

Axial patterning of the chondrichthyan pharyngeal endoskeleton and the origin of the jaw

Marie Christine Hirschberger

Downing College

March 2021



UNIVERSITY OF
CAMBRIDGE

This dissertation is submitted for the degree of Doctor of Philosophy
in Zoology

Declaration

This dissertation is the result of my own work and includes nothing which is the outcome of work done in collaboration except as declared in the preface and specified in the text.

This dissertation is not substantially the same as any work that has already been submitted before for any degree or other qualification except as declared in the preface and specified in the text.

This dissertation does not exceed the prescribed word limit of the School of Biology degree committee.

Summary

Classical comparative anatomical hypotheses propose that the upper and lower jaw evolved through modification of dorsal and ventral gill arch skeletal elements, respectively. These hypotheses were based largely on the skeletal anatomy of chondrichthyans (sharks, skates and holocephalans), but remain largely untested from a developmental perspective. Here, I test **1)** whether jaws and gill arches ancestrally shared common developmental patterning mechanisms, and **2)** whether the mandibular arch might carry anatomical vestiges of an ancestral gill-arch-like condition. To do this, I have used embryos of a cartilaginous fish, the little skate (*Leucoraja erinacea*), which has retained an ancestral organisation of the jaw and gill arch endoskeleton, and which possesses a reduced gill-like structure (a “pseudobranch”) on the back of the mandibular arch. Using candidate and RNAseq/differential gene expression analysis and mRNA *in situ* hybridisation, I find broad conservation of dorsoventral patterning mechanisms within pharyngeal arches – embryonic structures which contain the progenitors of the jaw and gill arch skeleton – as well as unique transcriptional features that may underpin distinct jaw and gill arch morphologies. The latter include unique gene expression features of jaw and gill arch muscle progenitors, and of developing gill lamellae. Finally, it has been historically speculated that the chondrichthyan pseudobranch derives from the hyoid (i.e. 2nd pharyngeal) arch. I demonstrate here, by cell lineage tracing, that the pseudobranch is, in fact, mandibular arch derived, that it shares gene expression features with developing gills, and that its supporting spiracular cartilage develops under the influence of a *shh*-expressing signalling centre, in a manner that parallels that *shh*-dependent development of branchial rays (i.e. cartilaginous appendages that support the respiratory lamellae of the gill arches). Taken together, this dissertation presents evidence for serial homology of the jaw and gill arch skeleton, and of an ancestral gill-arch nature of the mandibular arch of vertebrates.

Acknowledgements

The writing of this dissertation could not have been accomplished without the great deal of support I have received throughout my time as a PhD student.

First, I would like to thank my supervisor, Dr. Andrew Gillis, as well as all other members of the Gillis lab, past and present, for invaluable guidance, advice, and insights. It is an understatement to say that this work could not have been done without them and I feel enormously privileged to have been able to learn from them over the past four years. I am also indebted to the wider Evo-Devo community in Cambridge, which provides a greatly enriching environment for any young scientist.

When embarking upon this project, I certainly did not anticipate a pandemic to take a hold of the world when I got within six months of the finish line. In the face of this, I could not have completed this dissertation without the generous support of my funding body, the Biotechnology and Biological Sciences Research Council, as well as giant efforts on behalf of the University of Cambridge, the Zoology Department, Downing College, and the Gillis lab, which all worked together to allow for our work to continue in as safe an environment as possible despite COVID-19.

Finally, I would also like to thank my family and friends, without whom I could not have done this either.

Collaborations and publications

Chapter 3 includes tissue samples (skate pharyngeal arches, stages 23-26) collected by Dr. J. Andrew Gillis and cDNA libraries quality-controlled prior to sequencing by Dr. Stephen Clark.

Chapter 2 and 3 are in preparation for publication with *Molecular Biology and Evolution* (Oxford University Press), and currently available as a preprint on bioRxiv.

Parts of this work have been published as:

Hirschberger, C., Sleight, V. A., Criswell, K. E., Clark, S., & Gillis, J. A. (2021). Conserved and unique transcriptional features of pharyngeal arches in the skate (*Leucoraja erinacea*) and evolution of the jaw. *Molecular Biology and Evolution*. msab123.

Barske, L., Fabian, P., **Hirschberger, C.**, Jandzik, D., Square, T., Xu, P., Nelson, N., Yu, H.V., Medeiros, D.M., Gillis, J.A., & Crump, J. G. (2020). Evolution of vertebrate gill covers via shifts in an ancient Pou3f3 enhancer. *Proceedings of the National Academy of Sciences*, 117(40), 24876-24884.

Table of Contents

Chapter 1: Introduction	1
1.1 Jaw development	4
1.1.1 Pharyngeal arch development.....	4
1.1.2 Patterning the pharyngeal arches	5
1.1.3 Differences in pharyngeal arch development in jawed and jawless vertebrates	9
1.2 A brief history of jaw evolution	12
1.2.1 Classical models from the 19 th century	15
1.2.2 New heads and new mouths in the 1980s	19
1.2.3 Fossil evidence for a cyclostome-like arrangement of the pharyngeal endoskeleton in stem gnathostomes	20
1.2.4 The velum-transformational theory	23
1.2.5 Lamprey-based evo-devo models since the 2000s.....	25
1.2.6 Fossil evidence inconsistent with an ancestrally cyclostome-like condition in stem vertebrates	30
1.3 The return to serial homology	34
1.4 Summary	37
Chapter 2: Gnathostome jaw patterning mechanisms are conserved in the gill arches of the skate	38
2.1 Abstract	38
2.2 Introduction	39
2.2.1 Ventral patterning	41
2.2.2 Dorsal patterning.....	45
2.2.3 Intermediate patterning.....	46
2.2.4 Jaw patterning and serial homology.....	48
2.3 Methods	50
2.3.1 Embryo collection.....	50
2.3.2 cDNA synthesis, gene cloning and mRNA in situ hybridisation probe synthesis	50
2.3.3 Histology and in situ hybridization on sections and in wholemount.....	52
2.4 Results	54
2.4.1 Conservation of ventral gene expression patterns in the skate pharyngeal arches..	54

2.4.2 Conserved and divergent expression of dorsal patterning genes in the skate pharyngeal arches	56
2.4.3 Conservation of joint gene expression patterns in the skate pharyngeal arches.....	59
2.5 Discussion	61
2.5.1 Jaw patterning mechanisms known from bony fishes conserved across all pharyngeal arches in skate	61
2.5.2 Divergent expression of upper jaw markers known from bony fishes across all pharyngeal arches in skate	62
2.5.3 Conservation of jaw joint genes across all pharyngeal arches in skate	63
2.6 Summary	66
Chapter 3: Comparative transcriptomics reveal conserved and divergent transcriptional features of pharyngeal arches in the skate.....	67
3.1 Abstract	67
3.2 Introduction	68
3.2.1 RNA-seq in “non-model” organisms and the Trinity pipeline.....	68
3.2.2 Comparative transcriptomics of pharyngeal arch development in skate.....	70
3.3 Methods	73
3.3.1 RNA-seq and de novo transcriptome assembly.....	73
3.3.2 Differential gene expression analysis	76
3.3.3 Gene cloning, mRNA probe generation, histology and in situ hybridization on sections and in wholemount	76
3.4 Results	77
3.4.1 Quality control of the de novo pharyngeal arch transcriptome assembly	77
3.4.2 Sample correlation and biological replication analysis.....	82
3.4.3 ComBat batch effect correction	86
3.4.4 Differential gene expression analysis	88
3.4.5 Additional dorsoventrally polarised transcriptional features of the pharyngeal arches in skate	93
3.4.6 Distinct gene expression features within the mandibular and gill arch mesoderm ..	95
3.4.7 Gene expression features of presumptive gill epithelium and external gill buds	98
3.5 Discussion	100
3.5.1 Comparative transcriptomics add candidates to the dorsoventral patterning programme of developing pharyngeal arches in skate	100
3.5.2 Divergent patterning programmes within the mesodermal progenitors of the mandibular and gill arches	105

3.5.3 Novel gene expression features of the presumptive gill epithelium and external gill buds	106
3.6 Summary.....	107
Chapter 4: Vestigial gill structures derive from the mandibular arch of the skate.....	108
4.1 Abstract	108
4.2 Introduction	109
4.2.1 Interpreting the spiracle as evidence of the gill arch-like ancestry of the jaw	109
4.2.2 Interpreting the spiracle as a secondary derived feature.....	113
4.3 Methods	115
4.3.1 Embryo collection and fate mapping.....	115
4.3.2 mRNA in situ hybridisation	115
4.3.3 Immunofluorescence on paraffin sections.....	116
4.3.4 in ovo cyclopamine treatment, wholemount skeletal preparations and statistical analysis	116
4.4 Results	118
4.4.1 The skate pseudobranch is mandibular arch-derived	118
4.4.2 The skate pseudobranch and gills share cell and gene expression features	120
4.4.3 The skate spiracular cartilage and branchial rays share an embryonic origin from equivalent domains of shh-responsive mesenchyme	122
4.4.4 The skate spiracular cartilage and branchial rays share patterning mechanisms ...	125
4.5 Discussion	127
4.5.1 The mandibular arch origin of the pseudobranch	127
4.5.2 Serial homology of the spiracular cartilage and branchial rays.....	128
4.5.3 Spiracular cartilages and branchial rays throughout the palaeontological record..	131
4.6 Summary.....	135
Chapter 5: Discussion	136
5.1 A brief history of homology	138
5.2 Jaw-gill arch serial homology and the evolution of gnathostome jaws.....	141
5.3 Serially homologising beyond the jaws and gill arches in gnathostome body plan evolution.....	151
Supplementary files.....	155
References.....	157

Chapter 1:

Introduction

There are few other events in the history of vertebrates that are of such singular importance as the origin of the jaws. Gnathostomes (jawed vertebrates, or ‘jawed mouths’) entered the evolutionary stage in the Silurian period, 444–416 million years ago, and about 85 million years later, by the late Devonian period, they were already climbing the prehistoric shores well on their way to the colonisation of land (Janvier, 1996; Sansom et al., 2001; Anderson et al., 2011). Silurian assemblages and the dominance of jawless fishes (agnathans) over them were replaced by new assemblages composed almost exclusively of gnathostomes. Today, more than ninety-nine percent of all living vertebrates are jawed (Nelson, 2006). They have successfully adapted to a wide variety of ecosystems on every continent, from the skies to the deep sea, and range in size from a few millimetres to over 30 metres in length (Kardong, 2002).

The early gnathostomes possessed traits that unite modern vertebrates: chief among them was an embryonic cell population called neural crest cells, but also a large tripartite brain defined by the telencephalon, an inner ear with a vestibular system and semicircular canals, and sensory placodes, among other features (York and McCauley, 2020). The acquisition of articulated jaws on top of these vertebrate characteristics has long been thought of as the primary reason for the sweep to dominance by gnathostomes (Denison, 1961; Carroll, 1988; Janvier, 1996; Purnell, 2002). According to this view, jaws are the key feature that allowed gnathostomes to displace agnathans and successfully take over their ecological niches. However, this perspective has shifted over time as fossil evidence accumulated that shows the loss of jawless taxa does not neatly align with the rise of gnathostomes, as scenarios of competition would predict (Purnell, 2001). Instead, more recent work has illustrated that rather than directly outcompeting jawless taxa, early gnathostomes likely succeeded due to new ecological opportunities that became accessible because of jaws (Anderson et al., 2011). For example, feeding strategies such as macropredation and durophagy (the ability to eat exoskeleton-bearing or hard-shelled animals) or pelagic lifestyles were not common amongst

agnathans, but spread quickly amongst gnathostomes (Klug et al., 2010; Anderson et al., 2011). The emergence of a robust, jaw-bearing pharyngeal endoskeleton likely made these new strategies and lifestyles feasible, driving early gnathostome evolution and laying the groundwork for the jawed diversity we see today.

However, the exact origin of this body plan, i.e. the acquisition of a jaw from a jawless pharyngeal endoskeleton, remains an unanswered question in vertebrate evolution. The fossil record lacks key findings that show transitional states between the jawless and jawed vertebrates. In the absence of this evidence, centuries of research on the anatomy and development of the vertebrate body plan has offered many key insights, but no definite answers. As such, jaws still present a flagship problem in the study of evolutionary novelty.

The advent of evolutionary-developmental biology has shed new light on this long-standing question. Evolutionary-developmental biology, or evo-devo for short, is interested in the comparative link between development and morphology in order to infer ancestral relationships, or in other words, in the mechanisms of evolution and development that link the readout of the genotype with the structures of the phenotype (Hall, 2012a). This scientific strategy has led to an influx of research that frames the evolution of the jaw as the stepwise accumulation of changes in the development of the anterior pharyngeal endoskeleton across gnathostomes. However, the developmental data used to identify the set of changes that led to the origin of the jaw has almost exclusively stemmed from bony fishes, like zebrafish or mouse, and a jawless fish, the lamprey, as an outgroup. Chondrichthyans or cartilaginous fishes (sharks, rays, skates, and holocephalans) comprise the sister group to the bony fishes, but comparative data on pharyngeal development from this group has mostly been lacking from considerations on the origin of the jaw (Gillis et al., 2013; Compagnucci et al., 2013).

This dissertation aims to fill this gap and link pharyngeal development and anatomy in a cartilaginous fish, little skate (*Leucoraja erinacea*), to jaw development known from bony fishes. Cartilaginous fishes have retained the primitive dorsoventrally segmented organization of the gnathostome pharyngeal endoskeleton (i.e. a jaw and gill arch skeleton that is segmented into prominent palatoquadrate/Meckel's cartilage epi-/ceratobranchial elements, respectively), as well as a spiracle behind the jaw and open gill slits separating all

gill-bearing arches, as opposed to the presence of an opercular gill cover that permits for the reduction of individual gill-arch endoskeletal support in teleosts (Gillis et al., 2009a; Mallatt, 1996; Gillis et al., 2012). Through comparisons with their sister group, the bony fishes, the anatomical and developmental conditions in the last common ancestor of gnathostomes may be inferred.

In this introduction, I will briefly summarise pharyngeal development to discuss how the jaws first develop in the embryo. Then I will pair this developmental overview with the models of jaw evolution that have been constructed on its basis and discuss to what extent they match the evidence available from the fossil record. Finally, I will introduce the little skate as a model system and its power to connect pharyngeal development with anatomy to create an important step forward in solving the puzzle of jaw evolution.

1.1 Jaw development

As the vertebrate head plays a key role in ecology and evolution, it is also arguably the most complex part of vertebrate morphology. Its development reflects this complexity and involves an elaborate interplay of all three germ layers as well as cranial neural crest cells. Most of the craniofacial skeleton, including jaws, derive from pharyngeal arches – transient columns of tissue forming on the lateral surface of the developing head (Fig. 1.1A, Graham, 2001, 2003; Richmann and Lee, 2003).

1.1.1 Pharyngeal arch development

Pharyngeal arches form as the foregut endoderm establishes a series of paired out-pockets. These endodermal pouches contact and fuse with overlying ectoderm on the lateral surface of the embryo, forming openings between the foregut and the outside of the animal—the presumptive gills slits (Fig. 1.1A). The serial architecture of pharyngeal arches in the embryo confers a segmented origin onto the oropharyngeal apparatus that is often absent in the adult anatomy of amniotes (mammals, reptiles, and birds). The degree to which the clefts open during development varies. For example, in amniotes like mice and chickens, the posterior arches are only demarcated by endoderm contacting ectoderm, rather than fusing and subsequent clefts creating an opening through the two layers.

The columns of tissue left between the out-pocketing pouches of endoderm are the pharyngeal arches. Each arch consists of ectoderm on the external side of the embryo, endoderm on the interior side in the pharyngeal cavity, and a mesenchymal core of neural crest cells surrounding mesoderm (Fig. 1.1B). The neural crest component enters each arch after delaminating from the dorsal neural tube, undergoing an epithelial-to-mesenchymal transition and migrating along well-defined pathways (Theveneau & Mayor, 2012). Their migration occurs in three main streams, alongside a fourth population that migrates into the frontal-nasal region (Fig. 1.1C; Graham et al., 2003), outlined in detail below.

Each of the different embryonic cell types that comprise the pharyngeal arches gives rise to distinct derivatives. The ectodermal epithelium gives rise to the epidermis and the sensory neurons associated with each arch, while the endodermal epithelium gives rise to the gills (in

fishes) and the epithelial lining of the pharynx. The neural crest cells within each arch give rise to skeletal and connective tissues, and the mesodermal core to arch musculature and endothelial cells (Graham, 2001). From these components, the nerves, muscles, skeletal tissues and epithelial specialisations of the jaw and pharynx are formed.

1.1.2 Patterning the pharyngeal arches

As such, the pharyngeal arches consist of an iterative series of parallel columnar tissues, each of which gives rise to the same basic components. However, despite this shared basic blueprint of each arch, they are also patterned along the anterior-posterior axis and each pair of arches has an individual identity. In fishes, the first (mandibular) pharyngeal arch gives rise to the jaw, while the second (hyoid) arch forms a gill bearing arch that also functions to suspend the jaw from the braincase and in bony fish gives rise to the gill covering (opercular) skeleton, and a variable number of gill arches give rise to the elements of the pharynx and the gills (Graham, 2003; Gillis et al., 2013). In amniote tetrapods, the mandibular arch gives rise to the jaw and middle ear ossicles (malleus and incus in mammals), the hyoid arch forms the stapes, styloid process, and hyoid bone, and the more posterior pharyngeal arches give rise to the tracheal cartilages and other specialised elements of the pharyngeal apparatus like the thyroid, parathyroids and thymus (Fraser, 1882; Schilling & Kimmel, 1994; Crump et al., 2006, Medeiros & Crump, 2012; Graham & Richardson, 2012). Additionally, anterior to the mandibular arch there is a population of unsegmented neural crest cells that in tetrapods contribute to the frontonasal and maxillary prominences, which in turn give rise to the anterior skull, foreface, and parts of the upper jaw (Eberhart et al., 2006, Kontges & Lumsden, 1996; Wada et al., 2005). Hence, the pharyngeal arches form in a morphologically similar fashion, but the embryonic cell types within each arch have to be coordinated to construct distinct morphologies at the right time in the right place in order to ensure that the correct anteroposterior identity of each arch is generated.

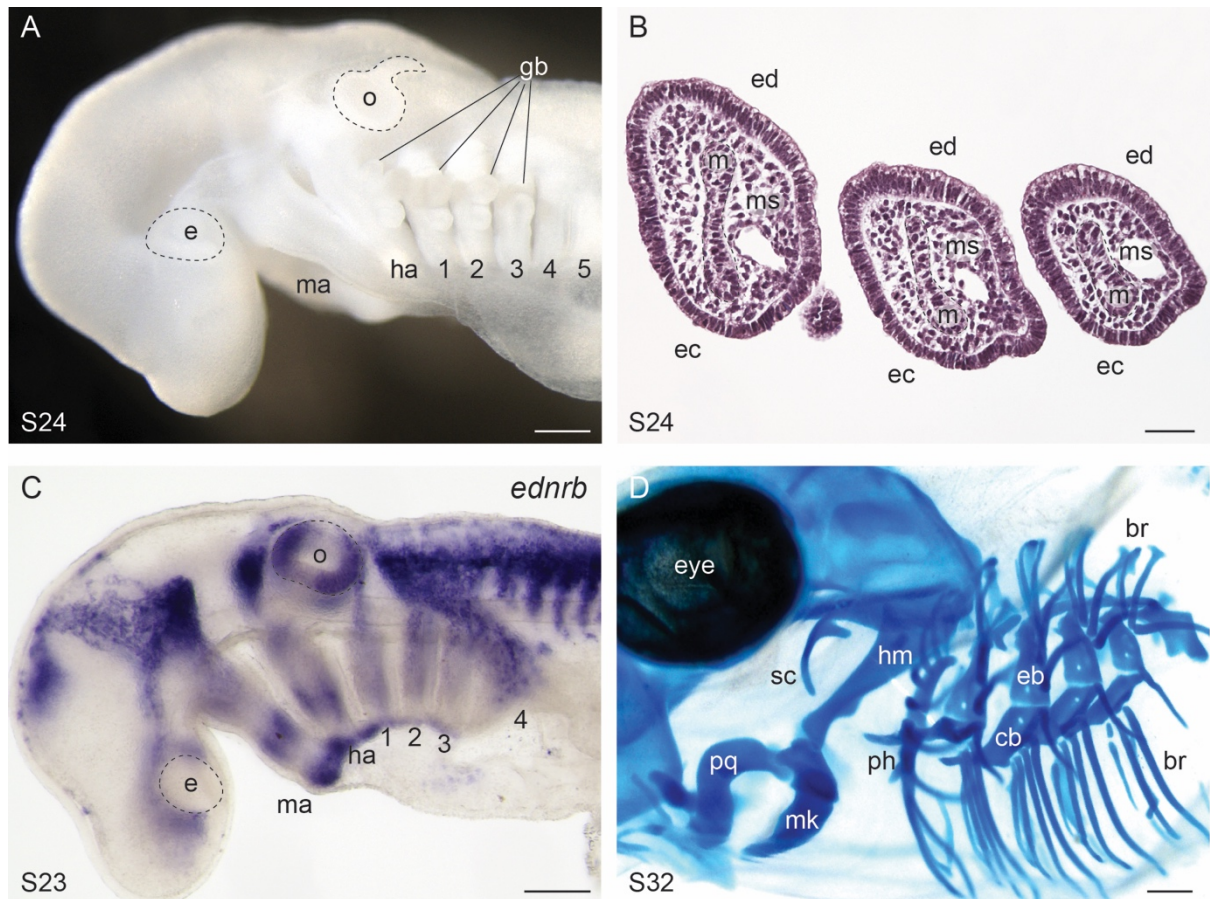


Figure 1.1: Pharyngeal arches and their skeletal derivatives in the little skate (*Leucoraja erinacea*).

(A) Pharyngeal arches are columns of tissue characterising the lateral embryonic head and pharynx. (B) Horizontal section through gill arches 1-3 at stage (S)24 showing the mesodermal core surrounded by mesenchyme, which is encased by endoderm on the inside and ectoderm on the outside of the animal. (C) Wholemount *in situ* hybridisation of migrating neural crest cell marker *ednrb* showing trigeminal, hyoid and postotic neural crest cell streams populating mandibular, hyoid, and gill arches, respectively. (D) Wholemount skeletal preparation at S32 shows dorsoventral jaw segmentation into palatoquadrate and Meckel's cartilage, jaw suspension from the braincase by the hyomandibula, and dorsoventral gill arch segmentation into epi- and ceratobranchial elements. Branchial rays are projecting from the gill arches. br: branchial ray; cb: ceratobranchial; e: eye; eb, epibranchial; ec: ectoderm; ed: endoderm; gb: gill buds; ha: hyoid arch; o: otic vesicle; ph: pseudohyal; pq: palatoquadrate; m: mesoderm; ma: mandibular arch; mk: Meckel's cartilage; ms: mesenchyme; sc: spiracular cartilage; 1-5: gill arches 1-5.

A specific class of homeobox-containing transcription factor genes, called *Hox* genes, are key body plan regulators across the animal kingdom, and the development of pharyngeal arches is a classic example of their rule: nested expression of the ‘*Hox* code’ establishes arch identity along the anteroposterior axis of the embryonic vertebrate pharynx (Hunt et al., 1991; Hunt & Krumlauf, 1991). In the mandibular arch, *Hox* gene expression is absent and this arch is filled by the trigeminal stream of migrating cranial neural crest cells (Fig. 1.1C), which originates from the midbrain and rhombomeres 1 and 2 of the hindbrain. These neural crest cells will give rise to neurons of the trigeminal ganglion and the skeleton of the lower and upper jaw (Lumsden et al., 1991; Schilling & Kimmel, 1994). The second, hyoid arch is characterised by expression of *Hoxa-2*. Gain- and loss-of-function experiments on *Hoxa-2* result in the transformation of the mandibular arch into the hyoid or vice versa (Gendron-Maguire et al. 1993; Rijli et al. 1993; Grammatopoulos et al. 2000; Pasqualetti et al. 2000). The hyoid stream of cranial neural crest cells migrating into this arch (Fig. 1.1C) originates from rhombomeres 3-5 of the hindbrain and will give rise to neurons of the proximal facial ganglion as well as the hyoid skeleton (Lumsden et al., 1991; Schilling & Kimmel, 1994). The post-hyoid, first gill arch is characterised by *Hoxa-2* and *Hoxa-3* expression, and in the posterior gill arches additional *Hoxb-4* is expressed (Couly et al., 1998). The caudal arches are populated by the post-otic stream of neural crest cells (Fig. 1.1C), which originates from rhombomeres 6 and 7 of the hindbrain and will give rise to neurons of the proximal and jugular ganglia and the skeletal components of the posterior pharyngeal arches (Lumsden et al., 1991; Schilling & Kimmel, 1994).

In addition to the anteroposterior polarisation, the gnathostome pharyngeal arches also give rise to an endoskeleton that is dorsoventrally segmented. This condition is most readily observed in extant chondrichthyans and, to a lesser extent, in bony fish like teleosts (Janvier, 1996). In chondrichthyans, the pharyngeal endoskeleton is partitioned dorsoventrally into the palatoquadrate and Meckel’s cartilage in the jaws, into the hyomandibula and ceratohyal in the hyoid, and into epibranchial and ceratobranchial elements in the gill arches, from which gill-supporting branchial rays project laterally (Fig. 1.1D; DeBeer, 1937; Gillis et al., 2009a).

This organisation can already be seen in the first jawed fishes that arose in the Silurian about 444–416 million years ago (Anderson et al., 2011; Kardong, 2012 DeLaurier, 2018). Amongst

these first gnathostomes were two main lineages: placoderms, whose exact interrelationships remain disputed, and acanthodians (Kardong, 2012; Brazeau & de Winter, 2015). Both are distinguished by already well-developed jaws (Kardong, 2012). For example, the jaws of the placoderms *Entelognathus* and *Romundina* bear a striking resemblance to modern gnathostomes (Dupret et al., 2014; Zhu et al., 2013), and in the placoderm *Compagopiscis croucheri* the lower jaw has been homologised to the mandibular-derived Meckel's cartilage of extant gnathostomes (Rücklin et al., 2012). Acanthodians such as *Ptomacanthus anglicus* and *Acanthodes bronni* possessed pharyngeal skeletal elements similarly reminiscent of extant gnathostomes, including the jaw components palatoquadrate and Meckel's cartilage, the hyoid derived hyomandibula, and the gill arch derived ceratobranchials (Brazeau, 2009; Brazeau & de Winter, 2015; Friedman & Brazeau, 2010). Thus, a chondrichthyan-like organisation of the pharyngeal endoskeleton likely represents the ancestral condition found in the first jawed fishes. It should be noted, however, that there are also bony elements preserved from placoderms that have been lost in chondrichthyans. For example, endochondral bone and the bony skeleton it forms is an ancestral feature of jawed vertebrates that has been lost in chondrichthyans (Brazeau et al., 2020).

In extant bony fishes, the dorsoventral segmentation of the pharyngeal endoskeleton is less readily observable. In teleosts like zebrafish, the principal segmentation is still visible, though the epibranchial elements of the gill arches are highly reduced as the hyoid arch derived opercle bone fulfils the function of covering the gills (Schilling & Kimmel, 1994). In amniotes, the endoskeletal organisation is even more derived: the mandibular arch gives rise to the dorsal maxillary and ventral mandibular processes, which are ossified during development and together form the jaw, but also to the lateral skull (Köntges & Lumsden, 1996), and in mammals elements of the middle ear, i.e. the malleus and incus (Reichert, 1837; see O'Gorman, 2005 for hyoid arch contributions to the middle ear). The post-hyoid arches do not undergo skeletogenesis or myogenesis while still in arch-form, and are instead largely remodelled into the larynx, which consists of cricoid and paired arytenoids, the thyroid and associated muscular and connective tissue elements, and which functions to connect the pharynx with the trachea (Poopalasundaram et al., 2019). As the *Hox* code patterns the anteroposterior axis of the pharyngeal arches, a '*Dlx* code' patterns the dorsoventral axis (though not in post-otic arches in amniotes, Poopalasundaram et al., 2019), and underpins

the dorsoventral segmentation so readily observed in chondrichthyans (Depew et al., 2002; Gillis et al., 2013; for an in-depth discussion of the dorsoventral patterning beyond the *Dlx* code see chapters 2 & 3).

1.1.3 Differences in pharyngeal arch development in jawed and jawless vertebrates

In an evolutionary-developmental context, the origin of the jaw may be regarded as the accumulation of developmental changes to the anteroposterior and dorsoventral patterning programme outlined above that work together to sculpt the jaw out of the mandibular arch. In this respect, it is useful to also consider the development of pharyngeal arches in jawless vertebrates, as the differences in patterning and morphogenetic constraints exhibited in this lineage in contrast to jawed vertebrates may serve to illuminate the evolution of differences in their oral apparatuses. The only two remaining lineages of jawless vertebrates alive today are lampreys and hagfishes. Historically, the evolutionary relationships between lampreys, hagfishes, and gnathostomes has been contentious (Shimeld & Donoghue, 2012; York & McCauley, 2020). But advances in molecular phylogenetics now firmly group lampreys and hagfishes together as a monophyletic lineage of cyclostomes ('round mouths'), which persist as the last living members of an ancient group of jawless fishes (Heimberg et al., 2010). Both lampreys and hagfish have migrating neural crest cells as well as most of the neural crest derivatives known from jawed vertebrates (Shigetani et al., 2002; Ota et al., 2007; McCauley & Bronner-Fraser, 2003). Lampreys are also characterised by distinct anatomies at larval (ammocoete) and adult stages, which are separated by a metamorphosis during which many larval tissues are remodelled into adult features (De Beer, 1937; Green & Bronner, 2014).

The craniofacial organisation of lampreys and hagfishes differs considerably from gnathostomes in several important aspects. The most obvious difference concerns the jaw: while in gnathostomes the mandibular arch gives rise to the upper and lower elements of the jaw, the lamprey mandibular arch gives rise to the velum, a muscular pumping organ with a small cartilaginous element in the middle (Fig. 1.2). Lampreys also possess a muscular upper and lower lips that derive largely from the premandibular domain (Johnels, 1948).

The gnathostome pharyngeal arches give rise to an endoskeleton that is jointed and divided into subsections along the dorsoventral axis. In contrast, living cyclostomes possess thin, unjointed branchial bars, which are fused together in a condition often referred to as a 'branchial basket' (Fig. 1.2; Janvier, 1996). These arise from pharyngeal arches three to nine (Morrison et al., 2000). In hagfish, the number of branchial bars is very low and stands at only two, although they still possess between 6 and 12 pairs of gill slits (Oisi et al., 2013). In lampreys, the branchial basket is also compartmentalised in a manner that has no immediate obvious equivalencies with the gnathostomes: respiration occurs in the ventral part, while the mouth is dorsally separated from it by the velum (Janvier, 1996).

The differences between gnathostomes and cyclostomes have proven to be an insightful starting point for models of jaw evolution. As cyclostomes are an early branching vertebrate lineage, which predates the origin of the jaw, comparisons between their anatomy and development and the mechanisms at play in gnathostomes might reveal important clues as to how the jaw originated.

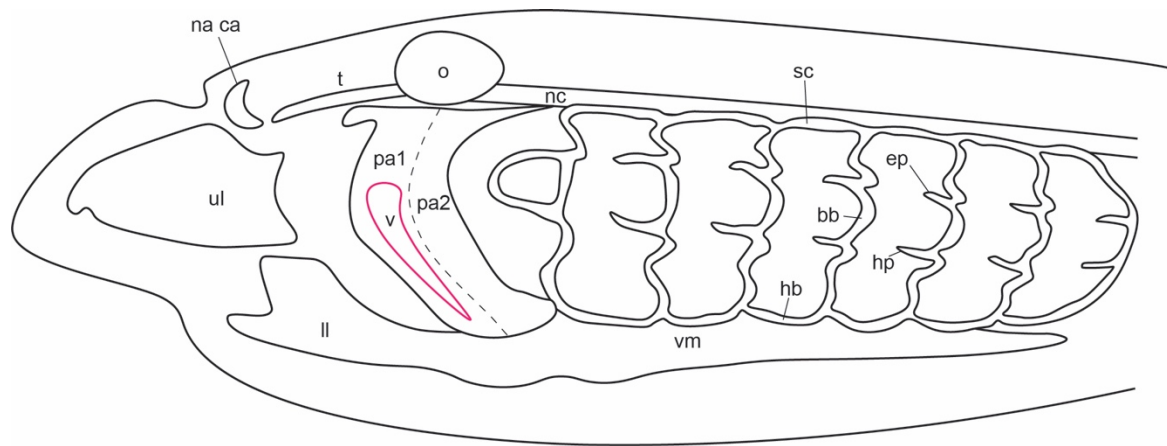


Figure 1.2 Larval (ammocoete) lamprey head. The upper lip (ul), lower lip (ll), first pharyngeal arch (pa1), second pharyngeal arch (pa2), and ventral pharynx (vm) are mainly comprised of mucocartilage. The mandibular arch derived velum (v) sits inside the anterior pharynx, outlined in pink. The posterior pharynx is supported by the branchial basket, consisting of fused, cartilaginous rods. Within this arrangement, dorsally and ventrally, the horizontal subchordal (sc) and hypobranchial (hb) bars frame the branchial bars (bb), from which the epitrematic (ep) and hypotrematic (hp) processes project laterally. na ca, nasal capsule; nc, notochord; o, otic vesicle; t, trabecula. Schematic adapted from Morrison et al., 2000, Meulemans & Crump, 2012, and Yokoyama et al., 2020.

1.2 A brief history of jaw evolution

In the developmental terms discussed above, the evolution of the jaw can be framed as the stepwise acquisition of the transcriptional and signalling programme that patterns the pharyngeal arches in gnathostomes, which in turn ultimately give rise to the jaws on the one hand and the gill arches on the other hand. However, this framing is a relatively modern one that only arose as our understanding of craniofacial development deepened. Jaw evolution models have existed for much longer than this developmental viewpoint.

Studies on the origin of the jaw predate Charles Darwin's 'On the Origin of Species'. One of the earliest treatises on jaw-gill arch similarities was published by embryologist and anatomist Heinrich Rathke in the first half of the 19th century (Rathke, 1827, 1832). Consistent with the worldview of natural philosophy at the time, Rathke framed all science as the search for the uniting laws that govern the natural world. In pursuit of this aim, he saw most value in an unbiased, comparative method, including ontogeny as well as anatomy. In his investigations in sharks, sturgeons, teleosts and frog larvae (and even lampreys, which he thought possessed fused jaw cartilages), Rathke was struck by the similar arrangement of gill-supporting cartilages to the jaw elements and speculated whether they might correspond (Rathke, 1832). Notably, Rathke also pointed out that all vertebrate embryos he studied, from lampreys to mammals, were united by the presence of pharyngeal arches separated by clefts early in development, an insight shared with von Baer, among others (Rathke, 1832).

These early anatomical investigations gave rise to the classic morphological theory of jaw evolution, which was based on the apparent anatomical similarity and correspondence of the upper and lower jaws to the upper and lower gill arch elements, respectively, and which suggested that the jaw in gnathostomes arose out of the transformation of a rostral gill arch (in detail outlined below; Sewertzoff, 1911, 1928; Goodrich, 1930; de Beer, 1937; Romer, 1966; Jarvik, 1980; Mallatt, 1984, 1996; Carroll, 1988; Janvier, 1996; Kuratani et al. 2001; Kuratani, 2004; DeLaurier, 2018). One of the main architects of this theory is Carl Gegenbaur, who also coined the term 'gnathostomata' (Gegenbaur, 1874). However, since the 19th century, the theory of jaw-gill arch serial homology has undergone transformations and faced

increasing opposition. Mainly due to the resolved phylogenetic relationships between living jawless and jawed vertebrates and an ever-increasing understanding of craniofacial organisation and development of the two groups, questions of homology between different parts of the oral and pharyngeal region in lampreys, gnathostomes, and fossil data have been raised (Janvier, 1996; Mallatt, 2008; Miyashita, 2016; Square et al., 2016; DeLaurier, 2018; Yokoyama et al., 2020). Today, the debate has mostly moved on to the specific evolutionary history of changes in the developmental programme that may create a set of jaws out of an ancestral jawless state, which is often assumed to be represented by a modern larval lamprey. To fully understand this paradigm shift—the rise and fall of transformational jaw-gill arch serial homology—we first have to trace the origins of this theory all the way back to the 19th century to first consider its origins and then discuss the emergence of subsequent models.

It is possible to partition previous models of jaw evolution into three stages (analogous to Janvier's 'three historical periods of segmental theory', 1996): classical models, new head/new mouth models, and finally modern evolutionary-developmental models (Table 1.1). The history of the jaw-gill arch serial homology theory, which is tested by this dissertation, can be traced through these three stages, from its origins, rise to dominance and subsequent fall from grace, to its recent reappraisal.

	Main Authors	Timeline	Main ideas	Main evidence
Classical models	Johann Wolfgang von Göthe and Lorenz Oken (pre-Darwin)	1820, 1807	Transformational vertebrae origin of the skull	Segmentation
	Carl Gegenbaur (post-Darwin)	1878	Serial homology of jaws and gill arches	Chondrichthyan anatomy
New heads/new mouths	R. Glenn Northcutt and Carl Gans	1980s	Neural crest derived features including jaws turned filter feeders into active predators	Neural crest cells, deuterostome phylogeny
	Jon Mallat	1996	Jaws first evolved for ventilation	Comparative cyclostome and chondrichthyan anatomy
Evo-devo models	Shigeru Kuratani, Yasuyo Shigetani, et al.	2002	Heterotopy Hypothesis: inductive tissue-interactions shifted posteriorly; jaws evolved as a morphological novelty	Gene expression in lampreys vs. amniotes
	Robert Cerny et al.	2010	Pre-Pattern and Co-Option: jaws evolved by co-option of 'joint genes' into a molecularly pre-patterned but unjointed mandibular arch	Gene expression in lampreys vs. zebrafish and amniotes, fossils
	Tetsuto Miyashita	2016	Mandibular Confinement: jaws evolved in four successive stages as the mandibular arch lost a role in ventilation and was spatially confined to contribute only to the jaw	Gene expression in lampreys vs. zebrafish and amniotes, fossils
	Claudia Compagnucci, Michael Depew et al.	2002, 2013	Hinge and Caps: jaw evolution is the acquisition of proximo-distal polarity into a branchial arch, forming appositional units separated by a hinge	Gene expression in lampreys vs. zebrafish and amniotes vs. chondrichthyans

Table 1.1: Models of jaw evolution from the late 19th century until today.

1.2.1 Classical models from the 19th century

As briefly hinted at above, the oldest models of jaw evolution from the 19th century were based on comparative anatomical and morphological data. Proto-evolutionary thought was permeating through the natural sciences, though Charles Darwin had not formalised it yet with the twin formula of natural selection and descent with modification (Darwin, 1859). Scientists interested in anatomy, such as Geoffroy Saint-Hilaire (1818), were convinced they could identify a common pattern or archetype that was once shared by all animals, and as such, their research was an attempt to order the differences and similarities across animals by classifying their morphological relationships to this hypothetical common pattern (Janvier, 1996). The first theories on transformations and homologies (at the time called ‘correspondences’ or ‘analogies’) can be traced back to this time, and studies on the jaw were no exception to these ideas. Segmentation was thought to be one such unifying feature shared to varying degrees across all animals, and the first theories on the transformational nature of the jaw specifically emerged out of a wider discussion on the segmentation of the vertebrate head (Janvier, 1996). Göthe (1820) and Oken (1807) are among the first authors to suggest that the vertebrate head once originated from serially homologous segments, and they viewed the skull, including the jaw, as an assemblage of modified vertebrae (Janvier, 1996).

However, through Darwin, Huxley, and other evolutionary thinkers, the philosophical search for an archetypal pattern once common to all animals was cast out and gave way to formal evolutionary thought that attempted to order animal variety by phylogenetic relationships instead of their closeness to a hypothetical ideal. The theories on the segmented origin of the skull were picked up by Huxley, who regarded both Göthe’s and Oken’s transformational vertebrae arguments as nonsensical (1858; Janvier, 1996), but agreed fundamentally that segmentation played a role in the development of vertebrate heads (Huxley, 1858; Goodrich, 1930). Finally, Carl Gegenbaur framed the problem of skull segmentation as one that included all craniofacial tissues, that is, also the nervous system, muscle, tendons, and other tissues in addition to endoskeletal elements (Gegenbaur, 1872, 1878; Janvier, 1996). Gegenbaur noticed the strikingly anatomical correspondence in the arrangement of jaws and gill arches in extant chondrichthyans, and suggested a theory of serial homology, whereby the jaw arose

out of the modified anterior-most gill arch (Fig. 1.3A; Gegenbaur, 1872). This theory considers the upper and lower jaws (palatoquadrate and Meckel's cartilage, respectively) to be modified upper and lower gill arch elements (epibranchials and ceratobranchials), jaw muscles to be modified branchial constrictors, the spiracular pseudobranch to be a vestigial gill, the trigeminal nerve to be a modified branchiomic nerve, and the maxillary or efferent pseudobranchial artery as a modified pharyngeal arch artery. In classical morphology, this view was cemented as the transformational origin theory of the jaw (Fig. 1.3B; Gegenbaur, 1872; Goodrich, 1930; Romer, 1966).

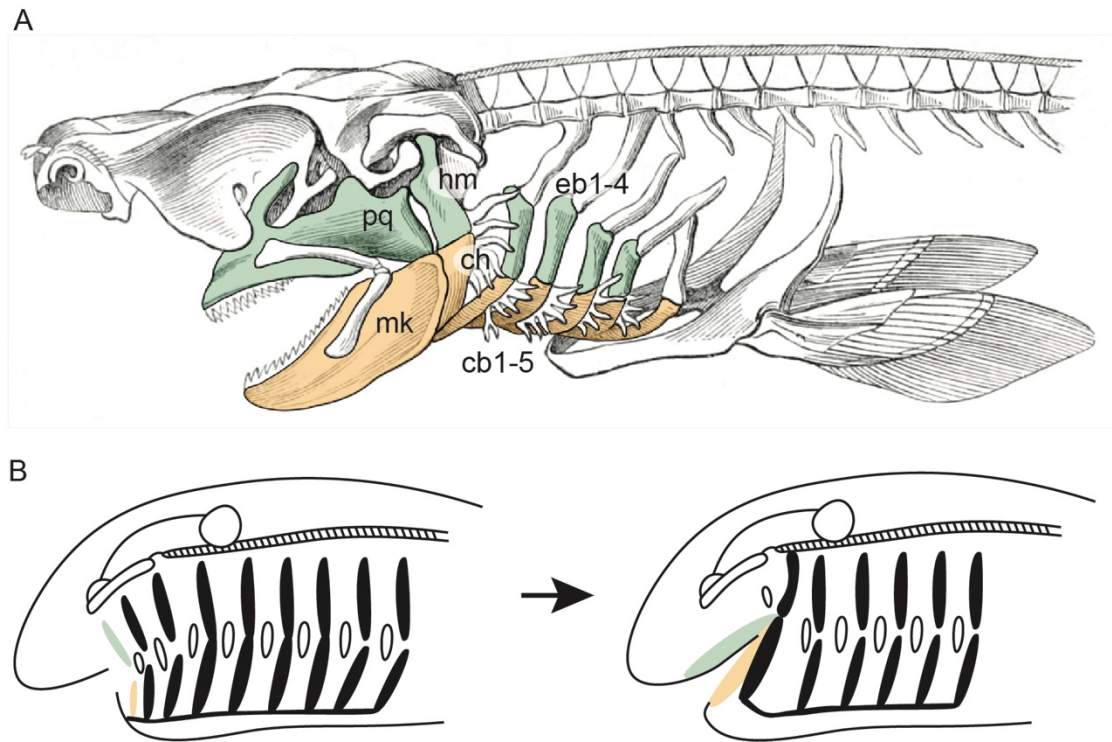


Figure 1.3 Classical models of jaw evolution. (A) Carl Gegenbaur's jaw-gill arch serial homology illustrated in a shark pharyngeal endoskeleton with anatomically equivalent dorsal and ventral skeletal elements in green and orange respectively. Redrawn after Owen, 1866. (B) Representative textbook scenario of jaw origin by transformation of an anterior gill arch. The anterior-most gill slit becomes the spiracle. Upper anterior gill arch/jaw in green, lower anterior gill arch/jaw in orange, redrawn from Janvier, 1996 and references therein. Cb1-5, ceratobranchials 1-5; ch, ceratohyal; eb1-4, epibranchials 1-4; hm, hyomandibula; mk, Meckel's cartilage; pq, palatoquadrate.

Some evolutionary thinkers of this time maintained assumptions that were tightly connected to the idealised theory of head segmentation, including Huxley. This mainly involves speculations on the hypothetical ancestral existence of a pre-mandibular arch (Huxley, 1874; Gegenbaur, 1898; Goodrich, 1930; Sewertzoff, 1928; de Beer, 1937; Jarvik, 1980; Kuratani, 2012). According to those ideas, the mandibular arch was originally specified as the second, rather than the first arch, and in gnathostomes the pre-mandibular arch has been adapted into the trabecula cartilage, which provided a cranial base for the rostrally expanded forebrain (Huxley, 1874; Goodrich, 1930; de Beer, 1937; Kuratani & Ahlberg, 2018). The morphological evidence cited in favour of this view is built around innervation, neurocranial anatomy, and mesodermal cavities thought to be associated with each pharyngeal arch. First, the trigeminal nerve (the anterior-most member of the branchiomic/pharyngeal nerves) emerges from two separate primordia, which was thought to reflect a dual-arch origin of this structure. The first one of these two trigeminal nerve primordia gives rise to the ophthalmic nerve and ganglion, while the second one gives rise to the maxillomandibular nerve components (Goodrich, 1930; de Beer, 1937). This led to the interpretation of the anterior, ophthalmic part of the trigeminal nerve as a secondarily degenerated nerve of the reduced premandibular arch (Kuratani et al., 2013). Secondly, the anterior neurocranium was thought to develop from paired rod-like cartilaginous primordia reminiscent of pharyngeal arches, and this was also interpreted as embryonic evidence of an ancestral pre-mandibular arch (Kuratani et al., 2013). Finally, elasmobranch embryos possess epithelial mesodermal cavities in the head during development, which were thought to correspond to the pharyngeal arches (Jarvik, 1980), and as the anterior-most one of these mesodermal cavities lacked such an association and was not linked to the mandibular arch, this was also weighed as evidence in favour of an ancestral premandibular arch that was assumed to have developed ventrally to this cavity. However, no pharyngeal pouch and no pharyngeal muscle develops anterior to the mandibular arch, no fossil jawless fish has been found to have possessed a premandibular arches (Janvier, 1996; Kuratani et al., 2013; Miyashita, 2016), and no *Dlx* genes are expressed anterior to the mandibular arch, and for these reasons the existence of such a hypothetical pre-mandibular arch has been discounted today (Kuratani et al., 2013). Nonetheless, speculations on this have been influential in previous models of jaw evolution; and the evolutionary history of the trabecula (part of the historical reason that invoked such an arch in the first place) has remained fruitful grounds for debate (Kuratani & Ahlberg, 2018).

1.2.2 New heads and new mouths in the 1980s

Around a hundred and twenty years after Gegenbaur's *Elements of Comparative Anatomy* (1859) became the standard textbook of evolutionary morphology, new insights from molecular and developmental data in the 1980s revolutionised our understanding of vertebrate phylogenetics. This led to a completely new conception of vertebrate evolution, jaws included (Northcutt & Gans, 1983; Mallat, 1984). In 1983, Northcutt and Gans put forward the 'New Head Hypothesis': they noted that most features unique to vertebrates are linked to the origin of the neural crest cells and the neurogenic placodes, and these embryonic features functioned together to derive a novel vertebrate head architecture (Gans and Northcutt, 1983; Gans, 1989, 93; Northcutt, 1996). The new head hypothesis framed the origin of vertebrates (and the subsequent origin of the jaws) as a transitional set of stages that started with benthic ciliary filter feeders, similar to living cephalochordates like amphioxus, followed by a shift to a proto-vertebrate lifestyle in which the pharynx became a muscular pump, consisting of neural-crest-derived pharyngeal bars and branchiomic muscles, which in turn enabled the shift from suspension feeding to suction feeding and finally to more active predation as the anterior pharyngeal muscular pump transformed into the first set of jaws (Northcutt, 2005). Several new lines of evidence united in support of this theory: large advances were made in understanding deuterostome phylogeny, ammocoetes were discovered to be larval lampreys and could as such be used in comparative studies on the development of jawless vertebrates as an outgroup to gnathostomes, and finally tritiated thymidine labelling experiments showed how extensively neural crest and placodes are contributing to vertebrate tissues, particularly in the head (Janvier, 1996).

It is important to note that this new head hypothesis modelled early vertebrate and subsequent gnathostome evolution as a transition from sessile filter feeding to active predation that could be represented by extant species, i.e. the non-vertebrate chordate amphioxus and the larval stages of jawless vertebrate lamprey. This marked a departure from mostly anatomical hypotheses that largely did not speculate on how ancestral lifestyles may have influenced the evolution of gnathostomes, to the broad assumption that the larval lamprey condition reflected a filter feeding lifestyle inherent to the ancestral condition of

gnathostome ancestors, and this assumption has influenced all subsequent theories on jaw evolution ever since.

In 1996, the new head scenario was complemented by the new mouth hypothesis put forward by Mallatt (1996, 2008). Mallatt also agreed with the hypothetical stepwise transition through several different lifestyles by early vertebrates before the acquisition of the jaw, but emphasised the role of ventilation in this transition. The new mouth theory proposes that the first pharyngeal bars enlarged to prevent water reflux during forceful expiration, meaning the presumptive jaws first enlarged to fulfil a ventilatory function, and only then evolved to grasp prey. The associated pharyngeal bars tilted forward, which shaped the once large mouth into a thin slit between jaws and lips, forming the buccopharyngeal cavity of gnathostomes. Larval lampreys (Fig. 1.2) and extant chondrichthyans (Fig. 1.3) are thought to represent various intermediate step along this route, as these lineages both have retained the ancestral pre-mandibular cheeks and lips that framed the primitive open mouth (Mallatt, 1996). Put together, this model suggests that the jawless ancestors of gnathostomes possessed unjointed branchial arches, akin to lampreys, but an increased level of activity associated with altered feeding strategies changed the way ventilation and prey-capture occurred, giving rise to jointed bars, a closing mouth, and jaws. This suggests few or no oral structures were lost during the acquisition of the jaw and nearly all of the retained homologs occupy the same relative positions in the head of chondrichthyans as in larval lampreys. For this reason, Mallatt's ventilation theory also denies the existence of a hypothetical premandibular arch and suggests that the upper lip in lampreys (Fig. 1.2), which is derived from the premandibular domain and which contains trigeminal nerve-innervated muscles and endoskeletal elements, is thought to be retained as the "lips" around the mouth as the mandibular arches tilted forward in early branching gnathostomes and living chondrichthyans.

1.2.3 Fossil evidence for a cyclostome-like arrangement of the pharyngeal endoskeleton in stem gnathostomes

The rise to prominence by lampreys as models of gnathostome ancestry prior to the emergence of the jaws was further underpinned by palaeontological evidence that largely

centred around fossilised impressions and scars preserved in headshields of extinct jawless fishes on the gnathostome stem. The jawless fishes in question were osteostracans, which lived from the middle Silurian to Devonian and comprise a series of successive sister clades to jawed vertebrates (Sansom et al., 2015), and galeaspids, which comprise the extinct sister clade to the group that is formed by osteostracans and crown gnathostomes (Gai et al., 2011). Together, osteostracans and galeaspids form successive outgroups to jawed fishes, and they are more closely related to gnathostomes than cyclostomes (Fig. 1.4). As such they have been considered informative in inferring which traits are considered ancestral or derived along the gnathostome stem.

Fossil evidence recovered from osteostracans and galeaspids includes casts of the trigeminal nerve, which supported the interpretation of a cyclostome-like upper lip deriving from a mandibular arch laterally overlapping with the premandibular domain (Wängsjö, 1952; Gai et al., 2011; Janvier, 1996; Miyashita, 2016). The preservation of muscle scars close to the second branch of the trigeminal nerve in osteostracans is also cited as cyclostome-like, as the muscle innervation of the equivalent branch of the trigeminal nerve in lampreys occurs in the same domain (Song & Boord, 1993; Janvier & Arsenault, 2007; Higashiyama & Kuratani, 2014; Miyashita, 2016).

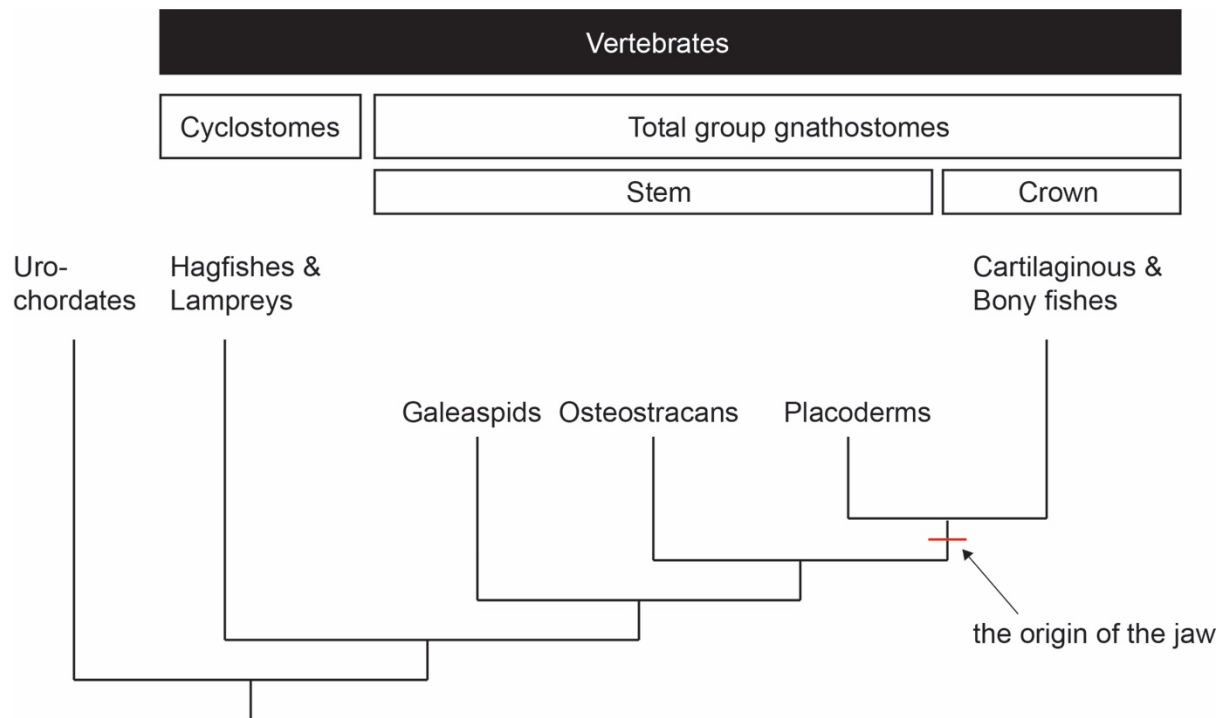


Figure 1.4: Vertebrate phylogeny. Jawless galeaspids and osteostracans as well as jawed placoderms are extinct groups on the gnathostome stem. Adapted from Gai & Zhu, 2012.

Other lines of evidence for a cyclostome-like condition in these jawless stem gnathostomes are drawn from the prebranchial cavities, which appear large enough to have housed a velum, and in some specific osteostracans such as *Dartmuthia*, preservations of the prebranchial cavity even suggest traces of the ventral attachment of a velum in this cavity (Janvier, 1985; Miyashita, 2016). Similarly, trace evidence and impressions of the prebranchial cavity in galeaspid have been interpreted as consistent with the innervation and veins associated with the velum in lampreys (Gai et al., 2011; Miyashita, 2016). Finally, it has also been suggested on a theoretical level that the rigid head shields and dermal scales inherent to these jawless fishes likely prohibited constrictions of the branchial cavity, which in turn would have prevented sufficient ventilatory flow in the absence of an additional ventilatory structure, necessitating the presence of a feature like the velum (Miyashita, 2016). Taken together, these palaeontological findings pointed to a scenario whereby the cyclostome-like organisation of the oropharyngeal region and endoskeleton, which is retained in living lampreys, was ancestrally shared by stem gnathostomes, and from this organisation, jaws likely originated.

1.2.4 The velum-transformational theory

The fossil evidence suggesting a cyclostome-like pharyngeal organisation in stem gnathostomes resulted in an increasing drive to homologise the components of lamprey and gnathostome pharyngeal endoskeletons, especially the velum and the jaw, as both derive from the first pharyngeal arch in lampreys and gnathostomes, respectively. The velum (Fig. 1.2) is a neural crest derived, cartilaginous structure unique to lampreys, which has a dual role in feeding and respiration in the anterior pharynx (Janvier, 1996). Attempts to homologise the velum with the gnathostome jaw have a long history (Ayers, 1931; Forey, 1995; Janvier, 1996), since jaws evolving from a velum-like condition appears like the most parsimonious scenario, if the velum-bearing lamprey condition of the pharyngeal endoskeleton is indeed ancestral. From this point of view, the jaw-gill arch serial homology hypothesis appears less likely, since the latter scenario involves an ancestral gill-arch losing its respiratory function and gaining a role in feeding—whereas the velum transformational

theory merely suggests an ancestral oropharyngeal device already functioning in feeding was adapted to clasp prey.

Consequently, the assumed cyclostome-like condition of stem gnathostomes and the increasing focus on comparative development and anatomy of extant jawed and jawless vertebrates ignited a debate on whether the ancestral mandibular arch had ever been gill-bearing. This is a prediction of the jaw-gill arch serial homology hypothesis, and this was an assumption that had largely been accepted as a given up to that point (de Beer, 1937; Goodrich, 1930; Janvier, 1996; Mallat, 1996). Classical anatomists had speculated that there had once been a complete gill slit between the mandibular arch and the hyoid, and that the paired openings in this place possessed by elasmobranchs (sharks, rays skates), called spiracles, represent a vestige of such a gill slit (Goodrich, 1930; Forey, 1995). But new comparisons with lampreys did not support this theory as they do not possess either a gill or a gill slit behind the velum-bearing mandibular arch (Maisey, 1989; Janvier, 1996; Morrison et al., 2000). The reduced, epithelial element inside the elasmobranch spiracles, termed 'pseudobranch', which anatomically strongly resembles a vestigial gill and had been interpreted as such, was discounted as a true gill since the water flow through the spiracles occurs in the opposite direction as across the gills in the gill arches (Janvier, 1996) and because its innervation and blood supply did not seem to match a gill-like organisation (Maisey, 1989; Miyashita, 2016). The clefts separating all arches, including the mandibular and hyoid arches, in the vertebrate embryo were discounted as evidence of serial homology, as they subsequently disappear in most groups. Developmentally, accumulating evidence of the power of *Hox* genes in body plan patterning and the '*Hox*-free default' state of the mandibular arch further served to decouple the mandibular arch from the posterior gill arches on a molecular level (Gendron-Maguire et al., 1993; Rijli et al., 1993). These findings were interpreted as evidence demonstrating that the apparent similarities between the mandibular and non-mandibular pharyngeal structures in gnathostomes, such as shared dorsoventral segmentation in chondrichthyans, require a patterning mechanism that acts independently of the pharyngeal *Hox* code and that had been acquired later in evolution than the ancestral, fundamental differences between the mandibular arch and the hyoid and gill arches (Miyashita, 2016). Consequently, it was now assumed that lampreys had retained the

ancestral condition and the mandibular arch across vertebrates had never been gill-like (Janvier, 1996; Forey, 1995).

Taken together, these findings have been interpreted as evidence consistent with the theory that the serially patterned derivatives of the mandibular arch in extant gnathostomes represent a derived, rather than ancestral, condition (Miyashita, 2016). According to this scenario, stem gnathostomes possessed a pharyngeal organisation reminiscent of cyclostomes, including a hypothetical velum or its equivalent structure that functioned for feeding or respiration. In the lineage leading to jawed fishes a reduction in the velar function occurred, and the velar cells were recruited to the novel structure of the jaw, particularly jaw articulation (Yokoyama et al., 2020). The velum-transformational hypothesis is challenged, however, by the fact that the velar muscles and cartilage develops from distinct mesodermal and mesenchymal subpopulations of mandibular arch cells, relative to the jaw cartilages (Yokoyama et al., 2020), which is reflected by the fact that the velar cartilages and muscles have no exact correspondences in gnathostomes and do not share a polarisation that could be compared to the upper and lower jaws, respectively (Miyashita, 2016). Nonetheless, the models of jaw evolution put forward since the 1980s all share one assumption: namely, cyclostomes have retained the ancestral pharyngeal endoskeletal organisation of vertebrates, and thus the jaw evolved out of a modified lamprey-like condition, as found in larval lampreys (Kuratani et al., 2005; Northcutt, 2005; Mallatt, 2008; Cerny et al., 2010; Square et al., 2016).

1.2.5 Lamprey-based evo-devo models since the 2000s

Current models of jaw evolution are still further advanced by novel developmental insights, such as the *Dlx* code (Depew et al., 2002) or transcriptional circuits regulating neural crest cells (Martik et al., 2019). Molecular biology techniques that extended the scope of developmental biology are continually improving, an ever-growing array of model species is becoming amenable to experimental manipulation, and high-resolution gene expression maps and gene regulation networks are being drawn. Consequently, the most recent suite of evo-devo hypotheses, put forward during the third era of jaw evolution models in my timetable of theories (Table 1.1), are mostly concerned with reconciling observed differences

in cell signalling, gene expression, and patterning functions between the lamprey and gnathostome pharyngeal arches, and aim to explain the derived gnathostome jaw as an elaboration upon a lamprey-like ancestral state. Specifically, the challenge has become to understand the genetic and developmental basis of how the robust and complex pharyngeal endoskeleton consisting of distinct cartilages connected by specialized joint tissue in gnathostomes emerged from the pharyngeal endoskeleton along the vertebrate stem, which is thought of as simple and unjointed like in lampreys. In molecular terms, the evolution of the jaw came to be viewed as the emergence of a patterning programme and inductive tissue interactions acting on the ectomesenchyme of the first pharyngeal arch to give rise to a dorsoventrally articulated jaw architecture, comprised of upper and lower elements, rather than a velum.

The heterotopic shift hypothesis of changing epithelial-mesenchymal interactions in vertebrate jaw evolution is such a theory, based on comparative studies in lamprey, chick and mouse development (Kuratani et al., 2001; Shigetani et al., 2002, 2005; Kuratani, 2005). It diverges from the new head and new mouth hypotheses of the 1980s-90s by abandoning the underlying assumption that the jaw evolved through a series of intermediate stages. Instead, the upper jaw is thought to have replaced, rather than be derived by, pre-existing adult structures. This is explained by a positional (heterotopic) shift that is proposed to have occurred in inductive tissue-interactions in the pre-gnathostome embryo. Kuratani and Shigetani et al. observed that the expression of genes such as *Bmp4*, *Msx1*, *Fgf8*, and *Dlx1* appears shifted posteriorly in the head of gnathostome embryos if compared to lamprey embryos, implying both that different developmental signals are being imparted on different domains of neural crest cells in the two lineages, and that signalling pathways as well as orthologous homeobox genes have been decoupled from their respective derivatives across vertebrates, i.e. lips vs. jaws (Shigetani et al., 2002). As a consequence of this positional shift of epithelial-mesenchymal signalling interactions, gnathostomes may have lost the ancestral upper lip that is still observed in lamprey today, and instead evolved the upper jaw as a morphological novelty, under the influence of the same signalling cascade that ancestrally patterns the upper lip (Shigetani et al., 2002; Kuratani, 2004; Kuratani, 2005; Kuratani, 2012). However, this hypothesis has been challenged by the presence of upper lips in chondrichthyans which correspond to premandibular-derived lamprey upper lips in terms of position,

innervation and vascularization: if jaws evolved through a posterior shift of signalling interactions that once functioned to pattern the premandibular upper lips in lamprey and are now patterning the mandibular-derived upper jaw, it seems difficult to reconcile this with the presence of both structures in the same place in a group of extant gnathostomes (Mallatt, 2008).

The pre-pattern co-option model proposes a different scenario that is based on similar observations (Cerny et al., 2010), but which returns to a continuation between the lamprey oropharyngeal apparatus and the gnathostome mandibular arch. This model frames the evolution of the jaw as the emergence of the joint in a previously un-jointed mandibular arch-derived skeleton. Cerny et al. (2010) observe gnathostome-like nested expression of *Dlx* genes, as well as combinatorial expression of *Msx*, *Hand* and *Gsc* genes along the dorsoventral axis of the lamprey pharyngeal arches, suggesting that gnathostome-like pharyngeal patterning predates the origin of the jaw. However, expression of the joint regulators *Bapx* and *Gdf5/6/7* is lacking from the first arch in lamprey larvae (Cerny et al., 2010). These data are assembled into the pre-pattern co-option model, whereby the jaws evolved by incorporation of *Bapx* and *Gdf5/6/7* into an already existing dorsoventral patterning program, which changed the hypothetical ancestrally unjointed, nonpolar first arch into the jointed, polarised mandibular arch of extant gnathostomes. However, this theory is challenged by the subsequent discovery that *bapx1* and *gdf5* expression is shared across all arches in skate, which decouples this joint specification programme from the jaw and instead indicates that this mechanism was ancestrally likely conserved across all arches in gnathostomes (Hirschberger et al., 2021; discussed in chapter 2). Furthermore, the mandibular arch in *P. marinus* is marked by *Dlx* gene expression that differs from gnathostomes: *DlxA* is expressed in a discontinuous manner, i.e. in distinct dorsal and ventral domains (Cerny et al., 2010). Ontogenetically, the oropharyngeal region in lamprey also does not simply give rise to an unjointed branchial bar, but a complex, multicomponent endoskeleton, and the velum transforms from a flow-generating structure to a valve that separates feeding (i.e. esophageal) and respiratory (i.e. pharyngeal) channels during morphogenesis (Johnels, 1948; Yao et al., 2011; Green & Bronner, 2014). Thus the lamprey mandibular arch lacks a clear polarised expression pattern of *Dlx* orthologues that corresponds to a ventral *Dlx5/6* domain nested in a dorsoventrally more extensive *Dlx1/2* domain as observed in gnathostomes, which

could be adapted into a jaw by the incorporation of *Gdf5/Bapx1* to the intermediate region. Rather, the uniquely lamprey-like domains of discontinuous *DlxA* expression then go on to give rise to endoskeletal elements that cannot be clearly homologised to gnathostome endoskeletal elements in the adult forms, i.e. the velum, which as part of the cusped feeding apparatus of adult lampreys allows for feeding by suctorial pumping (Hardisty, 1979). Taken together, the observation of nested *dlx* and *msx* expression in lampreys is a valuable asset in understanding the evolution of developmental patterning mechanisms in the pharyngeal arches across vertebrates, but the absence of *bapx* and *gdf* from the first arch in lamprey is equally likely to reflect a loss of these genes as the velum evolved as it is to reflect an ancestral absence from the first arch in early vertebrates.

The mandibular confinement hypothesis is also concerned with the apparent patterning similarities of the mandibular arch with the other pharyngeal arches, despite their assumed lack of shared ancestry (Miyashita, 2016). Miyashita postulates that if the latter is true, i.e. the jaw did not emerge out of a gill-arch-like condition, jawless stem gnathostomes should possess mandibular arch derivatives that were patterned in a different manner than the hyoid and gill arch derivatives. The observation that both developing mandibular and gill arches in extant gnathostomes are in fact patterned similarly thus requires an explanation. The mandibular confinement hypothesis suggests the gain of a gill-arch-like patterning programme by the mandibular occurred in tandem with the origin of jaws, owing to a spatial confinement of the mandibular arch mesenchyme by modified premandibular, hyoid, and hypobranchial interfaces. The newly confined mandibular derivatives of stem gnathostomes transformed from the musculoskeletal system that is highly expanded and derived in lamprey (lips, velum and first branchial bars of the branchial basket for feeding and ventilation) to its 'jaws-only' state for feeding (Miyashita, 2016). This shift is thought to have occurred stepwise via four stages that successively restricted the space filled by the mandibular mesenchyme: first, the lamprey-like unconfined mandibular mesenchyme in stem vertebrates gave rise to a broad domain of oropharyngeal structures, reaching anteriorly from the premandibular region to the posterior velum in the hyomandibular extension; then secondly, the anterior premandibular mesenchymal interface with the postoptic stream of trigeminal neural crest cells shifted to a crown-gnathostome-like state and the lamprey-like nasohypophyseal placode was split into two, leading to the loss of the lamprey upper lip and the gain of

gnathostome-like trabecula from the preoptic stream of trigeminal neural crest cells; thirdly, the posterior hyomandibular extension was lost also, leading to a crown-gnathostome-like hyoid interface with a spiracle and the loss of the velum, while the velar joint became the jaw joint precursor; until fourthly and finally, the last, mid-ventral mandibular mesenchyme extension was lost and the crown-gnathostome-like, narrow mandibular arch domain emerged, which was modelled into the jaws as the posterior branchial bars shifted medially, allowing the hypobranchial muscles to extend dorsally along the pharynx to attach to the jaws. During this sequence, the mandibular arch cell populations that would otherwise have differentiated into specialized feeding and ventilation structures as seen in lamprey, including the velum and upper lips, lost these ancestral fates and remodelled into the jaw apparatus. However, this hypothesis and its complex set of changes to pharyngeal development does not align perfectly with the fossil record: the mandibular confinement hypothesis explicitly assumes that a serially patterned pharynx is not the plesiomorphic vertebrate condition, i.e. the mandibular arch derivatives were already patterned distinctly in the vertebrate stem before the split of cyclostomes and gnathostomes (Miyashita, 2016). As discussed in detail below, this may not be the case. Secondly, while the gnathostome jaws and the lamprey velum share an embryonic origin from the mandibular arch mesenchyme, any contributions of the velum, such as its joint, to the jaw remains contentious (Yokoyama et al., 2020).

Finally, the hinge and caps model of jaw development first reframes jaw development as the evolution of a modular unit defined by two appositional components (Depew et al., 2002). In later incarnations, this model then attempts to bridge the developmental gap between the jawless lamprey and the jawed gnathostome condition by including developmental evidence from chondrichthyans (Depew et al., 2002; Depew & Compagnucci, 2007; Fish et al., 2011; Compagnucci et al., 2013). First, the hinge-and-caps model is based on the definition of the jaws as two modular, appositional units separated by a hinge. This architecture already predicts patterning polarity within the developing jaws, as the tissues within the appositional units, i.e. upper and lower jaws, have to acquire a positional identity relating to the hinge as well as to the neurocranium above the jaws. Hence, this approach frames jaw evolution as a question of changes in the polarity and varying mesenchymal competence along the dorsoventral axis. In testing this model, the authors observed that chondrichthyan embryos exhibit relative differences in gene expression locations (heterotopy) and timing

(heterochrony) if compared to amniotes like mice, and they consider this pattern to be the ‘baseline molecular bauplan’ for pharyngeal arch derived-jaws, from which the amniote jaws emerged (Depew et al., 2002; Depew & Compagnucci, 2007; Compagnucci et al., 2013). However, while this model is an excellent strategy to understand how the jaws develop in gnathostomes, and how this development has changes across gnathostomes to give rise to a wide variety of different phenotypes, it does not offer clear answers as to the origin of the jaws beyond the acquisition of the hinge-and-caps polarity by the mandibular arch.

While these models are supported by the trace evidence of cyclostome-like characteristics in stem gnathostomes (galeaspids and osteostracans), there is fossil evidence from the time period predating the split of the lineages leading to cyclostomes and stem gnathostomes (i.e. stem vertebrates) that conflicts somewhat with this view. If a cyclostome-like condition is indeed ancestral, we might expect species predating the split of cyclostomes and gnathostomes to possess these characteristics as well. In assessing whether the ancestral pharyngeal endoskeletal organisation of vertebrates really resembled modern cyclostomes, it is therefore important to test for the presence of these condition in stem vertebrates.

1.2.6 Fossil evidence inconsistent with an ancestrally cyclostome-like condition in stem vertebrates

The best place to start mapping the evolutionary history of the vertebrate pharyngeal organisation are the prehistoric oceans of the early- to mid-Cambrian (540 million years ago). There were no jawed fishes yet, but their early vertebrate ancestors were starting to populate the seas. During the early Cambrian era, stem vertebrates likely resembled modern amphioxus—a cephalochordate with a burrowing, suspension-feeding lifestyle that is driven by a muscular, ciliated, fibrous pharynx (Kardong, 2012). While it is difficult to ascertain whether this lifestyle is ancestral, the pharyngeal support for it is certainly shared by vertebrates recovered from this era. *Haikouella*, *Haikouichthys*, *Mylokunmingia* and *Metaspriggina* are four such fossil species, which all possessed a cartilaginous endoskeleton and a muscular pharynx, probably covered by gills (Holland & Chen, 2001; Mallatt & Chen, 2003; Shu et al., 2003; Morris & Caron, 2014). Although their exact phylogenetic relationships

remain contentious (e.g. whether *Mylokunmingia* and *Haikouichthys* group more closely to gnathostomes, hagfish or lampreys, Janvier, 1999), they are arguably all early vertebrates, and therefore present good starting points from which to map the acquisition of a modern jawed pharyngeal endoskeleton.

Haikouella is comparatively well studied, as more than three hundred specimens have been found to date (Holland & Chen, 2001). Extensive phylogenetic analyses suggest *Haikouella* is a sister lineage to craniates (chordates with skulls, i.e. the lineage comprising all living vertebrates including lampreys, hagfishes, and gnathostomes), and as such, the characteristics found in *Haikouella* may represent conditions found in the last common ancestor of cyclostomes and gnathostomes (Mallatt & Chen, 2003). While its mouth was fringed with buccal tentacles and likely supported by a cartilaginous band internally, the pharynx itself consisted of six bilateral pairs of branchial bars, which were in turn comprised of crossbanding discs and empty gaps, akin to the architecture of the mucocartilage in the gill arches of lamprey larvae (Holland & Chen, 2001). There is no evidence of gill filaments, and it is also not clear whether presumptive gill slits mapped onto the successive spaces between the pharyngeal arches, but each arch (seemingly including the first one) did bear conspicuous shadows on the posterior, which might be indicative of endoskeletal support points for gills (Holland & Chen, 2001; Mallatt & Chen, 2003). While the oral apparatus of *Haikouella* has been compared to the apparatus found in larval lampreys, this species does not appear to have possessed a branchial basket or a structure akin to a velum (Mallatt & Chen, 2003; Kuratani, 2004).

Mylokunmingia and *Haikouichthys* were originally described on the basis of a single, partially preserved fossil each (Shu et al., 1999; Holland & Chen, 2001). The specimen of *Mylokunmingia* possessed six pharyngeal clefts, each one accompanied by a relatively large pharyngeal pouch, which likely housed the gills (Shu et al., 1999). *Haikouichthys* was first described on the basis of a single animal as well, but the additional discovery of around 500 specimens has greatly improved our knowledge of this species (Shu et al., 2003). *Haikouichthys* possessed nine pharyngeal clefts and seven or eight associated branchial bars, which were posteriorly recurved and each apparently consisted of a single unit (Shu et al., 1999). This organisation of the pharyngeal endoskeleton is markedly different from the

cyclostome branchial baskets, and has been interpreted as reminiscent of the gnathostome ceratobranchials and hypobranchials (Shu et al., 2003). *Haikouichthys* also seems to have possessed gill-like lamellae between the branchial cartilages on the ventral side of the head, and these gill-like regions are occasionally partitioned in a way that suggests they were originally housed by pouches (Shu et al., 2003). As mentioned above, both *Mylokunmingia* and *Haikouichthys* have been grouped closer to lampreys than to the gnathostome stem, but these analyses vary (Shu et al., 2003). Other *Mylokunmingia* interpretations group it as a stem vertebrate, and suggest *Mylokunmingia*, with its hemibranch-like gills housed by pharyngeal pouches and rounded pharyngeal bars, may represent the most primitive of the stem-group gnathostomes, i.e. it diverged from the lineage that would eventually lead to gnathostomes after the cyclostomes had already split off (Hou et al., 2002). Wherever they may truly fall on the phylogenetic tree of vertebrates, these fossils show that the cyclostome pharyngeal endoskeleton is likely not an ancestral feature found in stem vertebrates, and that, in fact, we may assume a degree of dorsoventral polarisation to be present in the fishes that predate the split of the cyclostome and gnathostome lineages.

Most informative in this regard has been the recent reappraisal of *Metaspriggina* (Morris, 2008; Morris & Caron, 2014), a stem vertebrate recovered from the Middle-Cambrian (Simonetta & Insom, 1993). *Metaspriggina* possessed seven paired, bi-partite pharyngeal bars, an organisation that bears striking similarities to the epibranchials and ceratobranchials of extant gnathostomes, even more than the endoskeleton of *Haikouichthys* (Morris & Caron, 2014). Interestingly, the anterior-most pharyngeal bar of *Metaspriggina* is slightly thicker than the others, and also lacks an association with the posterior gills, which appear to have been housed by pouches much like in the other fossils described here. Phylogenetic analyses suggest *Metaspriggina* is a stem vertebrate, pre-dating the split of extant cyclostomes from gnathostomes, with close affinity to both *Haikouichthys* and *Mylokunmingia* (Morris & Caron, 2014). This is even more informative than *Mylokunmingia*, since this suggests a dorsoventrally polarised, bi-partite arrangement of the branchial bars may be a plesiomorphic vertebrate condition. Furthermore, it is important to stress that from none of the reconstructions of these early vertebrates a velum was ever recovered.

Thus, there is also fossil evidence consistent with the idea that a degree of dorsoventral polarity inherent to the pharyngeal arches is an ancestral feature of the last common ancestor of all vertebrates. This in turn suggests that the lack of such a polarity apparent in the branchial baskets of cyclostomes is thus likely a derived cyclostome feature. While it is still difficult to reconstruct the exact phylogenetic relationships among these fossil lineages, and the degree to which the preservation of their endoskeletons actually matches their original anatomy is debated, they all point towards a pharyngeal skeletal organization more closely resembling that of extant gnathostomes. In other words, a serially repeated set of bi-partite skeletal elements, could, in fact, be plesiomorphic for vertebrates. Hence, while there is some trace evidence from galeaspids and osteostracans that does not preclude the existence of cyclostome-like characteristics in these groups, such as a lamprey-like velum, it seems striking that these characteristics were likely not present in stem vertebrates predating the last common ancestors of cyclostomes and stem gnathostomes.

1.3 The return to serial homology

The fossils discussed above present a problem for the lamprey-based scenarios of jaw evolution. If the lamprey-like condition is a derived cyclostome feature, and a chondrichthyan-like organization of the pharyngeal endoskeleton represents the plesiomorphic condition of gnathostomes, might the evolutionary models that frame the acquisition of the jaw as a transformation of a lamprey into a modern jawed fish be based on the wrong assumptions? This line of thinking has led to a recent reappraisal of Gegenbaur's classical transformational theory of jaw-gill arch serial homology (Gillis et al., 2013; Siomava et al., 2020). However, while the lamprey-based models have seen extensive testing from developmental perspectives (for example Shigetani et al., 2005; Cerny et al., 2010; Miyashita, 2016), the serial homology theory has experienced comparatively little attention, despite initial positive results (Compagnucci et al., 2013; Gillis et al., 2013). This dissertation aims to rectify this situation: as Carl Gegenbaur recognized the striking similarities between the anatomical organization of the jaws and gills of chondrichthyans, his theory of serial homology of jaw evolution is rendered testable by the availability of cartilaginous and bony fish lineages with plesiomorphic pharyngeal endoskeletal organization for experimental manipulation.

The concept of homology remains the unifying theme of comparative anatomy and evolutionary biology (Wagner, 1989). It is always homology that is invoked whenever two or more biological units are compared and their relationship to each other is investigated, be they genes, cells, tissues, organs, structures, or even behaviors (Wagner, 1989, 2007, 2014; Hall, 2012a, b). However, exactly because it concerns so many different biological circumstances, homology is famously difficult to pin down. Various theoretical approaches frame homology in accordance with the concepts it is thought to underpin. These include sameness and identity (Wagner, 1989, 2007, 2014), synapomorphy and phylogeny (Cacraft, 2005), and morphological features as end-products of evolution and developmental processes, genes and gene networks as evolutionary processes themselves (Hall, 2012a). However, over the last few decades these different approaches have largely been organized by an increasing re-thinking of the hierarchical nature of homology (Wagner & Hall, 1994; Dickinson, 1995; Hall & Kerney, 2012; Rutishauser & Moline, 2005; Hall, 2012b). This

theoretical framework positions homology at several levels, which may not be interlinked, and at different processes in evolution (Abouheif, 1997; Sommer, 2008). Thus, homology may affect genes, their regulation, embryonic origins, and morphology—though homologous genes may not give rise to homologous structures across different species and homologous structures may not arise from homologous developmental processes.

The framework of homology as hierarchical in nature also transformed the understanding of serial homology. Serial homology was originally defined as “representative or repetitive relation in the segments of the same organism” (Owen, 1846), but through advances in developmental biology, concepts of serial homology now largely also include the repeated deployment of conserved developmental mechanisms (e.g. Van Valen, 1982; Roth, 1984; Wagner, 1989, 2007, 2014). In the original view, homology reflects continuity of descent: characters share ‘sameness’ when they share ancestry and when they can be connected through intermediate forms. In modern biology, and particularly through the lens of development, this shared ancestry can be unravelled on a molecular, genetic level: characters may be (serially) homologous on one level if they originate through the (iterative) deployment of shared or conserved developmental mechanisms.

If the parallel anatomical organisation of the gnathostome jaw and gill arch skeleton, noted by Gegenbaur, is indeed a product of serial homology, this leads to a testable prediction: if the jaw originated as the anterior-most element of an ancestral bi-partite branchial series, we would expect these elements to be delineated by shared developmental patterning mechanisms. Conversely, their anatomical divergence should be attributable to arch-specific variations on a core, conserved developmental programme. Hence, comparisons of the developmental and anatomical conditions observed in chondrichthyans with their sister group, the bony fishes, allow us to infer anatomical and developmental conditions in the last common ancestor of gnathostomes, and thus the origin of the jaw. In other words, the anatomical ‘sameness’ of the jaw and gill arch skeletal elements apparent at the level of morphology, can be tested for by the comparative search for common molecular mechanisms underpinning this ‘sameness’.

The second and third chapters of this dissertation test this exact prediction, i.e. serial homology on the basis of shared patterning mechanisms during development. Using candidate and RNA-seq/differential gene expression analysis and mRNA *in situ* hybridisation, I find broad conservation of dorsoventral patterning mechanisms within the pharyngeal arches as well as unique transcriptional features that may underpin distinct jaw and gill arch morphologies. The latter include unique gene expression features of jaw and gill arch muscle progenitors and of developing gill lamellae. In the fourth chapter of this dissertation, I test for serial homology on the basis of anatomy and return to the question of whether the mandibular arch ancestrally possessed a gill arch-like nature. Within the hierarchical framework of homology outlined above, this is a test for the ‘sameness’ of the mandibular and gill arches predicted by serial homology on an anatomical level: if the jaw arose out of a gill arch-like condition, we might expect anatomical vestiges of this condition to be found in some forms. In this chapter, using lineage tracing experiments, functional tests of cell signalling, and gene expression experiments, I detail the development of the internal anatomy of the spiracles (comprising the pseudobranch and spiracular cartilage) in skate and demonstrate the presence of a vestigial gill-slit on the back of the jaw.

The embryological model system that has been used for this project is the little skate, *Leucoraja erinacea*. The skate is emerging as a powerful developmental model system, with an increasing repertoire of experimental methods (Gillis et al., 2009b, 2012, 2016) and protocols for *in situ* gene expression analysis (Gillis et al. 2013, 2020). The skate pharyngeal arches are also relatively large and clearly segregated, which allows for the clear observation of gene expression features that are obscured or more difficult to image in more conventional bony fish model systems. Consequently, targeted studies that address specific comparative questions on pharyngeal arch patterning and development can easily be carried out in skate (Gillis et al., 2013, 2016b). In combination with its phylogenetic position as a representative of the sister group to bony fishes, this makes the skate the ideal model system to test Carl Gegenbaur’s classical jaw-gill arch serial homology theory from a developmental perspective.

1.4 Summary

Research on the evolution of the jaw has a long and rich history. The earliest scenarios of jaw origins emerged from philosophical considerations on the segmentation of the vertebrate head. In 1878, Carl Gegenbaur noticed the striking similarity of chondrichthyan jaws and gill arches and put forward the jaw-gill arch serial homology hypothesis, which frames the acquisition of the jaw as the transformation of the anterior-most element of an ancestral branchial series of gill arches into the jaw. In the 1980s, large advances in vertebrate phylogenetics and developmental biology led to new head and new mouth models, which shifted the attention onto larval lampreys as models of jawless vertebrate ancestry. In combination with palaeontological evidence that supported this view, stem gnathostomes were assumed to have arisen from a larval lamprey-like condition. Increasing knowledge on the molecular mechanisms of craniofacial development across vertebrates refined these hypotheses and led to the modern evo-devo era of jaw evolution models, during which scenarios such as the heterotopy hypothesis, the pre-pattern co-option model, the mandibular confinement hypothesis, and the hinge-and-caps model were put forward. However, re-interpretation of the fossil record questions whether stem gnathostomes really emerged from a lamprey-like condition. In the light of these recent findings, the classical jaw-gill arch hypothesis has received new attention. This dissertation aims to test the jaw-gill arch serial homology hypothesis on two levels of biological organisation: first, as recent advances in developmental biology have framed concepts of serial homology increasingly as the re-deployment of shared developmental mechanisms, I test for conserved patterning mechanisms across the pharyngeal arches. Secondly, I test for serial homology on the level of anatomy by demonstrating the existence of vestigial anatomical evidence of the gill-arch-like past of the jaws. To this end, I use the little skate (*Leucoraja erinacea*) as a model system, as cartilaginous fishes like the skate have retained an ancestral organisation of the craniofacial and pharyngeal endoskeleton. Each of these chapters presents evidence that is consistent with Gegenbaur's classical hypothesis of jaw-gill arch serial homology, first on the basis of development and secondly on the basis of anatomy. Together, I hope they serve to close significant gaps in the puzzle of gnathostome origins and shed new light on the shared ancestry of jaws and gill arches in vertebrates.

Chapter 2:

Gnathostome jaw patterning mechanisms are conserved in the gill arches of the skate

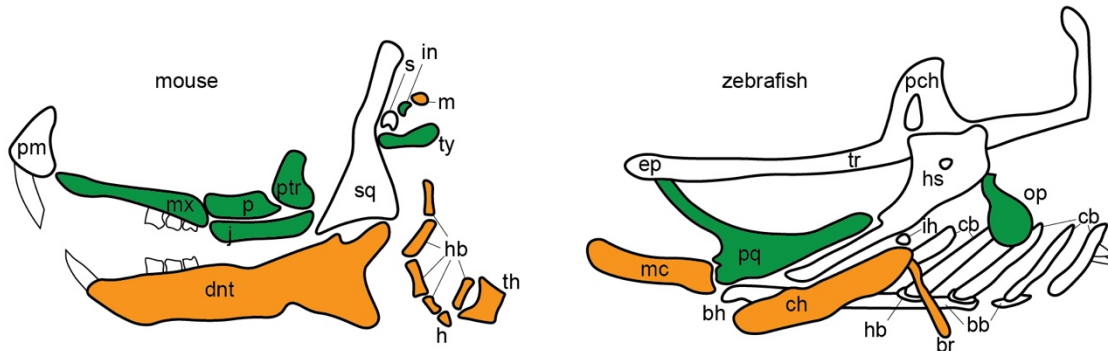
2.1 Abstract

The origin of the jaw is a long-standing problem in vertebrate evolution. Over a century ago, the anatomist Carl Gegenbaur proposed that the upper and lower jaw arose through modifications of the dorsal and ventral elements of the anterior-most gill arch, based on the strikingly similar anatomical organization of the jaws and gill arches of chondrichthyans (cartilaginous fishes – sharks, skates and rays), though this theory has largely been abandoned since. Here, I used candidate gene expression analyses to revisit this classical hypothesis of serial homology from a developmental perspective in a cartilaginous fish, the little skate (*Leucoraja erinacea*). If the jaw and gill arches are derived members of a primitive branchial series, I predict that they would share common developmental patterning mechanisms. I find that dorsoventral patterning mechanisms that are central to patterning the jaw of bony fishes are largely conserved across the developing mandibular, hyoid and gill arches in skate. Shared features include expression of genes encoding members of the ventralising BMP and endothelin signalling pathways, the joint markers *bapx1*, *gdf5*, discontinuous markers *barx1* and *gsc*, and the dorsal marker *pou3f3*. Additionally, I find shared expression of the endothelin receptors A and B in cranial neural crest cells, akin to previously described expression in lamprey but distinct from the condition in other gnathostomes, in which *ednra* marks cranial and *ednrb* marks trunk neural crest cells. My findings also point towards mesenchymal expression of *eya1/six1* as an ancestral feature of the dorsal mandibular arch of jawed vertebrates, while differences in notch signalling distinguish the mandibular and gill arches in skate. Taken together, these findings are consistent with serial homology of mandibular, hyoid and gill arch skeletal derivatives, but also highlight some molecular differences that may underpin the anatomical divergences of jaws and gill arches.

2.2 Introduction

Jaws are an iconic example of anatomical innovation, and a uniting feature of the jawed vertebrate (gnathostome) crown group (Gans & Northcutt 1983; Mallatt, 1996; Northcutt, 2005). The development of this feature is particularly well studied in bony fishes, though the anatomy of the oropharyngeal region varies widely across gnathostomes. While anatomically highly distinct, the bony and cartilaginous components of the jaws of bony fishes such as mouse and zebrafish (Fig. 2.1A) share a developmental origin from migrating cranial neural crest cells, which delaminate from the neural tube and undergo a set of complex epithelial-mesenchymal interactions (Santagati & Rijli, 2003; Brito et al., 2006). The frontonasal skeleton is formed from neural crest cells that emerge from the posterior diencephalon and anterior mesencephalon, while the mandibular (first) pharyngeal arch is populated by neural crest cells from the posterior mesencephalon and from rhombomeres 1 and 2 (Kontges & Lumsden, 1996; Santagati & Rijli, 2003). Along their path, a network of signalling interactions and transcription factors provide the spatial patterning information necessary for the correct formation of the dorsal and ventral segments of the jaw in bony vertebrates (Fig 2.1B). The complexity of this process and the delicate balance of cell signals and regulatory mechanisms required for coordinating cell growth, migration, differentiation, and apoptosis, is reflected by how often these steps are not finished completely: for example, cleft lips are some of the most common differential outcomes observed in human development (Leslie & Marazita, 2013). At the heart of the dorsoventral patterning process of the jaw in bony fishes sits the ‘*Dlx* code’, i.e. nested mesenchymal expression of genes encoding the *Dlx* family of transcription factors, which delineates upper (*Dlx1-2*), intermediate (*Dlx1,2,5,6*), or lower (*Dlx1-6*) mandibular arch derivatives (Depew et al., 2002). Upstream of the *Dlx* code, complex interactions of several signalling pathways, including endothelin-1, bone morphogenetic protein (*bmp*), and Jagged-Notch play a role in inducing correct *Dlx* expression. In turn, downstream of the *Dlx* code, other transcription factors mark dorsoventral identities of the developing jaw elements.

A



B

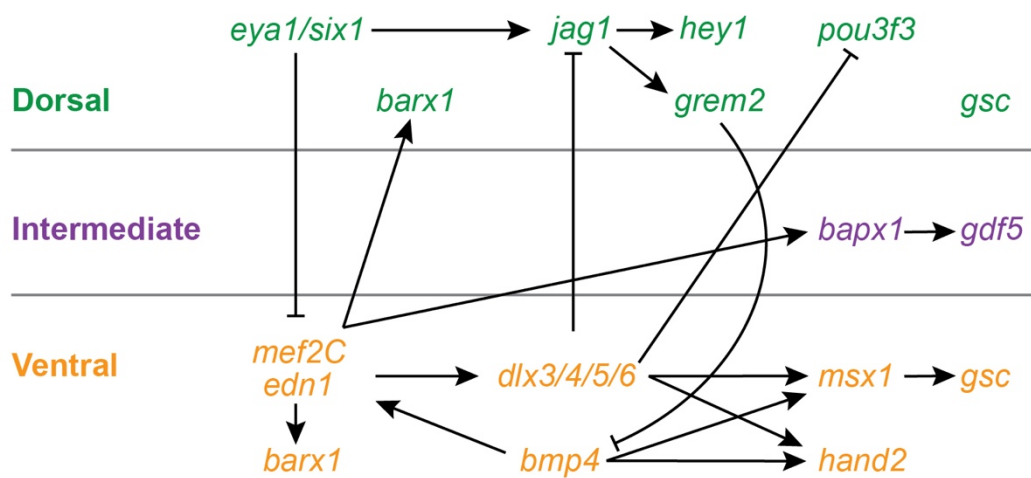


Figure 2.1: Jaw development in mouse and zebrafish. (A) Mouse (E18.5) and larval zebrafish (5dpf) pharyngeal anatomy, adapted from Clouthier et al., 2010. Bony or cartilaginous skeletal components in green or orange show defects if corresponding dorsal (green) or ventral (orange) patterning mechanisms outlined in (B) are genetically perturbed or suppressed. Shared colouration in green or orange across mouse and zebrafish skeletal elements does not imply homology. Rather, these elements comprise specialised mammalian or teleost jaw morphologies, which are nonetheless patterned by the same genes. (B) Patterning programme establishing dorsoventral identity in the jaw of bony fishes as established in mouse and zebrafish, adapted from Medeiros & Crump, 2012. bb, basibranchial; bh, basihyal; br, branchiostegal ray; cb, ceratobranchial; ch, ceratohyal; dnt, dentary; hb, hypobranchial; hs, hyosymplectic; ih, interhyal; in, incus; j, jugal; m, malleus; mc, Meckel's; mx, maxilla; op, opercle; p, palatine; pch, prechordal; pm, premaxilla; pq, palatoquadrate; ptr, pterygoid; s, stapes; sq, squamosal; th, thyroid; tr, trabecula; ty, tympanic ring.

2.2.1 Ventral patterning

Endothelin-1 (*edn1*) signalling is a particularly well-known pathway involved in dorsoventral patterning of the pharyngeal skeleton, specifically in establishing the identity of the lower jaw (Clouthier et al., 1998; Thomas et al., 1998; Clouthier and Schilling, 2004; Clouthier et al., 2000; Kimmel et al., 2003; Miller et al., 2000; Miller and Kimmel, 2001; Miller et al., 2003; Walker et al., 2006; Nair et al., 2007; Sato et al., 2008; Vieux-Rochas et al., 2010). In total, vertebrates possess three known Endothelin peptides, which all share an initial synthesis as a larger pre-pro-peptide, followed by modifications via furin proteases and endothelin converting enzymes (ECEs) to form mature ligands (Xu et al., 1994; Yanagisawa et al., 1998). Endothelin-1 signalling occurs through two G protein-coupled receptors, *Ednra* and *Ednrb*, both of which have been shown to cell-autonomously regulate neural crest development (Arai et al., 1990; Sakurai et al., 1990; Clouthier et al., 2003). *Edn1* is expressed by cells in the ventral pharyngeal arches, including ectoderm, core paraxial mesoderm and pharyngeal arch endoderm (Clouthier et al., 1998, Maemura et al., 1996), while its receptor in cranial neural crest cells in bony fishes, *Ednra*, is expressed in the mesenchyme across the pharyngeal arches (Clouthier et al., 1998, Yanagisawa et al., 1998). In the ventral arches, *Mef2C* functions with *Ednra* to induce expression of *Dlx5* and *Dlx6* (Miller et al., 2007; Verzi et al., 2007; Hu et al., 2015).

Studies in mice and zebrafish have demonstrated that genetic perturbations and targeted deletions of *Edn1* and *Ednra* result in severe bone malformations in the lower jaw, including homeotic transformations of lower jaw elements into upper jaw elements (Clouthier et al., 1998; Kurihara et al., 1994; Yanagisawa et al., 1998; Miller et al., 2000; Walker et al., 2006). In zebrafish, the first characterised *edn1* mutant was termed *sucker* due to characteristic malformations in Meckel's cartilage that produce a downturned mouth (Miller et al., 2000). The loss of *edn1* function affects ventral cartilages and bones of both the mandibular and hyoid arches, resulting in loss of the ceratohyal, the joints separating dentary (mandibular) and maxillary bones as well as cartilages, and a transformation of the rudimentary dentary bone into an element sharing similarities with the maxilla, suggesting a homeotic transformation of lower jaw elements into upper jaw elements. Posterior to the mandibular arch, similar defects occur, with the branchiostegal rays either missing or misshapen, and the

dorsal opercle bone assuming an enlarged form, again reminiscent of a homeotic transformation of the lower element into the upper element (Miller et al., 2000; Kimmel et al., 2003; Nair et al., 2007). In mice, deletion of *Edn1* also causes ventral defects and homeotic transformation of mandibular arch-derived structures into more maxillary-like structures, such as the formation of ectopic dorsal bones in the lower jaw and ectopic whisker barrels in the surface ectoderm covering the mandible (Ozeki et al., 2004; Ruest et al., 2004; Vieux-Rochas et al., 2010; Tavares et al., 2012). Endothelin-1 functions upstream of other signalling pathways and transcription factors, which together pattern the entire dorsoventral axis of the jaw in bony fishes, and consequently, lack of *Edn1* expression also leads to a loss of other genes with known expression domains in lower jaw primordia, such as the transcription factors *Dlx5/6*, *Hand2*, *Msx1*, and *Gsc* (Charite et al., 2001; Fukuhara et al., 2004; Miller et al., 2000).

In addition to patterning the skeletal elements of the jaw, *Edn1* may also play a role in patterning the jaw muscles. A classical model of cranial muscle development suggests that the mesodermal cores within each pharyngeal arch subdivide into distinct dorsal and ventral domains before assuming their individual arch-specific muscle identity (Edgeworth, 1935; Miyake et al., 1992; Kimmel et al., 2001; Ziermann & Diogo, 2018). The mesodermal expression of *edn1* in the ventral zebrafish mandibular and hyoid arches has been suggested to play a role in this model by patterning the premyogenic condensations of the intermandibularis and constrictor hyoideus ventralis muscles, respectively (Miller et al., 2000).

Another important signalling pathway involved in establishing ventral identity in the jaw across bony fishes is BMP signalling. Bmp ligands are expressed across facial primordia, where disturbances of this pathway via bead-implantation experiments result in lip and palate fusion in chick (Ashique et al., 2002; Barlow and Francis-West, 1997; Francis-West et al., 1994; Mina et al., 2002; Parsons & Albertson, 2009). *Bmp4* is also involved in the beak morphology variation observable in Darwin finches, a textbook example of species diversification by natural selection (Abzhanov et al., 2004). In this group of birds, *Bmp4* expression in the mesenchyme of the upper beak primordia is associated with deep and broad beak morphology, and misexpression of *Bmp4* in the upper jaw primordia of chick embryos akin to

the levels observed in broad-beaked Darwin finches leads to transformations in chick that strongly resemble the broad-beaked Darwin finch morphologies (Abzhanov et al., 2004). In mice, *Bmp4* controls transcriptional regulators that guide self-renewal, osteoblast differentiation and negative Bmp autoregulation in the developing jaw (Bonilla-Claudio et al., 2012). It is expressed in the oral epithelium of the lower mandible, where it induces the expression of lower jaw markers in the subjacent mesenchyme, such as *Msx1* and *Msx2*, and inhibits expression of intermediately expressed joint genes, such as *Barx1* (Tucker et al., 1998; Barlow et al., 1999), and *Nkx3.2/Bapx1* in chick (Wilson & Tucker, 2004). Loss of *Bmp4* in cultured mouse mandibles leads to a homeotic transformation of incisors to molars (Tucker et al., 1998), while ectopic *Bmp4* signal in the presumptive joint mesenchyme in chick depletes *Nkx3.2* expression and deletes the jaw joint, resulting in fusions of the quadrate and articular (Wilson & Tucker, 2004). Conversely, in zebrafish BMP signalling is required for the ventral expression of *edn1*, *hand2*, *dlx6a*, *msx1* and *nkx3.2* in the mandibular and hyoid arches and the correct formation of ventral and intermediate skeletal elements (Alexander et al., 2011). The ventral patterning function of *bmp4* is restricted by intermediate expression of *grem2*, which encodes a secreted Bmp antagonist (Zuniga et al., 2011). Ectopic BMP in the upper jaw primordia causes the expression of the ventral genes to expand dorsally, and results in malformations or transformations of dorsal skeletal elements into ventral ones, such as duplications of Meckel's cartilage in the position of the pterygoid process (anterior palatoquadrate - Alexander et al., 2011).

Taken together, *endothelin-1* and *bmp4* are key regulators of lower jaw identity across bony fishes. They promote ventral mesenchymal expression of *hand2*, *msx1*, *dlx5/6*, amongst other lower jaw markers, and confer lower jaw identity (Thomas et al., 1998; Yanagisawa et al., 2003; Funato et al., 2016; Alexander et al., 2011; Zuniga et al., 2011). They also instruct the *Dlx* code, i.e. nested expression of combinatorial *dlx* genes, which sit at the heart of the dorsoventral patterning network in the developing jaw in bony fishes (Qiu et al., 1997; Beverdam et al., 2002; Depew et al., 2002; Talbot et al., 2010).

Some of these ventralising genes are also expressed in the ventral pharyngeal arches of the jawless lamprey, suggesting they have a patterning role beyond the jaw. The core components of endothelin signalling are a vertebrate synapomorphy (Martinez-Morales et

al., 2007; Braasch & Schartl, 2014), and as such, the study of endothelin signalling has revealed interesting insights into vertebrate evolution as a whole. In the sea lamprey, *Petromyzon marinus*, *edn1* is expressed in the ectoderm surrounding the mouth and the pharyngeal arches as well as the mesodermal cores of each arch, while *ednra* and *ednrb* are expressed in late migratory and post-migratory skeletogenic neural crest cells in the head, which will give rise to the upper and lower lips and mucocartilage of the lamprey branchial basket (Square et al., 2016). This points to an early split in the functions of endothelin receptors A and B after the divergence of cyclostomes and gnathostomes: while in lamprey *ednra* and *ednrb* expression and function is shared by cranial neural crest cells, in gnathostomes *ednra* is restricted to the cranial neural crest and *ednrb* is restricted to the trunk neural crest cells (Square et al., 2016, 2020). A previous study in a different lamprey, the Japanese river lamprey, *Lethenteron japonicum*, also found *edn1* in the ectoderm around the mouth, in addition to the pharyngeal arch ectomesenchyme, while *ednra* was expressed in the same domains as in *P. marinus* (Kuraku et al., 2010; Square et al., 2016). The varying descriptions of the expression patterns of these genes in different lamprey species may reflect species-level differences, or differences in the observed stages, as Square et al. (2016) described lamprey larvae from mid-neurulation until the initial differentiation of the head skeleton, while Kurako et al. (2010) studied the mid-pharyngula stage.

Lampreys also express homologs of *dlx*, *hand* and *msx* genes (Kurako et al., 2010; Cerny et al., 2010). However, even more than differences in edn ligands, descriptions of observed *dlx* patterns have varied, with some authors describing uniform levels of *dlx* expression across the entire dorsoventral axis of the pharyngeal arches (Myojin et al., 2001; Neidert et al., 2001; Kuraku et al., 2010) and others describing nested expression akin to gnathostome-like expression patterns of the *Dlx* code (Cerny et al., 2010). These differences may also be a reflection of different stages being observed as well as difficulties in resolving orthology of lamprey and gnathostome *dlx* genes. The lamprey orthologs of *hand* and *msx*, however, are expressed in the ventral pharyngeal arches in all studies that examined them (Kurako et al., 2010; Cerny et al., 2010). Taken together, these data suggest the ventralising functions of endothelin, *hand* and *msx* as well as the dorsoventral patterning roles of the *Dlx* code predates the emergence of the jaw, consistent with a conserved role in ventralising the pharynx across vertebrates, rather than patterning the jaw specifically.

2.2.2 Dorsal patterning

The establishment of upper jaw identity is less well-studied than the lower jaw signalling pathways. This has led to an initial hypothesis that the upper jaw represents a default state of mandibular arch development, while the lower jaw requires specific signals. However, this view has changed over time, as specific regulators of upper jaw identity have been reported. One of the first markers of dorsal territory in the mandibular arch identified in mice was *Pou3f3*, which was discovered by systematically screening for downstream effectors of the *Dlx* code and which is expressed in the mesenchymal maxillary primordia (Jeong et al., 2008).

Subsequent studies in zebrafish and mice have established additional drivers of dorsal identity across the mandibular and hyoid arch. Much like the ventralising pathways described above, these signalling pathways and transcription factors conferring dorsal identity also function to restrict joint genes and ventral genes. In mouse, *Eya1* and *Six1* function in middle ear and craniofacial development (Xu et al., 1999; Laclef et al., 2003; Ozaki et al., 2004). They are co-expressed in the upper jaw primordium of the mandibular arch, where they inhibit expression of *Edn1* and induce expression of the dorsalising notch signalling component *Jag1* (Tavares et al., 2017). However, while loss of *Edn1* or its cranial neural crest cell receptor *Ednra* results in a homeotic transformation of the lower jaw into an upper jaw like structure, loss of Jagged-Notch signalling in mice does not cause significant changes in maxillary development (Tavares et al., 2017). Instead, *Six1* is required to restrict *Edn1* to the ventral mandibular arch endoderm, and *Six1*^{-/-} mice do show a partial homeotic transformation of the upper jaw into a lower jaw like structure (Tavares et al., 2017).

In contrast, in zebrafish Notch signalling components *jag1b* and *hey1* are expressed in the dorsal mesenchyme of the mandibular and hyoid arches and in the pouch endoderm, while *notch2* is expressed more widely throughout the pharyngeal arches (Zuniga et al., 2010). *notch2* morpholino and human jagged1 (*JAG1*) misexpression experiments have shown that in the absence of *notch2* expression, dorsal skeletal elements like the hyomandibular cartilage or the opercle bone assume ventral-like morphologies, while *JAG1* over-expression in zebrafish transforms the ventral Meckel's cartilage and ceratohyal cartilage into structures resembling the dorsal palatoquadrate and hyomandibular cartilages (Zuniga et al., 2010).

Notch signalling confers this upper jaw skeletal identity through *jag1b* and *hey1* and represses the transcription of *edn1* as well as other intermediate and ventral patterning genes, including *dlx3b/5a/6a*, *msxe*, *nkx3.2* and *barx1* (Zuniga et al., 2010; Barske et al., 2016). The discrepancies in the involvement of notch signalling in craniofacial development in mouse and zebrafish may be a consequence of the different fates of the mandibular and hyoid arch mesenchyme in the two lineages: whereas in zebrafish the jaw and hyoid bones and cartilages are derivatives of the cranial neural crest cells populating the mandibular and hyoid arch in the embryo, in mouse the jaw bones receive contributions from frontonasal neural crest cells and the ventral mandibular arch, while the dorsal mandibular and hyoid arch give rise to the ossicles of the middle ear. Therefore, it might be expected that pathways and transcription factors active in the dorsal mandibular and hyoid arches patterning the upper jaw in zebrafish to be involved in inner and middle ear development in mammals.

In contrast to the ventralising signal pathways and transcription factors discussed above, these dorsalising signalling cascades and transcription factors are not well studied in jawless fishes. This makes it difficult to resolve dorsal mandibular arch patterning mechanisms to the vertebrate stem and to understand whether these patterning activities are jaw-specific, or whether they were ancestrally more widely shared in the vertebrate pharyngeal arches prior to the emergence of the jaw, in parallel to how *edn-1* possesses a ventral patterning role in the lamprey pharyngeal arches.

2.2.3 Intermediate patterning

Finally, in bony fishes, the jaw joint is specified at the interface of these upper and lower jaw gene expression domains. The expression of the transcription factor *nkx3.2/bapx1* (Newman et al., 1997; Miller et al., 2003; Lukas & Olsson, 2018) and the secreted signalling molecule *gdf5* (Miller et al., 2003) mark the presumptive joint domain. In amphibians and zebrafish, morpholino experiments and genetic perturbations have shown that in the absence of *nkx3.2*, Meckel's cartilage and the palatoquadrate fuse, and this joint-less morphology may share similarities with the ancestral, jawless organisation of the pharyngeal endoskeleton in stem vertebrates before the origin of the jaw (Lukas & Olsson, 2018; Miyashita et al., 2020).

Zebrafish experiments have shown that *nkx3.2* is controlled by *edn1*, and similarly to amphibians, functional *nkx3.2* expression is required to form the jaw joint (Miller et al., 2003). Conversely, in mice, *Nkx3.2* expression marks an intermediate region in the mandibular arch, an ancestral joint region that has been modified in mammals to form middle ear ossicles, i.e. malleus and incus (Tribioli et al., 1997). In contrast to zebrafish, inactivation of *Nkx3.2* in mice does not affect the formation of a proper joint between malleus and incus (Tucker et al., 2004). This suggests that the transformation of the proximal jaw bones modifying the jaw articulation (the primary jaw joint) into the mammalian middle ear ossicles did not involve a loss of *Nkx3.2* expression in this region, but rather the loss of *Nkx3.2* regulation of *Gdf5* and *Gdf6*, which are both crucial joint regulators (Tucker et al., 2004).

In bony fishes, the presumptive joint domain is further flanked by expression of the transcription factors *barx1* and *gsc* (Miller et al., 2003; Nichols et al., 2013; Wilson & Tucker, 2004; Newman et al., 1997; Lukas & Olsson, 2018; Tucker et al., 2004; Trumpp et al., 1999). In mouse and zebrafish, *barx1* is expressed in the mesenchyme and is excluded from the joint-forming intermediate arch domains (Sperber & Dawid, 2008; Tissier-Seta et al., 1995). Genetic perturbations in zebrafish have shown that a loss of *barx1* expression results in ectopic joint formation, such as prominent gaps dividing Meckel's cartilage, the ceratohyal cartilage and the ceratobranchial cartilages (Nichols et al., 2013). Also in zebrafish, the transcription factor *gsc* is expressed in dorsal and ventral domains of the mandibular and hyoid arch (Miller et al., 2000; Miller et al., 2003). This expression is lost in *edn1* mutants and to a lesser extent in *hand2* mutants, which may explain the loss of the jaw joint in these fish (Miller et al., 2003).

It has been suggested that the gnathostome mandibular arch is distinguished from the posterior arches by the discontinuous expression of dorsal and ventral *gsc* and *barx* and intermediate expression of *nkx3.2* and *gdf5* in the presumptive jaw joint domain (Cerny et al., 2010). In the jawless lamprey *P. marinus*, gnathostome-like expression of *Barx*, *Bapx*, or *Gdf5/6/7* is lacking from the first arch (Cerny et al., 2010). Instead, continuous expression of *Barx* marks the ventral and intermediate domains of the first arch, while *Gdf5/6/7* and *Bapx* are completely absent from any pharyngeal arches in lamprey in this study (Cerny et al., 2010). These data have been assembled into the pre-pattern co-option model of jaw evolution, which frames the emergence of the jaw as the acquisition of these joint formation

genes into the mandibular arch, on top of an anterior-most arch already dorsoventrally prepatterned by *Dlx*, *Msx*, and *Hand* genes (Cerny et al., 2010). However, in the absence of clear palaeontological evidence demonstrating that the lamprey joint-less condition of the pharyngeal arches represents the stem vertebrate condition, it remains difficult to ascertain whether the absence of joint patterning genes in the mandibular arch is also the ancestral vertebrate condition.

2.2.4 Jaw patterning and serial homology

Over a century ago, the anatomist Karl Gegenbaur proposed a scenario of serial homology, whereby the upper and lower jaw arose through modifications of the dorsal and ventral elements of an anterior gill arch (Gegenbaur, 1878). Elements of Gegenbaur's hypothesis are testable from a developmental perspective. Over the past several decades, concepts of serial homology have evolved to centre largely around the iterative deployment or sharing of conserved developmental mechanisms (e.g. Van Valen, 1982; Roth, 1984; Wagner, 1989, 2007, 2014). If the parallel anatomical organisation of the gnathostome jaw and gill arch skeleton is a product of serial homology, these elements may be delineated by shared patterning mechanisms – and, conversely, their anatomical divergence may be attributable to arch-specific variations on a core, conserved developmental programme.

The little skate (*Leucoraja erinacea*) is uniquely suited to test for the presence or absence of such a shared patterning programme. As a cartilaginous fish, they are a member of the sister lineage to the bony vertebrates. By testing for features conserved between skate and other bony fish model systems, such as mouse, zebrafish, and chick, ancestral conditions for jawed vertebrates as a whole may be inferred. In comparison to these bony fish models, the pharyngeal arches in skate are also more readily observable on an anatomical level due to their size and clear dorsoventral segregation, which makes the skate an ideal system to answer targeted questions on pharyngeal arch patterning and development (Gillis et al., 2013, 2016b). For example, nested mesenchymal expression of *dlx* genes, that is, the *Dlx* code that specifies upper and lower jaw identity in bony fishes, has previously been shown to be conserved across all pharyngeal arches in skate, thereby suggesting it is a primitive feature of

the mandibular, hyoid and gill arches of jawed vertebrates (Gillis et al., 2013). Furthermore, the principal dorsal and ventral endoskeletal elements that emerge from the mesenchyme of all arches in skate derive from equivalent domains of this combinatorial *Dlx* gene expression, i.e. dorsal *dlx1/2* expressing arch mesenchyme gives rise to the palatoquadrate within the mandibular arch, the hyomandibula and pseudoepihyal within the hyoid arch, and the epibranchial within the first gill arch, while ventral *dlx1-6* expressing arch mesenchyme gives rise to Meckel's cartilage within the mandibular arch, the pseudoceratohyal within the hyoid arch, and the ceratobranchial within the first gill arch (Gillis et al., 2013). This developmental evidence from skate underpins how conserved axial patterning mechanisms give rise to putatively serially homologous skeletal elements. These data also point towards a common blueprint that primitively patterns the dorsoventral axis of all pharyngeal arches in jawed vertebrates. However, to what extent the signalling upstream and downstream of the *Dlx* code is conserved across all arches has not been determined yet, and this is what this chapter aims to test.

2.3 Methods

2.3.1 Embryo collection

L. erinacea embryos for mRNA in situ hybridisation were collected at the Marine Biological Laboratory (Woods Hole, MA, USA). Embryos were fixed in 4% paraformaldehyde overnight at 4°C, rinsed in phosphate-buffered saline (PBS), dehydrated stepwise into 100% methanol and stored in methanol at –20°C. Skate embryos were staged according to Ballard et al. (1993) and Maxwell et al. (2008).

2.3.2 cDNA synthesis, gene cloning and mRNA in situ hybridisation probe synthesis

Skate cDNA was generated using RNA extracted from S19-32 embryos. Total RNA was extracted from tissue samples on ice using 1mL Tri-Reagent (Sigma-Aldrich, UK) per 50-100mg of tissue in a manual glass homogenizer. After homogenisation, the sample was centrifuged at 12000g for 10 minutes at 4°C. The supernatant was isolated and left to rest for 5 minutes at room temperature. 200µL of chloroform was added per mL of Tri-Reagent used during homogenisation, before centrifugation at 13,000 rpm for 15 minutes at 4°C. The top aqueous layer was then isolated and mixed with 500µL of isopropanol per mL of Tri-Reagent used during homogenisation. Samples were allowed to rest for another 5 minutes at room temperature, followed by centrifugation at 13,000 rpm for 10 minutes at 4°C. The precipitated RNA pellet was washed with 1mL of 75% EtOH per 1mL of Tri-Reagent used during homogenisation. Samples were vortexed and centrifuged at 7500g for 5 minutes at 4°C. The RNA pellet was air-dried for 5-10 minutes and resuspended in RNase-free water.

cDNA synthesis was performed using the SuperScript III First-Strand Synthesis System (Invitrogen) according to manufacturer's instructions. Up to 5µg of previously isolated skate RNA was mixed with 1µl of 2µM oligo(dT) primer, 1µl of 10mM dNTP mix, and up to 10µl RNase-free water. The mixture was incubated at 65°C for 5 minutes and placed on ice for 1 minute. Then, 2µL of 10X RT buffer, 4µL 25mM MgCl₂, 2µL 0.1 M DTT, 1µL RNase-out, and 1µL Superscript RT were combined, and 10 µL of this mixture was added to the RNA mixture.

After gentle mixing and brief centrifugation, the samples were incubated at 50°C for 50 minutes, followed by termination of the reaction at 85°C for 5 minutes and placed on ice. 1µL RNase H was added to the sample and incubated for another 20 minutes at 37°C. cDNA was stored at -20°C.

Cloned fragments of skate cDNAs were PCR amplified from this embryonic cDNA template using REDTaq ReadyMix (Sigma). For 25µl polymerase chain reaction mixes, 18.25µl water, 2.5µl 10X RedTaq buffer, 0.5µl 10 mM dNTP mix, 0.63µl each of forward and reverse primers, 1.25µl cDNA template, and 1.25µl RedTaq were combined on ice. The PCR protocol consisted of 35 cycles of 30 seconds at 94°C, 30 seconds at 58°C and 1 minute at 72°C, followed by 1 cycle of 10 minutes at 72°C. PCR products were isolated and purified using the MinElute Gel Extraction Kit (Qiagen) and ligated into the pGemT-easy Vector System (Promega). Resulting plasmids were transformed into JM109 E. coli (Promega), and plasmid minipreps were prepared using an alkaline miniprep protocol: after growing cells to saturation, they were spun at 8000 rpm for 1 minute. Supernatant was removed and cells were resuspended in 150µL of 50mM glucose (0.9%), 25mM Tris, pH 8.0, 10mM EDTA buffer. 200 µl 0.2N NaOH, 1% SDS solution was added, and samples were mixed by inverting 6 – 8 times, followed by incubation for 5 minutes at room temperature. 150µl of acetate solution (50mL 5M potassium acetate, 25mL 17.5M glacial acetic acid, 11mL H₂O) was added, followed by mixing by inverting 6 – 8 times, and incubated for 5 minutes at room temperature. Samples were centrifuged for 2 minutes at room temperature. Supernatant was isolated and mixed with 900µl 100% EtOH, followed by incubation for 1 minutes at room temperature. Samples were centrifuged at 13,000 rpm for 7 minutes at room temperature. The resulting DNA pellets were washed with 700µl 70% EtOH, air-dried, and resuspended in 50µL H₂O.

Insert sequences were verified by Sanger Sequencing (University of Cambridge, Dept. of Biochemistry). Linearized plasmid was used as a template for in vitro transcription of DIG-labelled riboprobes for mRNA in situ hybridization, using 10X DIG-labelled rNTP mix (Roche) and T7 RNA polymerase (Promega), according to manufacturers' directions. Probe reactions were purified using the RNA Clean & Concentrator kit (Zymo Research). Sequences are available in Table S2.1.

2.3.3 Histology and *in situ* hybridization on sections and in wholemount

Prior to *in situ* hybridisations (ISH) on sections, embryos were embedded in paraffin and then cut. First, embryos were cleared with histosol twice for 20 minutes at room temperature, and then transitioned for 30 minutes each in 50% histosol:paraffin wax (Raymond Lamb, UK) at 60°C, followed by one overnight and five 1 hour washes in paraffin wax at 60°C. Embryos were then transferred to plastic moulds and positioned for sectioning. 8µm sections were cut on rotary microtome and stored on Superfrost Plus slides (VWR). For section ISH, slides were dewaxed twice for 5 minutes in Histosol, then rehydrated through a methanol gradient as above, then washed with DEPC-PBT. Hybridisation was performed under a glass coverslip in a humidified chamber overnight at 70°C with dig-labelled riboprobe diluted to 1ng/uL in hybridisation solution. Prehybridisation and hybridisation were performed as described for wholemount ISH, under coverslips in a slide incubator (Boekel) humidified with 50% formamide, 2X SSC. Slides were rinsed three times for 30 minutes each in wash solution at 70°C, then twice at room temperature in MABT. Antibody incubation and colour development were performed as described for wholemount ISH. Slides were mounted using Fluoromount G (SouthernBiotech).

For wholemount ISH, embryos were rehydrated through a methanol gradient into diethylpyrocarbonate (DEPC)-treated phosphate-buffered saline (PBS) with 0.1% Tween-20 (100%, 75%, 50%, 25% methanol in DEPC-PBT), then treated with a 1:2000 dilution of 10mg/mL proteinase K in DEPC PBT for 15 minutes at room temperature. Following a rinse in DEPC-PBT, embryos were re-fixed in 4% PFA/DEPC-PBS for 15 minutes at room temperature and washed in DEPC-PBT again. Specimens were prehybridised in hybridisation solution (5x SSC, 50% formamide, 1% SDS, 50ug/ml yeast tRNA, 25ug/ml heparin) for 1 hour at room temperature. Hybridisation was performed overnight at 70°C with dig-labelled riboprobe diluted to 1ng/uL in hybridisation solution. Embryos were washed twice for 1 hour each at 70°C in wash solution 1 (50% formamide, 2xSSC, 1% SDS), twice for 30 minutes each at 70°C in wash solution 3 (50% formamide, 1xSSC), then three times for 10 minutes at room temperature in MABT (0.1M maleic acid, 150mM NaCl, 0.1% Tween-20, pH 7.5). After blocking for 2 hours at room temperature in 20% sheep serum + 1% Boehringer blocking reagent in MABT, embryos were incubated overnight at 4°C with a 1:2000 dilution of anti-

digoxigenin antibody (Roche) in blocking buffer. Embryos were then washed in MABT (two quick rinses then five 30-minute washes), stored overnight in MABT at 4°C and equilibrated in NTMT (100mM NaCl, 100mM Tris pH 9.5, 50mM MgCl₂, 0.1% Tween-20). The colour reaction was initiated by adding BM Purple (Merck) to the embryos and stopped by transferring to PBS. Embryos were rinsed once in PBS, post-fixed in 4% PFA for 30 minutes, and graded into 75% glycerol in PBS for imaging. Negative controls (wholemound embryos and slides treated as above, but without added riboprobe) showed no signal.

For gelatin embedding, wholemount ISH embryos were equilibrated in a 15% w/v gelatin solution in PBS at 50°C for 1 hour, before being poured into plastic moulds, positioned for sectioning and left to cool. Gelatin blocks were then post-fixed in 4% PFA at 4°C for 4 days and rinsed in PBS. 50µm sections were cut using a Leica VTS1000 vibratome and mounted on Superfrost slides (VWR) using Fluoromount G (SouthernBiotech).

2.4 Results

2.4.1 Conservation of ventral gene expression patterns in the skate pharyngeal arches

I carried out a series of mRNA in situ hybridisation (ISH) experiments to test for shared expression of ventral patterning factors known from bony fishes in the pharyngeal arches of skate embryos. I found that *edn1* was expressed in the ventral/intermediate epithelium of the mandibular, hyoid and gill arches (Fig. 2.2A, B), while *ednra* was expressed throughout the mesenchyme of all pharyngeal arches (Fig. 2.2C, D). Additionally, skate embryos also exhibited shared expression of *ednrb* in ventral and intermediate mesenchyme across all pharyngeal arches, with a hint of polarising signal in the intermediate and ventral domains of the arches (Fig. 2.2E, F). I also found shared expression of edn signalling readout *mef2C* in the ventral and intermediate domain of all pharyngeal arches (Fig. 2.2G).

I also tested for the expression of bmp signalling components in skate pharyngeal arches and found shared *bmp4* expression in the ventral epithelium of all arches (Fig. 2.2H, I). Dorsal to this *bmp4* domain, I observed shared intermediate and dorsal expression of secreted bmp antagonist *gremlin2* in the mandibular, hyoid and gill arch epithelium (Fig. 2.2J, K). Finally, *hand2* and *msx1* expression was also shared by the ventral mesenchyme of all pharyngeal arches (Fig. 2.2L-N), indicating conservation of ventral BMP signalling across all pharyngeal arches in skate. Taken together, my findings point to conservation of ventral pharyngeal arch patterning mechanisms between bony and cartilaginous fishes, and across the mandibular, hyoid and gill arches of the skate, as well as a shared role of endothelin receptor A and B in cranial neural crest cells.

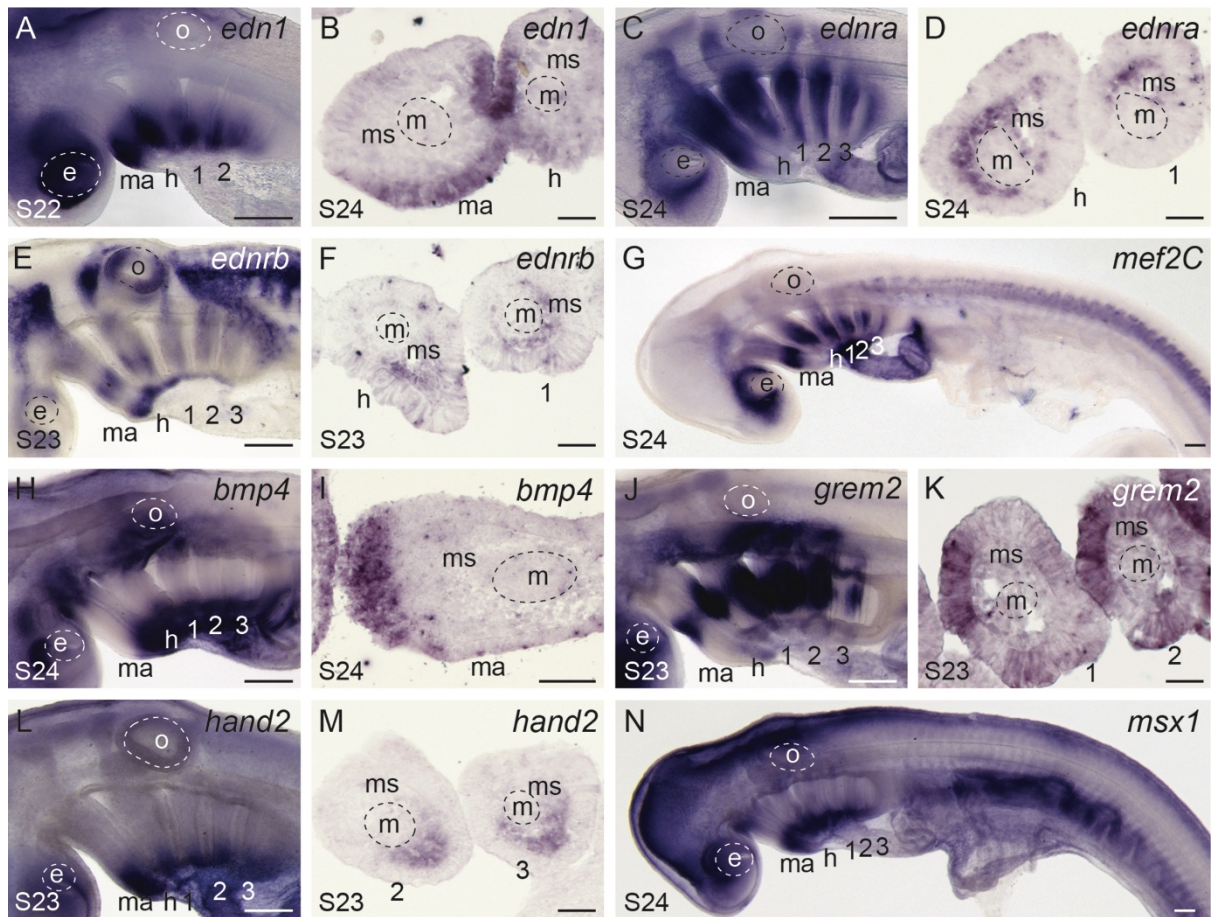


Figure 2.2: Conservation of ventral gene expression patterns in the skate mandibular, hyoid and gill arches. (A) At stage (S)22, *edn1* is expressed in the ventral domain of all pharyngeal arches, with transcripts localising to the (B) pharyngeal epithelium. (C) At S24 *ednra* is expressed along the entire DV axis of the pharyngeal arches, within (D) the mesenchyme. (E) At S23 *ednrb* is expressed in migrating neural crest streams, and also in distinct intermediate and ventral domains within (F) pharyngeal arch mesenchyme. (G) At S24 *mef2C* is expressed in the ventral and intermediate domains of all pharyngeal arches. (H) At S24 *bmp4* is expressed in ventral pharyngeal arch (I) epithelium, and (J) at S23 *grem2* is expressed in intermediate pharyngeal arch (K) epithelium. (L) At S23 *hand2* is expressed in the ventral (M) mesenchyme of each pharyngeal arch. (N) At S24 *msx1* is expressed ventrally in all pharyngeal arches. 1, 2, 3: gill arches; e, eye; h, hyoid; m, mesoderm; ma, mandibular; ms, mesenchyme; o, otic vesicle. Scale bars: A, C, E, G, H, J, L, N = 400um, B, D, F, I, K, M = 25um.

2.4.2 Conserved and divergent expression of dorsal patterning genes in the skate pharyngeal arches

To test for conservation of dorsal patterning factors in the pharyngeal arches of the skate, I first characterised the expression of the transcription factors *eya1*, *six1* and *pou3f3* by ISH. I found that *six1* (Fig. 2.3A-C) and *eya1* (Fig. 2.3D-F) were both expressed broadly in the mandibular, hyoid, and gill arches in skate, though there are tissue-level differences across the arches. While *six1* and *eya1* expression in the epithelium and mesodermal core was shared across the mandibular (Fig. 2.3B, E), hyoid and gill arches (Fig. 2.3C, F), mesenchymal expression of these factors was uniquely observed in the dorsal mandibular arch (Fig. 2.3B, E). In contrast, *pou3f3* expression was shared by the dorsal mesenchyme of the mandibular, hyoid, and gill arches (Fig. 2.3G-I). Taken together, these findings point towards an ancestral role for *eya1/six1* in patterning the upper jaw skeleton of gnathostomes, while *pou3f3* likely possesses a shared role in dorsal patterning across all pharyngeal arches.

I next tested for expression of genes encoding the notch signalling components *jag1* and *hey1*. *jag1* was expressed in the hyoid and gill arches of skate, but not in the mandibular arch, with the exception of very restricted expression in the posterior mandibular arch epithelium (Fig. 2.3J). In line with this, I also found strong expression of *hey1* (a notch signalling readout) throughout the mesenchyme of the hyoid and gill arches, but only very restricted expression within a subdomain of the posterior mandibular arch mesenchyme (Fig. 2.3K, L). The divergence in *hey1* signalling in the hyoid and gill arches and its near absence from the mandibular arch is not stage-specific and persisted through development. Spanning S24-27, the domain of *hey1* expression in the mandibular arch resolved into a thin line in the posterior mandibular mesenchyme immediately subjacent to the epithelium that separates the mandibular arch from the hyoid arch (Fig. 2.3M-O).

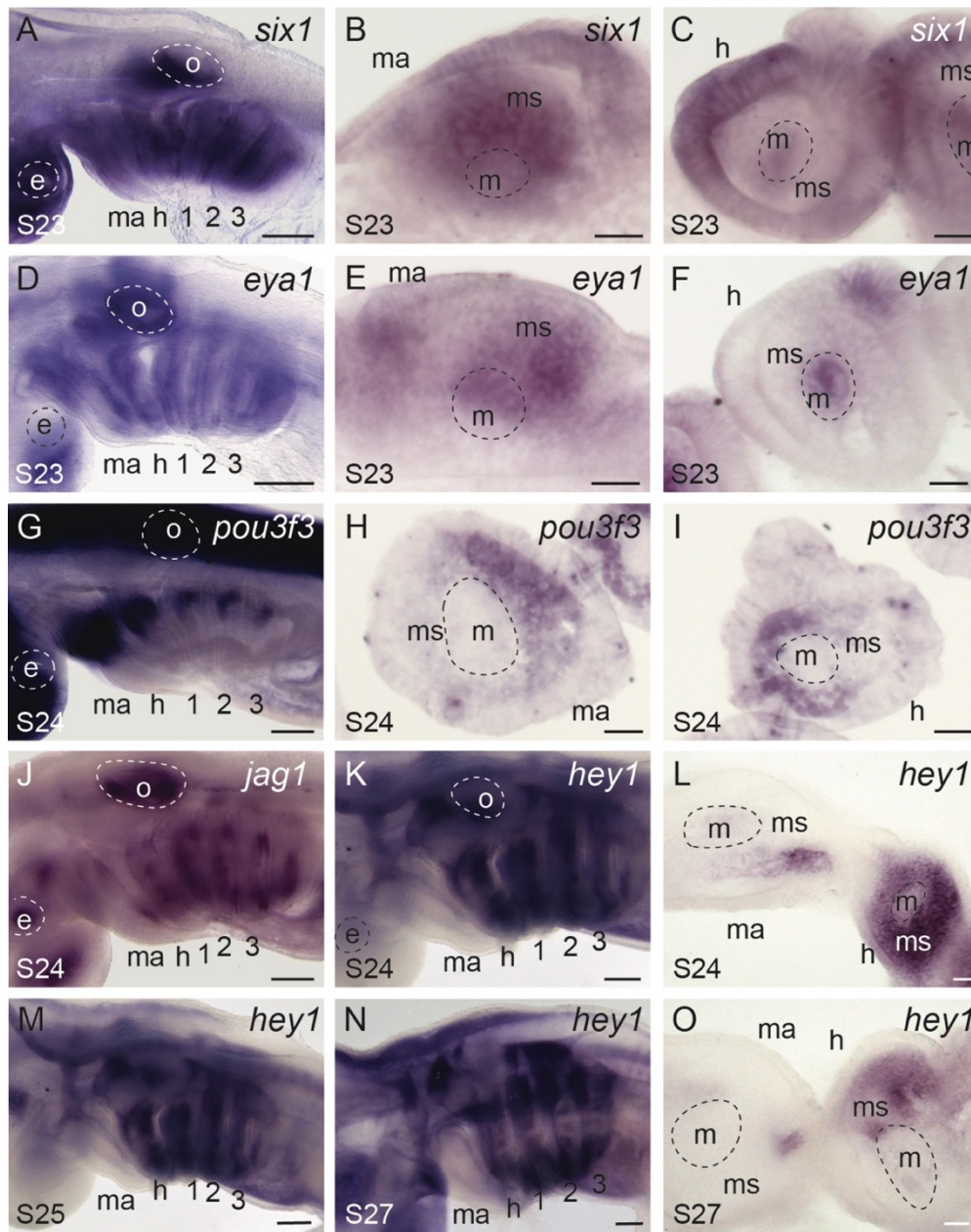


Figure 2.3: Conserved and divergent dorsal gene expression patterns in the skate mandibular, hyoid and gill arches. (A) At S23 *six1* is expressed in the (B) mesenchyme, core mesoderm and epithelium of the mandibular arch, and in the (C) the core mesoderm and epithelium of the hyoid and gill arches. (D) At S23 *eya1* is expressed in the (E) mesenchyme, core mesoderm and epithelium of the mandibular arch, and in the (F) the core mesoderm and epithelium of the hyoid and gill arches. (G) At S24 *pou3f3* is expressed in the dorsal mesenchyme of the (H) mandibular, (I) hyoid and gill arches. (J) *jag1* is expressed in the S24 mandibular, hyoid and gill arches, though (K) at S24 the notch signalling readout *hey1* is expressed (L) in a very restricted pattern within the mandibular arch mesenchyme, but

broadly throughout the hyoid and gill arch mesenchyme. (M) At S25 and (N) at S27 *hey1* is also expressed broadly throughout the hyoid and gill arches but only in a (O) very restricted domain in the mandibular mesenchyme. 1, 2, 3: gill arches; e, eye; h, hyoid; m, mesoderm; ma, mandibular; ms, mesenchyme; o, otic vesicle. Scale bars: A, D, G, J, K, M, N = 400um; B, C, E, F, H, I, L, O = 25um.

2.4.3 Conservation of joint gene expression patterns in the skate pharyngeal arches

Finally, to understand the extent to which jaw joint patterning genes are shared across the pharyngeal arches in skate, I tested for the expression patterns of the transcription factors *barx1*, *gdf5*, *nkx3.2*, which are known to play a role in joint formation in bony fishes, and *gsc*, which is expressed in two discontinuous domains that flank the developing jaw joint in zebrafish.

At S25, strong *barx1* expression (Fig. 2.4A) was shared across the endodermal epithelium and mesenchyme of the developing mandibular, hyoid and gill arches (Fig. 2.4B) in skate. This expression domain is discontinuous, with strong dorsal and ventral expression surrounding the presumptive joint domain, and matches the discontinuous dorsal and ventral expression of *gsc*, which was shared across all arches in skate in the same stage (Fig. 2.4C). Later, during S29, which just precedes chondrogenesis in skate, mesenchymal *gdf5* expression marked the intermediate domain of the mandibular, hyoid and gill arches (Fig. 2.4D, E). At S28, *nkx3.2* expression in the mesenchyme also marked the presumptive joint domains of all arches (Fig. 2.4F, G).

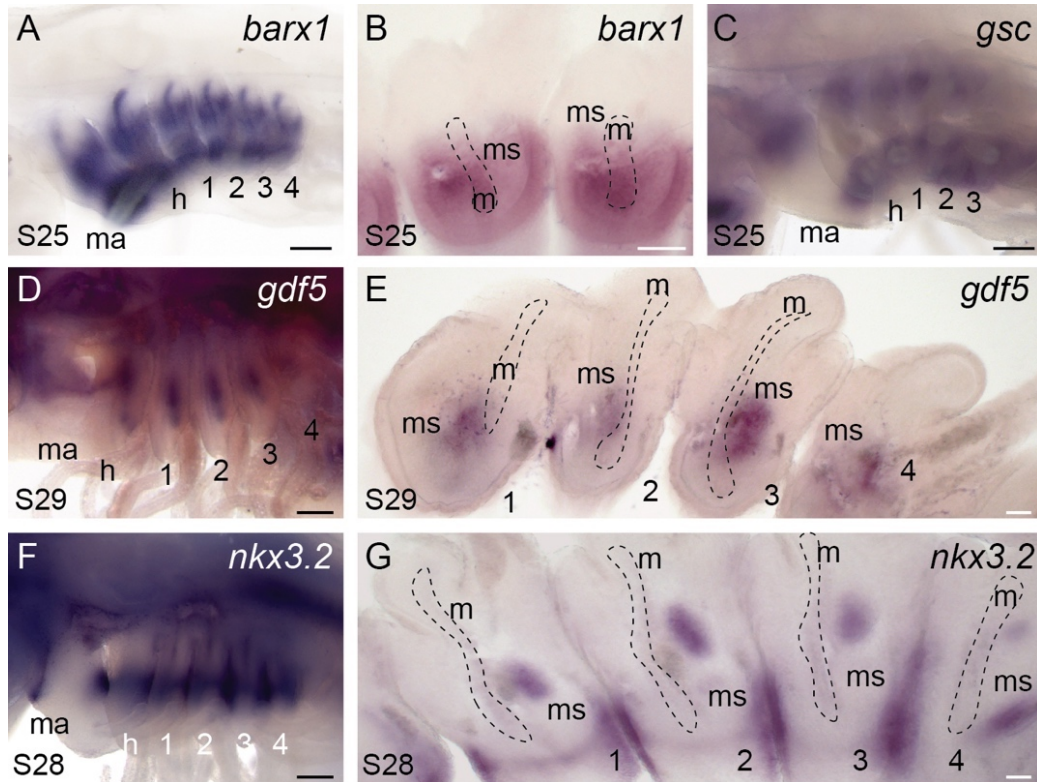


Figure 2.4: Conserved expression of joint markers and pro-chondrogenic transcription factors in the skate mandibular, hyoid and gill arches. (A) At S25 *barx1* is expressed in dorsal and ventral (B) mesenchyme across all pharyngeal arches, in a pattern that flanks the presumptive joint domain. (C) At S25 *gsc* is also expressed in dorsal and ventral domains of all pharyngeal arches, excluding the intermediate, presumptive joint domains. (D) At S29 *gdf5* is subsequently expressed in the intermediate (E) mesenchyme of all pharyngeal arches. (F) At S28 *bapx1* is expressed in the intermediate (G) mesenchyme and epithelium of all pharyngeal arches. 1, 2, 3: gill arches; e, eye; h, hyoid; m, mesoderm; ma, mandibular; ms, mesenchyme; o, otic vesicle. Scale bars: A, C, D, F = 400um; B, E, G = 25um.

2.5 Discussion

Taken together, these findings underscore a high degree of conservation of the jaw patterning mechanisms between bony and cartilaginous fishes. Additionally, as most of these jaw patterning mechanisms known from bony fishes are also conserved across all posterior pharyngeal arches in skate, this is consistent with shared patterning mechanisms underpinning the dorsoventral identity of all skeletal derivatives of the pharyngeal arches in gnathostomes. However, I also report some divergences in expression features between the mandibular, hyoid and gill arches in skate, which may underpin anatomical divergences observed between jaws and gill arches.

2.5.1 *Jaw patterning mechanisms known from bony fishes conserved across all pharyngeal arches in skate*

From amongst the suite of ventralising patterning mechanisms known from bony fishes, both *endothelin-1* and *bmp4* are shared by the ventral domains of all pharyngeal arches in skate. This is consistent with the conservation of the mechanisms conferring ventral jaw identity across bony fishes and cartilaginous fishes. However, the additional expression of *endothelin-1* and *bmp4* in the ventral hyoid and gill arches in skate further points to a ventralising patterning role of these signals beyond the jaw, though functional experiments perturbing their activity are needed to confirm this scenario. Shared expression of their downstream effectors, *hand2* and *msx1*, across all arches in skate is also consistent with this view. As *endothelin-1* is found in ventral pharyngeal arches in lamprey (Square et al., 2016, 2020), this points to endothelin as a likely regulator of ventral pharyngeal arch identity that predates the origin of the jaw.

Additionally, I find mesenchymal expression of *ednrb* in the pharyngeal arches of skate, an expression pattern previously unrecorded in other gnathostomes (Pla and Larue, 2003; Square et al., 2020). *ednrb* expression in craniofacial neural crest cells has so far only been described in a jawless fish, the lamprey (Square et al., 2020), suggesting that the expression observed in skate is a likely retention of ancestral *ednrb* expression in the pharyngeal arch

mesenchyme of vertebrates. In gnathostome model systems like mouse and zebrafish, cranial neural crest cells express *ednra*, while *ednrb* is restricted to trunk neural crest cells (Pla and Larue, 2003; Braasch et al., 2009). My findings from skate suggest that this specialisation of endothelin receptors in distinct neural crest cell populations, i.e. *ednra* expression in cranial neural crest and *ednrb* expression in trunk neural crest, occurred in the bony fish stem, rather than the gnathostome stem, as a comparison solely of lamprey and derived tetrapods may suggest (Square et al., 2020). Further studies of these endothelin receptors across early branching bony fishes are needed to resolve the exact mode and acquisition of the endothelin pathway specialisations across extant gnathostomes.

Interestingly, during the stage of skate development observed here, I was unable to detect *edn1* expression in the mesoderm of the pharyngeal arches. This contrasts with findings in mice, chicken and zebrafish, in which *edn1* is also expressed in mandibular and hyoid mesoderm (Clouthier et al., 1998; Nataf et al., 1998; Miller et al., 2000). The latter findings have led to the suggestion that *edn1* signalling might underpin myogenesis as well as skeletogenesis (Miller et al., 2000). Whether this is a developmental role of endothelin that is confined to bony fishes or whether this may occur during later stages of skate development and myogenesis requires further investigation.

2.5.2 Divergent expression of upper jaw markers known from bony fishes across all pharyngeal arches in skate

With respect to the dorsal jaw patterning genes examined here, there is some divergence in expression patterns of these genes amongst the pharyngeal arches in skate. Only one of the known upper mandibular arch markers examined here, *pou3f3* (Jeong et al., 2008), is shared across the dorsal mesenchyme of the mandibular, hyoid, and gill arches in skate, indicating a shared role in dorsal patterning across all pharyngeal arches. In contrast, my findings of mesenchymal *six1/eya1* expression unique to the mandibular mesenchyme are consistent with *six1* expression reported in mouse (Tavares et al., 2017) and chick (Fonseca et al., 2017), and point to an ancestral role for *eya1/six1* in patterning the upper jaw skeleton of gnathostomes, rather than the dorsal pharyngeal arch mesenchyme more broadly. However, the epithelial *eya1/six1* expression across the entire dorsoventral axis is shared across all

arches, implying a conserved role in epithelial patterning across the mandibular, hyoid and gill arches in skate, and revealing a level of tissue-specificity inherent to the function of *eya1/six1*.

My observations of the expression of notch signalling components in the pharyngeal arches in skate differ from patterns previously reported in zebrafish, both in terms of dorsoventral extent of expression (i.e. expression along the entire dorsoventral axis of the arch in skate, as opposed to the dorsal localisation seen in zebrafish), and the near exclusion of mesenchymal *hey1* expression from the mandibular arch in skate. It is possible that the upper jaw patterning function of *jag1* signalling is an ancestral feature of the gnathostome mandibular arch that has been lost or reduced in skate, or that this mechanism is a derived feature of bony fishes. Gene expression data for notch signalling components in the pharyngeal arches of cyclostomes are needed to resolve this.

2.5.3 Conservation of jaw joint genes across all pharyngeal arches in skate

Finally, my observations of the expression of jaw joint markers known from bony fishes in skate also shed light on the ancestral organisation of joint formation in the gnathostome pharyngeal endoskeleton. The expression patterns I observed are consistent with conservation of the pro-chondrogenic function of *barx1*, the joint patterning function of *bapx1* and *gdf5*, and the discontinuous expression of *gsc* across all intermediate joints separating the principal elements of the pharyngeal endoskeleton in cartilaginous fishes. A previous study of axial patterning gene expression in the pharyngeal arches of the jawless lamprey reported broad conservation of *dlx*, *hand* and *msx* expression across all pharyngeal arches, but a conspicuous absence of the joint markers *bapx* and *gdf* expression in the intermediate region of the first arch (Cerny et al., 2010). These observations led to the suggestion that co-option of the joint patterning factors to the intermediate region of the mandibular arch, on top of a pre-existing and deeply conserved dorsoventral patterning programme, was key to the evolutionary origin of the jaw (Cerny et al., 2010). My findings are consistent with the acquisition of intermediate *bapx1* and *gdf5* expression as a key step in the origin of the jaw joint, but suggest that this developmental mechanism was not primitively

mandibular arch-specific, and instead a conserved mechanism specifying joint fate in the skeleton of the mandibular, hyoid and gill arches of gnathostomes.

This candidate gene approach has revealed that a suite of transcription and signalling factors that confer upper and lower jaw and jaw joint identity also display polarised expression along the dorsoventral axis of the posterior pharyngeal arches in skate (Fig. 2.5A). Together with previous reports of shared expression of core components of the pharyngeal arch dorsoventral patterning network in cartilaginous and bony fishes (Gillis et al., 2013; Compagnucci et al., 2013), these findings point to a conserved transcriptional network patterning the dorsoventral axis of the mandibular, hyoid and gill arches in the gnathostome crown group (Fig. 2.5B, represented by the skate), and within the framework of serial homology as redeployment of shared patterning mechanisms, these findings are also consistent with serial homology of the gnathostome jaw, hyoid and gill arch skeleton.

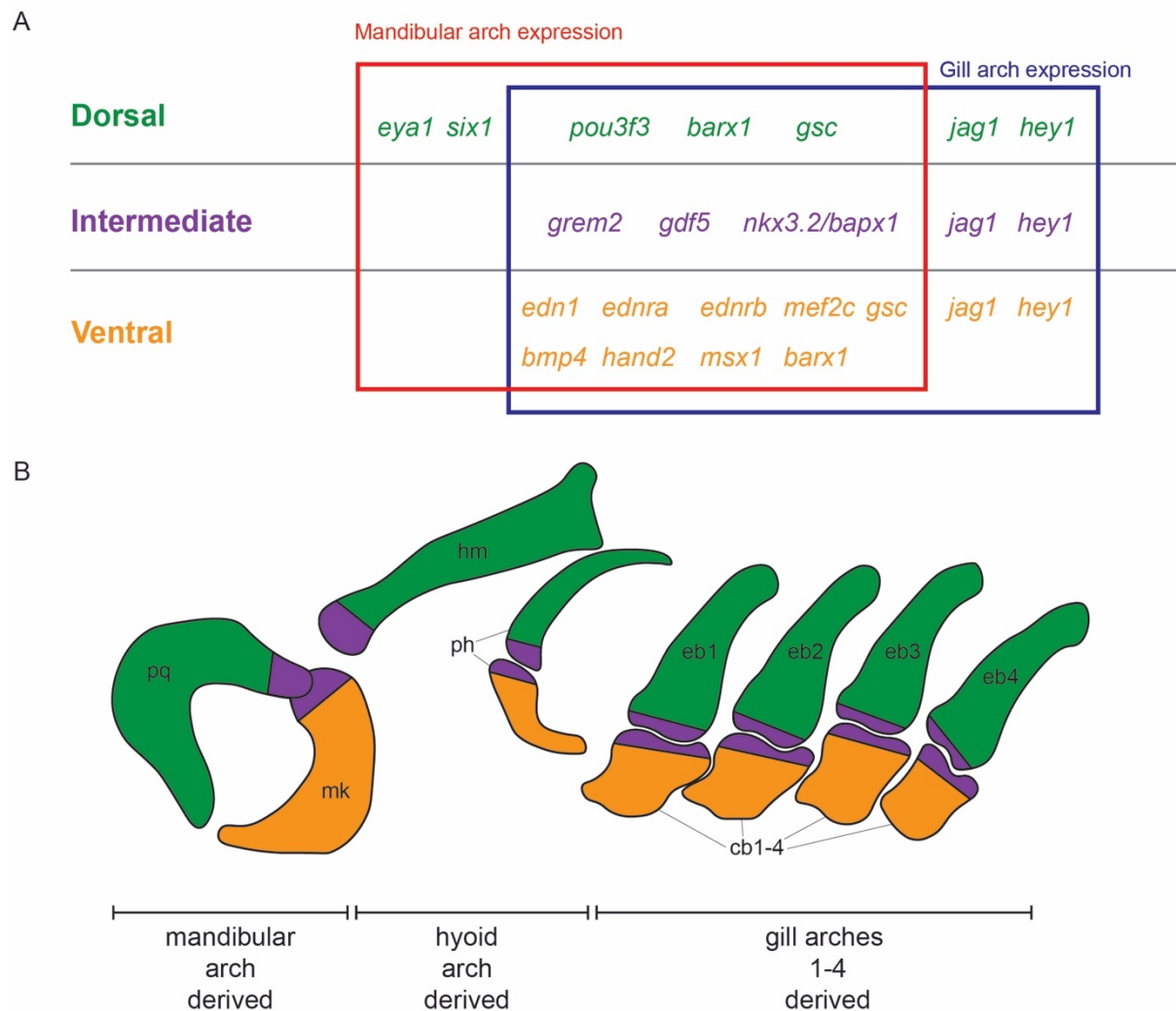


Figure 2.5: Conserved and divergent expression of jaw patterning candidates known from bony fishes in the skate mandibular, hyoid and gill arches. A) Red and blue squares indicate mandibular arch and gill arch expression, respectively. Genes listed in the overlap of the two squares are expressed across all pharyngeal arches, whereas expression listed solely in mandibular arch or gill arch squares is arch specific. Mandibular arch-specific expression of *eya1* and *six1* is restricted to the mesenchyme. B) Skate hatchling pharyngeal anatomy, adapted from Gillis et al., 2009a & 2013. Skeletal components in green, purple or orange indicate corresponding expression patterns from A) found in the respective pharyngeal arch primordia during ontogeny (for skeletal components of the jaw, hyoid and gill arch 1, their embryonic origin is demonstrated via lineage tracing experiments by Gillis et al., 2013). cb 1-4, ceratobranchials 1-5; eb 1-4, epibranchial 1-4; hm, hyomandibula; mk, Meckel's cartilage; ph, pseudohyoid; pq, palatoquadrate.

2.6 Summary

Here I have shown that jaw patterning mechanisms known from bony fishes are conserved in a cartilaginous fish, the little skate. Furthermore, I report that the vast majority of these patterning mechanisms are shared across all pharyngeal arches in skate, i.e. the hyoid and gill arches that sit posterior to the jaw. These signalling pathways and transcription factors include ventral endothelin signaling, *bmp4*, *hand2*, *msx1*, dorsal *pou3f3*, and joint regulators *barx1*, *gsc*, *gdf5* and *nkx2.3*. In combination with previous reports of shared expression of core components of this pharyngeal arch dorsoventral patterning network in jawless fishes, these findings point to a pan-pharyngeal transcriptional program that functions to pattern the dorsoventral axis and serially delineates pharyngeal skeletal segments not just in the last common ancestor of the gnathostome crown group, but more generally, in the last common ancestor of vertebrates. Furthermore, dorsoventral patterning mechanisms conserved across all pharyngeal arches in skate are consistent with serial homology of their skeletal derivatives, i.e. the jaw and gill arches.

Additionally, I also find divergent expression features that may underpin anatomical differences between the jaw and gill arches. In skate, mesenchymal *six1/eya1* expression is unique to the dorsal mandibular arch, while notch signalling is shared across the hyoid and gill arches and largely missing from the mandibular arch. Together, these molecular differences may delineate skeletal derivatives arising from these domains, i.e. the upper jaw and hyoid/gill arch skeletal elements, on top of the shared pan-pharyngeal axial patterning programme.

Chapter 3:

Comparative transcriptomics reveal conserved and divergent transcriptional features of pharyngeal arches in the skate

3.1 Abstract

While the transcriptome landscapes of jaw and pharyngeal arch development have been investigated extensively in bony fishes, comparative RNA-seq and differential gene expression analyses from the developing jaw and pharyngeal arches in cartilaginous fishes have been lacking. Here I have generated a *de novo* transcriptome assembly based on RNA-seq libraries generated from upper and lower jaw and gill arch progenitors in the little skate (*Leucoraja erinacea*). Using differential gene expression analyses, I have then tested for additional gene expression features that correlate with the common or distinct anatomical properties of the upper/lower jaw and upper/lower gill skeleton in skate. Within the mesenchyme, I report discontinuous expression of *sfrp2* and *twist2* in dorsal and ventral territories, and ventral expression of *hand1*, which are all shared across all pharyngeal arches. I also report *scamp5* as a novel marker of the dorsal mandibular arch mesenchyme in skate. Within the mesoderm, I report shared dorsal expression of *foxG1* and *six2*, and within the endoderm I report shared ventral expression of *nkx2.3* and *foxe4*. I also report novel transcriptional features that are differentially expressed within the mandibular arch vs. the gill arches. Within the mesoderm, I report mandibular arch-specific expression of *six2*, *tbx18*, and *pknox2*, and gill arch-specific expression of *lhx9*. Within the endoderm, I report gill arch-specific expression of *foxl2*, *gcm2*, *wnt2b* and *foxq1* marking the presumptive gill buds. This approach reveals additional gene expression patterns that are shared across all pharyngeal arches, as well as distinct gene expression patterns that may contribute to the unique anatomical features of the mandibular and gill arches of the skate.

3.2 Introduction

Next-generation high-throughput sequencing of transcriptomes (RNA-seq) has unlocked access to genetic ‘read-out’ information stored within any organism at an unprecedented scale and speed. By profiling the complete sets of RNA transcripts present in cells and quantifying the changing expression levels of each transcript during development and under different conditions, RNA-seq offers functional insights into cells, tissues, and organs at work (Wang et al., 2009). RNA-seq also stands in stark contrast to standard genomic applications. The latter are generally cost- and labour-intensive owing to genome sizes and repeat contents across vertebrates, and often require pre-existing high-quality genome sequences. RNA-seq data are comparatively inexpensive and provide rapid access to sequence information for routine downstream methods, such as primer design, phylogenetics, or marker construction (Haas et al., 2013).

3.2.1 RNA-seq in “non-model” organisms and the Trinity pipeline

RNA-seq methods also have the advantage of being applicable to non-standard model organisms, which may be of substantial developmental or evolutionary importance, but for which comprehensive assembled and annotated genomic sequences are lacking. The little skate (*Leucoraja erinacea*) is such a non-model organism. While the skate is emerging as a powerful experimental system amenable to lipophilic dye-based lineage tracing (Gillis et al., 2013), *in ovo* treatment with cell signalling inhibitors and cell proliferation trackers (Gillis et al., 2016), and multiplexed *in situ* gene expression analysis (Criswell et al., 2020; Sleight et al., 2020; Marconi et al., 2020), transcriptomic and genomic resources are limited. A previous skate transcriptome had been assembled based on sequences collected from six pooled embryos ranging in stage from 20–29 (King et al., 2011; Wyffels et al., 2014), while genomic DNA data was available based on data from a single stage 32 embryo, though no standard genome annotation data had been provided (King et al., 2011). The sequences of these previous transcriptome and genome datasets were generated using Illumina protocols for single-end sequencing on an Illumina Genome Analyzer II, while the transcriptome assembly was constructed using CLCBio Genome Workbench version 4 (King et al., 2011), which

possesses a *de novo* alignment algorithm that is not fully appropriate for RNA-seq projects. These resources are useful for downstream applications and routine molecular biology in the day-to-day laboratory work, but they lack tissue specificity and annotation data, and are also marred by misassembled sequences and overall low coverage.

Here, I was specifically interested in complementing the candidate approach outlined in the previous chapter with a comparative transcriptomic analysis of the dorsal and ventral domains of the mandibular and gill arches of the little skate. To this end, I have made use of Trinity, a *de novo* transcriptome assembly pipeline (Grabherr et al., 2011; Haas et al., 2013). The Trinity pipeline constructs transcriptomes without genome-based guidance. It consists of three sequentially employed, independent software modules (Inchworm, Chrysalis, and Butterfly) that work together to efficiently and robustly reconstruct transcriptomes from Illumina RNA-Seq data.

Briefly, the first and computationally most demanding software module, Inchworm, parses short-read data into the unique sequences of transcripts, which often generates full-length transcripts for dominant isoforms if the raw data is of appropriate quality, and then marks the unique portions of alternatively spliced transcripts. The assembled contigs (contiguous sequences generated by overlapping transcript reads representing consensus regions of RNA) are subsequently passed on to the Chrysalis module, which clusters the transcripts and computes de Bruijn graphs for each cluster. De Bruijn graphs are directed graphs representing pathways that connect pairs of nucleotide overlaps between the short sequences, akin to a game of dominoes in which the end point of one piece has to overlap with the beginning of the next piece, but in which connections can occur in parallel if end or start points match several other pieces. Each graph represents the transcriptional complexity (e.g. through splicing) at a given gene or locus. Finally, the last software module, Butterfly, assesses each de Bruijn graph and reports all the emerging transcripts, including full-length transcripts for alternatively spliced isoforms and transcripts that corresponds to paralogous genes (Grabherr et al., 2011; Haas et al., 2013).

A difficulty in this process lies in the accurate capturing of transcripts with shallow expression levels, particularly with regards to loci that produce several transcripts (isoforms) due to

alternative splicing events. Illumina short reads that are ultimately derived from a single exon can be part of multiple paths in the de Bruijn graphs, which makes any graph structure ambiguous and challenging to resolve. These issues are exacerbated if variants or lowly expressed transcripts occur only in a subset of sampled tissue types or time points. This can be combatted by stringent filtering methods of the raw data, but this in turn may exclude transcripts with low expression values from the assembly process (Hölzer & Marz, 2019). Keeping these potential pitfalls in mind is important when assessing sequencing protocols, parameter settings, and statistical approaches, in order to ensure potential computational issues are counterbalanced efficiently and the most accurate and complete *de novo* transcriptome assembly is generated.

3.2.2 Comparative transcriptomics of pharyngeal arch development in skate

In skate, I have used the Trinity pipeline to assemble RNA reads extracted from dorsal and ventral domains of the mandibular and gill arches into a *de novo* transcriptome, and to quantify the representation of these *de novo* transcripts across my sampled pharyngeal arch domains. As I was specifically testing for shared and/or divergent patterning mechanisms between the jaw and gill arches, I focused on the time period that spans the expression of the *Dlx* code, a key regulator of axial identity in the pharyngeal arches, i.e. S23-24 and S25-26 (Fig. 3.1A). In mouse, nested *dlx* expression has typically been restricted to the mandibular and hyoid arches (Depew et al., 2002), while in zebrafish, nested *dlx* expression has been observed in the post-hyoid gill arches, though the effects of perturbations of *dlx* gene expression or lineage tracing experiments of *dlx* expressing cells have only been analysed in mandibular and hyoid arch derivatives (Ellies et al., 1997; Verreijdt et al., 2006; Walker et al., 2006; Talbot et al., 2010; Barske et al., 2020). In skate the nested expression of the *dlx* genes has been described in the developing mandibular, hyoid and gill arches, and it has been demonstrated through lineage tracing that from these molecularly equivalent domains of combinatorial *Dlx* gene expression the principal dorsal and ventral endoskeletal segments of the jaw hyoid and gill arches originate (Gillis et al., 2013). Here, RNA was extracted from dorsal and ventral domains of the mandibular and first gill arch were collected by manual dissection from skate embryos at S23/24 and S25/26 (Fig. 3.1B, C).

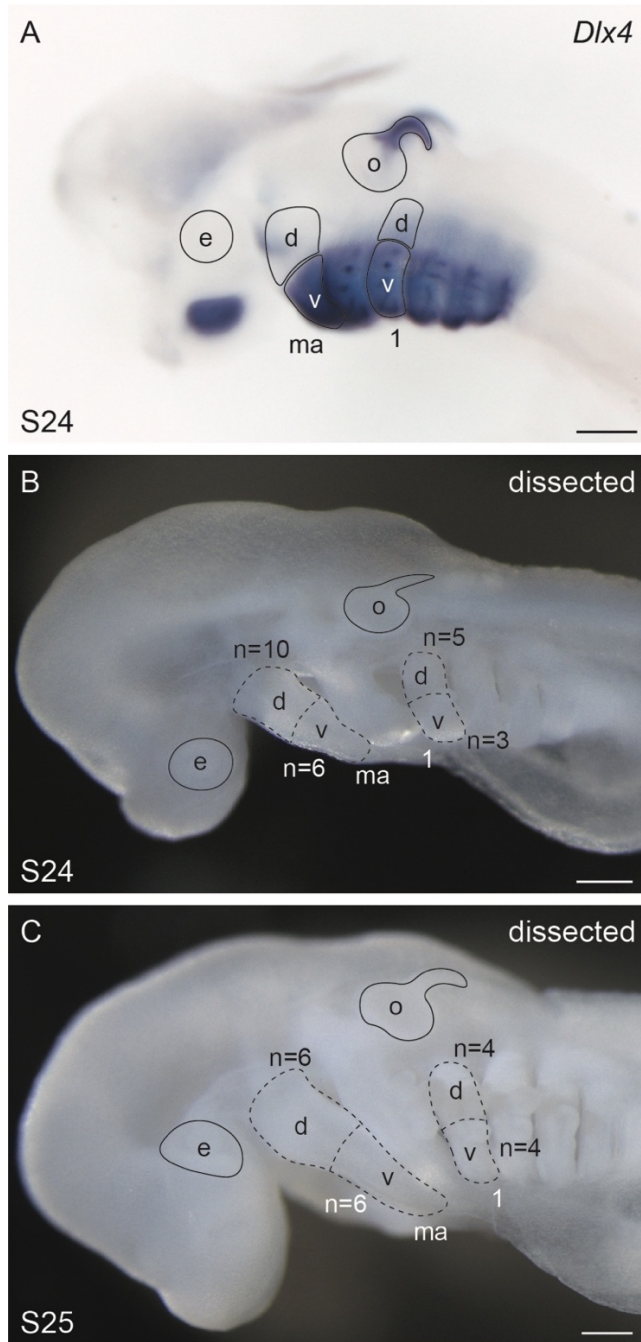


Figure 3.2: Pharyngeal arch domains sampled for RNA extraction. (A) Previously established *Dlx* gene expression was used to mark dorsal and ventral domain boundaries. (B) Dorsal and ventral mandibular arch domains and dorsal and ventral gill arch domains dissected at S23-24. (C) Dorsal and ventral mandibular arch domains and dorsal and ventral gill arch domains dissected at S25-26. d, dorsal; e, eye; ma, mandibular arch; o, otic vesicle; v, ventral; 1, gill arch 1. Scale bars: 400um

Based on the assembly and quantification of the resulting sequencing data, I then conducted a differential gene expression analysis to identify transcriptional differences associated with the progenitors of the jaw and gill arch endoskeleton in skate, using the R package EdgeR. After biological validation through *in situ* hybridisation, I identified *foxG1*, *six2*, *sfrp2* and *twist2*, *nkx2.3*, *hand1* and *foxe4* as potential markers of dorsoventral identity across all pharyngeal arches in skate, and I report *scamp5* as a novel marker of the dorsal mandibular arch. The unbiased comparative transcriptomics approach also revealed transcriptional features of arch-specific musculature and gill primordia: I report *six2*, *tbx18*, and *pknox2* as markers of the mandibular arch mesoderm, *lhx9* as a novel marker of the gill arch mesoderm, and finally endodermal *foxl2*, *wnt2b* and *foxq1* as novel markers of the gill buds in skate. Taken together, these findings point to a conserved gene regulatory network underlying the primitively shared organisation of the gnathostome mandibular, hyoid and gill arch skeleton, and highlight additional transcriptional features that correlate with the developmental and anatomical diversification of jaws and gill arches within gnathostomes.

3.3 Methods

3.3.1 RNA-seq and de novo transcriptome assembly

Total RNA was extracted from upper mandibular arch (n=10), lower mandibular arch (n=6), upper gill arch (n=5) and lower gill arch (n=3) domains at stage (S)23/24 and from upper mandibular arch (n=6), lower mandibular arch (n=6), upper gill arch (n=4) and lower gill arch (n=4) domains at S25/26 (Table 3.1). Samples were only taken from one side of the embryo. S23-24 and S25-26 span the expression of the *Dlx* code, a key regulator of axial identity in the pharyngeal arches, and manual dissections of upper and lower arch primordia were guided by morphological landmarks correlating with dorsal (*dlx1/2+*) and ventral (*dlx1-6+*) expression (Gillis et al., 2013). Occasionally, dissected tissue samples from dorsal or ventral domains of the mandibular and gill arch were morphologically large enough to generate two tissue samples for library preparation at once (this was accounted for later during statistical testing). Tissue dissection of S23-26 embryos was performed by Dr. Andrew Gillis. In addition to the S23-24 and S25-26 samples, I also dissected upper mandibular arch (n=4), lower mandibular arch (n=4), upper gill arch (n=4) and lower gill arch (n=4) domains from 5 S29 embryos, though these libraries were not considered by the differential gene expression analysis.

Embryo	Tissues sampled	Stage
A	GAD, GAV, MAD (2x), MAV	Stage 23-24
B	GAD, GAV, MAD (2x), MAV	
C	GAD (2x), MAD (2x), MAV (2x)	
D	GAD, GAV, MAD (2x), MAV (2x)	
E	GAD, GAV (2x), MAD (2x), MAV (2x)	Stage 25-26
F	GAD (2x), GAV (2x), MAD (2x), MAV (2x)	
G	GAD, GAV, MAD (2x), MAV (2x)	
H	GAD, GAV, MAD, MAV	
I	GAD, GAV, MAD, MAV	Stage 29
J	GAD, GAV, MAD, MAV	
K	GAD, GAV, MAD, MAV	
L	GAD, GAV, MAD, MAV	

Table 3.1: Pharyngeal arch domains dissected and subjected to RNA extraction. Individual embryos are labelled alphabetically A-L. GAD = gill arch dorsal, GAV = gill arch ventral, MAD = mandibular arch dorsal, MAV = mandibular arch ventral.

Dissected tissue samples were initially preserved in RNAlater, and total RNA was then extracted using the RNAqueous-Micro Total RNA Isolation Kit (ThermoFisher). Library prep was performed using Smart-seq2 (Picelli et al., 2014) with 10 cycles of cDNA amplification. Indexed S23/24 and S25/26 libraries were pooled and sequenced using the HiSeq4000 platform (paired end sequencing, 150bp read length) at the CRUK genomics core facility (University of Cambridge, Cancer Research UK Cambridge Institute). cDNA library quality control and subsequent sequencing was performed by Dr. Stephen J. Clark at the Babraham Institute in Cambridge, UK. In addition to the above, I prepared libraries from the dorsal mandibular arch (n=5), ventral mandibular arch (n=5), dorsal gill arch (n=5) and ventral gill arch (n=5) domains of S29 skate embryos as described above, which were sequenced using the NovaSeq 6000 (paired end sequencing, 150bp read length) at Novogene Co., Ltd. Reads from these libraries were included in the *de novo* transcriptome assembly, but are not analysed further in this current work.

A total of 2,058,512,932 paired raw reads were generated. Low quality read and adapter trimming was conducted with Trim Galore! (0.4.4) with the quality parameter set to 30 and phred cut-off set to 33. Reads shorter than 65 bp were discarded. After trimming adapters and removing low quality reads a total of 1,348,098,076 reads were retained. Normalisation (max coverage 30) reduced this to a further 54,346,196 reads. The *de novo* strand-specific assembly based on these reads was generated using Trinity 2.6.6 with default parameters (Grabherr et al., 2011; Haas et al., 2013). The N50 of that assembly was 1009bp, and the Ex90N50 (the N50 statistic computed as usual but considering only the topmost highly expressed transcripts that represent 90% of the total normalized expression data, meaning the most lowly-expressed transcripts are excluded) was 1906bp. Post-assembly quality control was carried out using Trinity's toolkit or gVolante.

The code used for assembling the transcriptome is available as Script S.3.1. For quality control and sample correlation analyses I employed scripts provided by the Trinity pipeline (<https://github.com/trinityrnaseq/trinityrnaseq/wiki/QC-Samples-and-Biological-Replicates>).

3.3.2 Differential gene expression analysis

Trinity transcript quantification was performed alignment-free using salmon (Patro et al., 2017) to estimate transcript abundance in TPM (Transcripts Per Kilobase Million). The genes differentially expressed along the dorsoventral axis within each arch, or across the anterior-posterior axis between dorsal and ventral domains of each arch, were screened for using edgeR with a cutoff of FDR (false discovery rate) ≤ 0.05 . Table S3.1 for candidates for validation, Tables S3.2-5 for stages 24/25 and Tables S3.6-9 for stages 25/26 are available in the supplementary material to this dissertation. Within EdgeR, a negative binomial additive general linear model with a quasi-likelihood F-test was performed. Model design accounted for repeated sampling of tissues from the same individual and p-values were adjusted for multiple testing using the Benjamin-Hochberd method to control the false discovery rate (FDR ≤ 0.05) (Fig. S1 A-D). This code is available in Script S3.1 and S3.2 in the supplemental material. The transcripts were putatively annotated based on sequence similarity searched with blastx against Uniprot (<http://www.uniprot.org/>).

3.3.3 Gene cloning, mRNA probe generation, histology and *in situ* hybridization on sections and in wholemount

Gene cloning of additional candidates identified through differential gene expression analysis, mRNA *in situ* hybridisation probe synthesis as well as histology and *in situ* hybridizations were performed as described in chapter 2. Probe sequences are also listed in in Table S2.1.

3.4 Results

3.4.1 Quality control of the *de novo* pharyngeal arch transcriptome assembly

After I had completed the *de novo* skate pharyngeal arch transcriptome using the Trinity pipeline, based on the tissue samples of skate upper and lower mandibular and gill arch primordia across S23/24, S25/26 and S29, I tested the quality of the resulting assembly. The resulting read and assembly statistics as well as read representation and assembly quality control statistics are summarised in table 3.2 below.

Reads		
	Raw reads	2058512932
	Trimmed reads	1348098076
	Normalised reads	54346196
Assembly		
	Total Trinity transcripts	549531
	Total Trinity genes	364865
	% GC	46.26
Statistics based on all isoforms per gene		
	N50	1009
	Ex90N50	1906
	Median length	635
	Average length	818
Read representation	Average read content per library	93%
BUSCO, Core Vertebrate Gene set	Total # of core genes queried:	233
	# of core genes detected	
	Complete:	207 (89.98%)
	Complete + partial:	225 (96.57%)
	# of missing core genes:	8 (3.43%)

Table 3.2: Skate pharyngeal arch *de novo* transcriptome assembly statistics.

In order to assess the quality and degree of fragmentation inherent to the assembly, I next set out to compute the Nx and ExN50 statistic. The contig Nx statistic is widely used to assess transcriptome quality. It is defined as the sequence length of the shortest contig at x% of the total transcriptome and reflects the degree of fragmentation inherent to the assembly. Traditionally, the Nx is calculated as the N50 so that at least half (50%) of all assembled nucleotides are covered by transcript contigs of at least the N50 length value. A high N50 number implies the transcriptome is characterised by a high number of full-length transcripts. Here, the N50 of this skate pharyngeal arch transcriptome is 1009bp, meaning half of the assembled nucleotides belong to contigs that measure at least 1009bp in length. While the Nx statistic is widely used in genomics and transcriptomics, the Trinity pipeline (Grabherr et al., 2011) also suggests computing the ExN50 statistic (<https://github.com/trinityrnaseq/trinityrnaseq/wiki/Transcriptome-Contig-Nx-and-ExN50-stats>). In this elaboration of the N50 statistic, the N50 is computed for the top-most highly expressed genes that represent x% of the total normalized expression data. In order to calculate this statistic, the transcript abundance estimation has to be completed first. Then the gene expression is defined as all transcript isoform expression summed up, and the gene length is computed as the mean of the isoform lengths, weighted by expression. In other words, the N50 is calculated for a subset of top highly expressed transcripts covered by x% of sample-wise normalized reads. If high values of “x” in ExN50 are close to the maximum of the plotted curve, this means the assembly includes good coverage of long transcripts. Specifically, if the ExN50 curve has a maximum of “x” at 90%, the assembly is considered to provide good coverage and deeper sequencing is unlikely to improve the quality assembly.

Here, a plot of the ExN50 of this skate pharyngeal arch transcriptome assembly (Fig. 3.2) reveals that while the original N50 value measures 1009bp in length, this statistic is influenced by a number of lowly expressed transcripts or transcript fragments. If these were excluded from the N50 calculation, i.e. if only the top highly expressed transcripts covered by 90% of sample-wise normalized reads were included (the 494577 most highly expressed transcripts out of the total of 549531 transcripts), the N50 would increase to 1906 bp. This is close but not quite the maximum of the curve shown in Fig 3.2., meaning the assembly likely contains some lowly expressed and short contigs that may be a result of somewhat low read coverage confounding the assembly. However, this spike is very close to the 90% threshold indicated

by the dotted line, suggesting that read coverage is very close to ideal values. Additionally, the very early spike in Fig. 3.2 also shows that there is a very small subset of transcripts, representing 5% or less of the normalised reads of the assembly, that measure up to 2500 bp in length.

To further test the quality of the *de novo* assembled skate pharyngeal arch transcriptome, I employed the Benchmarking Universal Single-Copy Orthologs (BUSCO) assessment through gVolante (Nishimura et al., 2017) and checked to what extent the original libraries aligned to the novel assembly. This approach revealed a high degree of completeness of the transcriptome. On average, 93% of each original library aligned to the *de novo* assembly, and 97% of 233 vertebrate core genes (99.69% of 978 metazoan core genes) queried through gVolante (Nishimura et al, 2017) were found completely or partially within it.

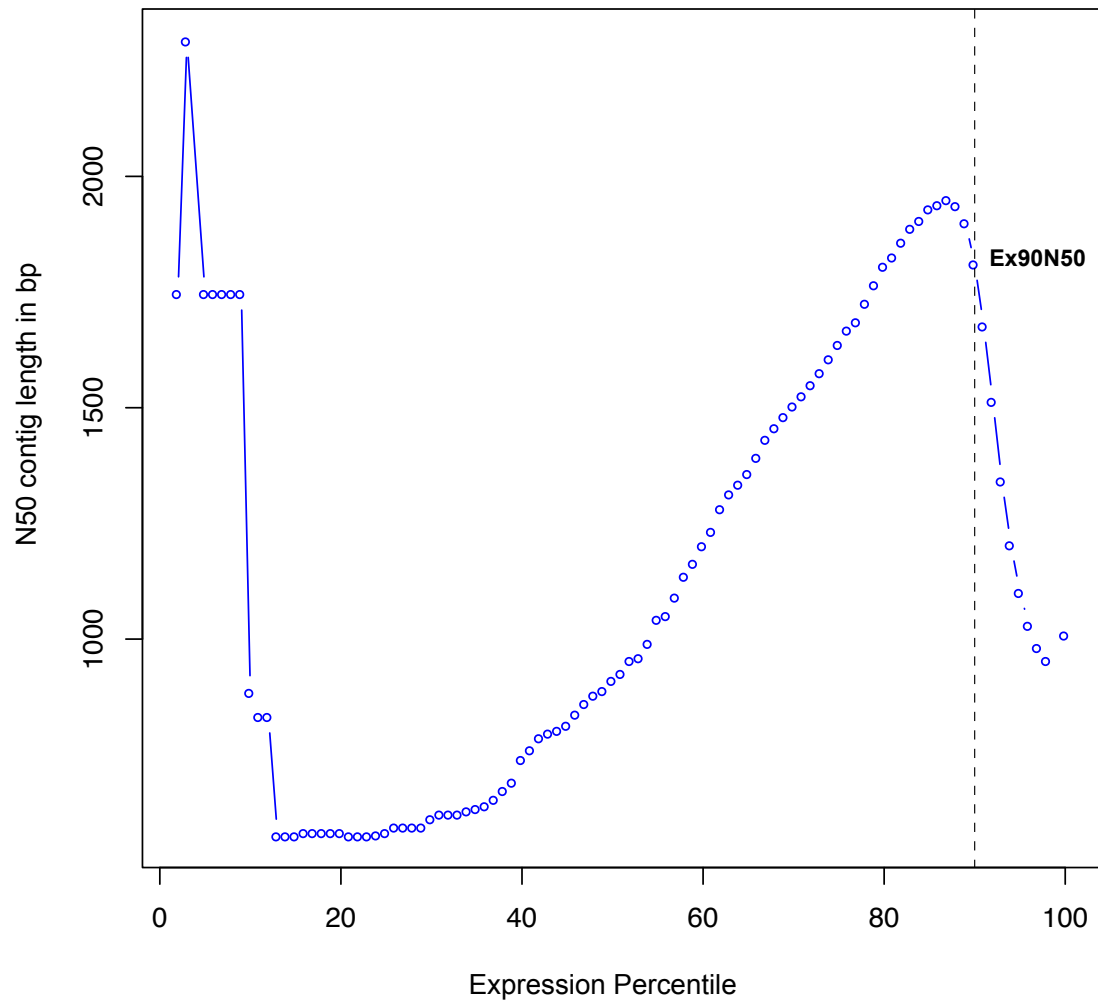


Figure 3.2. Transcriptome assembly statistics: ExN50. Vertical dashed line is drawn through the Ex90N50 statistic, i.e. the N50 if only 90% of the topmost transcripts are considered. This shows that if the 10% most lowly expressed transcripts are excluded from the N50 computation, the N50 increases to 1906 bp. The early spike in the curve suggests there are some transcripts that are very long (around 2500 bp) but represent only a very small percentage in the assembly (less than 5%).

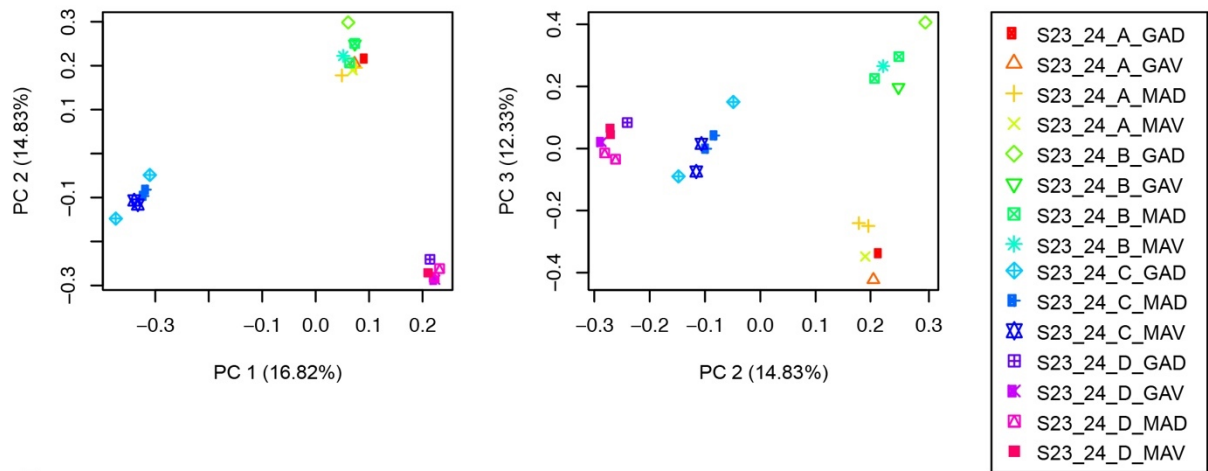
3.4.2 Sample correlation and biological replication analysis

After transcript quantification, I next set out to identify possible batch effects and other issues within the data to ensure that my biological replicates of dissected skate pharyngeal arches are correlated according to tissue type rather than their stages or the individual embryos from which the samples originated. To this end, I computed Principal Component Analyses (PCA – Fig. 3.3) and performed hierarchical clustering to generate a sample correlation matrix (Fig. 3.4).

Principal Component Analysis

A

Stage 23-24: Embryos A-D



B

Stage 25-26: Embryos E-G

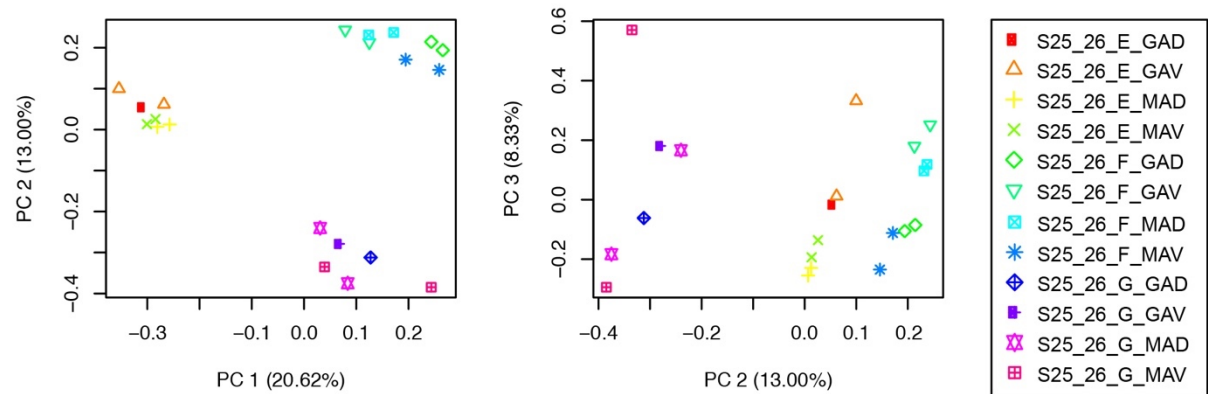


Figure 3.3: Principal Component Analyses (PCA) of the skate pharyngeal arch samples. A) Especially amongst S23-24 embryo samples but also amongst B) S25-26 embryo samples, the PCA shows a strong individual batch effect: samples group by embryo of origin, rather than tissue type. GAD = gill arch dorsal; GAV = gill arch ventral; MAD = mandibular arch dorsal; MAV = mandibular arch ventral.

Both the PCA plots and the hierarchical clustering via the sample correlation matrix identified a strong batch effect inherent to the sequenced samples. The PCA (Fig. 3.3) showed that after linear combinations of the original gene expression values to define a new set of unrelated variables (the principal components), the variance of the data is dominated by the identities of the embryos from which the samples originated (embryos A-D at stage 23/24 and embryos E-G at stage 25/26). The sample correlation matrix (Fig. 3.4) identified the same issue, but also showed that within each group of samples originating from the same embryo, the samples group along the anteroposterior axis. For example, in embryo E, which is colour-coded blue in the hierarchical clustering, samples from the gill arch group together and samples from the mandibular arch group together, with the exception of a single ventral gill arch sample (Fig. 3.4).

3.4.3 ComBat batch effect correction

Taken together, the sample correlation and biological replication analyses showed a strong batch effect that reflected variation due to the identity of the embryo from which the samples originated, rather than variation due to the tissue type of each sample (dorsal/ventral mandibular arch or dorsal/ventral gill arch). If this was left unattended prior to any subsequent differential gene expression analysis, this analysis may have inadvertently revealed genes differentially enriched across individual embryos, for example due to minor variations in age or other conditions during sampling, rather than genes involved in conferring axial identity across the pharyngeal arches. To counteract the batch effect, I therefore employed a batch correction method, ComBat-Seq, which uses empirical Bayes methodology, i.e. a negative binomial regression model, to recover the signal of the biological tissue types within the sample data (Johnson et al., 2007; Leek et al., 2012; Zhang et al., 2020).

Multi-dimensional scaling (MDS) analysis is a complementary means to PCA plots in visualising the level of variation amongst samples of a dataset (Mead, 1992). While PCA plots visualise percentile variation across data reduced into orthogonal principal components, MDS plots chart pairwise variations inherent to a group of samples into an abstract Cartesian space. Here, I have generated MDS plots of the pharyngeal arch samples prior to (Fig. 3.5A) and after ComBat batch removal (Fig. 3.5B), to visualise the results of this batch effect removal technique. The graphs show that ComBat effectively accounts for the batch removal during statistical testing. After this adjustment, MDS plots show samples clustering according to tissue type. In other words, passing the full gene expression matrix alongside a separate batch argument through the empirical Bayesian framework of the ComBat function results in corrected gene expression values from which batch effects have been removed. Consequently, MDS plot shows that the samples now group according to tissue type (Fig. 3.5B). Interestingly, the MDS plot also visualises the anteroposterior and dorsoventral axes along dimension 1 and 2, respectively: while samples from dorsal gill arch tissue group with each other and samples from ventral gill arch tissue also group together, they form a bigger cluster that groups away from the other two clusters that represent mandibular arch samples.

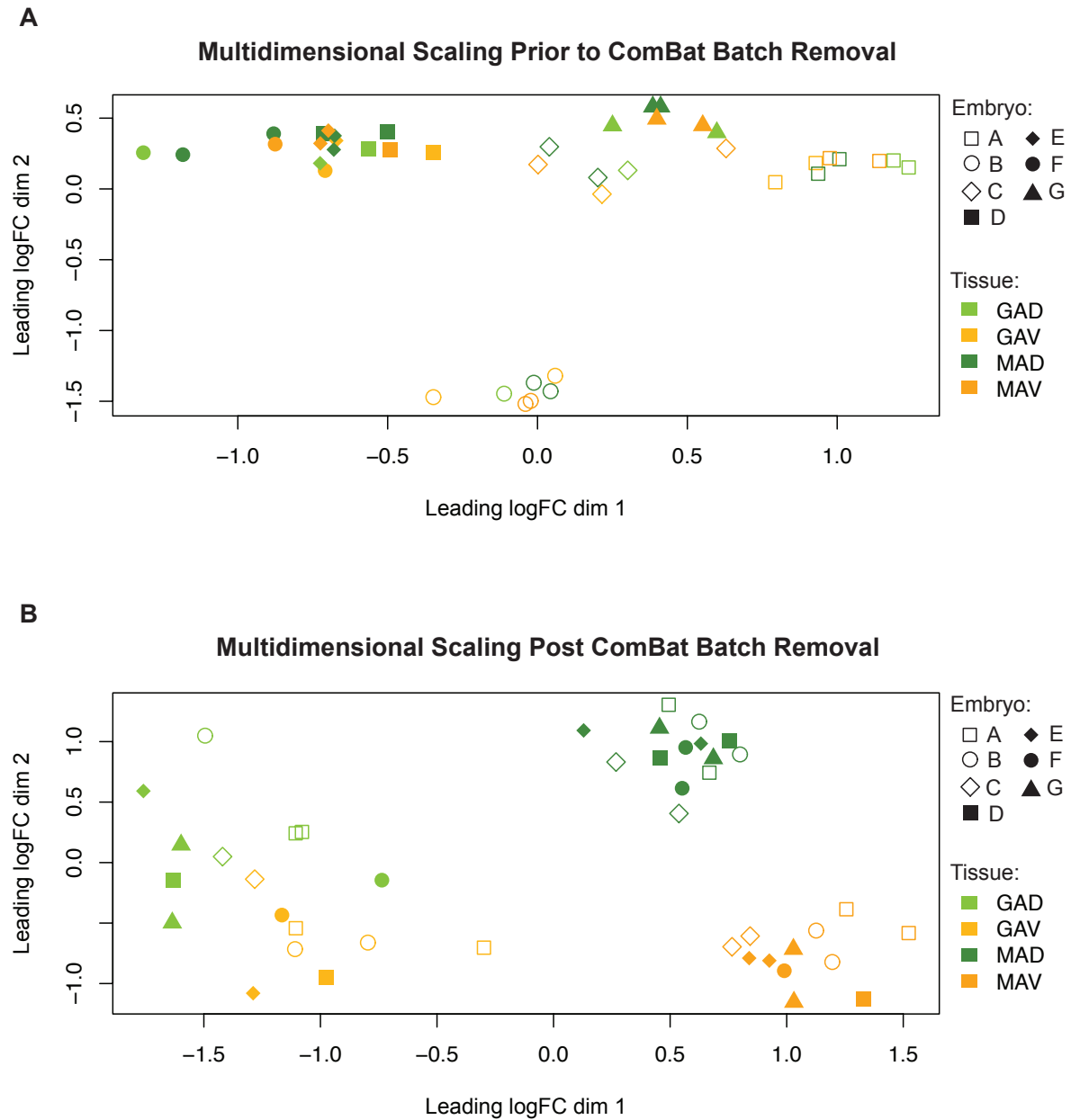


Figure 3.5: Multidimensional scaling plots prior to and after ComBat batch removal. (A) Much like the PCA, the Multi-Dimensional Scaling (MDS) analysis of the original samples shows grouping according to individual embryo from which samples were derived. **(B)** After ComBat batch removal, the variation in the adjusted data is now explained by tissue type, rather than embryo of origin. Embryos A-D: S23-24, embryos E-G: S25-26; Tissue: GAD = gill arch dorsal, GAV = gill arch ventral, MAD = mandibular arch dorsal, MAV = mandibular arch ventral.

3.4.4 Differential gene expression analysis

After quality control had been completed and the batch effect had been addressed, I next set out to complete a differential gene expression analysis across the sampled skate pharyngeal arch domains. First, within EdgeR, the ComBat method outlined above was used, i.e. a negative binomial additive general linear model with a quasi-likelihood F-test was performed. This model design accounted for repeated sampling of tissues from the same individual and p-values were adjusted for multiple testing using the Benjamin-Hochberd method to control the false discovery rate ($FDR \leq 0.05$). Based on this method I identified a number of transcripts as differentially expressed, defined as greater than a 2-fold change between tissue types with an adjusted P-value less than 0.05 (\log_2 -fold changes $[\log_2FC] > 1$, P-value adjusted using Benjamin-Hochberd method < 0.05), within and between arch types at S23-24 and S25-26 (Table 3.3). Complete lists of differentially expressed genes are found in the appendix (Table S3.1 shows candidates selected for validation, Tables S3.2-5 show all differentially expressed genes for stages 24/25 and Tables S 3.6-9 for stages 25/26). Additionally, I visualised the gene expression analyses using Volcano plots (Fig. 3.6-7).

Dorsoventral comparisons	Gill arch S23/24	Mandibular Arch S23/24	Gill Arch S25/26	Mandibular Arch S25/26
Dorsal	10	57	11	46
Ventral	9	54	21	44
Anteroposterior comparisons	Dorsal S23/24	Ventral S23/24	Dorsal S25/26	Ventral S25/26
Gill arch	238	83	45	919
Mandibular arch	200	105	71	691

Table 3.3: Number of significantly expressed transcripts per differential gene expression analysis between and within mandibular and gill arches.

The identification of differentially expressed transcripts within and between arches was corroborated by the correct identification of several known or expected genes within the appropriate spatial territory – e.g. *hand2* and *edn1* were identified as differentially expressed within ventral territories (Fig. 3.6), and *otx2* and *hox* genes were identified as differentially expressed within the mandibular and gill arch territories, respectively (Fig. 3.7). To further biologically validate the findings of this analysis, I selected up to eight of the topmost differentially expressed transcription factors or signalling pathway components per comparison (excluding those already queried by the candidate gene approach or those with well-known functions in axial patterning of the pharyngeal skeleton), and attempted to clone fragments for *in situ* gene expressions analysis. Out of these 37 uniquely identified genes (Table S3.1), I generated riboprobes for an additional 15 candidates, and tested spatial expression of these candidates by mRNA *in situ* hybridisation (ISH).

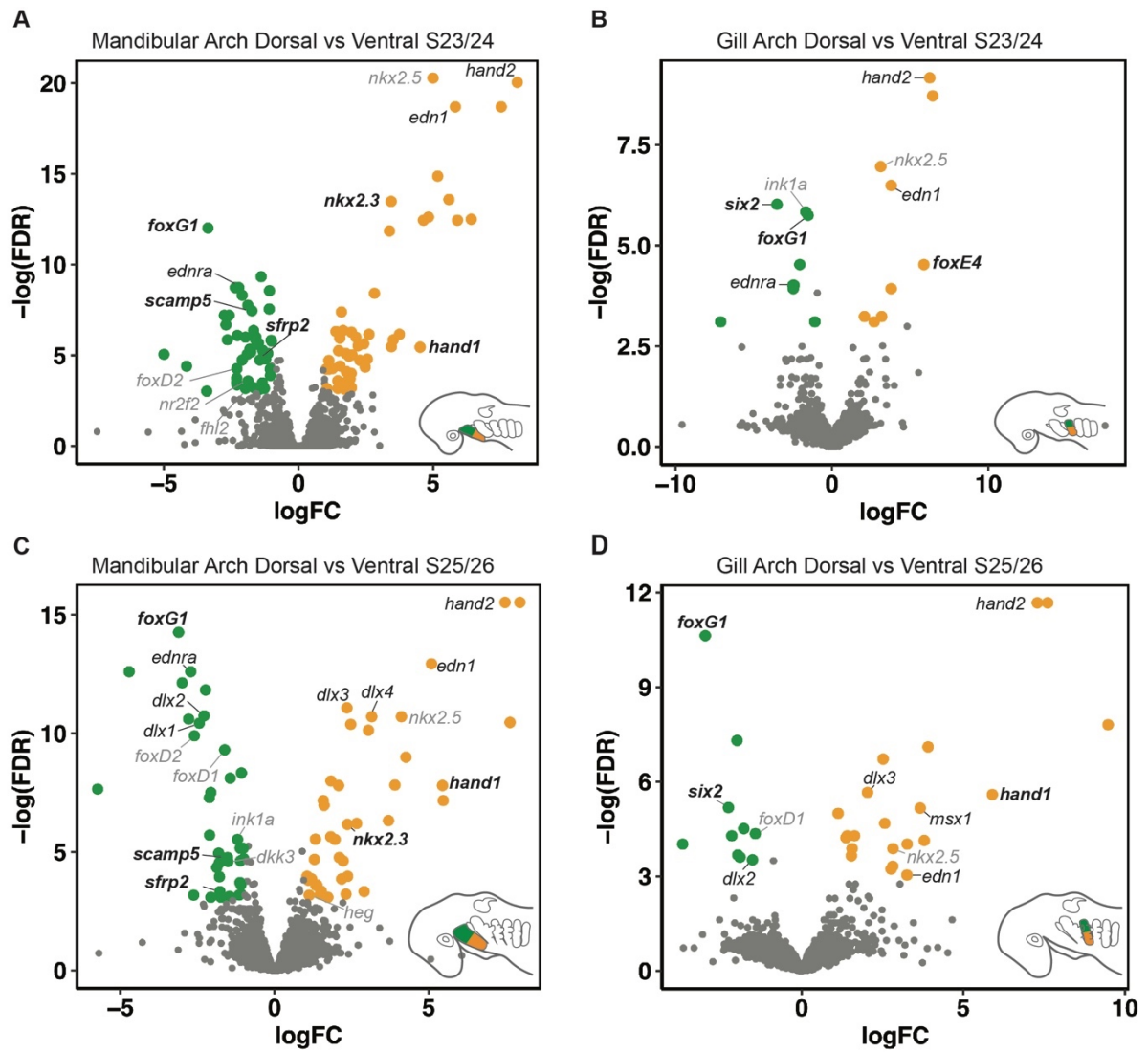


Figure 3.6: Differential gene expression analysis of dorsal and ventral domains of skate pharyngeal arches. Volcano plots illustrate genes that are significantly differentially expressed within the dorsal and ventral domains of the (A) mandibular arch at S23/24, (B) the first gill arch at S23/24, (C) the mandibular arch at S25/26 and (D) the first gill arch at S25/26. Genes with established roles in pharyngeal arch axial patterning are in simple italics, additional genes for which I provide *in situ* validation are in bold italics, and additional factors highlighted by this analysis but not validated by ISH are in grey italics. Schematic skate heads depict which tissues were compared: dorsal mandibular/gill arch in green, ventral mandibular/gill arch in orange.

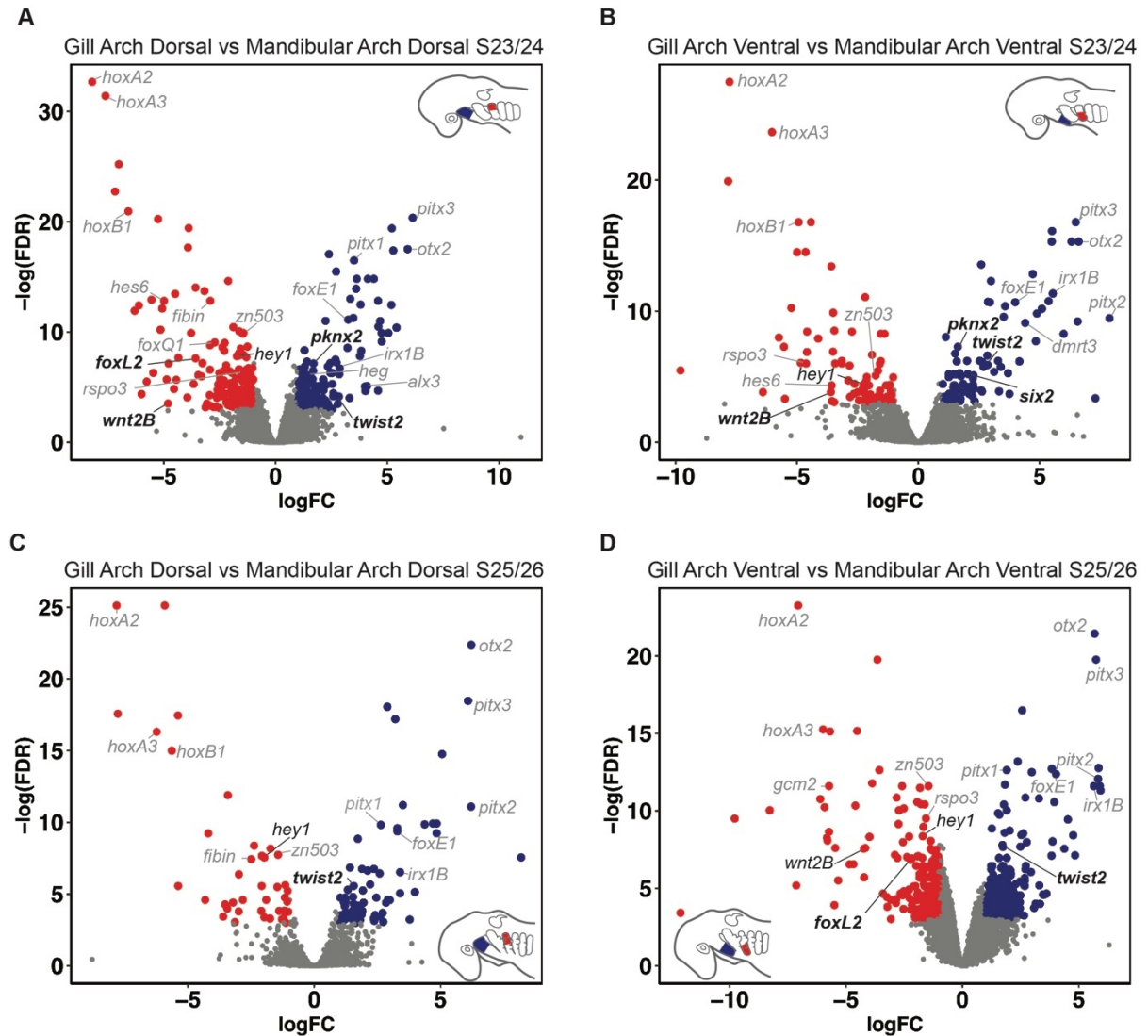


Figure 3.7 Differential gene expression analysis of anterior and posterior upper and lower domains of skate pharyngeal arches. Volcano plots illustrate genes that are significantly differentially expressed (A) between the dorsal domains of the mandibular and the gill arch at S23/24, (B) between the ventral domains of the mandibular and the gill arch at S23/24, (C) between the dorsal domains of the mandibular and the gill arch at S25/26 and (D) between the ventral domains of the mandibular and the gill arch at S25/26. Genes with established roles in pharyngeal arch axial patterning are in simple italics, additional genes for which I provide *in situ* validation are in bold italics, and additional factors highlighted by this analysis but not validated by ISH are in grey italics. Schematic skate heads depict which tissues were compared: anterior mandibular/gill arch in red, posterior mandibular/gill arch in blue.

3.4.5 Additional dorsoventrally polarised transcriptional features of the pharyngeal arches in skate

Among candidates differentially expressed in the dorsal mandibular or gill arch territories, I selected *foxG1*, *sfrp2* and *twist2* for validation by mRNA ISH. In my differential gene expression analysis, *foxG1* was enriched in dorsal pharyngeal arch territories, while *sfrp2* and *twist2* were both overexpressed in the dorsal mandibular arch specifically. ISH confirmed this prediction for *foxG1*, but the expression patterns of *sfrp2* and *twist2* diverged from the differential gene expression results. *foxG1* was expressed in the dorsal domains of the mandibular, hyoid and gill arches in skate (Fig. 3.8A), and this signal originated from the dorsal epithelium and dorsal core mesoderm of each pharyngeal arch (Fig. 3.8B). *sfrp2* and *twist2* expression was not dorsal mandibular arch specific, rather, they were expressed in discontinuous dorsal and ventral domains to the exclusion of the presumptive joint domains across the mandibular, hyoid and gill arches in skate (Fig. 3.8C, E), localising to the dorsal and ventral mesenchyme in each arch (Fig. 3.8D, F). However, in each case, the dorsal mandibular arch domain displayed stronger levels of signal than the morphologically smaller upper and lower gill arch domains (Fig. 3.8C, E), which may explain why the differential gene expression showed both *sfrp2* and *twist2* transcripts enriched in upper jaw primordia.

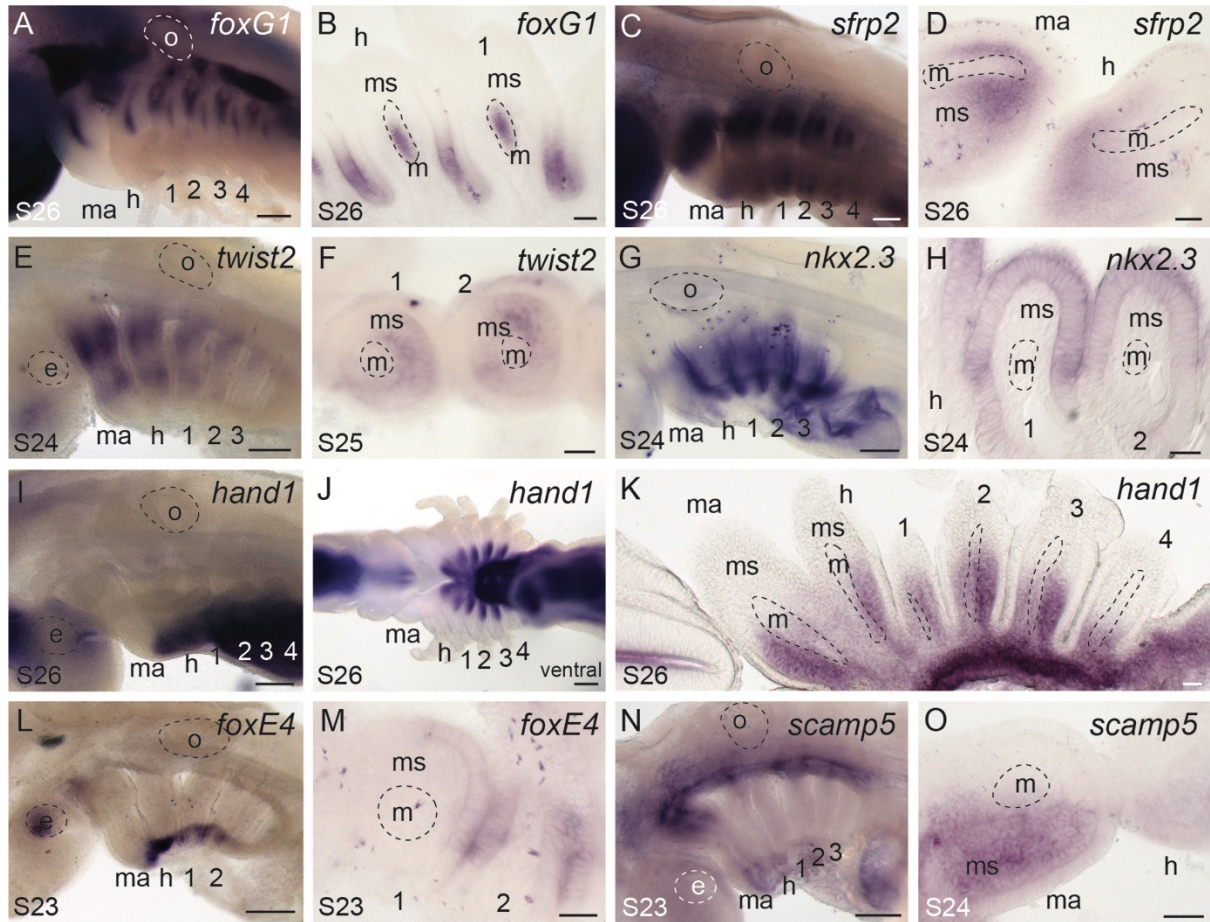


Figure 3.8: Additional genes exhibiting polarised expression along the DV axis of skate pharyngeal arches. (A) At S26 *foxG1* is expressed in dorsal (B) pharyngeal arch epithelium and core mesoderm of skate mandibular, hyoid and gill arches. (C) At S26 *sfrp2* is expressed in dorsal and ventral (D) mesenchyme of each pharyngeal arch, excluding the intermediate domains. (E) At S24 *twist2* is also expressed in dorsal and ventral (F) mesenchyme of each pharyngeal arch, excluding the intermediate domains. (G) At S24 *nkx2.3* is expressed in the ventral and intermediate (H) epithelium of each pharyngeal arch. (I) At S26 *hand1* transcripts localise to the (j) ventral (L) mesenchyme of each pharyngeal arch. (L) At S23 *foxE4* is expressed in the ventral extreme of the pharyngeal region, (M) with transcripts localising to the epithelium. (N) At S23 *scamp5* is expressed in the dorsal (O) mesenchyme of the mandibular arch. 1, 2, 3, 4: gill arches 1-4; e, eye; h, hyoid; m, mandibular arch; me, mesoderm; ms, mesenchyme; o, otic vesicle. Scale bars: A, C, E, G, I, J, K, L, N = 400um; B, D, F, H, M, O = 25um.

Among genes with enriched expression in ventral pharyngeal arch territories, I selected *nkx2.3*, *hand1* and *foxE4* for validation by mRNA ISH. My differential gene expression analysis predicted *nkx2.3* as a marker of the lower mandibular arch, *hand1* as a marker of all ventral territories, and *foxE4* as a marker of the ventral gill arch. Much like the dorsally overexpressed genes selected for validation, ISH did not fully confirm these predictions. ISH showed *nkx2.3* was expressed in the ventral and intermediate endoderm not just within the mandibular, but also within the hyoid and gill arches in skate (Fig. 3.8G, H). *hand1* was similarly expressed in ventral domains across all pharyngeal arches, though within the mesenchyme (Fig. 3.8I-K). *foxE4* was also expressed in narrow domains of the ventral mandibular, hyoid and gill arches in skate (Fig. 3.8L), localising to the pharyngeal endoderm (Fig. 3.8M).

Finally, this analysis also highlighted several transcripts that were differentially expressed between pharyngeal arch territories, but that were not immediately annotated by BLAST against UniProt/Swiss-Prot, and that required further manual annotation by BLASTing against the larger NCBI non-redundant (nr) database. Amongst these was *scamp5*, which was predicted to be a marker of the upper jaw in skate, as my differential gene expression analysis consistently recovered it as overexpressed in the dorsal mandibular arch if compared to the ventral mandibular arch, across S23-24 and S25-26. ISH confirmed that *scamp5* is indeed a marker of dorsal mandibular arch mesenchyme in skate (Fig. 3.8N, O).

3.4.6 Distinct gene expression features within the mandibular and gill arch mesoderm

Additionally, I also used my differential gene expression analysis to test for genes with anteroposterior-specific enrichment, i.e. mandibular arch or gill arch-specific expression domains. Amongst candidates predicted to be differentially expressed in the mandibular arch, I selected *six2* and *pknox2* for validation by mRNA ISH. I also included *tbx18* as a potential additional marker of mandibular arch identity, as previous work had discovered *tbx18* expression in the developing jaw, though not in the gill arches in skate (Criswell et al., 2020). Amongst candidates predicted to be overexpressed in the gill arch, I selected *lhx9*, *foxl2*, *gcm2*, *wnt2b* and *foxq1* for validation. As opposed to the genes with predicted overexpression in dorsal or ventral domains, all predicted markers of anteroposterior identity were confirmed

by ISH. They did, however, differ in terms of the tissues that they were expressed in: one group of these genes, comprising *six2*, *pknox2*, *tbx18* and *lhx9* marked the mesoderm, whereas a second group, comprising *foxl2*, *gcm2*, *wnt2b* and *foxq1*, marked the endoderm.

ISH showed expression of *six2* in the mesodermal core of the skate mandibular arch as well as in the dorsal epithelium across all pharyngeal arches (Fig. 3.9A, B). *pknox2* (Fig. 3.9C, D) and *tbx18* (Fig. 3.9E, F) were expressed exclusively in the mandibular arch mesoderm, to the exclusion of the hyoid and gill arches in skate. *lhx9*, on the other hand, was expressed in the mesodermal cores of the hyoid and gill arches, excluding the mandibular arch (Fig. 3.9G-H). Together, these ISH results confirmed the differential gene expression analysis, which had returned all of these genes as putative markers of anteroposterior identity.

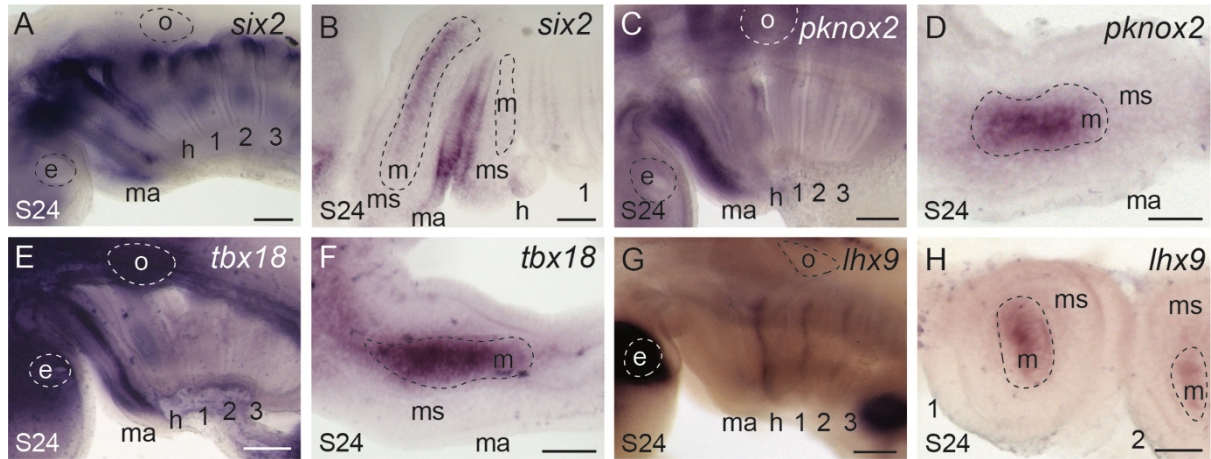


Figure 3.9: Distinct gene expression features of mandibular and hyoid/gill arch muscle progenitors. (A) At S24, *six2* is expressed dorsally across all pharyngeal arches, in addition to a thin expression domain along the dorsoventral axis unique to the mandibular in skate. (B) *six2* is expressed uniquely in the mesoderm of the mandibular across the dorsoventral axis, in addition to the dorsal epithelium of each arch. (C) At S24, *pknox2* is also expressed solely in the mandibular (C) core mesoderm. (D) At S24, *tbx18* expression uniquely marks the (E) mesoderm of the mandibular arch in skate. (G) At S24, *lhox9* expression is restricted to the hyoid gill arches in skate, where (H) it marks the core mesoderm of each arch. 1, 2, 3, 4: gill arches 1-4; e, eye; h, hyoid; m, mandibular arch; me, mesoderm; ms, mesenchyme; o, otic vesicle. Scale bars: A, C, E, G = 400um, B, D, F, H = 25um.

3.4.7 Gene expression features of presumptive gill epithelium and external gill buds

From amongst the genes with enriched expression in gill arch territories, I also selected *foxl2*, *gcm2*, *wnt2b* and *foxq1* for validation by mRNA ISH. While they shared this predicted enrichment with *lhx9*, their expression domains differed from *lhx9* in terms of the tissues they were expressed in: I found *foxl2* expression was shared by the gill-forming endodermal epithelium and developing gill buds of all pharyngeal arches as well as in the core mesoderm of each pharyngeal arch (Fig. 3.10A, B). The endodermal expression domain of *foxl2* also includes the presumptive spiracular primordium - i.e. the precursors of the reduced gill lamellae of the mandibular arch (Fig. 3.10A). *gcm2* expression was similarly shared throughout the developing gill buds of the hyoid and gill arches (Fig. 3.10C, D), as was *wnt2B* expression (Fig. 3.10E, F) and *foxq1* (Fig. 3.10G, H). In contrast to *foxl2*, expression of *gcm2*, *wnt2b*, and *foxq1* was absent from the mandibular arch. This validation by ISH showed that my differential gene expression had accurately predicted the gill-arch specific expression patterns of *gcm2*, *wnt2b*, and *foxq1*, though not of *foxl2*, which was also found in the mandibular arch. However, as *foxl2* marks the gill buds, the enrichment of *foxl2* transcripts in samples originating from the first gill arch as opposed to the mandibular arch is likely an artefact of the morphology of the gill bud on the first gill arch, which is much larger if compared to the thin ridge of *foxl2* expression in the presumptive spiracular primordium on the mandibular arch (Fig. 3.10A, B)

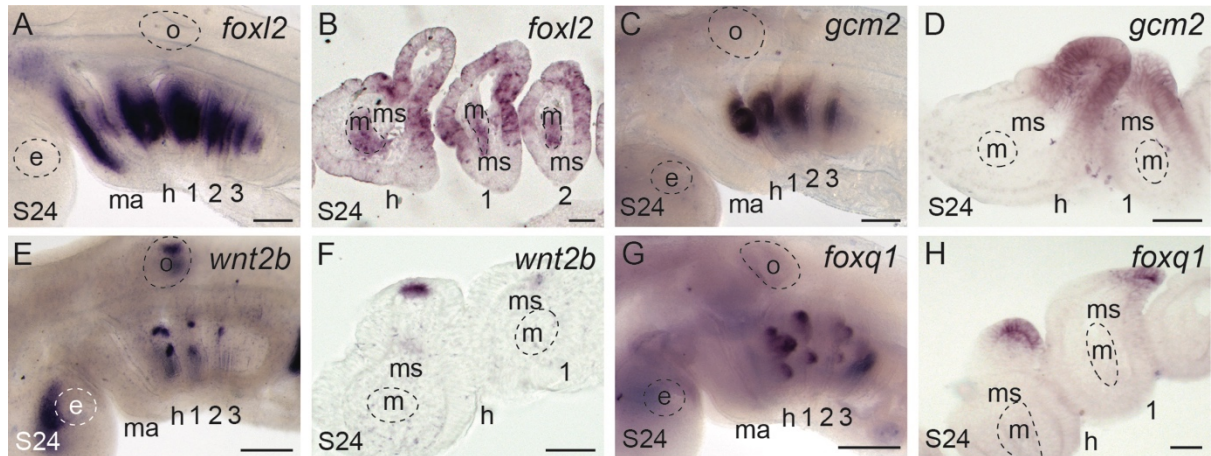


Figure 3.10: Conserved and novel molecular markers of gill development. (A) At S24 *foxl2* expression marks the (B) gill-forming epithelium and core mesoderm of all pharyngeal arches in skate. (C) At S24 *gcm2* expression also marks (D) the endoderm and developing gill buds of the hyoid and gill arches. (E) At S24 *wnt2b* is expressed in the (F) tips of the out-budding gills. (G) At S24, *foxq1* is also expressed in the (H) tips of developing gill buds. 1, 2, 3, 4: gill arches 1-4; e, eye; h, hyoid; m, mandibular arch; me, mesoderm; ms, mesenchyme; o, otic vesicle. Scale bars: A, C, E, G = 400um; B, D, F, H = 25um.

3.5 Discussion

Here first assembled a *de novo* transcriptome from upper and lower mandibular and gill arch primordia in skate, and then subsequently tested these samples for differentially expressed genes through a series of differential expression analyses that screened for transcriptional features enriched within and between arch samples. From amongst the resulting additional candidates of axial identity markers, I further biologically validated 15 genes through *in situ* hybridisation, which extends the list of genes with known dorsoventrally and anteroposteriorly polarised expression in the gnathostome pharyngeal arches and reveals new molecular markers of mandibular and gill arch derivatives.

3.5.1 Comparative transcriptomics add candidates to the dorsoventral patterning programme of developing pharyngeal arches in skate

Some of the genes identified here by differential gene expression analysis and validated through *in situ* hybridisation as sharing expression patterns that are polarised along the dorsoventral axis of the pharyngeal arches in skate (Fig. 3.11), are known to play roles in craniofacial development. Therefore, the expression patterns established here in skate complement previous findings from bony fishes and, occasionally, lamprey.

	Mandibular arch expression						Gill arch expression	
Dorsal	<i>scamp5</i> <i>six2</i> <i>tbx18</i> <i>pknox2</i>	<i>foxg1</i>	<i>foxl2</i>	<i>twist2</i>	<i>sfrp2</i>	<i>lhx9</i>		
Intermediate	<i>six2</i> <i>tbx18</i> <i>pknox2</i>		<i>foxl2</i>	<i>nkx2.3</i>		<i>lhx9</i>	<i>gcm2</i> <i>wnt2b</i> <i>foxq1</i>	
Ventral	<i>six2</i> <i>tbx18</i> <i>pknox2</i>	<i>hand1</i>	<i>foxe4</i>	<i>twist2</i> <i>nkx2.3</i>	<i>sfrp2</i>	<i>lhx9</i>	<i>gcm2</i> <i>wnt2b</i> <i>foxq1</i>	

Figure 3.11 Additional patterning candidates identified by differential gene expression analysis and ISH validation. Red and blue squares indicated mandibular arch and gill arch expression, respectively. Genes listed in the overlap of the two squares are expressed across all pharyngeal arches, whereas expression listed solely in mandibular arch or gill arch squares are arch specific.

foxG1, here shown to be expressed in the dorsal epithelium and mesoderm of the mandibular, hyoid and gill arches in skate (Fig. 3.8A, B), functions in the morphogenesis of the forebrain in mice (Tao & Lai, 1992; Dou et al., 1999; Hanashima et al., 2002). More recently, *FoxG1* has been shown to play a role in neurocranial and pharyngeal skeletal development in mice, where it is expressed in the cephalic surface ectoderm (Compagnucci & Depew, 2020). In the absence of *FoxG1*, expression patterns of various transcription factors and signalling cascade components in the upper jaw primordium are disrupted: in *FoxG1*^{-/-} mice, *Bmp4* expression in the lower jaw is unaffected, but an additional epithelial domain of *Bmp4* expression in the distalmost tip of the upper jaw primordia expands dorsally towards the eye, while *Fgf8*, usually expressed in the oral ectoderm (Abu-Issa et al., 2002), is lost from the upper jaw epithelium (Compagnucci & Depew, 2020), and the usually ventral expression of *Pitx1* and the typical expression of *Msx1* in the distal ‘caps’ of the upper and lower jaw in mice also expand within the upper jaw primordia (Compagnucci & Depew, 2020). In combination with the epithelial expression shared across the dorsal domains across all pharyngeal arches in skate, this points to a likely ancestral role of *foxG1* in regulating dorsal polarity of pharyngeal arch derivatives across all arches within gnathostomes.

In contrast to its role in cranial surface ectoderm patterning, the dorsal mesodermal expression of *foxG1* in the pharyngeal arches I report here has not been extensively investigated. However, this mesodermal expression domain of *foxG1* may underpin a classic model of cranial muscle development, which posits that pharyngeal arch mesodermal cores subdivide into distinct dorsal and ventral domains before assuming their individual muscle identity (Edgeworth, 1935; Kimmel et al., 2001). Not many transcription factors or signalling pathways have of yet been identified in playing functional roles in this model, with the exception of ventral *edn1* (discussed in chapter 1) and dorsal *engrailed* expression in muscle progenitors in zebrafish (Kimmel et al., 2001). Dorsal *foxG1* expression matches the first step in this scenario, which is the subdivision of dorsal and ventral domains of mesoderm inside the cores of each pharyngeal arch. Hence, *foxG1* may be a promising new candidate in the developmental patterning programme underpinning this classical model of cranial muscle development across gnathostomes.

I find that *sfrp2* (Fig. 3.8C, D) and *twist2* (Fig. 3.8E, F) share discontinuous expression domains in the dorsal and ventral mesenchyme of skate pharyngeal arches, excluding the presumptive joint domains, reminiscent of *gsc* and prochondrogenic transcription factor *barx1* (see chapter 2). In chick, *sfrp2* is expressed in migrating cranial neural crest cells (Terry et al., 2000), while in mouse, it is expressed in the mesenchyme of the maxillary and mandibular domains of the mandibular arch (Leimeister et al., 1998). *sfrp2* is also expressed in the pharyngeal arches in zebrafish (Tendeng & Houart, 2006), where RNA-seq experiments found it to be enriched in cranial neural crest cells of the dorsal mandibular and hyoid arches (Askary et al., 2017). However, wholemount fluorescent *in situ* hybridisation in zebrafish detected *sfrp2* expression only in the dorsal mesoderm, and TALEN and CRISPR induced early frameshift mutations in this gene did not lead to any observable skeletal craniofacial phenotypes (Askary et al., 2017). My findings in skate conflict somewhat with the findings in zebrafish: in my ISH experiments I did not find corresponding expression of *sfrp2* in the mesoderm, though I did detect expression in the dorsal pharyngeal arch mesenchyme domains—as well as in ventral mesenchyme domains across all arches.

twist2 encodes a basic helix-loop-helix transcription factor that is expressed in the dermis, cranial mesenchyme, pharyngeal arches and tongue of the mouse (Li et al., 1995), and in the mesenchyme of the mandibular and hyoid arches in chick (Scaal et al., 2001). Human nonsense mutations in *twist2* are linked to Setleis syndrome, a focal facial dermal dysplasia, and *twist2* knockout mice exhibit a similar facial phenotype (Tukel et al., 2010). In combination with the findings in skate, i.e. dorsal and ventral domains to the exclusion of the presumptive joint domains across all arches, this is suggestive of a conserved role of *sfrp2* and *twist2* in cranial neural crest patterning.

nkx2.3, *foxE4* and *hand1* were among the genes with predicted expression in ventral pharyngeal arch territories, and their shared ventral expression across all pharyngeal arches in skate matches previous findings on their expression and function across other taxa. *nkx2.3* is expressed in the endodermal lining of the pharynx in frog, mouse and zebrafish (Evans et al., 1995; Biben et al., 2004; Lee et al., 1996), and in addition to the expression in skate this suggests a conserved role of *nkx2.3* in patterning the ventral pharynx across gnathostomes. *hand1* functions in cardiac morphogenesis in mouse (Srivastava et al., 1995; Riley et al., 1998),

but is also expressed in the ventral mesenchyme of the pharyngeal arches (Clouthier et al., 2000). Targeted deletion of *hand1* alone does not result in craniofacial defects, though ablation of *hand1* on a *hand2* heterozygous background results in ventral midline defects within the jaw skeleton, suggesting a dosage dependent role for hand genes in mandibular skeletal patterning (Barbosa et al., 2007). Skate *hand1* expression (Fig. 8I-K) largely overlaps with the ventral mesenchymal expression of *hand2* (Chapter 2, Fig. 2.4), consistent with an ancestral combinatorial role for Hand genes patterning the ventral pharyngeal arch skeleton of gnathostomes. Finally, *foxE4* is expressed in the pharyngeal endoderm of non-teleost ray-finned fishes (Minarik et al., 2017), and in the endostyle (an endodermally-derived secretory organ and putative evolutionary antecedent of the thyroid gland) in amphioxus (Yu et al., 2002; Hiruta et al., 2005). The conserved *foxE4* expression in ventral pharyngeal endoderm in skate (Fig. 8L, M) points to an ancestral role for this transcription factor in pharyngeal endodermal patterning. Taken together, *nkx2.3*, *hand1* and *foxE4* may play a conserved role in patterning the ventral pharyngeal arches and their derivatives across gnathostomes (and potentially across chordates in the case of *foxE4*).

Finally, this work suggests *scamp5* as a novel player in patterning the mandibular arch mesenchyme and upper jaw. *scamp5* encodes a secretory carrier membrane protein expressed in the synaptic vesicles of neuroendocrine tissues (Fernández-Chacón & Südhof, 2000; Han et al., 2009), and falls within the same topologically associated domain as single nucleotide polymorphisms associated with orofacial clefting in humans (Carlson et al., 2018). Although this gene has not been previously implicated in pharyngeal arch skeletal patterning, the above observations, combined with the novel *in situ* expression in skate, highlight this gene as promising candidates for further study. Expression analyses and functional characterisation of these genes in bony fish model systems will reveal whether the expression patterns reported here are general features of gnathostomes, or derived features of cartilaginous fishes, and possible undiscovered roles for these gene products in craniofacial skeletal development.

3.5.2 Divergent patterning programmes within the mesodermal progenitors of the mandibular and gill arches

The mesodermal cores of vertebrate pharyngeal arches give rise to the branchiomic musculature, i.e. the muscles of mastication and facial expression in mammals and the muscles of the jaw and gill arches in fishes (Tzahor & Evans, 2011; Ziermann & Diogo, 2019; Sleight & Gillis, 2020). The segmented arrangement of the mesoderm sequestered into the arch cores has long been of scientific interest and was studied in concert with questions on head segmentation of vertebrates (Kimmel et al., 2001). Some elements of the pharyngeal myogenic developmental programme are also serial in nature, and genes such as *Tbx1* (Kelly et al., 2004), *Islet-1* (Nathan et al., 2008), *Lhx2* (Harel et al., 2012), *myosin heavy chain* (Ziermann et al., 2017) and *MyoD* (Schilling and Kimmel, 1997; Poopalasundaram et al., 2019) are shared across the mesodermal cores of all pharyngeal arches. Other genes are arch-specific and regulate the development of distinct muscular features. For example, mandibular arch specific *Pitx2* specifies jaw musculature in mice, in part through positive regulation of core mesodermal *Six2* expression (Shih et al., 2007). It therefore appears as though pharyngeal arch myogenesis is regulated by a core transcriptional programme, with additional arch-specific gene expression directing specific branchiomic muscle identities.

six2, *tbx18*, and *pknox2*, the markers of mandibular arch mesoderm identified here through ISH in skate, as well as the mesodermal marker of the hyoid and gill arches, *lhx9*, may play a role in this muscle specification programme. *Tbx18* expression within the mandibular arch has previously been reported in mouse (Kraus et al. 2001), zebrafish (Begemann et al., 2002) and chick (Haenig & Kispert, 2004), while *Pknox2* has previously been reported from microarray analysis of the mouse mandibular arch (Feng et al., 2009). However, neither *Tbx18* nor *Pknox2* have yet been implicated in the development of mandibular arch-derived musculature. Furthermore, *lhx9* marking the mesodermal cores of the hyoid and gill arches, but not the mandibular arch is a feature so far unreported in any other taxon. Taken together, these findings highlight an ancestral role for *six2* in patterning mandibular arch-derived musculature in jawed vertebrates, possibly in conjunction/parallel with *tbx18* and *pknox2*, as well as *lhx9* as a novel marker of hyoid and gill arch muscle progenitors.

3.5.3 Novel gene expression features of the presumptive gill epithelium and external gill buds

The gills of fishes derive from the endodermal epithelium of the hyoid and gill arches (Gillis & Tidswell, 2017; Hockman et al., 2017; Warga & Nüsslein-Volhard, 1999). In skate, gills form initially as a series of transient embryonic external gill filaments, which are eventually remodelled and resorbed into internal gill lamellae (Pelster & Bemis, 1992). The differential expression analysis presented here revealed a number of genes to be differentially expressed between the mandibular and first gill arch, some of which proved, through ISH validation, to be markers of developing gills in skate. *foxl2* is expressed in the gill-forming endodermal epithelium and developing gill buds of all pharyngeal arches, including the presumptive spiracular primordium - i.e. the putative precursors of the vestigial gill lamellae of the mandibular arch (see next chapter), as well as in the core mesoderm of each pharyngeal arch (Fig. 3.10A, B), which is consistent with previous reports of *foxL2* expression from mouse (Jeong et al., 2008; Marongiu et al., 2015) and the shark, *Scyliorhinus canicula* (Wotton et al., 2007). The *gcm2* expression in the developing gills in skate (Fig. 3.10C, D) matches expression patterns observed in the developing gills of shark and zebrafish (Hogan et al., 2004; Okabe & Graham, 2004), and was therefore likely ancestrally required for gill development in gnathostomes. However, there are no previous reports of *wnt2b* or *foxq1* expression during gill development in other taxa, pointing to a possible novel role for these factors in driving outgrowth of external gill filaments.

3.6 Summary

Here I have generated a *de novo* transcriptome of the dorsal and ventral mandibular and gill arch territories of the skate, and I have used this assembly as the basis for differential gene expression analyses to identify potential novel gene expression features of these territories. From this analysis, I validate and report shared dorsal epithelial and mesodermal expression of *foxG1*, discontinuous expression of *sfrp2* and *twist2*, and ventral expression of *nkx2.3*, *hand1*, and *foxe4* across all pharyngeal arches in skate. Taken together, these expand the conserved transcriptional network patterning the dorsoventral axis of the mandibular, hyoid and gill arches in the gnathostome crown group, and provide further developmental evidence consistent with the hypothesis of serial homology of the gnathostome jaw, hyoid and gill arch skeleton.

Additionally, this work also uncovered distinct transcriptional features of the mandibular and gill arches in skate, including dorsal mesenchymal expression *scamp5* in the mandibular arch, mandibular arch mesoderm-specific expression of *six2*, *tbx18* and *pknox2*, hyoid and gill arch mesoderm-specific expression of *lhx9*, and gill-bud specific expression of *foxl2*, *gcm2*, *wnt2b* and *foxq1*. These gene expression features may reflect arch-specific divergences from the ancestral pharyngeal dorsoventral patterning programme, possibly functioning downstream of global anteroposterior patterning mechanisms (e.g. the *Hox* code of the vertebrate head). According to this view, the mesenchymal *scamp5* expression may be involved in upper jaw skeletogenesis while *six2*, *tbx18* and *pknox2* pattern the mandibular muscles, functioning in parallel with local signals from the oral epithelium to effect anatomical divergence of the mandibular arch derivatives. Conversely, mesodermal and endodermal gene expression features unique to the gill-bearing hyoid and gill arches, i.e. mesodermal *lhx9* and endodermal *foxl2*, *gcm2*, *wnt2b* and *foxq1* may underpin the evolution and development of arch-specific muscular and gill fates, respectively.

Chapter 4:

Vestigial gill structures derive from the mandibular arch of the skate

4.1 Abstract

Behind the jaw of cartilaginous fishes (sharks, skates and rays) sits a gill-like epithelial elaboration called a “pseudobranch”. It was classically thought that this structure is a vestige of the ancestral gill-arch like condition of the jawed vertebrate mandibular arch. However, hypotheses of jaw evolution by transformation of a gill arch have been largely abandoned, owing to a gap in the jawed vertebrate fossil record, and the pseudobranch is now regarded as a derivative of the second (hyoid) pharyngeal arch. Here, I demonstrate by cell lineage tracing in the skate (*Leucoraja erinacea*) that the pseudobranch does, in fact, derive from the mandibular arch, and that it shares gene expression features and cell types with developing gills. I also show that the mandibular arch pseudobranch is supported by a spiracular cartilage, and that this cartilage is patterned by a *shh*-expressing epithelial signalling centre. This parallels the condition seen in gill arches, where cartilaginous appendages called branchial rays support the respiratory lamellae of the gills, and are patterned by a *shh*-expressing gill arch epithelial ridge (GAER). Taken together, these findings support serial homology of jawed vertebrate mandibular and gill arch derivatives, and an ancestral gill arch-like nature of the mandibular arch.

4.2 Introduction

Most elasmobranchs (sharks, rays, and skates) possess a small hole behind each eye called a spiracle (Fig. 4.1A). These spiracles provide a passageway for water from outside the animal into the buccopharyngeal chamber (Ridewood, 1896; Goodrich, 1909, 1930; El-Toubi, 1947; Romer, 1970; Barry et al. 1988; Tomita et al., 2018). Inside each spiracle sits an epithelial, gill-like feature, called pseudobranch (Fig. 4.1B). In elasmobranchs, the pseudobranch is internally supported by a small cartilaginous element in the anterior wall of the spiracle, called spiracular cartilage (Fig. 4.1C, Ci), which in skates is characterised by a leaf-shaped appearance. Spiracles first emerge during the embryonic development of the pharyngeal arches, when the first pharyngeal pouch contacts overlying surface ectoderm, delineating the mandibular (first) and hyoid (second) pharyngeal arches. Later in development, the resulting slit between these two arches is reduced to a small spiracular opening that shifts dorsally, and that sits immediately behind the eye (Goodrich, 1958; Barry et al., 1988). Spiracles are also found in early branching bony fishes (coelacanth, sturgeon, paddlefish and bichirs), and are therefore likely a plesiomorphic feature of gnathostomes (jawed fishes). In bichirs, which are known for lung-based respiration similar to lungfish and tetrapods, spiracles have been adapted for air-breathing (Graham et al., 2014) and they have been suggested to have possessed a similar function in stem tetrapodomorphs during the transition from water to land (Clack, 2007). Teleost fishes do not possess a spiracle, though they have retained a pseudobranch on the inner surface of the opercular gill cover (Laurent & Dunel-Erb, 1984).

4.2.1 Interpreting the spiracle as evidence of the gill arch-like ancestry of the jaw

The classical theory of jaw-gill arch serial homology in vertebrate evolution proposes that the gnathostome jaw originated through transformation of the anterior-most gill arch (Gegenbaur, 1878; Romer, 1970). This theory interprets the gnathostome jaw and other mandibular arch derived features as modified from a gill arch-like condition, implying the ancestral existence of a gill bearing mandibular arch. Because of the anatomical similarities between the mandibular pseudobranch and gills—i.e. the shared structure and histology of their lamellae, and their location in contact with water of the pharyngeal cavity (Fig. 4.1D)—

the pseudobranch has historically been interpreted as a vestigial gill on the mandibular arch, while the spiracle has been interpreted as a vestigial gill slit (Mallatt, 1996; Wegner, 2015). Fossil evidence of spiracles support this view, as paired spiracles are indeed found in early stem gnathostomes as well as stem bony and cartilaginous fishes (Stensiö, 1947; Young and Zhang, 1992; Zhu et al., 2013, King et al. 2017; Burrows et al., 2020), and generally match the interpretation of a reduced first gill slit, which was displaced dorsally as the hyoid moved to support the jaws. The presence of spiracles in fossils is also often inferred from notches in skull roofing elements or spiracular grooves, for example in placoderms (Young & Zhang, 1992) and actinopterygians (e.g. Gardiner, 1984; Basden et al., 2000), though these notches and grooves alone do not provide further insights into the interior organisation of the spiracles.

Elasmobranchs also possess a series of paired appendages that project laterally from their gill arches, known as branchial rays (Fig. 4.1B, C), which function to provide skeletal support to the gills (Gillis et al., 2009a, Gillis & Hall, 2016). The relationship between branchial rays and their associated gill arch cartilages bears a striking resemblance to that of the spiracular cartilage and the jaw skeleton (Fig. 4.1E-G), and this has led to the interpretation of the spiracular cartilage as a vestige of mandibular arch branchial rays (Gegenbaur, 1872, 1878; Holmgren & Stensiö, 1936; El-Toubi, 1947). This proposed correspondence is rooted not only in their anatomical organisation and appearance—the latter is particularly apparent in some sharks, as their spiracular cartilages develop as slender rods, which closely resemble branchial rays—but also because they chondrify later than the jaw elements, much like the branchial rays chondrify later than the epi- and ceratobranchial cartilages of the gill arches (El-Toubi, 1947). In skates, the spiracular cartilage is similarly positioned in association with the palatoquadrate of the jaw (Fig. 4.1E), but rather resembles a leaf-like sheet of cartilage that spans the space between two slender cartilaginous thickenings at either end (Fig. 4.1Ci, E).

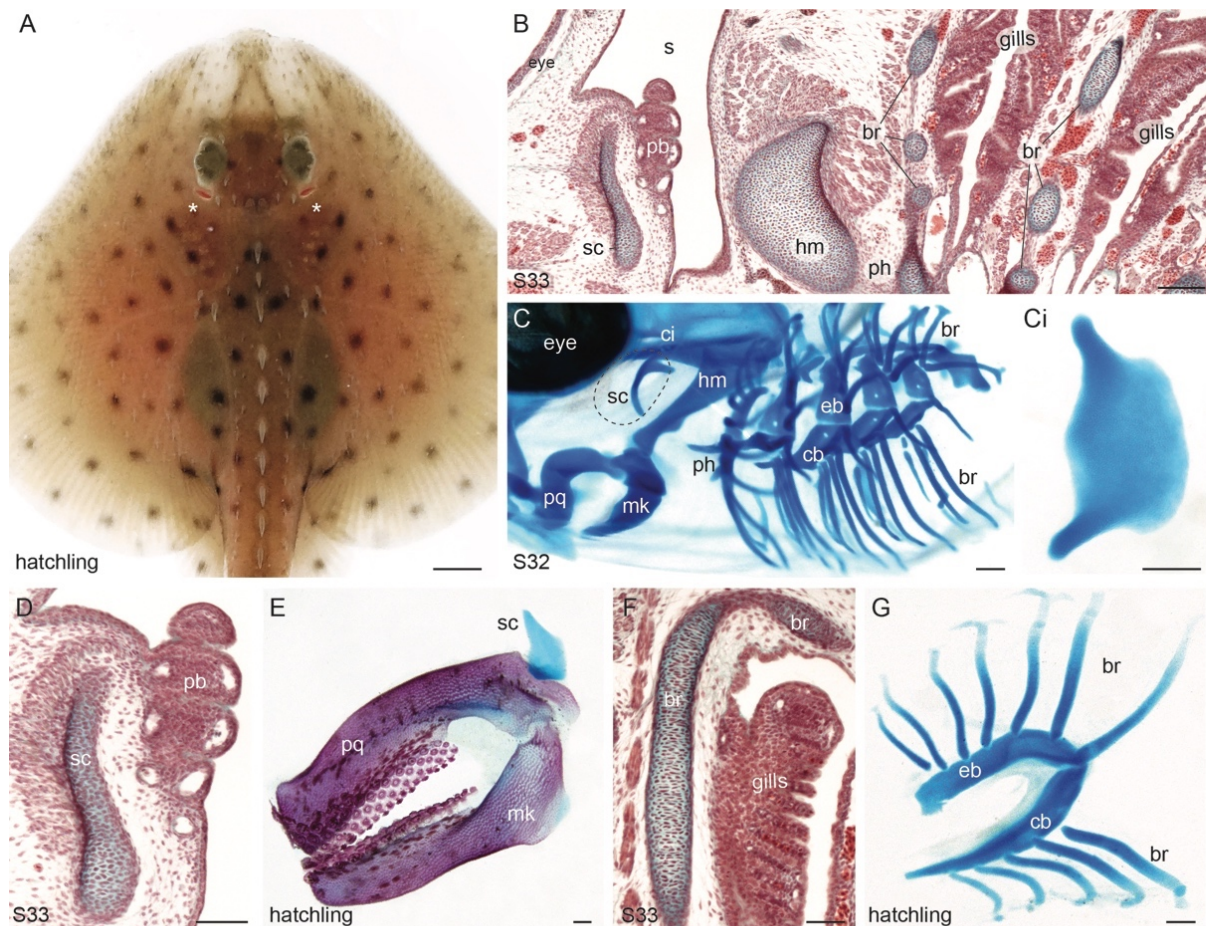


Figure 1: Spiracle, pseudobranch and spiracular cartilage in the little skate (*Leucoraja erinacea*).

(A) Dorsal view of a little skate hatchling. The spiracles behind the eyes are marked with white asterisks. (B) Horizontal section of a stage (S)33 skate embryo showing the spiracular region, including the spiracle, pseudobranch and spiracular cartilage, and two anterior-most gill slits. Section stained with Masson's trichrome. (C) Lateral view of a skeletal preparation of a S32 skate embryo showing the serial arrangement of upper and lower jaws (palatoquadrate and Meckel's cartilage, respectively) and spiracular cartilage, and upper and lower gill arches (epibranchials and ceratobranchials, respectively) bearing branchial rays. (Ci) Frontal view of a dissected skate spiracular cartilage. (D) Horizontal section of the anterior wall of a S33 spiracle: the gill-like pseudobranch is an epithelial feature projecting from the anterior wall of the spiracle, internally supported by the spiracular cartilage. (E) Lateral view of a hatchling skate jaw, demonstrating its close association with the spiracular cartilage. (F) Horizontal section of a S33 gill slit: the respiratory lamellae of the gills are internally supported by branchial rays. (G) Frontal view of a hatchling skate gill, with branchial rays projecting

laterally. br, branchial rays; eb, epibranchial; hm, hyomandibula; mk, Meckel's cartilage; pb, pseudobranch; ph, pseudohyal; pq, palatoquadrate; s, spiracle; sc, spiracular cartilage; scalebars: A=3cm; B-Ci, E, G=500um; D, F=50um

4.2.2 Interpreting the spiracle as a secondary derived feature

The classical interpretation of the pseudobranch as a vestigial gill and the spiracular cartilage as a vestigial branchial ray has recently been called into question. There is no evidence for a gill arch-like nature of the mandibular arch in extant jawless vertebrates (cyclostomes), in which the first arch gives rise to the velum, rather than to a gill-bearing branchial arch, and there is some fossil evidence that suggests a cyclostome-like oropharyngeal skeletal condition may reflect the condition in the gnathostome stem (Janvier, 1996; Miyashita, 2016). If the cyclostome condition is indeed ancestral, this would imply that the mandibular arch was always ancestrally distinct from the gill arches and this would instead suggest that the pseudobranch is a secondarily acquired and derived feature of jawed vertebrates.

There is also little functional evidence for a respiratory role for the pseudobranch in elasmobranchs, which further undermines the idea that it represents a vestigial gill (Laurent & Dunel-Erb, 1984; Maisey, 1989). Water is taken in through the spiracles, rather than expelled as it is through the gill slits, and the pseudobranch blood supply is arranged in such a way that it receives only oxygenated blood (Allis, 1916; Mallatt, 1996; Miyashita, 2016). This anatomical organisation may allow for sustained ventilatory flow to the gills when the mouth is buried in substrate or engaged in prey manipulation (Graham et al., 2014). In teleosts, the blood supply to the pseudobranch is similarly arterialized. Hence, across fishes, the pseudobranch has been mainly investigated for its chemosensory and osmoregulatory functions (Laurent & Dunel-Erb, 1984). The assumption that the pseudobranch is mandibular-arch-derived has also been questioned (Maisey, 1989; Miyashita, 2016). Its innervation by the facial nerve and partial blood supply from the lateral hypobranchial artery may reflect a different embryonic origin than from the mandibular arch. An alternative hypothesis has therefore been forward, which suggests that the pseudobranch is a hyoid arch derivative.

Here I experimentally test serial homology of the pseudobranch and its supporting spiracular cartilage with the gill arch gill lamellae and branchial rays in the skate. I demonstrate by cell lineage tracing that the pseudobranch is indeed mandibular arch-derived, and I report shared molecular and cell type features of the skate pseudobranch and gills. I also investigate embryonic similarities between the spiracular cartilage and gill arch branchial rays, and

demonstrate that both derive from domains of skeletogenic mesenchyme that are responsive to corresponding *sonic hedgehog* (*shh*)-expressing epithelial signalling centre. Finally, I show that stage-specific loss of hedgehog signalling results in reduction or loss of the spiracular cartilage, in a manner that parallels the corresponding reduction of the gill arch branchial ray skeleton. Taken together, these findings are consistent with the historical interpretation of the pseudobranch and spiracular cartilage as vestigial gill arch structures that derive from the mandibular arch in skate.

4.3 Methods

4.3.1 Embryo collection and fate mapping

All animal work complied with protocols approved by the Institutional Animal Care and Use Committee at the Marine Biological Laboratory (MBL) in Woods Hole, U.S.A. Skate (*Leucoraja erinacea*) eggs were obtained from the Marine Resources Centre of the MBL. Staging was carried out according to Maxwell et al. (2008) and Ballard et al. (1993). Embryos for histological and gene expression analyses were fixed in 4% paraformaldehyde (PFA) in 1X phosphate-buffered saline (PBS) overnight at 4°C, prior to dehydration and storage in methanol at -20°C. Embryos for cell lineage tracing experiments were maintained in a flow-through seawater system at ~15°C. For labelling of skate embryos at S22 (for broad mandibular arch lineage tracing), eggs were windowed, and microinjection of the mandibular arch with CM-Dil was performed *in ovo*, according to Gillis et al. (2017). For labelling of skate embryos at S27 (for focal mesenchymal lineage tracing beneath the mandibular arch *shh* expression domain), embryos and attached yolk sacs were taken out of the egg and transferred to a Petri dish of seawater containing ethyl 3-aminobenzoate methanesulfonate salt (MS-222, Sigma). CellTracker CM-Dil (Invitrogen), diluted in 0.3M sucrose from a 5µg/µl stock in ethanol, was microinjected into the mandibular arch using a Picospritzer pressure injector. Eggs containing labelled S22 embryos were re-sealed using the cyanoacrylate adhesive Krazy glue and a piece of donor eggshell, while embryos labelled at S27 were allowed to recover in seawater and returned to their egg-cases. After development in a flow-through seawater table for 6-10 weeks, embryos were fixed in 4% PFA in PBS overnight at 4°C, rinsed three times in PBS and stored at 4°C in PBS with 0.01% sodium azide.

4.3.2 mRNA in situ hybridisation

mRNA *in situ* hybridisation for *foxl2* (MW457610), *gata2*, *shh* (EF100667) and *ptc* (EF100663) was performed in wholemount and on paraffin sections according to the protocols detailed in Chapter 2.

4.3.3 Immunofluorescence on paraffin sections

Slides to be used for immunofluorescence were dewaxed in histosol and rehydrated through a descending ethanol series into 1X PBS + 0.1% Triton X-100 (PBT). For antigen retrieval, slides were preheated in distilled water for 5 minutes at 60°C, transferred to prewarmed antigen retrieval solution (10mM sodium citrate, pH6.0) and incubated for 25 minutes at 95°C. Slides were then cooled in a freezer for 30 minutes. Slides were rinsed 3 × 10 min in PBT, blocked for 30 min in 10% sheep serum and incubated in primary antibody under a parafilm coverslip in a humidified chamber overnight at 4°C. Primary antibodies used for this experiment were rabbit anti-5HT (Merck S5545; diluted 1:250 in block) and mouse anti-SV2 (Developmental Studies Hybridoma Bank; diluted 1:100 in block). The next day, slides were rinsed 3 × 5 min in PBT and incubated in secondary antibody under a parafilm coverslip in a humidified chamber overnight at 4°C. Secondary antibodies used for this experiment were goat anti-rabbit 488 (ThermoFisher A11008; diluted 1:500 in block) and goat anti-mouse 633 (ThermoFisher A21050; diluted 1:500 in block). Slides were then rinsed 3 × 10 min in PBT and coverslipped with Fluoromount G containing DAPI (Southern Biotech). Negative controls (slides treated as above, but with no primary antibody) showed no signal.

4.3.4 *in ovo* cyclopamine treatment, wholemount skeletal preparations and statistical analysis

Skate eggs have an approximate internal chamber volume of 12ml. In order to achieve an *in ovo* cyclopamine concentration of 20 µM, 25 µl of 9 mM stock solution of cyclopamine in dimethylsulfoxide (DMSO) was injected into skate eggs at S27 or S29, using a syringe and 30-gauge needle (as per Gillis & Hall, 2016). For controls, an equivalent volume of DMSO was injected. Injected embryos were grown to S32, and surviving embryos (n=12/28 and n=7/19 for cyclopamine treatment at S27 and cyclopamine treatment at S29, and n=4/5 and n = 5/5 for DMSO control treatment at S27 and at S29, respectively) were fixed as described above and analysed for skeletal defects after skeletal preparation.

For wholemount staining of the endoskeleton, skate embryos were transitioned from 100% methanol through 100% ethanol into 70% ethanol at room temperature. Embryos were then stained for cartilage matrix with 20% w/v Alcian Blue 8GX dissolved in acetic ethanol (3:7 glacial acetic acid: absolute ethanol) for 24 hours with gentle rocking at room temperature. Embryos were destained in acetic ethanol for 24 hours, and then rehydrated through a descending ethanol series (70%, 50%, and 25% ethanol in ddHOH, 24 hours/wash). After a wash in ddHOH, embryos were soaked in 1% trypsin (Fisher) in 2% sodium tetraborate for 20 minutes. Subsequently, embryos were cleared in a 0.5% KOH solution as needed. Embryos were then moved through a graded 0.5% w/v KOH/glycerol series of 24 hours each (3:1, 1:1, 1:3 0.5% KOH:glycerol). Final skeletally prepared specimens were stored in 80% glycerol at 4°C and manually dissected for photography.

For the statistical analysis, dissected left spiracular cartilages of each embryo were imaged on a Leica M165FC stereomicroscope, and surface area of each cartilage was measured using Fiji ImageJ (Schindelin et al., 2012) and normalised against total embryo length. Measurements are available in Table S4.1 To test for statistically significant differences among the means of normalised spiracular cartilage area for each group (DMSO, cyclopamine at S27, cyclopamine at S29), a Kruskal-Wallis analysis of variance was performed, followed by a Dunn's test with Bonferroni correction to identify which pairwise comparisons were statistically significantly different. The same statistical analysis confirmed no significant difference between normalised spiracular cartilage area of DMSO-treated vs. wild-type (n=3) spiracular cartilages at S32 (p=0.305).

4.4 Results

4.4.1 *The skate pseudobranch is mandibular arch-derived*

It has been speculated that, despite its close association with the jaw, the pseudobranch is actually a derivative of the hyoid arch (Maisey, 1989; Miyashita, 2016). I therefore sought to directly test the embryonic origin of the skate pseudobranch. We and others have previously reported expression of the transcription factor *foxl2* in the pharyngeal arches of skate and shark embryos, in a pattern that seemingly delineates the presumptive gill-forming epithelium, including a domain of expression in the posterior mandibular arch which may correspond with the presumptive pseudobranch (Wotton et al., 2007; Hirschberger et al. 2021 – Fig. 4.2A). To test the mandibular arch origin of the pseudobranch, I broadly labelled the dorsal-intermediate mandibular arch in skate embryos at S23 with the lipophilic dye CM-Dil (Fig. 4.2B). By S23, the first pharyngeal endodermal pouch has fused with the surface ectoderm, permitting me to broadly and specifically label mandibular arch tissues without risk of contaminating the hyoid arch.

Injected embryos were reared until S32, at which point the pseudobranch has fully differentiated. In 9/11 labelled embryos, I readily observed CM-Dil-positive cells throughout the entirety of the pseudobranch (Fig. 4.2C, C'). CM-Dil-positive cells were recovered throughout the pseudobranch lamellae (Fig. 4.2Ci), as well as in the endothelial lining of the pseudobranch vasculature (Fig. 4.2Cii). No CM-Dil positive cells were recovered in any hyoid arch-derived features. These findings conclusively demonstrate the mandibular arch origin of the pseudobranch in skate.

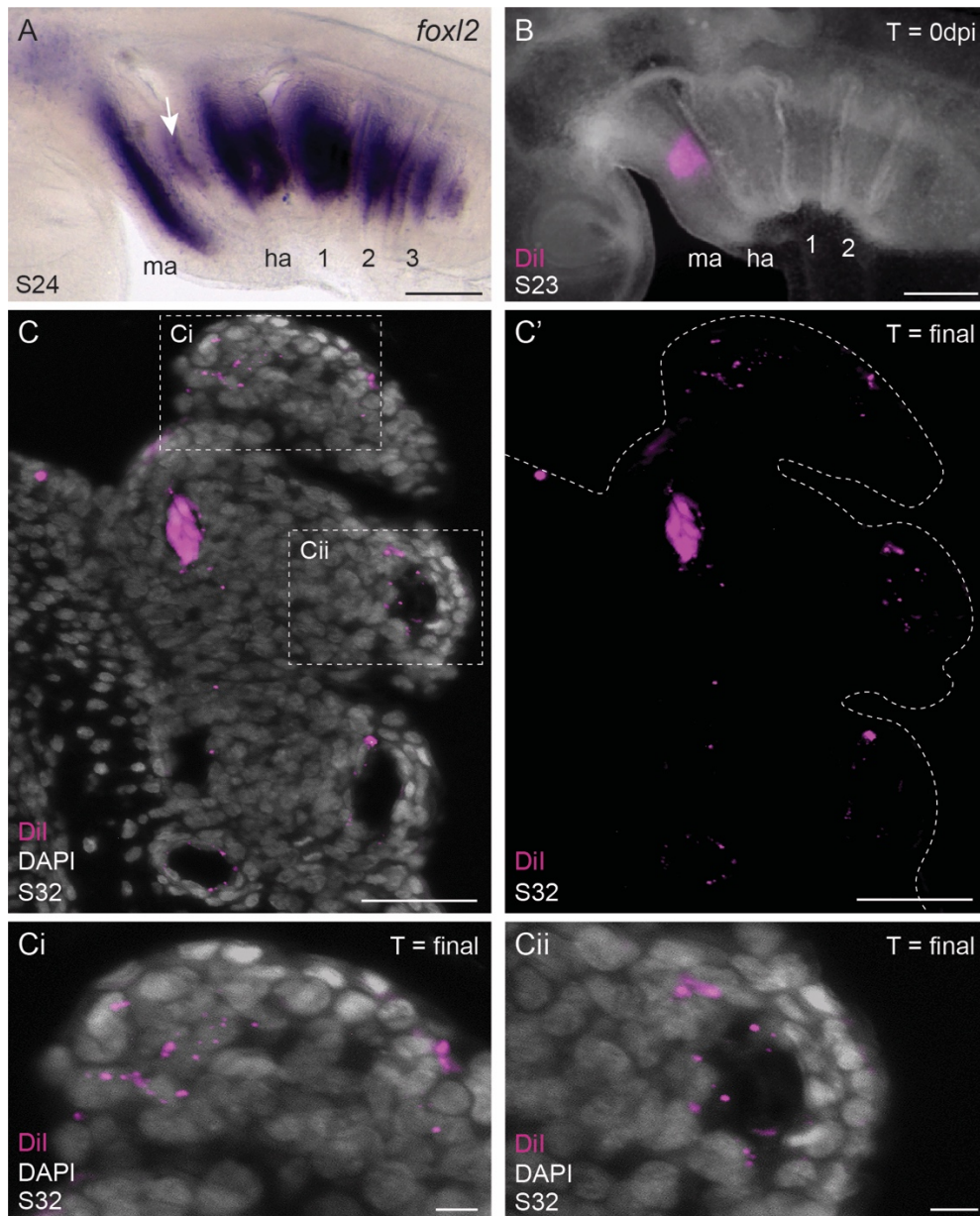


Figure 4.2: The skate pseudobranch is mandibular-arch-derived. (A) At S24, skate embryos express *foxl2* in the mesodermal core of each pharyngeal arch, and in the presumptive gill epithelium of each arch (including an epithelial domain on the mandibular arch which may correspond with the future pseudobranch). (B) Microinjection of CM-Dil in the posterior dorsal-intermediate mandibular arch of skate embryos at S23 results in broad, specific labelling of mandibular arch derivatives at S32, including (C-Ci) the pseudobranch throughout the pseudobranch (Ci) gill-like lamellae and (Cii) blood vessels. ha, hyoid arch; ma, mandibular arch; sc, spiracular cartilage; 1-3: gill arches 1-3, scale bars: Ai, Aii, Aiii, Di, Dii, Diii, li, lii= 5um, A-I=50um.

4.4.2 The skate pseudobranch and gills share cell and gene expression features

If the pseudobranch is indeed a vestigial mandibular arch gill, we might expect the pseudobranch and gills to share cell types and gene expression features. Bony fish gills possess neuroepithelial cells (NECs), which function to mediate physiological responses to hypoxia, and which are identifiable by their immunoreactivity for serotonin and synaptic vesicle glycoprotein 2 (Dunel-Erb et al., 1982; Jonz & Nurse, 2003, 2005; Hockman et al., 2017). Immunofluorescent detection of serotonin (5-HT) and synaptic vesicle glycoprotein 2 (SV2) confirms conservation of this putative hypoxia-sensitive neuroepithelial cell type in the tips of the gill lamellae of S33 skate embryos (Fig. 4.3A, 2Ai-iii). Using mRNA *in situ* hybridisation (ISH), I also found that skate gill lamellae express the transcription factors *foxl2* and *gata2* during development (Fig. 4.3B-C). *foxl2* expression localised to the epithelium of the gill lamellae (Fig. 4.3B), while *gata2* was found predominantly in the mesenchyme-derived cores of the gill lamellae (Fig. 4.3C).

Immunostaining and ISH on sections also reveal conservation of the above gene expression features in the skate pseudobranch. I found 5HT/SV2+ NECs in the tips of the pseudobranch lamellae (Fig. 4.3D, Di-Diii), as well as expression in the pseudobranch of *foxl2* (Fig. 4.3E) and *gata2* (Fig. 4.3F). Much like in the hyoid and gill arch-derived gills, *foxl2* expression in the mandibular-derived pseudobranch localised to the epithelium of the gill-like element (Fig. 4.3E), while *gata2* was expressed in the core of the pseudobranch (Fig. 4.3F). These experiments reveal shared cell types and gene expression features between the pseudobranch and gills of the skate, consistent with the serial homology of these structures.

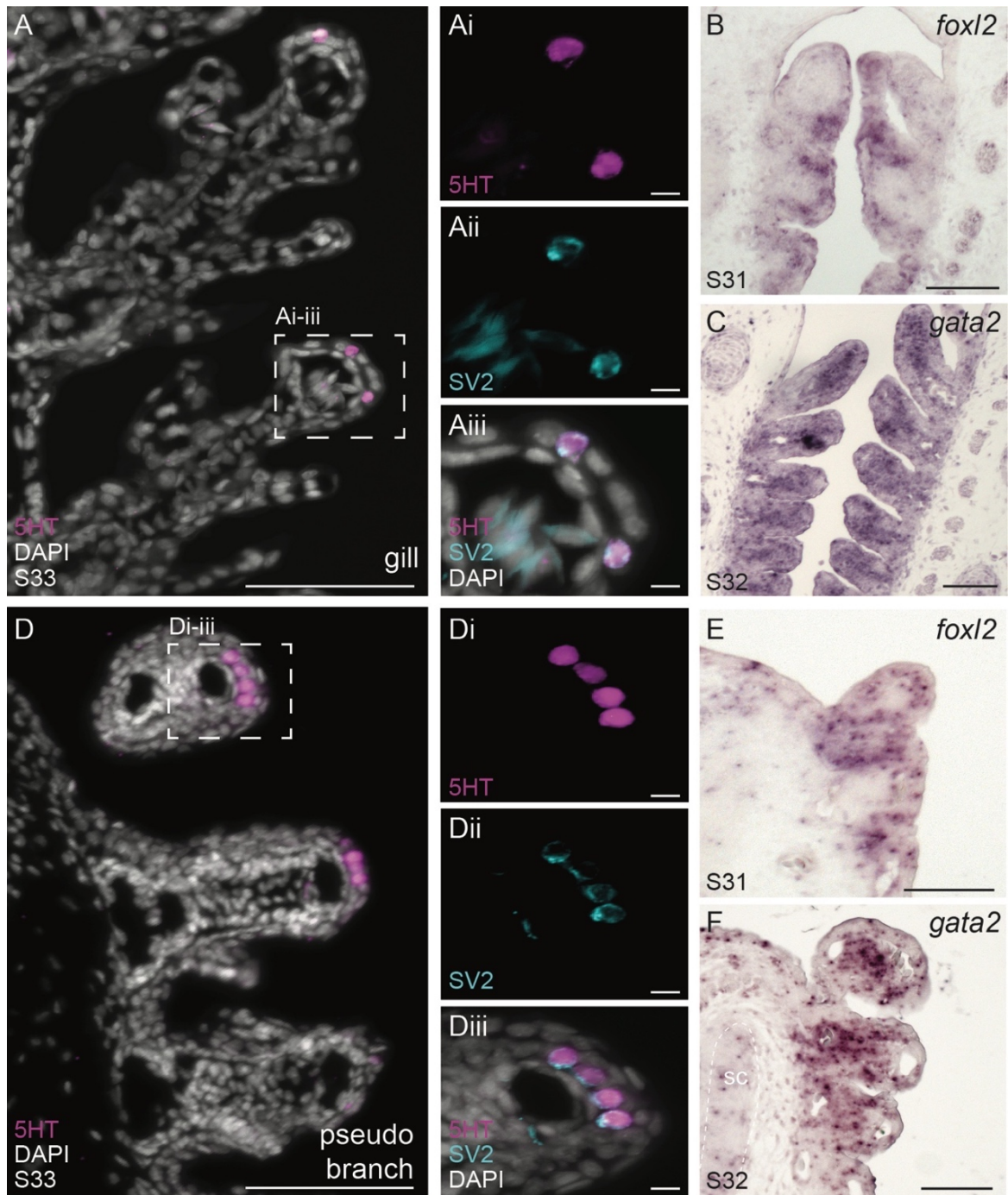


Figure 4.3: The skate pseudobranch shares gene expression features with gills: (A, Ai-iii) The gills of a S33 skate embryo possess hypoxia-sensitive neuroepithelial cells (NECs), which may be recognised by their immunoreactivity for (Ai) serotonin (5HT) and (Aii) synaptic vesicle glycoprotein 2 (SV2). Skate gills also express (B) *foxl2* and (C) *gata2* during development. (D) The pseudobranch of a S33 skate embryo also possesses (Di-iii) 5HT/SV2+ NECs, and also expresses (E) *foxl2* and (F) *gata2* during development. sc, spiracular cartilage; scalebars: A, B, C, D, E, F = 50um; Ai-iii, Di-iii = 5um

4.4.3 The skate spiracular cartilage and branchial rays share an embryonic origin from equivalent domains of *shh*-responsive mesenchyme

The cartilaginous branchial rays of that support the gill lamellae of the hyoid and gill arches of skates and sharks are patterned by a *shh*-expressing epithelial signalling centre called the gill arch epithelial ridge (GAER – Gillis et al., 2009b, Gillis et al., 2011; Gillis & Hall, 2016). In these arches, *shh* is initially broadly expressed in the posterior arch epithelium, and this expression then resolves into the GAER as the arches undergo their lateral expansion. Cell lineage tracing has shown that branchial rays develop from GAER *shh*-responsive mesenchyme, and inhibition of GAER *shh* signalling results in a truncation/reduction of the branchial ray skeleton (Gillis et al., 2009b; Gillis & Hall, 2016).

To compare spiracular cartilage development to the branchial rays, I first characterised *shh* expression in the developing mandibular arch of the skate. I found that by S23, *shh* was broadly expressed in the posterior epithelium of the skate mandibular arch (Fig. 4.4A-B), with this expression resolving into a GAER-like ridge of *shh*-expressing cells along the posterior margin of the mandibular arch by S27 (Fig. 4.4C-D). This ridge of *shh* expression persisted into S29, when it delineated the anterior edge of the spiracle (Fig. 4.4E-F). The patterns of *shh* expression in the mandibular arch closely resemble GAER *shh* expression of the branchial ray-bearing hyoid and gill arches and led me to speculate about their possible skeletal patterning function within the mandibular arch.

To test the fate of mesenchyme underneath the *shh*-expressing GAER of the skate mandibular arch, I labelled this tissue by microinjection of the lipophilic dye CM-Dil in skate embryos at S27 (Fig. 4.4G). Using this approach, I was able to label *ptc*⁺ (i.e. *shh*-responsive) mesenchymal cells underneath the mandibular arch GAER (Fig. 4.4H-I), rear injected embryos until S32, and then assess the contribution of that tissue to the mandibular arch skeleton. Histological analysis of labelled embryos revealed CM-Dil-positive cells throughout the spiracular cartilage (Fig. 4.4J, K; n=22/29, also see Fig. S4.1), as well as in the connective tissue surrounding the spiracular cartilage. These experiments indicate that, like gill arch branchial rays, the spiracular cartilage develops from GAER *shh*-responsive mesenchyme of the mandibular arch.

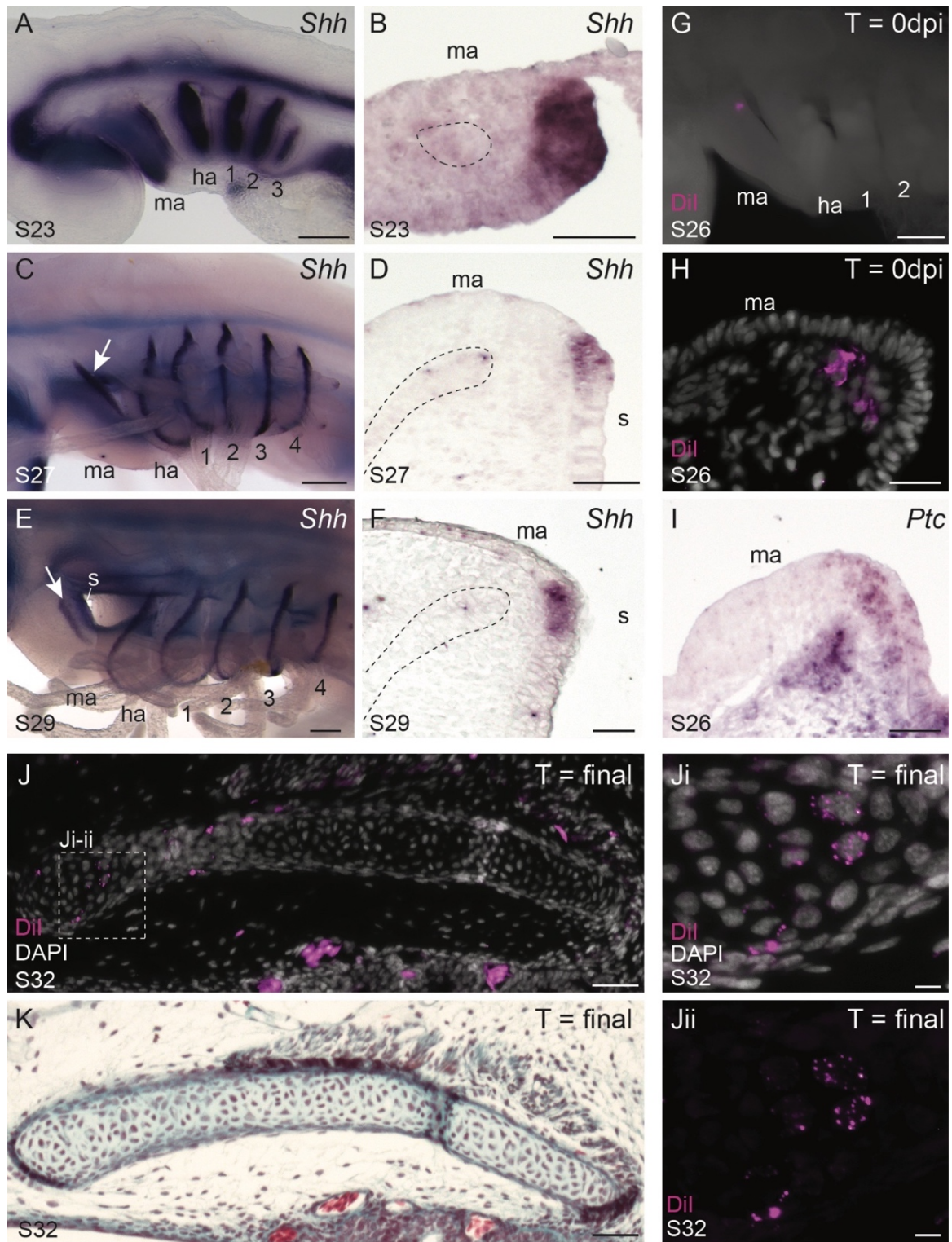


Figure 4.4: The skate spiracular cartilage derives from *shh*-responsive mandibular arch mesenchyme.

(A) At S23, *shh* is expressed broadly throughout the posterior epithelium of all pharyngeal arches in skate, including (B) in the posterior endodermal lining of the mandibular arch. (C, D) At S27 and (E, F) S29 the pharyngeal arch *shh* expression has resolved to a thin ridge of cells

(the gill arch epithelial ridge – GAER) that runs along the leading edge of the hyoid and first four gill arches. GAER-like expression of *shh* is also present on the mandibular arch, adjacent to the spiracle (s), highlighted by white arrows. (G-I) Labelling of the *ptc*-expressing mesenchyme subjacent to the mandibular arch GAER at S26/27 results in (J-K) CM-Dil+ chondrocytes throughout the spiracular cartilage at S32. ha, hyoid arch; ma, mandibular arch; s, spiracle; 1-4: gill arches 1-4; scalebars: A, C, E, G = 300um, B, D, F, H, I, J, K = 30um, Ji, Jii = 5um

4.4.4 The skate spiracular cartilage and branchial rays share patterning mechanisms

Finally, I set out to test whether mandibular arch GAER shh signalling patterns the spiracular cartilage in a manner that is comparable to the GAER patterning function of the gill arches. Inhibition of sonic hedgehog signalling by cyclopamine treatment at S27 results in a reduction of gill arch mesenchymal cell proliferation and a reduction in the number of branchial rays (Gillis & Hall, 2016). To test the effects of hedgehog signalling inhibition on development of the spiracular cartilage, I conducted *in ovo* cyclopamine treatments with skate embryos at S27 and S29, and assessed surviving embryos for spiracular cartilage defects at S32. Given the 2-dimensional sheet-like nature of the skate spiracular cartilage, my test for spiracular cartilage reduction consisted of unilateral (left) spiracular cartilage dissection, measurement of spiracular cartilage area (standardised against total embryo length), and pairwise comparisons of mean ratios between control and cyclopamine-treated embryo groups.

Control (DMSO-treated) skate embryos (n=4 at S27, n=5 at S29) showed no observable spiracular cartilage defects (Fig. 4A, A'), and the spiracular cartilage area was not significantly different from wildtype S32 embryos (n = 3, not shown). Conversely, cyclopamine treatment at S27 led to striking spiracular cartilage defects (Fig. 4B, B', C, C'; n= 11/12), and to an overall significant reduction in spiracular cartilage area, relative to control (Fig. 4D, D'). Defects with cyclopamine treatment at S27 ranged from complete loss of the spiracular cartilage to a highly reduced, rod-like phenotype. In contrast, cyclopamine treatment at S29 resulted in spiracular cartilages with some slightly abnormal morphology (Fig. 4D, D'), but no significant reduction in spiracular cartilage area, relative to control (Fig. 4E). These findings reveal a shared role for GAER shh signalling in patterning the spiracular cartilage and branchial rays, and a shared period in development during which shh signalling is required for development of the spiracular cartilage and branchial rays.

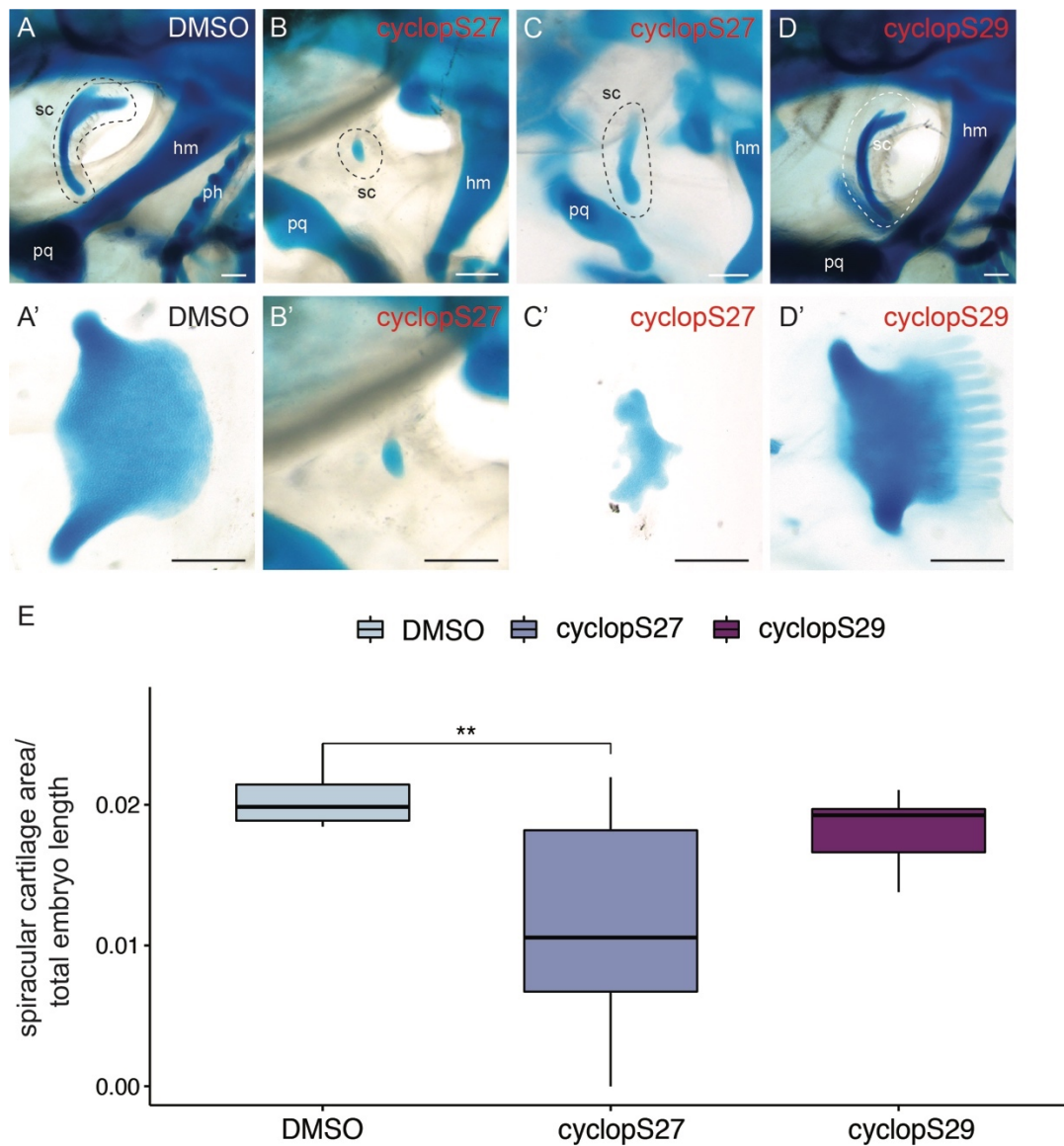


Figure 4.5: Shh-dependant patterning of the skate spiracular cartilage. Spiracular cartilage morphology from (A-A') DMSO treated skate embryos, and from skate embryos treated with 20uM cyclopamine *in ovo* at (B-B', C-C') S27 and (D-D') S29. (E) Cyclopamine treatment at S27 results in significant reduction of the spiracular cartilage (as measured by cartilage area/total embryo length) relative to DMSO controls ($p=0.008$), while cyclopamine treatment at S29 resulted in no significant difference in the size of the spiracular cartilage ($p=0.887$). The Kruskal-Wallis test was performed as a non-parametric alternative to an one-way ANOVA, and followed by a Dunn's test with Bonferroni correction ($\chi^2 = 9.965$, $n = 28$). hm, hyomandibula; ph, pseudohyal; pq, palatoquadrate; sc, spiracular cartilage. Scalebars = 500um.

4.5 Discussion

The spiracle and its associated structures – i.e. the pseudobranch and, in elasmobranchs, the spiracular cartilage – have long been regarded by classical anatomists and evolutionary biologists as vestigial gill elements on the back of the jaw (Gegenbaur, 1872; Ridewood, 1896; Goodrich, 1909; El-Toubi, 1947). This idea meshes well with the interpretation of the jaw as a derived gill arch, an idea put forward by the classical theory of jaw-gill arch serial homology. However, after fossil evidence emerged from stem gnathostomes that seemed to suggest a cyclostome-like organisation as the ancestral condition from which jaws evolved (Maisey 1989; Janvier, 1996; Miyashita, 2016), the interpretation of the spiracle and its internal anatomy as the remnants of an ancestral gill arch has largely been abandoned. In cyclostomes like lamprey, the mandibular arch has no gill-bearing function, and no gill-slit exists between the mandibular and hyoid (Janvier, 1996), rendering the interpretation of the spiracle and its internal anatomy as vestigial gill slit elements highly unlikely. Consequently, the pseudobranch has been interpreted as a derived chemoreceptive structure that converges on a gill-like morphology (Miyashita, 2016), and as a derivative of the hyoid arch (Allis, 1916 in *Polydontus*; Maisey, 1989 and Miyashita, 2016 in elasmobranchs).

4.5.1 *The mandibular arch origin of the pseudobranch*

My fate-mapping experiments show unequivocally that the pseudobranch is derived from the mandibular arch in skate. Suggestions to the contrary (Maisey, 1989; Miyashita, 2016) are based on the partial irrigation of the pseudobranch from the oxygenated efferent hyoidean artery, described by Allis (1916), and its innervation by the facial nerve, which generally supplies the hyoid arch (Laurent & Dunel-Erb, 1984). However, these features are not necessarily diagnostic of an embryonic origin from the hyoid arch. For example, in earlier work Allis (1900) regarded the portion of the hyoidean artery that supplies the pseudobranch in the bowfin fish *Amia* as belonging to the mandibular, and further suggested that the dorsal portion of the efferent pseudobranchial artery relates to the palatoquadrate in the same way as the branchial arteries relate to their respective arches—an arrangement in line with the serial homology of these elements in *Amia*. In several elasmobranchs, Allis (1916) found the

afferent pseudobranchial artery that supplies the pseudobranch (which he called ‘spiracular gill’) to be formed by a merging of vessels deriving from the afferent mandibular artery as well as the anterior hyoidean artery. In a classical anatomical study of elasmobranchs, De Beer finds the same shared supply by both the true mandibular vessel and the cross-commissure from the efferent hyoid artery to the pseudobranch, and further describes the efferent pseudobranchial artery as the dorsal portion of the mandibular vessel (De Beer, 1924). This leaves no doubt that the mandibular-derived pseudobranch is also irrigated by mandibular-derived vessels, which parallels blood supply to the gills on the gill arches (Mallatt, 1996), and corresponds to its embryonic origin in the first arch.

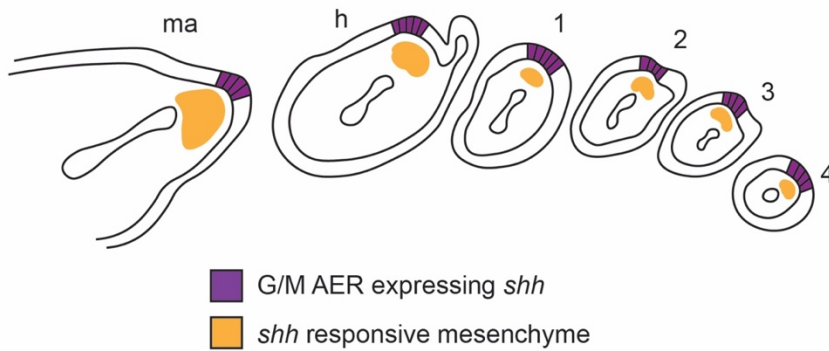
Further, the facial nerve is also known to innervate non-mandibular derived structures. For example, in teleosts, the facial nerve broadly supplies chemoreceptive organs like taste buds and the anterior dorsal fin of the rockling *Ciliata mustela* (Kotrschal et al., 1993) or the maxillary barbels of the Japanese sea catfish *Plotosus japonicus* (Kanwal et al., 1987; Caprio et al., 2015). In cartilaginous fishes, the facial nerves have been described as forming a complex of four parts that supply part of the lateral line system on the head (ophtalmicus superficialis), the cheeks (buccal ganglion), the palatine (roof of the mouth), as well as the hyomandibular nerve (Ewart, 1889). Other cranial nerves also supply structures beyond the pharyngeal arch with which they are associated: for example, in mice, the maxillary aspect of the mandibular arch-derived trigeminal nerve also supplies structures that stem from the more anteriorly located frontonasal prominence, which is a derivative of the premandibular mesenchyme (Higashiyama & Kuratani, 2014). These morphological findings underscore the difficulty of ascertaining arch origin based on innervation alone, and the importance of direct cell lineage tracing for resolving questions of embryonic origin.

4.5.2 Serial homology of the spiracular cartilage and branchial rays

The skate pseudobranch is endoskeletally supported by the spiracular cartilage, and this element has been serially homologised with the branchial rays, which support the gill lamellae on the gill arches in the same anatomical arrangement (Gegenbaur, 1872; El-Toubi, 1947). My gene expression and lineage tracing analyses of the mandibular arch provide a developmental explanation for this anatomical correspondence: all pharyngeal arches in skate share a

common signalling centre—an epithelial ridge of *shh* signalling on the posterior margin, termed GAER, which patterns the subjacent *shh*-responsive mesenchyme (Fig. 4.6A). In the hyoid and gill arches, this *shh*-responsive mesenchyme gives rise to the branchial rays (Gillis et al., 2009; Gillis & Hall, 2016), while in the mandibular arch, the *shh*-responsive mesenchyme gives rise to the spiracular cartilage (Fig. 4.6B). Inhibition of hedgehog signalling via cyclopamine treatment results in a reduction of the spiracular cartilage, akin to defects observed in the endoskeletal elements of the branchial rays after the same treatment (Gillis et al., 2009; Gillis & Hall, 2016). The shared embryonic origin from equivalent domains of *shh*-responsive mesenchyme on the pharyngeal arches is developmental evidence consistent with the historical interpretation of the spiracular cartilage as a vestigial branchial ray (Gegenbaur, 1872; Holmgren & Stensiö, 1936; El-Toubi, 1947).

A. Epithelial ridges of *shh* expression in the pharyngeal arches



B. *shh* patterned pharyngeal endoskeletal elements

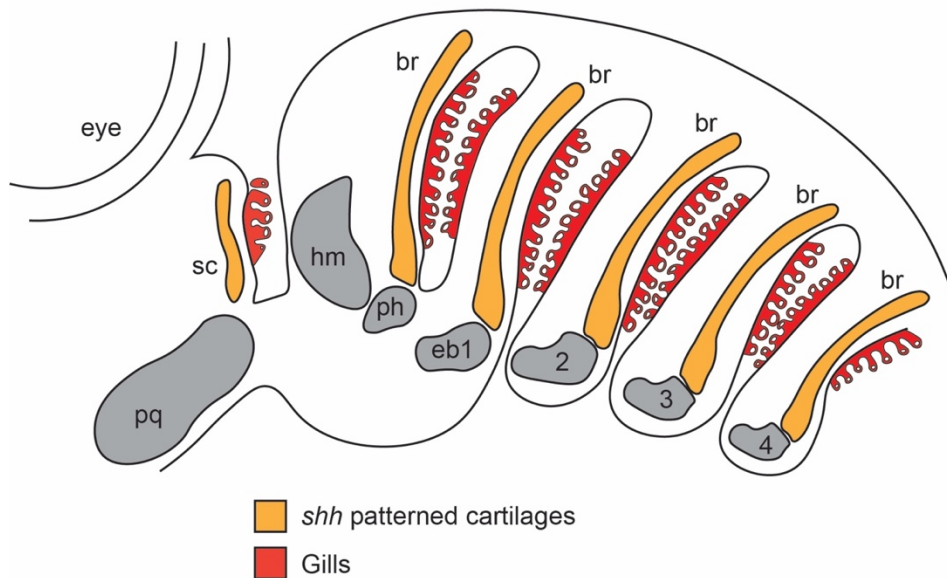


Figure 4.6: Schematic representation of the skate gill arch epithelial ridge (GAER) across all pharyngeal arches and serial homology of spiracular cartilage and branchial rays. A) All pharyngeal arches in embryonic skates possess an epithelial ridge of *shh* signalling (GAER) (purple) that signals to subjacent arch mesenchyme (orange). B) The *shh* responsive mesenchyme in the mandibular arch gives rise to the spiracular cartilage (orange), while the *shh* responsive mesenchyme in the hyoid and gill arches gives rise to the branchial rays (orange) in the adult skate. Thus the spiracular cartilage not only shares an anatomically similar arrangement with the branchial rays, i.e. they provide skeletal support to the gills (red), they are also patterned by the same *shh* pathway. br: branchial rays; eb 1-4, epibranchials 1-4; ha: hyoid arch; hm, hyomandibula; ph: pseudohyal; pq: palatoquadrate; ma: mandibular arch; sc: spiracular cartilage; 1-4: gill arches 1-4.

However, it should be noted that the *shh* signalling emanating from the GAER on the hyoid and gill arches also has a role in anteroposterior patterning the gill arches (Gillis & Hall, 2016), which could not be detected conclusively in the mandibular arch by my cyclopamine experiments. In chondrichthyans, gill arches are marked by a clear anteroposterior polarity as branchial rays articulate with the epi- and ceratobranchial cartilages along their posterior margins (Gillis et al., 2009a, b). If *shh* signalling is inhibited by cyclopamine at S22, though not at S27 or S29, this anteroposterior polarity is lost and misshapen epi- and ceratobranchial cartilages articulate along the midlines of the gill arches (Gillis & Hall, 2016). An equivalent polarity defect in the articulation of the spiracular cartilage to the upper jaw could not be established here: cyclopamine treatment at S22 results in complete deletion of the spiracular cartilage, and there is also no clear anatomical readout of the anteroposterior axis in the spiracular cartilage that is comparable to the articulation of the branchial rays to the gill arches and that could be quantified or qualified in a similar manner to establish anteroposterior polarity defects.

4.5.3 Spiracular cartilages and branchial rays throughout the palaeontological record

While this work presents the developmental mechanisms allowing for the anatomical correspondence of the pseudobranch to the gills and the spiracular to the branchial rays in extant elasmobranchs, there is still little fossil evidence available that traces the evolution of these features along the gnathostome stem. To date, both branchial rays and spiracular cartilages have only been resolved to the chondrichthyan stem and assessing the exact evolutionary history of branchial rays amongst chondrichthyans (i.e. elasmobranchs and holocephalans) is a long-standing issue in vertebrate evolution (Gillis et al., 2011). Elasmobranchs are characterised by open gill slits, in which an interbranchial septum projects beyond the respiratory gill lamellae. The branchial rays function in providing skeletal support to the gills from within these protective gill flaps (Gillis et al., 2009a). Holocephalans, the sister group of elasmobranchs, possess branchial rays only on the hyoid arch, where they form an opercular gill cover, and in the absence of clear branchial ray homologs outside of chondrichthyans it is difficult to polarise the acquisition of these endoskeletal arrangements, i.e. which of these two conditions is likely ancestral (Maisey, 1984, 1989, 2012; Gaudin, 1991;

Schaeffer & Williams, 1997; Lund & Grogan, 1997; Janvier, 1996). More recent developmental analyses of the holocephalan *Callorhinchus milii* indicate that branchial rays on the post-hyoid arches are indeed present as small, chondrified projections from the ceratobranchials of the first three post-hyoid gill arches, and that the holocephalan operculum likely originated via a change in *shh* signalling on the hyoid arch that ensures prolonged, operculum-forming branchial ray outgrowth—alongside holocephalan-specific changes in a deeply conserved enhancer element that drives expression of the gill cover regulator *pou3f3* across gnathostomes in general (Gillis et al., 2011; Barske et al., 2020). In combination with palaeontological evidence suggesting the reduction of branchial rays in the post-hyoid gill arches along the holocephalan stem (Maisey, 1989; Coates & Sequeira, 2001; Janvier, 1996), the vestigial branchial rays in extant holocephalans may thus be interpreted as a feature retained from the ancestral elasmobranch-like organisation of the branchial rays across all gill arches in stem chondrichthyans (Gillis et al., 2011). However, there is also some fossil evidence consistent with a prominent bony opercular gill cover on the hyoid arch in a stem gnathostome (Zhu et al., 2013) and stem chondrichthyans (Dick, 1978; Dearden et al., 2019), which may be interpreted as pointing the other way, i.e. towards a single, hyoid arch-derived gill cover in the last common ancestor of extant gnathostomes, and the subsequent acquisition of separate, branchial ray supported gill covers in the posterior gill arches in the chondrichthyan stem. However, these separate findings of functional opercula components in stem group fossils can also be interpreted as independent origins of a similar gill cover strategy (and independent loss of branchial rays in some stem chondrichthyans – Gillis et al., 2011). Fundamentally, our inability to resolve the acquisitions of these different conditions (a holocephalan-like single opercular gill cover on the hyoid vs. elasmobranch-like branchial ray supported septa across all gill arches) reflects a high level of anatomical variation found in a small number of pre-Devonian stem chondrichthyans available for study, which as a group are generally already under-sampled (Coates et al., 2018). As thin, filigree endoskeletal elements, branchial rays also preserve exceptionally poorly across the fossil record. To accurately reconstruct the evolutionary history of branchial ray expansion and reduction across chondrichthyans, a detailed reappraisal of chondrichthyan phylogeny and pharyngeal anatomy is necessary.

Spiracles, when present, are often difficult to interpret in the fossil record as well. For example, some placoderms—a paraphyletic assemblage of fishes which includes some of the earliest jawed vertebrates—possessed an opening in the position of a hypothetical spiracle (Young & Zhang, 1992; Arsenault et al., 2004), but distinguishing this feature from other gaps in their heavy dermal armour remains challenging. Similarly, tracing the internal vestiges of potential pseudobranch innervation and irrigation presents a difficult approach, though some have described fossilised grooves in stem gnathostomes and stem osteichthyan skulls that may represent the remnants of the efferent pseudobranchial artery (Goodrich, 1930; Gardiner, 1984; Basden & Young, 2001).

A notable exception to this dearth of fossilised spiracular elements is the recent description of the spiracular endoskeleton of the Middle Devonian acanthodiform *Cheiracanthus murchisoni*, which provides the most complete fossilised spiracle in a stem chondrichthyan described to date (Burrow et al., 2020). *Cheiracanthus* appears to have been characterised by the presence of both gill bars and a sheet of cartilage in each spiracle, potentially forming a valve that allowed for controlled water flow over the pseudobranch. This gill bar-like condition of the spiracular cartilage bears a strong anatomical resemblance to branchial rays—instead of a continuous sheet of cartilage, *Cheiracanthus* possessed a set of thin rods arranged in parallel like branchial rays inside the spiracle (Burrow et al., 2020). Interestingly, *Cheiracanthus* was a nektonic fish that did not possess teeth and thus had no need to sustain waterflow through the buccopharyngeal chamber while its mouth was engaged in prey manipulation, and it does not seem to have lived a benthic life, meaning the spiracle would not have been needed for water intake while the mouth was buried in substrate (Burrow et al., 2020). Hence, the spiracle in *Cheiracanthus* may have retained an ancestral respiratory function. *Cheiracanthus* can thus be interpreted as the transitional state between hypothetical ancestral gnathostome with an unconstrained first gill slit and a gill-arch-like mandibular arch on the one hand, and the derived condition of extant elasmobranchs bearing paired spiracles containing a reduced pseudobranch and spiracular cartilage derived from the mandibular arch on the other hand. Historically, El-Toubi acknowledged that in dogfish hatchlings the spiracular cartilages are broader than at earlier developmental stages, meaning an oblique cross-section may very well represent them as small sheets rather than rods of cartilage (El-Toubi, 1947). Furthermore, the dorsal ends of dogfish hatchling spiracular

cartilages appear to merge and fill the space between them with connective cartilage—perhaps indicating the transition from a rod-like branchial-ray-like appearance to the continuous sheet observed in skate. Further comparative studies on the anatomy and development of the spiracular cartilages across extant elasmobranchs are needed to establish the variety of spiracular cartilages, which may also aid in further understanding the evolutionary history of their morphology.

Taken together, these findings support a scenario whereby a mandibular arch-derived pseudobranch is likely an ancestral feature of gnathostomes. While pseudobranchs are widely present in osteichthyans, lineage tracing data from osteichthyans are still needed to formally test the mandibular arch origin of the pseudobranch in this group. The presence of spiracular cartilages, however, cannot be inferred beyond the chondrichthyan stem, much like their putative gill arch serial homologues, the branchial rays. Nevertheless, the mandibular-arch origin of both features, and their apparent similarity to the gills and gill support skeleton in chondrichthyans is consistent with the spiracle as a vestigial mandibular arch gill structure that is serially homologous with those of the more posterior pharyngeal arches. This view is not compatible with scenarios that suggest stem gnathostomes were characterised by a cyclostome-like condition in their oropharyngeal region, as cyclostomes do not possess a gill slit behind the jaw (Janvier, 1996; Miyashita, 2016). In the absence of transitory fossils showcasing the stepwise acquisition of the jawed condition along the gnathostome stem, it is difficult to support or refute either hypothesis, i.e. jaw-gill arch serial homology or a transformational cyclostome scenario, on palaeontological evidence alone. However, the anatomical and developmental evidence reported here strongly point towards the ancestral gill slit-like nature of the spiracle in chondrichthyans. This stands in opposition to views that suggest that the mandibular arch was always ancestrally distinct from the gill arches and the spiracle and its internal anatomy converged on a secondarily derived gill-like nature for chemosensory or osmoregulatory reasons.

4.6 Summary

Here I have reported cell lineage tracing evidence that shows conclusively for the first time that the pseudobranch, here in skate, is a mandibular arch derivative. By also identifying gene expression features and cell types (*foxl2*, *gata2*, NECs) shared between the pseudobranch and gills, I further present strong evidence in favour of interpreting the pseudobranch as a vestigial gill on the back of the jaw in skate. By identifying a shared signalling centre emanating sonic hedgehog signalling in the posterior margin of the mandibular, hyoid and gill arches, which drives spiracular cartilage and branchial ray development, and by demonstrating that equivalent domains of mesenchyme, equally competent to respond to this shh signal, give rise to both spiracular cartilage and branchial rays, I have also presented strong evidence in favour of interpreting the spiracular cartilage as a vestigial branchial ray on the mandibular in skate. As a vestigial gill slit that ancestrally separated the jaw and hyoid arch is a prediction of the classical anatomical hypothesis of jaw-gill arch serial homology, this work provides further developmental evidence consistent with an ancestral gill-arch-like condition of the mandibular arch and serial homology of the jaw and gill arches.

Chapter 5: Discussion

The emergence of jaws was a critical event in vertebrate history, but the acquisition of this morphological innovation has been a long-standing question in vertebrate evolution. As outlined in chapter 1, most modern developmental hypotheses of jaw evolution aim to explain the origin of the gnathostome jaw by modification of a cyclostome-like condition – for example via a heterotopic shift in epithelial-mesenchymal interactions restricting skeletogenic transcription factor expression to the mandibular arch (Shigetani et al., 2002), by confinement of the embryonic progenitors of ancestrally distinct rostral pharyngeal skeletal elements to the mandibular arch, and subsequent assimilation of mandibular arch derivatives to segmented skeletal arrangement found in more caudal arches (Miyashita, 2016), or by co-option of a developmental mechanism promoting joint fate into a mandibular arch that is otherwise largely gnathostome-like in its dorsoventral patterning (Cerny et al., 2010). These hypotheses, in turn, are predicated on the assumption that the cyclostome-like pharyngeal skeleton reflects an ancestral vertebrate condition. There is some palaeontological support for this view, though this comes in the form of inferred cyclostome-like skeletal conditions from casts of cranial nerve paths and muscle scars inside the dermal head shield of stem-gnathostomes, and not from direct observation of endoskeletal preservation (Janvier, 1996; Miyashita, 2016).

More recent palaeontological data originating from Cambrian stem-vertebrates has started to shift this view. A recent reappraisal of the Cambrian stem-vertebrate *Metaspriggina walcotti* (Morris, 2008) has found that this animal possessed seven paired gill bars, each segmented into bipartite dorsal and ventral elements, reminiscent of the epi- and ceratobranchials of the gill arches of crown gnathostomes (Morris & Caron, 2014). If this reconstruction reflects an accurate preservation of the ancestral pharyngeal endoskeleton – and if the most rostral of these segmented bars is derived from the first pharyngeal arch – this would imply that a pharyngeal skeletal organization more closely resembling that of crown gnathostomes (i.e. with a serially repeated set of segmented skeletal derivatives arising

from each pharyngeal arch, exemplified by chondrichthyans) could, in fact, be plesiomorphic for vertebrates. It would follow that differences between cyclostome and gnathostome pharyngeal skeletons reflect cyclostome divergence from the plesiomorphic condition retained in gnathostomes, rather than vice versa. In light of this scenario, attention has returned to the parallel anatomical organisation of the gnathostome jaw and gill arch skeleton and the classical hypothesis of jaw-gill arch serial homology built on this observation (Gillis et al., 2013).

Here I have tested the hypothesis of jaw-gill arch serial homology at two levels of biological organisation in a cartilaginous fish, the little skate (*Leucoraja erinacea*): first, at the level of gene expression features and axial patterning mechanisms, and second, at the level of vestigial gill arch-like features of the mandibular arch. Specifically, I used a candidate approach to demonstrate that conserved dorsoventral patterning mechanisms underpin the development of the jaw in bony fishes and the pharyngeal arches in skate. Then I used a comparative transcriptomics approach to identify additional members of this conserved pharyngeal patterning program as well as unique transcriptional features that may underpin distinct jaw and gill arch morphologies in skate. Finally, moving from the molecular level of patterning mechanisms to the level of anatomy, I tested for the vestigial presence of the ancestral gill-arch like condition of the jawed vertebrate mandibular arch in the form of the pseudobranch and spiracular cartilage on the back of the jaw of cartilaginous fishes. My findings contrast strongly with the view that the cyclostome-like pharyngeal skeleton reflects an ancestral gnathostome condition. Instead, this work suggests serial homology of jawed vertebrate mandibular and gill arch patterning mechanisms and their anatomical derivatives. However, before discussing these arguments in more depth, which combine patterning mechanisms and morphology to infer homology, I will briefly discuss the concept of homology itself, and how it has evolved over time to include criteria of anatomy as well as developmental biology.

5.1 *A brief history of homology*

Famously, homology can be defined in many different ways, but on a broad level, it revolves around the manifestation of continuity or identity of information (Roth, 1984). Classical comparative anatomy of the 19th century was concerned with the search for common body plans or archetypes. In this context, homology originated as a concept that underpins ‘sameness’ of morphological characters, famously defined as “the same organ in different animals under every variety of form and function” (Owen, 1843). Serial homology is a special case of homology, which was originally defined, also by Owen, as “representative or repetitive relation in the segments of the same organism” (Owen, 1848). In other words, serial homology applies when iterated parts (appendages, subunits) of the same organism are compared, and is most apparent in animals with a modular (metameric) body plan, i.e. when the manifestation of ‘sameness’ occurs within the same individual organism. As such, serial homology has been of longstanding interest to anatomists and evolutionary thinkers. For instance, Charles Darwin, the architect of modern evolutionary biology, invoked serial homology when he considered the origins of repeated vertebrae in back-boned animals or the iterated floral organs in the flowers of angiosperms (Darwin, 1859). However, since the times of Owen and Darwin, the concept of serial homology has been transformed considerably. Owen’s ‘sameness’ aimed to describe how serially homologous features are ultimately all variants of the same idealistic archetype, from which different organisms deviate in their own ways (Owen, 1843; Van Valen, 1982). In Owen’s words, serially homologous features are “manifestations of some higher type of organic conformity on which it has pleased the divine Architect to build up certain of his diversified living works” (Owen, 1848). For Darwin, descent with modification and natural selection were the two workhorses of evolution (Darwin, 1859) and therefore also the explanation for (serial) homology: Owen’s archetype was simply an ancestral condition, and homologous characters are evidence of phylogenetic relationships and shared ancestry.

In modern evolutionary biology, similarities in structure, in anatomical position, as well as embryonic origins are used as criteria to infer homology. Considerations on the ‘sameness’ of putative serially homologous features therefore also involve the mechanisms of development

that generate these features in the embryo. While previous definitions of homology mostly view homologous characters as the consequence of evolutionary diversification of morphologies over time and infer homology by reconstructing phylogenetic relationships, more recent developmental definitions explicitly view (serial) homologues as the consequence of common developmental mechanisms that are (iteratively) redeployed during ontogeny. Broadly, the continuity of information, from which all definitions of homology are ultimately drawn, thus became located in the same “subprograms” of development that may be re-used repeatedly (Van Valen, 1982), via developmental pathways that consist of phylogenetically related genetic components (Roth, 1984). In this view, serial homology amongst iterative features, such as vertebrae or limbs, may be inferred on the basis of an underlying modular developmental program, which is duplicated and then re-deployed in a new location or at a new time—in addition to common anatomical features (Hall, 1995). However, several new problems originated from the inclusion of development as a criterion to infer homology, which led to increasingly specific definitions of (serial) homology in attempts to circumvent these issues.

A strict definition of homology as a result of development involving ‘genealogically-related’ genetic elements complicates homologising entire structures if they partially derive from different developmental pathways (Roth, 1984). This has led to suggestions of a continuum of serial homology on a developmental basis, from identical, strongly homologous features, e.g. two thoracic vertebrae in the same animal, to weakly homologous features that simply derive from the same germ layer, e.g. cranial and trunk muscles in the same animal, which are both mesoderm derivatives. Within this sliding scale framework, the continuum of serial homology was measured by the developmental steps at which developmental paths diverge (Roth, 1984). However, this definition eliminates all putatively (serially) homologous characters from consideration that do not originate via the same developmental pathways. A classic example often invoked to illustrate this point are body segments across insects: as a lineage, insects are nested within arthropods, which are exclusively comprised of segmented animals, and there is no unsegmented sister lineage to insects that could suggest a loss of arthropod-like segmentation prior to their emergence. Nonetheless, genes that are essential for segmentation in the fruit fly *Drosophila melanogaster*, i.e. the pair-rule genes *fushi tarazu* (*ftz*) and *even skipped* (*eve*), are not fulfilling a pair-rule function in the grasshopper

Schistocerca americana, in which they instead mark the central nervous system (Pankratz & Jackle, 1993; Patel et al., 1992; Dawes et al., 1994). However, their anatomical correspondence and their phylogenetic past leave no doubt that the fruit fly and grasshopper body segments are homologous features—but a strict developmental definition of serial homology revolving around the ‘genealogically’ related pair-rule genes would question their homology.

This problem can be addressed in several different ways. For example, it has been proposed to distinguish between homologous characters that result from shared pathways or divergent developmental pathways, i.e. syngeny vs. allogeny (Butler & Saidel, 2000). A different approach is taken by the theory of ‘character identity networks’, which is concerned with the historical continuity of the gene regulatory networks that underpin putatively homologous characters, rather than the expression of individual homologous genes (Wagner, 2007, 2014). Through testing for these character identity networks, it can be established whether a body part is a novelty or a derived feature serially homologous to a different structure—for example, if the gnathostome jaw and gill arches share a character identity network that specifies their identities during development.

Taken together, this era of developmental homology concepts ignited a long-standing (and ongoing) debate on the presence and absence of homology at the molecular level at which developmental processes and patterns operate (Dickinson, 1995). In other words, re-deployed developmental programs may diverge with or without consequences for the phenotypic readout (Hall, 1995), which decouples homology on the morphological and the developmental level. One solution to this conundrum is considering homology as a hierarchical concept: while some characters may be homologous on an anatomical level, they may not be generated by homologous developmental processes (Dickinson, 1995; Abouheif, 1997; Wagner, 2014). This renders hypotheses of homology testable from different perspectives, and allows us to revisit classical hypotheses, which were originally based on anatomy, using modern techniques of developmental biology.

5.2 Jaw-gill arch serial homology and the evolution of gnathostome jaws

Here, I have applied the hierarchical line of thinking about homology to the question of jaw origins in gnathostome vertebrates by testing for serial homology on molecular and anatomical levels of biological organisation: I report common patterning mechanisms in the form of gene expression domains that unite all pharyngeal arches, and I demonstrate the presence of gill-arch vestiges on the back of the jaw in skate.

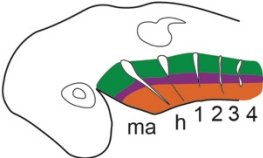
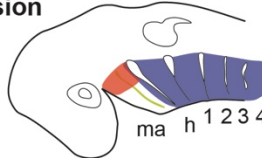
The combination of candidate and differential gene expression analysis outlined in chapters two and three has revealed a suite of transcription and signalling factors that display polarised expression along the dorsoventral axis of the pharyngeal arches in skate. The overwhelming majority of these genes, for example dorsal territory marks such as *pou3f3* and *foxg1*, joint factors such as *bapx1* and *gdf5*, and ventralising *endothelin* and *bmp4*, share expression in the mandibular, hyoid and gill arches (serially shared genes in Fig. 5.1A). Together with previous reports of shared expression of core components of the pharyngeal arch dorsoventral patterning network in cartilaginous and bony fishes, such as the *dlx* genes (Gillis et al., 2013; Compagnucci et al., 2013), these findings point to a conserved transcriptional network patterning the dorsoventral axis of the mandibular, hyoid and gill arches in the gnathostome crown group, and serial homology of the gnathostome jaw, hyoid and gill arch skeleton (Fig. 5.1B).

Additionally, I report distinct transcriptional features of the mandibular and gill arches in skate (arch specific genes in Fig. 5.1A). These include mandibular arch-specific expression of *six1*, *eya1* and *scamp5* in the dorsal mesenchyme and expression of *six2*, *tbx18* and *pknox2* in the mesoderm; and hyoid and gill arch-specific mesodermal expression of *lhx9* and endodermal expression of *gcm2*, *wnt2b* and *foxq1* in developing gills. The mandibular arch-specific mesenchymal gene expression features may reflect jaw-specific divergence from the ancestral pharyngeal dorsoventral patterning program and may function downstream of global anteroposterior patterning mechanisms (e.g. the *Hox* code of the vertebrate head) and in parallel with local signals from oral epithelium to effect anatomical divergence of the

mandibular arch skeleton (Hunt & Krumlauf., 1991; Rijli et al., 1993; Couly et al., 1998, 2002; Hunter and Prince, 2002). The mesodermal and endodermal gene expression features may underlie the evolution of arch-specific muscular and gill fates, respectively. Expression of *eya1*, *six1*, *six2*, *tbx18* and *pknox2* may therefore be ancestral features of the gnathostome mandibular arch, while *lhx9*, *gcm2*, *wnt2b* and *foxq1* may be ancestral features of the gnathostome gill arches. However, depending on comparative expression data from other lineages, it is also feasible to infer that some of these expression patterns may be skate- or chondrichthyan-specific: for example, as notch signalling has been found to play a critical role in patterning the mandibular arch derivatives in mouse and zebrafish (Zuniga et al., 2010; Barske et al., 2016; Tavares et al., 2017), the near absence of expression of the notch signalling readout *hey1* from the mandibular arch may be a derived feature of the skate or chondrichthyans more broadly, or a retention of an ancestral vertebrate condition that has been lost in bony fishes. Comparative data on notch signalling from jawless fishes is needed to resolve the likely ancestral role of notch signalling in patterning the vertebrate mandibular arch.

In light of Cambrian stem vertebrates displaying a bi-partite, dorsoventrally polarised organisation of the pharyngeal endoskeleton in the fossil record, i.e. *Metaspriggina*, it is worth speculating whether the pan-pharyngeal transcriptional program described here in skate could have functioned to pattern the dorsoventral axis and to serially delineate pharyngeal skeletal segments not just in the last common ancestor of the gnathostome crown group, but more generally, in the last common ancestor of vertebrates (Fig. 5.1B). In other words, the serially shared core components of the pharyngeal arch patterning network as found in skate might predate the origin of the gnathostome body plan and could reflect the retention of a patterning program ancestral to vertebrates, while arch specific gene expression patterns, such as dorsal mandibular arch *eya1/six1* expression in the mesenchyme (Fig. 5.1A), may be associated with the evolution of the jaw.

A Core components of the pharyngeal arch dorsoventral and anteroposterior patterning program in gnathostomes as found in skate (*Leucoraja erinacea*)

Serially shared genes			Arch specific genes		
Tissue	Epithelial	Mesenchymal	Tissue	Epithelial	Mesenchymal
■	<i>shh, foxg1, foxl2, eya1, six1</i>	<i>dlx1/2, pou3f3, barx1, gsc, twist2, sfrp2</i>	■		<i>eya1, six1, scamp5</i>
■	<i>shh, grem2, foxl2, nkx2.3, eya1, six1</i>	<i>dlx1/2/5/6, bapx1, gdf5</i>	■	<i>lhx9, gcm2, wnt2b, foxq1</i>	<i>hey1</i>
■	<i>shh, edn1, bmp4, nkx2.3, foxe4, eya1, six1</i>	<i>dlx1-6, mef2c, barx1, msx1, gsc, hand1, hand2, twist2, sfrp2</i>	■	<i>six2, tbx18, pknox2</i>	
Expression 			Expression 		

B Evolution of the gnathostome jaws

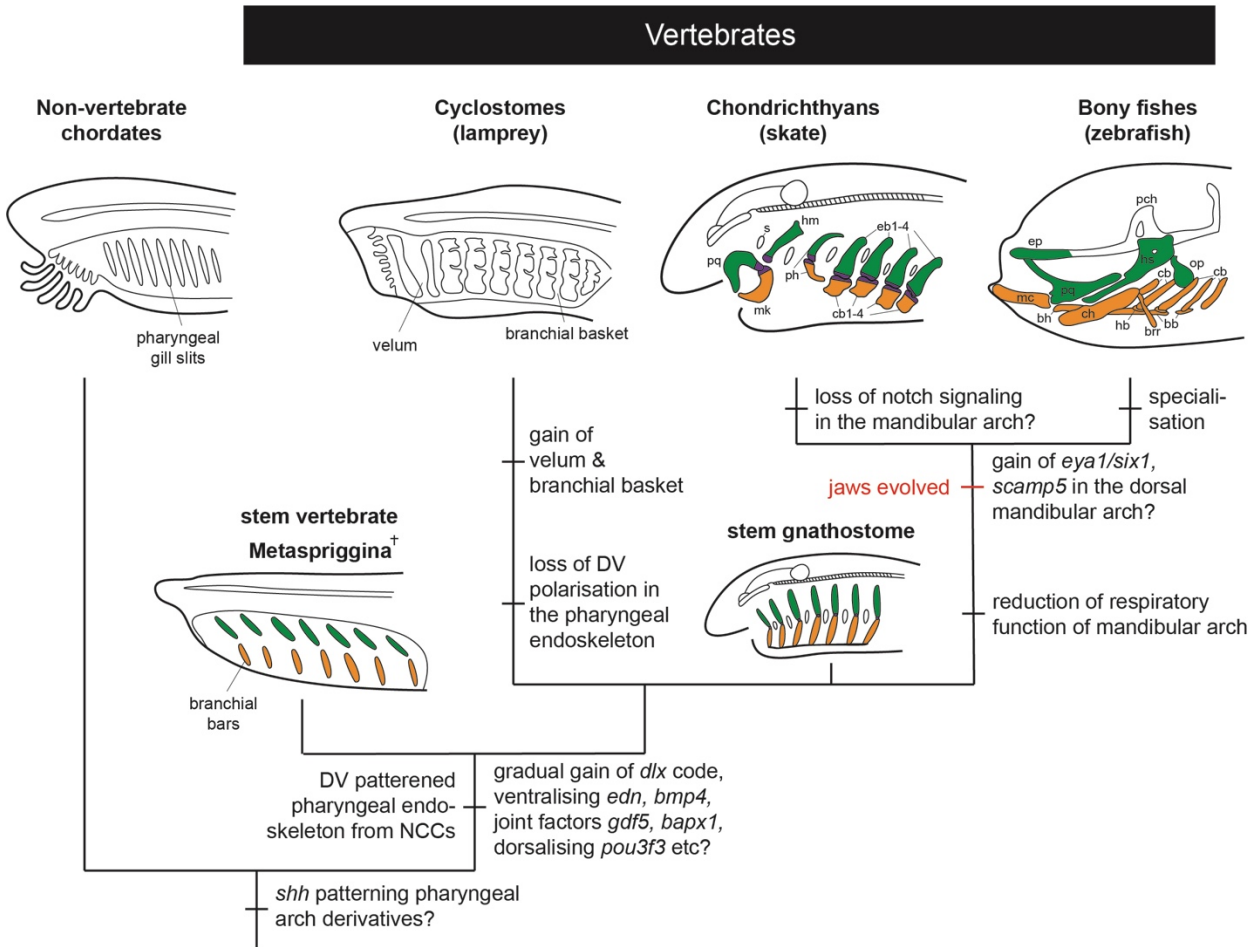


Figure 5.1: The origin of gnathostome jaws via molecular and anatomical serial homology.

(A) Summary of polarised gene expression patterns within skate pharyngeal arches. Serially shared genes possess expression patterns that are serially repeated across the mandibular, hyoid and gill arches in skate. These expression features may comprise an ancestral core pharyngeal arch dorsoventral patterning program for gnathostomes, and underlie serial homology of the jaw, hyoid and gill arch skeleton. Genes in bold italic are likely candidates of such an ancestral network as they are also found in lamprey (though their expression in larval lampreys may not correspond exactly to the dorsoventral expression pattern found in skate). Arch specific genes possess expression patterns that are unique to one or to a subset of pharyngeal arches in skate and may underlie the anatomical divergences of jaws and gill arches, on top of primitively similar molecular and anatomical identities of all arches. (B) The evolution of dorsoventral patterning in the pharyngeal endoskeleton of vertebrates and serial homology of jaws and gill arches. As the dorsoventrally patterned pharyngeal endoskeleton derived from neural crest cells evolved in stem vertebrates, such as *Metaspriggina*, this was likely underpinned molecularly by the gradual gain of the dorsoventral patterning code active during pharyngeal arch development. Ancestrally, jawless stem gnathostomes thus possessed pharyngeal arches that were patterned dorsoventrally by a shared transcriptional network, which iteratively gave rise to serially homologous, bi-partite gill arches in the adult anatomy, each separated by gill slits. In the lineage leading to cyclostomes, this bi-partite, dorsoventrally segregated organisation was lost and the velum and branchial basket instead evolved as pharyngeal arch derivatives. In the lineage leading to gnathostomes such as skate or zebrafish, however, the mandibular arch eventually gained a unique molecular patterning mechanism on top of the pan-pharyngeal code that transformed its derivative, the ancestral first gill arch, into jaws. The gill slit ancestrally separating the first, mandibular-arch-derived arch from the second, hyoid-arch-derived arch was transformed into the spiracle. bb, basibranchial; bh, basihyal; br, branchial rays; brr, branchiostegal ray; cb, ceratobranchial; ch, ceratohyal; eb, epibranchial; hb, hypobranchial; hs, hyosymplectic; hm, hyomandibula; mc, Meckel's; mk, Meckel's cartilage; op, opercle; pch, prechordal; pq, palatoquadrate, pb, pseudobranch; ph, pseudohyal; s, spiracle.

In the fourth chapter of this dissertation, I investigate the theory of jaw-gill arch serial homology on an anatomical level by testing whether the ancestral nature of the mandibular arch may have been gill arch-like. This is a prediction of the classical theory of jaw-gill arch serial homology, which proposes that jaws originated through transformation of the anterior-most gill arch (Gegenbaur, 1878; Romer, 1966). In contrast, most modern developmental hypotheses of jaw evolution assume the jaw originated out of a non-gill bearing, cyclostome-like condition, and since lampreys do not possess a gill slit separating the first two pharyngeal arches, this also implies that ancestrally no gill slit separated the jaw and hyoid arch. Therefore, the idea that the jaw might bear remnants of a gill arch-like past has been largely discounted and features reminiscent of a gill slit on the back of the jaw, i.e. the spiracle, have been interpreted as secondarily derived. However, I find strong evidence consistent with a vestigial gill element in the spiracle of the skate.

I report that the embryonic mandibular arch in skate possesses a signalling centre that strongly resembles the gill arch epithelial ridge (GAER) on the hyoid and gill arches. These serially repeated epithelial signalling centres all express *shh*, which functions to pattern the subjacent, skeletogenic mesenchyme, giving rise to the spiracular cartilage on the mandibular arch and the branchial rays on the hyoid and gill arches in skate. The shared embryonic origin from equivalent domains of *shh*-responsive mesenchyme on the pharyngeal arches is developmental evidence consistent with the historical interpretation of the spiracular cartilage as a vestigial branchial ray (Gegenbaur, 1872; Holmgren & Stensiö, 1936; El-Toubi, 1947). Furthermore, I report that in skate the pseudobranch is indeed mandibular arch-derived, and that it shares molecular and cell type features with the respiratory gill filaments of the gill arches. These conserved anatomical, developmental, and molecular similarities—i.e. shared endoskeletal support for the gill filaments by cartilage elements derived from *shh*-responsive mesenchyme, shared gene expression during gill morphogenesis, and shared NECs, respectively—strongly point to the pseudobranch being a vestigial gill element. Taken together, this work provides a mechanistic explanation for the correspondence of the pseudobranch to gill filaments and the correspondence of the spiracular cartilage to branchial rays. In the context of a putative branchial series in stem gnathostomes, this further suggests the mandibular arch and hyoid arch were ancestrally separated by a gill slit, unlike in modern

cyclostomes, and that this ancestral gill slit has been retained in the form of the spiracle (Fig. 5.1B).

Pseudobranchs are also widely present in bony fishes, suggesting that this feature is likely ancestral to gnathostomes, though lineage tracing experiments are needed to confirm whether the bony fish pseudobranch is a mandibular arch derivative as well. However, there is currently no evidence for a spiracular cartilage homologue or branchial rays outside of elasmobranchs, which indicates that these elements are likely derived features of cartilaginous fishes. While the spiracular cartilage-branchial ray correspondence can consequently only be resolved to the chondrichthyan lineage, my findings still lead to the conclusion that the spiracle indeed represents a vestigial gill slit. Within it, a reduced gill element is retained, which in chondrichthyans is supported by a vestigial branchial ray, i.e. the spiracular cartilage. These interpretations of the anatomy and development in skate are in agreement with the classical interpretations of these structures as vestiges of the gill-arch like past of the mandibular arch (Gegenbaur, 1872; Ridewood, 1896; Goodrich, 1909; El-Toubi, 1947), but stand in stark contrast to most modern developmental hypotheses of jaw evolution, which frame the acquisition of this morphological novelty as a transformation of a cyclostome-like past. Instead, the evidence presented here, in combination with recent reappraisal of *Metaspriggina* and the changing view on the ancestral pharyngeal endoskeleton as dorsiventrally polarised and bi-partite (Morris & Caron, 2014), suggests that the differences between cyclostome and gnathostome pharyngeal skeletons reflect cyclostome divergence from the plesiomorphic condition retained in gnathostomes (Fig. 5.1B), rather than vice versa.

Further evidence for this shift in thinking on gnathostome origins comes from the recent recovery of larval stem lampreys from the Paleozoic that lack the typical characteristics of ammocoetes and instead show adult-like traits, including a cusped feeding apparatus and posteriorly united branchial baskets (Miyashita et al., 2020). The morphological similarities between larval lampreys and invertebrate chordates thus likely resulted from the convergence of these two lineages on a similar lifestyle, i.e. filter-feeding, rather than a retaining of an ancestral condition in ammocoetes (Miyashita et al., 2020). It follows that the pharyngeal endoskeletal condition found in the larvae of extant lampreys is a derived

condition of crown group lampreys. Given this fossil evidence, the larvae of extant lampreys cannot provide a model of the hypothetical ancestral conditions of the pharyngeal endoskeleton in early jawless vertebrates or stem gnathostomes. While there is still a dearth of comparable fossil evidence on the condition in the gnathostome stem to fill this gap, this shifts the focus back on scenarios that do not assume a larval lamprey-like condition in stem gnathostomes, such as jaw-gill arch serial homology.

Consequently, when considered alongside comparative data from bony fishes, the findings reported here may lead to a new model of jaw evolution that combines the anatomical arguments in favour of jaw-gill arch serial homology put forward by Carl Gegenbaur with the molecular and developmental data provided by the little skate. As outlined above, the serially shared, pan-pharyngeal transcriptional program (Fig. 5.1A) may have functioned to pattern the dorsoventral axis and to iteratively confer pharyngeal skeletal identity not just in the last common ancestor of the gnathostome crown group, but more generally, in the last common ancestor of vertebrates, coincident with the origin of pharyngeal endoskeletal segmentation (Fig. 5.1B). Over the course of evolution, along the anteroposterior axis of the pharyngeal endoskeleton, this may have given rise to a primitive series of dorsal, intermediate, and ventral skeletal elements and associated nerves, muscles and connective tissues, which through changes in functions associated with ventilation and predation have been modified into the jaw, hyoid and gill arches of modern gnathostomes. It seems feasible to speculate that stem gnathostomes underwent large-scale changes in life history strategies in terms of increasing reliance on predation as mode of feeding, as suggested by the new head and new mouth models of vertebrate evolution (Northcutt & Gans, 1983; Mallat, 1984), though their ancestral state likely did not resemble the oropharyngeal organisations of modern-day lampreys.

To test this hypothesis and better understand the acquisition of this patterning mechanisms in the vertebrate stem, it would be of considerable interest to test for the expression of orthologous genes in the chordate sister groups to vertebrates, i.e. urochordates (tunicates) and cephalochordates (amphioxus), to determine whether or to which degree the pharyngeal patterning mechanisms are conserved across chordates. The neural crest cell derived, collagenous pharyngeal endoskeleton is a vertebrate-specific innovation (Janvier, 1996), as

are some of the pharyngeal patterning components, e.g. endothelin ligands (Martinez-Morales et al., 2007; Braasch & Schartl, 2014). However, other aspects of the pharynx, such as out-pocketing endoderm and associated transcription factors, are deeply conserved within deuterostomes (Gillis et al., 2012; Simakov et al., 2015). Similarly, the oral skeleton of the cephalochordate amphioxus *Branchiostoma floridae*, which otherwise lacks neural crest cells, has been shown to possess cellular cartilage akin to the cartilage found in vertebrates (Jandzik et al., 2015). This has led to the suggestion that the evolution of the vertebrate head skeleton involved the recruitment of the genetic mechanisms in the mesendoderm that drives cellular cartilage differentiation in amphioxus (a gene encoding a clade-A fibrillar collagen, *ColA*, and the transcription factors *SoxE* and *SoxD*) by the novel neural crest cells, and the spread of the resulting collagenous cartilage from the oral region into the pharynx and the head (Jandzik et al., 2015). As the robust pharyngeal endoskeleton evolved, the developmental changes in the vertebrate head may have been intertwined with the acquisition of the axial patterning program outlined in Fig. 5.1A., giving rise to the ancestrally polarized mandibular, hyoid and gill arches and their derivatives from cranial neural crest cells in stem vertebrates.

Three different scenarios underpinning the acquisition of the axial patterning program seem feasible: The first possibility is the redeployment of transcription factors or epithelial signalling interactions from previous functions in development to the pharynx, akin to how the collagen-generating *SoxD/E-ColA* gene regulatory network in the oral apparatus of cephalochordates has likely been recruited by the neural crest cells in stem vertebrates. For example, the dorsal marker *pou3f3*, the joint markers *nkx3.2* and *gdf5*, and ventral markers *hand1*, *hand2* and *msx1* may have each been recruited from elsewhere during development by the same neural crest cells as they incorporated *SoxD/E* and *ColA*. This may have underpinned the dorsoventral polarisation across the pharyngeal endoskeleton in stem vertebrates as the collagenous endoskeleton of the pharynx evolved. If this is the case, we may predict expression of orthologous genes fulfilling patterning roles outside the pharynx in non-vertebrates. This may be the case for the *hand* transcription factors, which function in early heart formation, a process that has a deep metazoan origin and is largely conserved in flies and mammals, and accordingly expression of *hand* orthologues is also found during cardiogenesis in flies and vertebrates (Srivastava et al., 1995; Han & Olson, 2005; Han et al., 2006). As the vertebrate pharynx evolved, expression of *hand* orthologues originally from the

developing heart may have been extended into the ventral pharyngeal arch mesenchyme to confer lower arch identity. Testing for the presence and expression of *hand* genes in larval amphioxus may resolve this question.

The second possibility is the components of the pharyngeal patterning program may have already played a role in patterning the non-neural crest derived head and pharynx across non-vertebrate chordates and maintained this function as the novel neural crest cells begun migrating into the new, vertebrate-specific pharynx. Members of the patterning network that underwent this scenario can be expected to be expressed in equivalent domains of the pharynx in non-vertebrate chordates. A possible candidate for this scenario is *foxe4*, which in skate marks the ventralmost pharyngeal endoderm and has already been shown to also be expressed in the amphioxus pharyngeal endoderm (Yu et al., 2002). Similarly, on the dorsal side of the patterning program, expression of *Brn1/2/4*, a member of the POU3 class of transcription factors and potential amphioxus orthologue of *pou3f3*, has been described in the dorsal amphioxus pharynx (Candiani et al., 2002).

The third possibility is *de novo* evolution of genes in the vertebrate stem as the vertebrate pharynx evolved. These genes and signalling pathways are expected to be vertebrate specific novelties. This scenario is exemplified by endothelin ligands and receptors, which pattern the ventral pharynx in the earliest branching lineage of vertebrates, i.e. cyclostomes (Square et al., 2016, Square et al., 2020), but are not found in non-vertebrate animals (Martinez-Morales et al., 2007; Braasch & Scharl, 2014). This suggests the role of endothelins in patterning the neural crest cells originated alongside this vertebrate-specific cell population (Square et al., 2020).

Finally, it should be noted that there is no evidence of a comparable patterning network in another tissue that predates the origin of vertebrates, which makes a ‘wholesale’ re-deployment by the patterning network outlined in Fig. 5.1A highly unlikely. Similarly, the mesenchyme populating the pharyngeal arches in vertebrates is a novelty, and not found in non-vertebrate chordates. Therefore, it seems feasible that the acquisition of the pharyngeal patterning program was a gradual process, and its individual components, like mesenchymal *hand* genes, were redeployed for novel functions in the pharynx on top of previous gene

expression, such as endodermal *foxe4*, while others arose *de novo*, like endothelin signalling. Nonetheless, only comparative studies in non-vertebrate chordates can resolve the exact mode of acquisition by which the axial patterning program achieved its role within the pharyngeal arches of stem vertebrates.

Consequently, previous hypotheses of jaw evolution like the heterotopic shift in epithelial-mesenchymal interactions (Shigetani et al., 2002) or the pre-pattern co-option model (Cerny et al., 2010) that frame the acquisition of the jaw by rewiring the patterning mechanisms in the oropharyngeal region of a lamprey-like stem gnathostome, may actually highlight the developmental changes that correlate with the loss of dorsoventral polarity in the pharyngeal endoskeleton, the emergence of the branchial basket, and other peculiarities of cyclostomes. For instance, the epithelial signalling acting upon the pre-mandibular mesenchyme caudal to the eye in the lamprey, which gives rise to upper lip and which is shared by the mandibular arch in gnathostomes (Shigetani et al., 2002) may reflect a unique adaptation of the premandibular mesenchyme in lampreys (i.e. the upper and lower lips) that cannot easily be homologized with gnathostome derivatives of this region, rather than an ancestral state of patterning mechanisms, which had to be adapted to allow for the emergence of jaws from this region. The loss of *Gdf5* and *Nkx3.2/Bapx1* expression from the intermediate region of the mandibular arch in lampreys (Cerny et al., 2010) may underpin the development of a different morphological novelty, i.e. the velum and its cartilaginous support element. The patterning mechanisms conserved between lamprey and gnathostomes, such as ventral *edn1* and *hand* expression (Square et al., 2016; Square et al., 2020), have often been interpreted as a ‘ground plan’ upon which gnathostomes have added transcriptional elaboration, e.g. *Gdf5* and *Nkx3.2/Bapx1* expression, but in accordance with the scenarios described above it also seems feasible to hypothesize that the patterning mechanisms found in lamprey represents a reduced or simplified version of the ancestral patterning network, in which core features, such as endothelin signals patterning migrating neural crest cells, are preserved, while others have been lost, simplified, or otherwise derived, relative to the gnathostome pharyngeal patterning network.

5.3 Serially homologising beyond the jaws and gill arches in gnathostome body plan evolution

Recent fate mapping experiments in skate have shown that the mandibular and hyoid arch skeleton derives exclusively from neural crest cells, but the gill arch skeleton is characterized by a dual origin from both the neural crest and the mesoderm, while the pectoral fin skeleton is exclusively mesoderm derived (Sleight et al., 2020). As skeletogenic primordia in the skate hyoid and gill arches and in the tetrapod limb bud share responsiveness to shh signalling in terms of anteroposterior axis establishment and proliferative expansion (Gillis et al., 2009b; Gillis & Hall, 2016), these findings demonstrate a common competence of gill arch and fin/limb skeletal progenitors to respond to shh signals in cartilaginous fishes. This conserved competence has been interpreted as consistent with putative serial homology of the skeletal derivatives of the gill arches and the fin/limbs (Sleight et al., 2020). Traditionally, serial homology has been thought of as necessitating shared embryonic origin (Hall, 1995), but this new view decouples serial homology on an anatomical level from strict germ layer fates, and instead shifts the focus on conserved developmental competence, in this case within the vertebrate skeleton.

Here I have shown that a shared shh signalling centre (GAER) also plays a role in patterning a mandibular arch-derived appendage in skate, i.e. the spiracular cartilage. Thus, I provide evidence for further anterior competence of skeletogenic mesenchyme to respond to shh in a similar fashion as the gill arches and fins. In this context, it is interesting to note that the subsequent patterning of the skeletal derivatives of pharyngeal arches and fin/limb buds, i.e. the jaw, gill arches, and pectoral fin/limb skeleton, also share commonalities across gnathostomes. For example, genes like *barx1*, *nkx3.2* and *gdf5* are also active in skeletogenesis in the mesoderm-derived skeleton of the fins/limbs in bony fishes, e.g. in synovial joint formation (Tissier-Seta et al., 1995; Church et al., 2005; Crotwell et al., 2007; Storm & Kingsley, 1996; Brunet et al., 1998; Merino et al., 1999; Hartmann & Tabin, 2001). Another example is *Bmp4* and its expression in the apical ectodermal ridge at the distal end of the limb bud, which is a key player in regulating limb development (Duprez et al., 1996; Pizette et al., 2001; Ahn et al., 2001; Selever et al., 2004; Wang et al., 2004)—as well as in

lower jaw development. The overlap of these developmental patterning programs, i.e. axial patterning of the pharynx and the limbs across gnathostomes, seems striking. As the jaw and paired fins are both gnathostome synapomorphies, the evolution of the developmental fates of the skeletogenic mesenchyme and mesoderm in the pharyngeal arches and fin buds, respectively, may have been driven by the acquisition the patterning mechanisms as outlined in Fig. 5.1A, as a shared response or common competence to respond to similar signalling centres such as the GAERs. In other words, these two evolutionary innovations of the gnathostome body plan—jaws and paired fins—may share ancestry as pharyngeal arch derivatives and may therefore have shared a common, serially-repeated patterning program. This scenario is based on the decoupling of germ layer origin, meaning the axial patterning program was retained by all skeletogenic tissues, i.e. the mesenchyme of the mandibular and hyoid arches, the mesenchyme and mesoderm of the gill arches, and the mesoderm of the fin buds.

This view provides a mechanistic framework for the putative serial homology across the jaw, gill arches, and the pectoral fin skeleton originally suggested by Carl Gegenbaur (1878): while the skeletogenic primordia of the jaw, gill arches, and the pectoral girdle and fin do not share common embryonic origins from the same germ layer, they do share a conserved competence to respond to *shh* signalling emanating from posterior marginal ridge (Sleight et al., 2020) and they share the repeated deployment of axial patterning mechanisms, such as regulators of joint formation or *bmp* signalling. However, there is currently no clear evidence from the fossil record to support or refute this theory (Coates, 2003), and in the absence of such palaeontological data other theories such as the fin-fold hypothesis (Thacher, 1877; Balfour, 1881; Mivart, 1879; Tanaka et al., 2002; Tulenko et al., 2016) have been put forward. The shared expression of joint markers and chondrogenesis regulators across pharyngeal arches and developing limb buds also lacks a neat correspondence that complicates inferring clear-cut serial homology on a developmental basis alone. In the original theory put forward by Gegenbaur, the (shoulder) girdle of tetrapods represents a modified gill arch and the limb/fin skeleton (stylopod, zeugopod, autopod) represents modified branchial rays, but the signalling I have described in the pharyngeal arches in skate cannot be easily mapped from the pharyngeal arches onto the limb bud: in skate, intermediate expression of *gdf5* in the pharyngeal arches marks presumptive joint domains in the gill arches, i.e. the hypothetical

ancestral girdle, whereas in tetrapods, *gdf5* marks presumptive joint domains in the digits, i.e. the autopod (e.g. Hartmann & Tabin, 2001). This may imply two different scenarios if the gill arch-fin serial homology view holds true: on the one hand, if there is a correspondence between these different joint domains in gill arches vs. limbs, the classical gill arch-fin serial homology could also have involved a topographic shift of gene expression patterns playing a role in joint formation. In other words, the putative shoulder girdle antecedent, i.e. the gill arch, ancestrally possessed a joint marked by *gdf5* expression, which then shifted to the limb skeleton as the limb evolved. On the other hand, the shared expression of *gdf5* in the skate gill arches and in tetrapod limb buds may simply be a reflection of a conserved role of *gdf5* in joint formation, and lack any meaningful role in the putative serial homology of gill arches and limbs. Further comparative gene expression studies of known limb bud regulators across the pharyngeal arches are needed to test this more comprehensively. Nonetheless, the expression features of pharyngeal arches of a cartilaginous fish presented here may thus prove to be informative with regards to other evolutionary theories on the gnathostome body plan and may provide insightful developmental data to rework the framing of serial homology across vertebrate evolution.

To find out what truly differentiates the jaw from the gill arches on a molecular level, it would be interesting to pair the RNA-seq and differential gene expression experiments presented here with chromatin immunoprecipitation and DNA sequencing (ChIP-seq) and assays for transposase-accessible chromatin with high-throughput sequencing (ATAC-Seq). ChIP-seq and ATAC-Seq are used to profile epigenetic modifications and chromatin accessibility on a genome-wide scale, i.e. they reveal the non-coding DNA regions such as transcription factor binding sites involved in the spatiotemporal regulation of gene expression at base-pair resolution (Park, 2009; Buenrostro et al., 2015). However, both techniques require the availability of a high-quality genome for reference—which has only been recently completed in skate (by Professor José Luis Gómez-Skarmeta, unpublished). In the context of jaw evolution and patterning of the pharyngeal endoskeleton in skate, these methods could be used to map the genome regulatory landscapes along the dorsoventral and anteroposterior axis of the developing jaw and gill arches (particularly the skeletogenic mesenchyme). This approach might yield the exact gene regulatory network that commands cell population differentiation into the principal components of the pharyngeal endoskeleton in skate, i.e.

Meckel's cartilage and palatoquadrate in the mandibular arch, and cerato- and epibranchial cartilages in the gill arches, respectively. For example, by comparing the epigenomic profiles of each of these skeletogenic cell populations, putative *cis*-regulatory elements may be mapped that underpin how dorsal expression of the transcription factors *eya1* and *six1* in the mandibular arch mesenchyme informs differentiation into the skeletal elements of the upper jaw. Additionally, by comparisons of the dynamics of gene expression and chromatin accessibility within skate to the genome regulatory landscapes across vertebrates, the evolution of the diversity of pharyngeal skeletal derivatives may be elucidated—i.e. the changes in the regulatory elements that underpin how for example despite shared *dlx* transcription factor expression across cyclostomes as well as gnathostomes, the pharyngeal arches in lamprey form a velum and a branchial basket, while they give rise to the jaws and gill arches in fishes, and finally the jaw and middle ear ossicles in tetrapods.

Hence, while there still is a gap in the fossil record and no evidence exists to support or refute the hypothesis of jaw-gill arch serial homology on palaeontological evidence alone, the combination of anatomical and developmental data from skate which I have assembled here may serve as a stepping-stone in the bridge across this gap. There is now a consistent wealth of developmental and anatomical evidence that suggests the jaw is indeed a derived, serially homologous element of an ancestral branchial series, and my data from skate further describe a vestigial gill on the back of the jaw in chondrichthyans—consistent with a gill-arch-like past of the mandibular arch, and consistent with Gegenbaur's classical hypothesis of jaw-gill arch serial homology. Put together, it is my hope that these findings serve to answer important questions in vertebrate evolution.

Supplementary files

Chapter 1:

There are no supplementary files associated with this chapter.

Chapter 2:

Table S2.1.xlsx = List of accession numbers and sequences associated with the skate genes whose expression I have described throughout chapters 2-4.

Chapter 3:

Script S3.1.xlsx = Bash script containing the code used to assemble the *Leucoraja erinacea* pharyngeal arch transcriptome from trimmed, cleaned, and normalised read data.

Script S3.2.R = R script containing the code used to identify differentially expressed genes and generate associated plots across pharyngeal arch samples from S23-24.

Script S3.3.R = R script containing the code used to identify differentially expressed genes and generate associated plots across pharyngeal arch samples from S25-26.

Table S3.1.xlsx = Differentially expressed *Leucoraja erinacea* genes selected for validation through ISH and associated expression patterns, if available

Table S3.2.xlsx = *Leucoraja erinacea* genes differentially expressed in ventral vs dorsal gill arches at S23/24.

Table S3.3.xlsx = *Leucoraja erinacea* genes differentially expressed in ventral vs dorsal mandibular arches at S23/24.

Table S3.4.xlsx = *Leucoraja erinacea* genes differentially expressed in dorsal mandibular arch vs dorsal gill arch at S23/24.

Table S3.5.xlsx = *Leucoraja erinacea* genes differentially expressed in ventral mandibular arch vs ventral gill arch at S23/24.

Table S3.6.xlsx = *Leucoraja erinacea* genes differentially expressed in ventral vs dorsal gill arches at S25/26.

Table S3.7.xlsx = *Leucoraja erinacea* genes differentially expressed in ventral vs dorsal mandibular arches at S25/26.

Table S3.8.xlsx = *Leucoraja erinacea* genes differentially expressed in dorsal mandibular arch vs dorsal gill arch at S25/26.

Table S3.9.xlsx = *Leucoraja erinacea* genes differentially expressed in ventral mandibular arch vs ventral gill arch at S25/26.

Chapter 4:

Figure S4.1.jpg = Additional mandibular arch cell lineage tracing results showing broad CM-Dil+ chondrocyte contributions throughout spiracular cartilages at S32.

References

- Abouheif, E. (1997). Developmental genetics and homology: a hierarchical approach. *Trends in ecology & evolution*, 12(10), 405-408.
- Abu-Issa, R., Smyth, G., Smoak, I., Yamamura, K. I., & Meyers, E. N. (2002). Fgf8 is required for pharyngeal arch and cardiovascular development in the mouse. *Development*, 129(19), 4613-4625.
- Abzhanov, A., Protas, M., Grant, B. R., Grant, P. R., & Tabin, C. J. (2004). Bmp4 and morphological variation of beaks in Darwin's finches. *Science*, 305(5689), 1462-1465.
- Abzhanov, A., Tabin C.J. (2004) Shh and Fgf8 Act Synergistically to Drive Cartilage Outgrowth during Cranial Development'. *Developmental Biology* 273(1): 134–48.
- Ahn, K., Mishina, Y., Hanks, M. C., Behringer, R. R., & Crenshaw, E. B. (2001). BMPR-IA signaling is required for the formation of the apical ectodermal ridge and dorsal-ventral patterning of the limb. *Development*, 128(22), 4449-4461.
- Alexander, C., Zuniga, E., Blitz, I. L., Wada, N., Le Pabic, P., Javidan, Y., Zhang T., Cho K.W., Gage Crump J.G. & Schilling, T. F. (2011). Combinatorial roles for BMPs and Endothelin 1 in patterning the dorsal-ventral axis of the craniofacial skeleton. *Development*, 138(23), 5135-5146.
- Allis, E. P. (1900). Pseudobranchial Circulation in *Amia calva*. *Zool. Jahrb.*, Oct.
- Allis, E. P. (1916). The so-called mandibular artery and the persisting remnant of the mandibular aortic arch in the adult selachian. *Journal of Morphology* 27, 99 – 118.
- Anderson, P. S., Friedman, M., Brazeau, M. D., & Rayfield, E. J. (2011). Initial radiation of jaws demonstrated stability despite faunal and environmental change. *Nature*, 476(7359), 206-209.
- Arai, H., Hori, S., Aramori, I., Ohkubo, H., & Nakanishi, S. (1990). Cloning and expression of a cDNA encoding an endothelin receptor. *Nature*, 348(6303), 730-732.
- Arsenault, M., Desbiens, S., Janvier, P., and Kerr, J. (2004). New data on the soft tissues and external morphology of the antiarch *Bothriolepis canadensis* (Whiteaves, 1880), from the Upper Devonian of Miguasha, Québec, p. 439-454. In Arratia, G., Wilson, M.V.H., and Cloutier, R. (eds.), *Recent Advances in the Origin and Early Radiation of Vertebrates*. Verlag Dr. Friedrich Pfeil, Munich.
- Ashique, A. M., Fu, K. and Richman, J. M. (2002). Endogenous bone morphogenetic proteins regulate outgrowth and epithelial survival during avian lip fusion. *Development* 129, 4647-4660
- Askary, A., Xu, P., Barske, L., Bay, M., Bump, P., Balczerski, B., Bonaguidi M. & Crump, J. G. (2017). Genome-wide analysis of facial skeletal regionalization in zebrafish. *Development*, 144(16), 2994-3005.
- Ayers, H. (1931). Vertebrate cephalogenesis. VI. A. The velum—its in head building—the hyoid. The Velata. The origin of the vertebrate head skeleton. B. Myxinoid characters inherited by the teleostomi. *Journal of Morphology*, 52(2), 309-371.
- Balfour, F. M. (1881). On the Development of the Skeleton of the Paired Fins of Elasmobranchii, considered in Relation to its Bearings on the Nature of the Limbs of the Vertebrata. In *Proceedings of the Zoological Society of London* (Vol. 49, No. 3, pp. 656-670). Oxford, UK: Blackwell Publishing Ltd.

- Ballard, W. W., Mellinger, J. & Lechenault, H. (1993). A series of normal stages for development of *Scyliorhinus canicula*, the lesser spotted dogfish (*Chondrichthyes: Scyliorhinidae*). *J. Exp. Zool.* 267, 318–336 (1993).
- Barbosa, A. C., Funato, N., Chapman, S., McKee, M. D., Richardson, J. A., Olson, E. N., & Yanagisawa, H. (2007). Hand transcription factors cooperatively regulate development of the distal midline mesenchyme. *Developmental biology*, 310(1), 154–168.
- Barlow, A. J. and Francis-West, P. H. (1997). Ectopic application of recombinant BMP-2 and BMP-4 can change patterning of developing chick facial primordia. *Development* 124, 391–398.
- Barlow, A. J., Bogardi, J. P., Ladher, R., & Francis-West, P. H. (1999). Expression of chick Barx-1 and its differential regulation by FGF-8 and BMP signaling in the maxillary primordia. *Developmental dynamics*: 214(4), 291–302.
- Barry, M. A., Hall, D. H. & Bennett, M. V. L. (1987). The elasmobranch spiracular organ. *J. Comp. Physiol. A* 163, 85–92.
- Barske, L., Fabian, P., Hirschberger, C., Jandzik, D., Square, T., Xu, P., Nelson, N., Yu, H.V., Medeiros, D.M., Gillis, J.A. and Crump, J.G., 2020. Evolution of vertebrate gill covers via shifts in an ancient Pou3f3 enhancer. *Proceedings of the National Academy of Sciences*, 117(40), pp.24876–24884.
- Basden, A. M., Young, G. C., Coates, M. I., & Ritchie, A. (2000). The most primitive osteichthyan braincase? *Nature*, 403(6766), 185–188.
- Begemann, G., Gibert, Y., Meyer, A., & Ingham, P. W. (2002). Cloning of zebrafish T-box genes *tbx15* and *tbx18* and their expression during embryonic development. *Mechanisms of development*, 114(1–2), 137–141.
- Beverdam, A., Merlo, G. R., Paleari, L., Mantero, S., Genova, F., Barbieri, O., Janvier, P. & Levi, G. (2002). Jaw transformation with gain of symmetry after *Dlx5/Dlx6* inactivation: mirror of the past? *genesis*, 34(4), 221–227.
- Biben C., Wang C., Harvey RP. (2004). NK-2 class homeobox genes and pharyngeal/oral patterning: *nkx2-3* is required for salivary gland and tooth morphogenesis. *Int J Dev Biol.* 46(4): 415–22.
- Bonilla-Claudio, M., Wang, J., Bai, Y., Klysik, E., Selever, J., & Martin, J. F. (2012). Bmp signaling regulates a dose-dependent transcriptional program to control facial skeletal development. *Development*, 139(4), 709–719.
- Braasch, I. & Scharf, M. (2014). Evolution of endothelin receptors in vertebrates. *Gen. Comp. Endocrinol.* 209, 21–34.
- Braasch, I., Volff, J. N. & Scharf, M. (2009). The endothelin system: evolution of vertebrate-specific ligand-receptor interactions by three rounds of genome duplication. *Mol. Biol. Evol.* 26, 783–799.
- Brazeau, M. D. (2009). The braincase and jaws of a Devonian “acanthodian” and modern gnathostome origins. *Nature*, 457(7227), 305–308.
- Brazeau, M. D., & de Winter, V. (2015). The hyoid arch and braincase anatomy of *Acanthodes* support chondrichthyan affinity of “acanthodians.” *Proceedings. Biological Sciences*, 282(1821), 20152210.
- Brazeau, M. D., Giles, S., Dearden, R. P., Jerve, A., Ariunchimeg, Y. A., Zorig, E., Sansom R., Guillerme T. & Castiello, M. (2020). Endochondral bone in an Early Devonian ‘placoderm’ from Mongolia. *Nature Ecology & Evolution*, 4(11), 1477–1484.

- Brito, J. M., Teillet, M. A., & Le Douarin, N. M. (2006). An early role for sonic hedgehog from foregut endoderm in jaw development: ensuring neural crest cell survival. *Proceedings of the National Academy of Sciences*, 103(31), 11607-11612.
- Brunet, L. J., McMahon, J. A., McMahon, A. P., & Harland, R. M. (1998). Noggin, cartilage morphogenesis, and joint formation in the mammalian skeleton. *Science*, 280(5368), 1455-1457.
- Buenrostro, J. D., Wu, B., Chang, H. Y., & Greenleaf, W. J. (2015). ATAC-seq: a method for assaying chromatin accessibility genome-wide. *Current protocols in molecular biology*, 109(1), 21-29.
- Burrow, C.J., Newman, M.J., den Blaauwen, J.L. (2020) First evidence of a functional spiracle in stem chondrichthyan acanthodians, with the oldest known elastic cartilage. *J. Anat.* 236: 1154– 1159.
- Candiani, S., Castagnola, P., Oliveri, D., & Pestarino, M. (2002). Cloning and developmental expression of *AmphiBrn1/2/4*, a POU III gene in amphioxus. *Mechanisms of development*, 116(1-2), 231-234
- Caprio, J., Shimohara, M., Marui, T., Kohbara, J., Harada, S., & Kiyohara, S. (2015). Amino acid specificity of fibers of the facial/trigeminal complex innervating the maxillary barbel in the Japanese sea catfish, *Plotosus japonicus*. *Physiology & behavior*, 152, 288-294.
- Carlson, J. C., Anand, D., Butali, A., Buxo, C. J., Christensen, K., Deleyiannis, F., Hecht, J.T., Moreno, L.M., Orioli, I.M., Padilla, C. & Leslie, E. J. (2019). A systematic genetic analysis and visualization of phenotypic heterogeneity among orofacial cleft GWAS signals. *Genetic epidemiology*, 43(6), 704-716.
- Carroll, R. L. (1988). Vertebrate paleontology and evolution. New York: Freeman and Company.
- Cerny, R., Cattell, M., Sauka-Spengler, T., Bronner-Fraser, M., Yu, F., & Medeiros, D. M. (2010). Evidence for the prepattern/cooption model of vertebrate jaw evolution. *Proceedings of the National Academy of Sciences*, 107(40), 17262-17267.
- Charité, J., McFadden, D.G., Merlo, G., Levi, G., Clouthier, D.E., Yanagisawa, M., Richardson, J.A. and Olson, E.N., 2001. Role of *Dlx6* in regulation of an endothelin-1-dependent, *dHAND* branchial arch enhancer. *Genes & development*, 15(22), pp.3039-3049.
- Chen, J. K., Taipale, J., Young, K. E., Maiti, T., & Beachy, P. A. (2002). Small molecule modulation of *Smoothed* activity. *Proceedings of the National Academy of Sciences*, 99(22), 14071-14076.
- Church, V., Yamaguchi, K., Tsang, P., Akita, K., Logan, C., & Francis-West, P. (2005). Expression and function of *Bapx1* during chick limb development. *Anatomy and embryology*, 209(6), 461-469.
- Clack J. A., (2007). Devonian climate change, breathing, and the origin of the tetrapod stem group. *Integrative and Comparative Biology*, Volume 47(4), 510–523.
- Clouthier, D. E., Hosoda, K., Richardson, J. A., Williams, S. C., Yanagisawa, H., Kuwaki, T., Kumada, M., Hammer, R.E. & Yanagisawa, M. (1998). Cranial and cardiac neural crest defects in endothelin-A receptor-deficient mice. *Development*, 125(5), 813-824.
- Clouthier, D. E., Williams, S. C., Yanagisawa, H., Wieduwilt, M., Richardson, J. A., & Yanagisawa, M. (2000). Signaling pathways crucial for craniofacial development revealed by endothelin-A receptor-deficient mice. *Developmental biology*, 217(1), 10-24.

- Clouthier, D. E., Williams, S. C., Hammer, R. E., Richardson, J. A., & Yanagisawa, M. (2003). Cell-autonomous and nonautonomous actions of endothelin-A receptor signaling in craniofacial and cardiovascular development. *Developmental biology*, 261(2), 506-519.
- Clouthier, D. E., & Schilling, T. F. (2004). Understanding endothelin-1 function during craniofacial development in the mouse and zebrafish. *Birth Defects Research Part C: Embryo Today: Reviews*, 72(2), 190-199.
- Clouthier, D. E., Garcia, E., & Schilling, T. F. (2010). Regulation of facial morphogenesis by endothelin signaling: insights from mice and fish. *American Journal of Medical Genetics Part A*, 152(12), 2962-2973.
- Compagnucci, C., Debiais-Thibaud, M., Coolen, M., Fish, J., Griffin, J. N., Bertocchini, F., Minoux, M., Rijli, F.M., Borday-Birraux, V., Casane, D. & Depew, M. J. (2013). Pattern and polarity in the development and evolution of the gnathostome jaw: both conservation and heterotopy in the branchial arches of the shark, *Scyliorhinus canicula*. *Developmental biology*, 377(2), 428-448.
- Compagnucci C., Depew M.J. (2020). Foxg1 organizes cephalic ectoderm to repress mandibular fate, regulate apoptosis, generate choanae, elaborate the auxiliary eye and pattern the upper jaw. Forthcoming. *BioRxiv*, 5 February 2020.
- Couly, G., Grapin-Botton, A., Coltey, P., Ruhin, B., & Le Douarin, N. M. (1998). Determination of the identity of the derivatives of the cephalic neural crest: incompatibility between Hox gene expression and lower jaw development. *Development*, 125(17), 3445-3459.
- Coates MJ, Sequeira SEK (2001) A new stethacanthid chondrichthyan from the Lower Carboniferous of Bearsden, Scotland. *J Vert Paleont* 21:438–459.
- Coates, M. I. (2003). The evolution of paired fins. *Theory in Biosciences*, 122(2-3), 266-287.
- Coates, M. I., Finarelli, J. A., Sansom, I. J., Andreev, P. S., Criswell, K. E., Tietjen, K., Rivers, M. L., & La Riviere, P. J. (2018). An early chondrichthyan and the evolutionary assembly of a shark body plan. *Proceedings of the Royal Society B: Biological Sciences*, 285(1870), 20172418.
- Cracraft, J. (2005). Phylogeny and evo-devo: characters, homology, and the historical analysis of the evolution of development. *Zoology*, 108(4), 345-356.
- Criswell, K. E., & Gillis, J. A. (2020). Resegmentation is an ancestral feature of the gnathostome vertebral skeleton. *Elife*, 9, e51696.
- Crotwell, P. L., & Mabee, P. M. (2007). Gene expression patterns underlying proximal–distal skeletal segmentation in late-stage zebrafish, *Danio rerio*. *Developmental dynamics*, 236(11), 3111-3128.
- Crump, J. G., Swartz, M. E., Eberhart, J. K., & Kimmel, C. B. (2006). *Moz*-dependent Hox expression controls segment-specific fate maps of skeletal precursors in the face. *Development*, 133(14), 2661-2669.
- Darwin, C. (1859). *On the Origin of Species by Means of Natural Selection Or the Preservation of Favoured Races in the Struggle for Life*. International Book Company.
- Dawes, R., Dawson, I., Falciani, F., Tear, G. & Akam, M. (1994). *Dax*, a locust Hox gene related to *fushi-tarazu* but showing no pair-rule expression. *Development* 120, 1561–1572.
- Dearden, R. P., Stockey, C., Brazeau, M. D. (2019). The pharynx of the stem-chondrichthyan *Ptomacanthus* and the early evolution of the gnathostome gill skeleton. *Nat. Commun.* 10, 2050.
- De Beer, G. R. (1937). *The Development of the Vertebrate Skull*. Oxford: Clarendon.
- De Beer, G. R. (1924). Studies on the Vertebrate head. I. Fish. *Quart. J. Micr. Sci.* 68, 11

- Denison, R. H. (1961). Feeding mechanisms of Agnatha and early gnathostomes. *American Zoologist*, 177-181.
- Depew, M. J., & Compagnucci, C. (2008). Tweaking the hinge and caps: testing a model of the organization of jaws. *Journal of Experimental Zoology Part B: Molecular and Developmental Evolution*, 310(4), 315-335.
- Depew, M. J., Lufkin, T. & Rubenstein, J. L. R. (2002). Specification of jaw subdivisions by Dlx genes. *Science* 298, 381–385.
- Dick, J. R. F. (1978). On the Carboniferous shark *Tristychius arcuatus* Agassiz from Scotland. *Trans R Soc Edinb* 70:63–109.
- Dickinson, W. J. (1995). Molecules and morphology: where's the homology? *Trends in Genetics*, 11(4), 119-121.
- Dou, C. L., Li, S., & Lai, E. (1999). Dual role of brain factor-1 in regulating growth and patterning of the cerebral hemispheres. *Cerebral cortex*, 9(6), 543-550.
- Dunel-Erb, S., Bailly, Y., & Laurent, P. (1982). Neuroepithelial cells in fish gill primary lamellae. *Journal of Applied Physiology*, 53(6), 1342-1353.
- Dupret, V., Sanchez, S., Goujet, D., Tafforeau, P., & Ahlberg, P. E. (2014). A primitive placoderm sheds light on the origin of the jawed vertebrate face. *Nature*, 507(7493), 500–503.
- Duprez, D., Bell, E. J. D. H., Richardson, M. K., Archer, C. W., Wolpert, L., Brickell, P. M., & Francis-West, P. H. (1996). Overexpression of BMP-2 and BMP-4 alters the size and shape of developing skeletal elements in the chick limb. *Mechanisms of development*, 57(2), 145-157.
- Eberhart, J. K., Swartz, M. E., Crump, J. G., & Kimmel, C. B. (2006). Early Hedgehog signaling from neural to oral epithelium organizes anterior craniofacial development. *Development*, 133(6), 1069-1077.
- Edgeworth, F.H. (1935). *The Cranial Muscles of Vertebrates*. Cambridge: Cambridge University Press.
- El-Toubi M.R. (1947). The development of the spiracular cartilages of the spiny dogfish, *Acanthias vulgaris*. *Biological. Bulletin* 93: 287-295.
- Ellies, D. L., Langille, R. M., Martin, C. C., Akimenko, M. A., & Ekker, M. (1997). Specific craniofacial cartilage dysmorphogenesis coincides with a loss of dlx gene expression in retinoic acid-treated zebrafish embryos. *Mechanisms of development*, 61(1-2), 23-36.
- Evans, S. M., Yan, W., Murillo, M. P., Ponce, J., & Papalopulu, N. (1995). tinman, a Drosophila homeobox gene required for heart and visceral mesoderm specification, may be represented by a family of genes in vertebrates: XNkx-2.3, a second vertebrate homologue of tinman. *Development*, 121(11), 3889-3899.
- Ewart, J. C. (1889). On the cranial nerves of elasmobranch fishes. Preliminary communication. *Proceedings of the Royal Society of London*, 45(273-279), 524-537.
- Feng, W., Leach, S. M., Tipney, H., Phang, T., Geraci, M., Spritz, R. A., Hunter, L.E. & Williams, T. (2009). Spatial and temporal analysis of gene expression during growth and fusion of the mouse facial prominences. *PloS one*, 4(12), e8066.
- Fernández-Chacón, R., & Südhof, T. C. (2000). Novel SCAMPs lacking NPF repeats: ubiquitous and synaptic vesicle-specific forms implicate SCAMPs in multiple membrane-trafficking functions. *Journal of Neuroscience*, 20(21), 7941-7950.
- Fish, J. L., Villmoare, B., Köbernick, K., Compagnucci, C., Britanova, O., Tarabykin, V., & Depew, M. J. (2011). Satb2, modularity, and the evolvability of the vertebrate jaw. *Evolution & development*, 13(6), 549-564.

- Fonseca, B. F., Couly, G., & Dupin, E. (2017). Respective contribution of the cephalic neural crest and mesoderm to SIX1-expressing head territories in the avian embryo. *BMC developmental biology*, 17(1), 1-15.
- Forey, P. L. (1995). Agnathans recent and fossil, and the origin of jawed vertebrates. *Reviews in Fish Biology and Fisheries*, 5(3), 267-303.
- Francis-West, P. H., Tatla, T. and Brickell, P. M. (1994). Expression patterns of the bone morphogenetic protein genes Bmp-4 and Bmp-2 in the developing chick face suggest a role in outgrowth of the primordia. *Dev. Dyn.* 201, 168-178.
- Fraser, A. (1882). On the development of the ossicula auditus in the higher Mammalia. *Philosophical Transactions of the Royal Society of London*, (173), 901-925.
- Friedman, M., & Brazeau, M. D. (2010). A reappraisal of the origin and basal radiation of the Osteichthyes. *Journal of Vertebrate Paleontology*, 30(1), 36–56.
- Fukuhara, S., Kurihara, Y., Arima, Y., Yamada, N., & Kurihara, H. (2004). Temporal requirement of signaling cascade involving endothelin-1/endothelin receptor type A in branchial arch development. *Mechanisms of development*, 121(10), 1223-1233.
- Funato, N., Kokubo, H., Nakamura, M., Yanagisawa, H., & Saga, Y. (2016). Specification of jaw identity by the Hand2 transcription factor. *Scientific reports*, 6(1), 1-14.
- Gai, Z., & Zhu, M. (2012). The origin of the vertebrate jaw: Intersection between developmental biology-based model and fossil evidence. *Chinese Science Bulletin*, 57(30), 3819-3828.
- Gai, Z., Donoghue, P. C. J., Zhu, M., Janvier, P. & Stampanoni, M. (2011). Fossil jawless fish from China foreshadows early jawed vertebrate anatomy. *Nature* 476, 324–327.
- Gans C., Northcutt R. G. (1983). Neural crest and the origin of vertebrates: a new head. *Science* 220(4594): 268–73.
- Gardiner, B. G. (1984). The relationships of the palaeoniscoid fishes, a review based on new specimens of *Mimia* and *Moythomasia* from the Upper Devonian of Western Australia. *Bulletin of the British Museum of Natural History (Geology)* 37(4): 173–428
- Gaudin, T. J. (1991). A re-examination of elasmobranch monophyly and chondrichthyan phylogeny. *Neues Jahrbuch für Geologie und Paläontologie-Abhandlungen*, 133-160.
- Gegenbaur, C. (1878). Elements of Comparative Anatomy. MacMillan and Co.
- Gendron-Maguire, M., Mallo, M., Zhang, M., & Gridley, T. (1993). Hoxa-2 mutant mice exhibit homeotic transformation of skeletal elements derived from cranial neural crest. *Cell*, 75(7), 1317-1331.
- Geoffroy Saint-Hilaire E. Philosophie anatomique. 1818. J.B. Baillière, Paris.
- Gillis, J. A., Dahn, R. D. & Shubin, N. H. (2009a). Chondrogenesis and homology of the visceral skeleton in the little skate, *Leucoraja erinacea* (Chondrichthyes: Batoidea). *J. Morphol.* 270, 628–643
- Gillis JA, Dahn RD, Shubin NH (2009b). Shared developmental mechanisms pattern the gill arch and paired fin skeletons in vertebrates. *Proceedings of the National Academy of Sciences*. 106: 5720-5724.
- Gillis, J. A., Rawlinson, K. A., Bell, J., Lyon, W. S., Baker, C. V., & Shubin, N. H. (2011). Holocephalan embryos provide evidence for gill arch appendage reduction and opercular evolution in cartilaginous fishes. *Proceedings of the National Academy of Sciences*, 108(4), 1507-1512.
- Gillis, J. A., Modrell, M. S., & Baker, C. V. H. (2012). A timeline of pharyngeal endoskeletal condensation and differentiation in the shark, *Scyliorhinus canicula*, and the paddlefish, *Polyodon spathula*. *Journal of Applied Ichthyology*, 28(3), 341-345.

- Gillis J.A., Modrell M.S., Baker C.V.H. (2013). Developmental evidence for serial homology of the vertebrate jaw and gill arch skeleton. *Nat Commun.* 4: 1436.
- Gillis, J. A., & Hall, B. K. (2016). A shared role for sonic hedgehog signalling in patterning chondrichthyan gill arch appendages and tetrapod limbs. *Development*, 143(8), 1313-1317.
- Gillis J.A., Tidswell O.R.A. (2017). The origin of vertebrate gills. *Curr. Biol.* 27(5): 729–32.
- Goodrich, E. S. (1930). Studies on the structure and development of vertebrates. London: Macmillan
- Goodrich, E.S. (1909). Part IX. Vertebrata Craniata. Fascicule 1. Cyclostomes and fishes. In: E.R. Lankester. A Treatise on Zoology. London: Macmillan, pp. xvi+518.
- Göthe, J. W. (1820). Dem Menschen wie den Tieren ist ein Zwischenknochen. Erstdruck in: Zur Naturwissenschaft überhaupt, besonders zur Morphologie (Stuttgart/Tübingen), 1. Band, 2. Heft.
- Graham, A. (2001). The development and evolution of the pharyngeal arches. *Journal of anatomy*, 199(1-2), 133-141.
- Graham, A. (2003). Development of the pharyngeal arches. *American Journal of Medical Genetics Part A*, 119(3), 251-256.
- Graham, A., & Smith, A. (2001). Patterning the pharyngeal arches. *Bioessays*, 23(1), 54-61.
- Graham, A., & Richardson, J. (2012). Developmental and evolutionary origins of the pharyngeal apparatus. *EvoDevo*, 3(1), 1-8.
- Graham, J.B., Wegner, N.C., Miller, L.A., Jew, C.J., Lai, N.C., Berquist, R.M. et al. (2014). Spiracular air breathing in polypterid fishes and its implications for aerial respiration in stem tetrapods. *Nature Communications*, 5, 6.
- Grammatopoulos, G. A., Bell, E., Toole, L., Lumsden, A., & Tucker, A. S. (2000). Homeotic transformation of branchial arch identity after Hoxa2 overexpression. *Development*, 127(24), 5355-5365.
- Green, S. A., & Bronner, M. E. (2014). The lamprey: a jawless vertebrate model system for examining origin of the neural crest and other vertebrate traits. *Differentiation*, 87(1-2), 44-51.
- Haas, B.J., Papanicolaou, A., Yassour, M., Grabherr, M., Blood, P.D., Bowden, J., Couger, M.B., Eccles, D., Li, B., Lieber, M. and MacManes, M.D. (2013). De novo transcript sequence reconstruction from RNA-seq using the Trinity platform for reference generation and analysis. *Nature protocols*, 8(8), pp.1494-1512.
- Haenig B., Kispert A. (2004). Analysis of TBX18 expression in chick embryos. *Dev. Genes Evol.* 214.8: 407-411.
- Hall, B. K. (1995). Homology and embryonic development. *Evolutionary biology*, 1-37.
- Hall, B. K. (2012a). Evolutionary developmental biology (Evo-Devo): Past, present, and future. *Evolution: Education and outreach*, 5(2), 184-193.
- Hall, B. K. (2012b). Homology: The hierarchical basis of comparative biology. Academic Press.
- Hall, B. K., & Kerney, R. (2012). Levels of biological organization and the origin of novelty. *Journal of Experimental Zoology Part B: Molecular and Developmental Evolution*, 318(6), 428-437.
- Han, Z., & Olson, E. N. (2005). Hand is a direct target of Tinman and GATA factors during Drosophila cardiogenesis and hematopoiesis. *Development*, 132(15), 3525-3536
- Han, Z., Yi, P., Li, X., & Olson, E. N. (2006). Hand, an evolutionarily conserved bHLH transcription factor required for Drosophila cardiogenesis and hematopoiesis. *Development*, 133(6), 1175-1182.

- Han, C., Chen, T., Yang, M., Li, N., Liu, H., & Cao, X. (2009). Human SCAMP5, a novel secretory carrier membrane protein, facilitates calcium-triggered cytokine secretion by interaction with SNARE machinery. *The Journal of Immunology*, 182(5), 2986-2996.
- Hanashima, C., Shen, L., Li, S. C., & Lai, E. (2002). Brain factor-1 controls the proliferation and differentiation of neocortical progenitor cells through independent mechanisms. *Journal of Neuroscience*, 22(15), 6526-6536.
- Hardisty, M. W. (2013). *Biology of the Cyclostomes*. Springer.
- Harel, I., Maezawa, Y., Avraham, R., Rinon, A., Ma, H. Y., Cross, J. W., Leviatan, N., Hegesh, J., Roy, A., Jacob-Hirsch, J. & Tzahor, E. (2012). Pharyngeal mesoderm regulatory network controls cardiac and head muscle morphogenesis. *Proceedings of the National Academy of Sciences*, 109(46), 18839-18844.
- Hartmann, C., & Tabin, C. J. (2001). Wnt-14 plays a pivotal role in inducing synovial joint formation in the developing appendicular skeleton. *Cell*, 104(3), 341-351.
- Heimberg, A. M., Cowper-Sal, R., Sémon, M., Donoghue, P. C., & Peterson, K. J. (2010). microRNAs reveal the interrelationships of hagfish, lampreys, and gnathostomes and the nature of the ancestral vertebrate. *Proceedings of the National Academy of Sciences*, 107(45), 19379-19383.
- Higashiyama, H. & Kuratani, S. (2014). On the maxillary nerve. *Journal of Morphology* 275, 17–38.
- Hirschberger, C., Sleight V.A., Criswell K.E., Clark S.J., Gillis J.A. (2021). Conserved and Unique Transcriptional Features of Pharyngeal Arches in the Skate (*Leucoraja Erinacea*) and Evolution of the Jaw. (forthcoming.) *BioRxiv*
- Hiruta, J., Mazet, F., Yasui, K., Zhang, P., & Ogasawara, M. (2005). Comparative expression analysis of transcription factor genes in the endostyle of invertebrate chordates. *Developmental dynamics*, 233(3), 1031-1037.
- Hockman, D., Burns, A. J., Schlosser, G., Gates, K. P., Jevans, B., Mongera, A., Baker, C. V. (2017). Evolution of the hypoxia-sensitive cells involved in amniote respiratory reflexes. *Elife*, 6, e21231.
- Hogan, B. M., Hunter, M. P., Oates, A. C., Crowhurst, M. O., Hall, N. E., Heath, J. K., Prince, V.E & Lieschke, G. J. (2004). Zebrafish *gcm2* is required for gill filament budding from pharyngeal ectoderm. *Developmental biology*, 276(2), 508-522.
- Holland, N. D., & Chen, J. (2001). Origin and early evolution of the vertebrates: New insights from advances in molecular biology, anatomy, and palaeontology. *BioEssays*, 23(2), 142–151.
- Holmgren, N., Stensiö, E. 1936. *Kranium und Visceralskelett der Acranier, Cyclostomien und Fische in Handbuch der vergleich. Anatomie der Wirbeltiere*, ed. by L. Bolck, etc., Bd. iv. Berlin & Wien.
- Hölzer, M., & Marz, M. (2019). De novo transcriptome assembly: A comprehensive cross-species comparison of short-read RNA-Seq assemblers. *GigaScience*, 8(5), giz039.
- Hu, J., Verzi, M.P., Robinson, A.S., Tang, P.L.F., Hua, L.L., Xu, S.M., Kwok, P.Y. and Black, B.L., (2015). Endothelin signaling activates Mef2c expression in the neural crest through a MEF2C-dependent positive-feedback transcriptional pathway. *Development*, 142(16), pp.2775-2780.
- Hunt, P., Gulisano, M., Cook, M., Sham, M. H., Faiella, A., Wilkinson, D., Boncinelli, E. & Krumlauf, R. (1991). A distinct Hox code for the branchial region of the vertebrate head. *Nature*, 353(6347), 861-864.

- Hunt, P., & Krumlauf, R. (1991). Deciphering the Hox code: clues to patterning branchial regions of the head. *Cell*, 66(6), 1075-1078.
- Huxley, T. H. (1859). I. The Croonian Lecture.—On the theory of the vertebrate skull. *Proceedings of the Royal Society of London*, (9), 381-457.
- Jandzik, D., Garnett, A. T., Square, T. A., Cattell, M. V., Yu, J. K., & Medeiros, D. M. (2015). Evolution of the new vertebrate head by co-option of an ancient chordate skeletal tissue. *Nature*, 518(7540), 534-537.
- Janvier, P. (1996). Early vertebrates. Oxford: Clarendon.
- Janvier, P. (1999). Catching the first fish. *Nature* 402:21-22.
- Janvier, P. (1985). Les Thyestidiens (Osteostraci) du Silurien de Saaremaa (Estonie). Première partie: morphologie et anatomie. *Annales de Paleontologie* 71, 83–147
- Janvier, P. & Arsenault, M. (2007). The anatomy of *Euphanerops longaeus* Woodward, 1900, an anaspid-like jawless vertebrate from the Upper Devonian of Miguasha, Quebec, Canada. *Geodiversitas* 29, 143–216.
- Jarvik, E. (1980). Basic structure and evolution of vertebrates. Academic Press, London.
- Jeong, J., Li, X., McEvilly, R. J., Rosenfeld, M. G., Lufkin, T., & Rubenstein, J. L. (2008). Dlx genes pattern mammalian jaw primordium by regulating both lower jaw-specific and upper jaw-specific genetic programs. *Development*, 135(17), 2905-2916.
- Johnels, A. G. (1948). On the development and morphology of the skeleton of the head of *Petromyzon*. *Acta Zool.* 29, 139-279.
- Johnson, W. E., Li, C., & Rabinovic, A. (2007). Adjusting batch effects in microarray expression data using empirical Bayes methods. *Biostatistics*, 8(1), 118-127
- Jollie, M. Chordate Morphology. Reinhold, New York, USA (1962)
- Jonz, M. G. and Nurse, C. A. (2003). Neuroepithelial cells and associated innervation of the zebrafish gill: a confocal immunofluorescence study. *J. Comp. Neurol.* 461, 1-17.
- Jonz, M. G., & Nurse, C. A. (2005). Development of oxygen sensing in the gills of zebrafish. *Journal of Experimental Biology*, 208(8), 1537-1549.
- Kanwal, J. S., Hidaka, I., & Caprio, J. (1987). Taste responses to amino acids from facial nerve branches innervating oral and extra-oral taste buds in the channel catfish, *Ictalurus punctatus*. *Brain research*, 406(1-2), 105-112.
- Kardong, K. V. (2012). Vertebrates: Comparative anatomy, function, evolution (6th ed.). New York, NY: McGraw-Hill.
- Kelly, R. G., Jerome-Majewska, L. A., & Papaioannou, V. E. (2004). The del22q11. 2 candidate gene *Tbx1* regulates branchiomic myogenesis. *Human molecular genetics*, 13(22), 2829-2840.
- Kimmel, C. B., Miller, C. T., & Keynes, R. J. (2001). Neural crest patterning and the evolution of the jaw. *Journal of Anatomy*, 199(1-2), 105-120.
- Kimmel, C. B., Ullmann, B., Walker, M., Miller, C. T., & Crump, J. G. (2003). Endothelin 1-mediated regulation of pharyngeal bone development in zebrafish. *Development*, 130(7), 1339-1351.
- King, B. L., Gillis, J. A., Carlisle, H. R., & Dahn, R. D. (2011). A natural deletion of the HoxC cluster in elasmobranch fishes. *Science*, 334(6062), 1517-151.
- King, B., Qiao, T., Lee, M.S.Y., Zhu, M. and Long, J.A. (2017) Bayesian Morphological Clock Methods resurrect placoderm monophyly and reveal rapid early evolution in jawed vertebrates. *Systematic Biology*, 66, 499– 516.
- Klug, C., Kroeger, B., Kiessling, W., Mullins, G.L., Servais, T., FRÝDA, J., Korn, D. and Turner, S., 2010. The Devonian nekton revolution. *Lethaia*, 43(4), pp.465-477.

- Kontges, G., & Lumsden, A. (1996). Rhombencephalic neural crest segmentation is preserved throughout craniofacial ontogeny. *Development*, 122(10), 3229-3242.
- Kotrschal, K., Whitear, M., & Finger, T. E. (1993). Spinal and facial innervation of the skin in the gadid fish *Ciliata mustela* (Teleostei). *Journal of Comparative Neurology*, 331(3), 407-417.
- Kraus, F., Haenig, B., & Kispert, A. (2001). Cloning and expression analysis of the mouse T-box gene *Tbx18*. *Mechanisms of development*, 100(1), 83-86.
- Kumada, M., Hammer, R. E., & Yanagisawa, M. (1998). Cranial and cardiac neural crest defects in endothelin-A receptor-deficient mice. *Development*, 125(5), 813-824.
- Kuraku, S., Takio, Y., Sugahara, F., Takechi, M., & Kuratani, S. (2010). Evolution of oropharyngeal patterning mechanisms involving *Dlx* and endothelins in vertebrates. *Developmental Biology*, 341(1), 315-323.
- Kuratani, S., Nobusada, Y., Horigome, N., & Shigetani, Y. (2001). Embryology of the lamprey and evolution of the vertebrate jaw: insights from molecular and developmental perspectives. *Philosophical Transactions of the Royal Society of London. Series B: Biological Sciences*, 356(1414), 1615-1632.
- Kuratani, S. (2004). Evolution of the vertebrate jaw: comparative embryology and molecular developmental biology reveal the factors behind evolutionary novelty. *Journal of Anatomy*, 205(5), 335-347.
- Kuratani, S. (2005). Craniofacial development and the evolution of the vertebrates: the old problems on a new background. *Zoological science*, 22(1), 1-19.
- Kuratani, S., & Ahlberg, P. E. (2018). Evolution of the vertebrate neurocranium: problems of the premandibular domain and the origin of the trabecula. *Zoological letters*, 4(1), 1-10.
- Kuratani, S., Adachi, N., Wada, N., Oisi, Y., & Sugahara, F. (2013). Developmental and evolutionary significance of the mandibular arch and prechordal/premandibular cranium in vertebrates: revising the heterotopy scenario of gnathostome jaw evolution. *Journal of Anatomy*, 222(1), 41-55.
- Kurihara, Y., Kurihara, H., Suzuki, H., Kodama, T., Maemura, K., Nagai, R., Oda, H., Kuwaki, T., Cao, W. H., Kamada, N. et al. (1994). Elevated blood pressure and craniofacial abnormalities in mice deficient in endothelin-1. *Nature* 368, 703-710.
- Laclef, C., Souil, E., Demignon, J., & Maire, P. (2003). Thymus, kidney and craniofacial abnormalities in *Six1* deficient mice. *Mechanisms of development*, 120(6), 669-679.
- Laurent, P., & Dunel-Erb, S. (1984). 9 The Pseudobranch: Morphology and Function. *Fish physiology*, 10, 285-323.
- Lee, K. H., Xu, Q., & Breitbart, R. E. (1996). A *Newtman*-Related Gene, *nkx2.7*, Anticipates the Expression of *nkx2.5* in Zebrafish Heart and Pharyngeal Endoderm. *Developmental biology*, 180(2), 722-731.
- Leek, J. T., Johnson, W. E., Parker, H. S., Jaffe, A. E., & Storey, J. D. (2012). The *sva* package for removing batch effects and other unwanted variation in high-throughput experiments. *Bioinformatics*, 28(6), 882-883.
- Leimeister, C., Bach, A., & Gessler, M. (1998). Developmental expression patterns of mouse *sFRP* genes encoding members of the secreted frizzled related protein family. *Mechanisms of development*, 75(1-2), 29-42.
- Leslie, E. J., & Marazita, M. L. (2013, November). Genetics of cleft lip and cleft palate. In *American Journal of Medical Genetics Part C: Seminars in Medical Genetics* (Vol. 163, No. 4, pp. 246-258).

- Li, L., Cserjesi, P., & Olson, E. N. (1995). Dermo-1: a novel twist-related bHLH protein expressed in the developing dermis. *Developmental biology*, 172(1), 280-292.
- Lukas, P., Olsson, L. (2018). Bapx1 Is required for jaw joint development in amphibians. *Evol Dev.* 20(6): 192–206.
- Lumsden, A., Sprawson, N., & Graham, A. (1991). Segmental origin and migration of neural crest cells in the hindbrain region of the chick embryo. *Development*, 113(4), 1281-1291.
- Lund, R., & Grogan, E. D. (1997). Relationships of the Chimaeriformes and the basal radiation of the Chondrichthyes. *Reviews in Fish Biology and Fisheries*, 7(1), 65-123.
- Maemura, K., Kurihara, H., Kurihara, Y., Oda, H., Ishikawa, T., Copeland, N. G., Gilbert, D. J., Jenkins, N. A. and Yazaki, Y. (1996). Sequence analysis, chromosomal location, and developmental expression of the mouse preproendothelin-1 gene. *Genomics* 31, 177-184.
- Maisey, J. G. (1984). Higher elasmobranch phylogeny and biostratigraphy. *Zoological Journal of the Linnean Society*, 82(1-2), 33-54.
- Maisey, J. G. (1989). Visceral skeleton and musculature of a Late Devonian shark. *Journal of Vertebrate Paleontology*, 9(2), 174-190.
- Maisey, J. G. (2012). What is an 'elasmobranch'? The impact of palaeontology in understanding elasmobranch phylogeny and evolution. *Journal of Fish Biology*, 80(5), 918-951.
- Mallatt, J. (1996). Ventilation and the origin of jawed vertebrates: a new mouth. *Zool J Linnean Soc* 117(4): 329–404.
- Mallatt, J. (1984). Early vertebrate evolution: pharyngeal structure and the origin of gnathostomes. *Journal of Zoology*, 204(2), 169-183.
- Mallatt, J. (1985). Reconstructing the life cycle and the feeding of ancestral vertebrates. In *Evolutionary Biology of Primitive Fishes* (pp. 59-68). Springer, Boston, MA.
- Mallatt, J. (2008). The origin of the vertebrate jaw: neoclassical ideas versus newer, development-based ideas. *Zoological science*, 25(10), 990-998.
- Mallatt, J., & Chen, J. (2003). Fossil sister group of craniates: Predicted and found. *Journal of Morphology*, 258(1), 1–31.
- Marconi, A., Hancock-Ronemus, A., & Gillis, J. A. (2020). Adult chondrogenesis and spontaneous cartilage repair in the skate, *Leucoraja erinacea*. *Elife*, 9, e53414.
- Marongiu, M., Marcia, L., Pelosi, E., Lovicu, M., Deiana, M., Zhang, Y., Puddu, A., Loi, A., Uda, M., Forabosco, A., Schlessinger, D. & Crisponi, L. (2015). FOXL2 modulates cartilage, skeletal development and IGF1-dependent growth in mice. *BMC developmental biology*, 15(1), 1-14.
- Martik, M. L., Gandhi, S., Uy, B. R., Gillis, J. A., Green, S. A., Simoes-Costa, M., & Bronner, M. E. (2019). Evolution of the new head by gradual acquisition of neural crest regulatory circuits. *Nature*, 574(7780), 675-678.
- Martinez-Morales, J. R., Henrich, T., Ramialison, M. & Wittbrodt, J. (2007). New genes in the evolution of the neural crest differentiation program. *Genome Biol.* 8, R36.
- Maxwell EE, Fröbisch NB, Heppleston AC. 2008. Variability and conservation in late chondrichthyan development: ontogeny of the winter skate (*Leucoraja Ocellata*). *Anat Rec.* 291(9): 1079–87.
- McCauley, D. W., & Bronner-Fraser, M. (2003). Neural crest contributions to the lamprey head. *Development*, 130(11), 2317-2327.

- Mead, A. (1992). Review of the development of multidimensional scaling methods. *Journal of the Royal Statistical Society: Series D (The Statistician)*, 41(1), 27-39
- Merino, R., Macias, D., Ganan, Y., Economides, A. N., Wang, X., Wu, Q., Stahl, N., Sampath, K.T., Varona, P. & Hurle, J. M. (1999). Expression and Function of Gdf-5 during Digit Skeletogenesis in the Embryonic Chick Leg Bud. *Developmental biology*, 206(1), 33-45.
- Miller, C. T., Schilling, T. F., Lee, K., Parker, J., & Kimmel, C. B. (2000). sucker encodes a zebrafish Endothelin-1 required for ventral pharyngeal arch development. *Development*, 127(17), 3815-3828.
- Miller, C. T., & Kimmel, C. B. (2001). Morpholino phenocopies of endothelin 1 (sucker) and other anterior arch class mutations. *genesis*, 30(3), 186-187.
- Miller, C. T., Yelon, D., Stainier, D. Y., & Kimmel, C. B. (2003). Two endothelin 1 effectors, hand2 and bapx1, pattern ventral pharyngeal cartilage and the jaw joint. *Development*, 130(7), 1353-1365.
- Miller, C. T., Swartz, M. E., Khuu, P. A., Walker, M. B., Eberhart, J. K., & Kimmel, C. B. (2007). mef2ca is required in cranial neural crest to effect Endothelin1 signaling in zebrafish. *Developmental biology*, 308(1), 144-157.
- Mina, M., Wang, Y. H., Ivanisevic, A. M., Upholt, W. B., & Rodgers, B. (2002). Region-and stage-specific effects of FGFs and BMPs in chick mandibular morphogenesis. *Developmental dynamics*, 223(3), 333-352.
- Minarik, M., Stundl, J., Fabian, P., Jandzik, D., Metscher, B. D., Psenicka, M., Gela, D., Osorio-Pérez, A., Arias-Rodriguez, L., Horáček, I. & Cerny, R. (2017). Pre-oral gut contributes to facial structures in non-teleost fishes. *Nature*, 547(7662), 209-212.
- Mivart, S. G. (1879) XII. Notes on the fins of Elasmobranchs, with Considerations on the Nature and Homologues of Vertebrate Limbs. *The Transactions of the Zoological Society of London* 10:439–484.
- Miyake, T., McEachran, J. D. and Hall, B. K. (1992). Edgeworth's legacy of cranial muscle development with an analysis of muscles in the ventral gill arch region of batoid fishes (*Chondrichthyes: Batoidea*). *J. Morph.* 212, 213-256.
- Miyashita, T. (2016). Fishing for jaws in early vertebrate evolution: a new hypothesis of mandibular confinement. *Biological Reviews*, 91(3), 611-657.
- Miyashita, T., Baddam, P., Smeeton, J., Oel, A.P., Natarajan, N., Gordon, B., Palmer, A.R., Crump, J.G., Graf, D. and Allison, W.T., 2020. nkx3. 2 mutant zebrafish accommodate jaw joint loss through a phenocopy of the head shapes of Paleozoic jawless fish. *Journal of Experimental Biology*, 223(15).
- Morris, S. C. (2008). A Redescription of a Rare Chordate, *Metaspriggina Walcottii* Simonetta and Insom, from the Burgess Shale (Middle Cambrian), British Columbia, Canada. *Journal of Paleontology*, 82(2), 424-430.
- Morris, S. C., & Caron, J. B. (2014). A primitive fish from the Cambrian of North America. *Nature*, 512(7515), 419-422.
- Morrison, S. L., Campbell, C. K., & Wright, G. M. (2000). Chondrogenesis of the branchial skeleton in embryonic sea lamprey, *Petromyzon marinus*. *The Anatomical Record*, 260(3), 252-267.
- Myojin, M., Ueki, T., Sugahara, F., Murakami, Y., Shigetani, Y., Aizawa, S., Hirano S., & Kuratani, S. (2001). Isolation of Dlx and Emx gene cognates in an agnathan species, *Lampetra japonica*, and their expression patterns during embryonic and larval development: conserved and diversified regulatory patterns of homeobox genes in vertebrate head evolution. *Journal of Experimental Zoology*, 291(1), 68-84.

- Nair, S., Li, W., Cornell, R., & Schilling, T. F. (2007). Requirements for Endothelin type-A receptors and Endothelin-1 signaling in the facial ectoderm for the patterning of skeletogenic neural crest cells in zebrafish. *Development*, 134(2), 335-345.
- Nataf, V., Grapin-Botton, A., Champeval, D., Amemiya, A., Yanagisawa, M., & Le Douarin, N. M. (1998). The expression patterns of endothelin-A receptor and endothelin 1 in the avian embryo. *Mechanisms of development*, 75(1-2), 145-149.
- Nathan, E., Monovich, A., Tirosh-Finkel, L., Harrelson, Z., Rousso, T., Rinon, A., Harel, I., Evans, S.M. & Tzahor, E. (2008). The contribution of Islet1-expressing splanchnic mesoderm cells to distinct branchiomic muscles reveals significant heterogeneity in head muscle development. *Development*, 135(4), 647-657.
- Neidert, A. H., Virupannavar, V., Hooker, G. W., & Langeland, J. A. (2001). Lamprey Dlx genes and early vertebrate evolution. *Proceedings of the National Academy of Sciences*, 98(4), 1665-1670.
- Nelson, J. S. (2006). *Fishes of the World*. (Wiley)
- Newman, C. S., Grow, M. W., Cleaver, O., Chia, F., & Krieg, P. (1997). Xbp, a Vertebrate Gene Related to bagpipe, Is Expressed in Developing Craniofacial Structures and in Anterior Gut Muscle. *Developmental biology*, 181(2), 223-233.
- Nichols, J. T., Pan, L., Moens, C. B., & Kimmel, C. B. (2013). barx1 represses joints and promotes cartilage in the craniofacial skeleton. *Development*, 140(13), 2765-2775.
- Nikitina, N., Sauka-Spengler, T., & Bronner-Fraser, M. (2008). Dissecting early regulatory relationships in the lamprey neural crest gene network. *Proceedings of the National Academy of Sciences*, 105(51), 20083-20088.
- Nishimura, O., Hara, Y., & Kuraku, S. (2017). gVolante for standardizing completeness assessment of genome and transcriptome assemblies. *Bioinformatics*, 33(22), 3635-3637.
- Northcutt, R. G. The new head hypothesis revisited. 2005. *J. Exp. Zool. Part B* 304B(4): 274–97.
- O'Gorman, S. (2005). Second branchial arch lineages of the middle ear of wild-type and Hoxa2 mutant mice. *Developmental dynamics: an official publication of the American Association of Anatomists*, 234(1), 124-131.
- Oisi, Y., Ota, K. G., Kuraku, S., Fujimoto, S., & Kuratani, S. (2013). Craniofacial development of hagfishes and the evolution of vertebrates. *Nature*, 493(7431), 175-180.
- Okabe M., Graham A. (2004). The origin of the parathyroid gland. *Proc Natl Acad Sci U S A* 101(51): 17716–19.
- Oken, L. (1807). *Über die Bedeutung der Schädelknochen*. Bamberg und Würzburg, JA. Göbhart.
- Ota, K. G., Kuraku, S., & Kuratani, S. (2007). Hagfish embryology with reference to the evolution of the neural crest. *Nature*, 446(7136), 672-675.
- Owen, R. (1843). *Lectures on comparative anatomy and physiology of the invertebrate animals, delivered at the Royal College of Surgeons in 1843*. London: Longman, Brown, Green & Longmans.
- Owen, R. (1846). Report on the archetype and homologies of the vertebrate skeleton. Report of the sixteenth meeting of the British Association for the Advancement of Science (pp. 169–340). London: John Murray.
- Owen, R. (1866). *On the anatomy of vertebrates*. (Vol. 1). Longmans, Green.

- Ozaki, H., Nakamura, K., Funahashi, J.I., Ikeda, K., Yamada, G., Tokano, H., Okamura, H.O., Kitamura, K., Muto, S., Kotaki, H. & Sudo, K. (2004). Six1 controls patterning of the mouse otic vesicle. *Development*, 131(3), pp.551-562.
- Ozeki, H., Kurihara, Y., Tonami, K., Watatani, S., & Kurihara, H. (2004). Endothelin-1 regulates the dorsoventral branchial arch patterning in mice. *Mechanisms of development*, 121(4), 387-395.
- Pankratz, M. J. & Jackle, H. in *The Development of Drosophila melanogaster* (eds Bate, M. & Martinez-Arias, A.) 467–516 (Cold Spring Harbor Laboratory Press, Plainview, 1993).
- Park, P. J. (2009). ChIP-seq: advantages and challenges of a maturing technology. *Nature reviews genetics*, 10(10), 669-680.
- Parsons, K. J., & Albertson, R. C. (2009). Roles for Bmp4 and CaM1 in shaping the jaw: evo-devo and beyond. *Annual review of genetics*, 43, 369-388.
- Pasqualetti, M., Ori, M., Nardi, I., & Rijli, F. M. (2000). Ectopic Hoxa2 induction after neural crest migration results in homeosis of jaw elements in *Xenopus*. *Development*, 127(24), 5367-5378.
- Patel, N. H., Ball, E. F. & Goodman, C. S. Changing role of *even-skipped* during the evolution of insect pattern formation. *Nature* 357, 339–342 (1992).
- Patro, R., Duggal, G., Love, M. I., Irizarry, R. A., & Kingsford, C. (2017). Salmon provides fast and bias-aware quantification of transcript expression. *Nature methods*, 14(4), 417-419.
- Pelster, B., Bemis, W. E. (1992). Structure and function of the external gill filaments of embryonic skates (Raja Erinacea). *Respir. Physiol.* 89(1): 1–13.
- Picelli, S., Faridani, O. R., Björklund, Å. K., Winberg, G., Sagasser, S., & Sandberg, R. (2014). Full-length RNA-seq from single cells using Smart-seq2. *Nature protocols*, 9(1), 171-181.
- Pizette, S., Abate-Shen, C., & Niswander, L. (2001). BMP controls proximodistal outgrowth, via induction of the apical ectodermal ridge, and dorsoventral patterning in the vertebrate limb. *Development*, 128(22), 4463-4474.
- Pla, P., & Larue, L. (2003). Involvement of endothelin receptors in normal and pathological development of neural crest cells. *International Journal of Developmental Biology*, 47(5), 315-325.
- Poopalasundaram, S., Richardson, J., Scott, A., Donovan, A., Liu, K., & Graham, A. (2019). Diminution of pharyngeal segmentation and the evolution of the amniotes. *Zoological letters*, 5(1), 1-9.
- Purnell, M. A. (2001). Scenarios, selection, and the ecology of early vertebrates. Major events in early vertebrate evolution, 188-208.
- Purnell, M. A. (2002). Feeding in extinct jawless heterostracan fishes and testing scenarios of early vertebrate evolution. *Proceedings of the Royal Society of London. Series B: Biological Sciences*, 269(1486), 83-88.
- Qiu, M., Bulfone, A., Ghattas, I., Meneses, J. J., Christensen, L., Sharpe, P. T., Presley R., Pedersen R.A., Rubenstein, J. L. (1997). Role of the Dlx homeobox genes in proximodistal patterning of the branchial arches: mutations of Dlx-1, Dlx-2, and Dlx-1 and-2 alter morphogenesis of proximal skeletal and soft tissue structures derived from the first and second arches. *Developmental biology*, 185(2), 165-184.
- Rathke, H. (1827). Bemerkungen über den innern Bau des Querder (Ammocoetes branchialis) und des kleinen Neunauges (Petromyzon planeri). *Neueste Schriften der Naturf. Gesellsch. Danzig. Bd II.*

- Rathke, H. (1832). Anatomisch-philosophische Untersuchungen über den Kiemenapparat und das Zungenbein der Wirbelthiere. E. Frantzen.
- Reichert, K. B. (1837). Über die Visceralbögen der Wirbelthiere im Allgemeinen und deren Metamorphosen bei den Vögeln und Säugethieren. *Arch. Anat. Phys. Wiss. Med.*, 1837, 120-220.
- Richman, J. M., & Lee, S. H. (2003). About face: signals and genes controlling jaw patterning and identity in vertebrates. *Bioessays*, 25(6), 554-568.
- Ridewood, W.G. (1896) On the spiracle and associated structures in elasmobranch fishes. *Anatomischer Anzeiger*, 11, 425– 433.
- Rijli, F. M., Mark, M., Lakkaraju, S., Dierich, A., Dollé, P., & Chambon, P. (1993). A homeotic transformation is generated in the rostral branchial region of the head by disruption of Hoxa-2, which acts as a selector gene. *Cell*, 75(7), 1333-1349.
- Riley, P., Anaon-Cartwright, L., & Cross, J. C. (1998). The Hand1 bHLH transcription factor is essential for placentation and cardiac morphogenesis. *Nature genetics*, 18(3), 271-275.
- Romer, A. S. (1970). The vertebrate body. Philadelphia: Saunders.
- Romer, A. S. (1966). Vertebrate Paleontology. University of Chicago Press, Chicago.
- Roth, V. L. (1984). On homology. *Biological Journal of the Linnean Society*, 22(1), 13-29.
- Rücklin, M., Donoghue, P. C. J., Johanson, Z., Trinajstić, K., Marone, F., & Stampanoni, M. (2012). Development of teeth and jaws in the earliest jawed vertebrates. *Nature*, 491(7426), 748–751.
- Rutishauser, R., & Moline, P. (2005). Evo-devo and the search for homology (“sameness”) in biological systems. *Theory in Biosciences*, 124(2), 213-241.
- Sakurai, T., Yanagisawa, M., Takuwa, Y., Miyazaki, H., Kimura, S., Goto, K. and Masaki, T. (1990). Cloning of a cDNA encoding a non-isopeptide-selective subtype of the endothelin receptor. *Nature* 348, 732-735.
- Sansom, I. J., Smith, M. M., Smith, M. P., & Ahlberg, P. E. (2001). The Ordovician radiation of vertebrates. Major events in early vertebrate evolution, 156-171.
- Sansom, R. S., Randle, E., & Donoghue, P. C. (2015). Discriminating signal from noise in the fossil record of early vertebrates reveals cryptic evolutionary history. *Proceedings. Biological sciences*, 282(1800), 20142245.
- Santagati, F., & Rijli, F. M. (2003). Cranial neural crest and the building of the vertebrate head. *Nature Reviews Neuroscience*, 4(10), 806-818.
- Sato, T., Kurihara, Y., Asai, R., Kawamura, Y., Tonami, K., Uchijima, Y., Heude, E., Ekker, M., Levi, G. & Kurihara, H. (2008). An endothelin-1 switch specifies maxillomandibular identity. *Proceedings of the National Academy of Sciences*, 105(48), 18806-18811.
- Scaal, M., Füchtbauer, E. M., & Brand-Saberi, B. (2001). cDermo-1 expression indicates a role in avian skin development. *Anatomy and embryology*, 203(1), 1-7.
- Schaeffer, B., & Williams, M. (1977). Relationships of fossil and living elasmobranchs. *American Zoologist*, 17(2), 293-302.
- Schilling, T. F., & Kimmel, C. B. (1994). Segment and cell type lineage restrictions during pharyngeal arch development in the zebrafish embryo. *Development*, 120(3), 483-494.
- Schilling, T. F., & Kimmel, C. B. (1997). Musculoskeletal patterning in the pharyngeal segments of the zebrafish embryo. *Development*, 124(15), 2945-2960.
- Schindelin, J., Arganda-Carreras, I., Frise, E., Kaynig, V., Longair, M., Pietzsch, T., Preibisch, S., Rueden, C., Saalfeld, S., Schmid, B., Tinevez, J.Y & Cardona, A. (2012). Fiji: an open-source platform for biological-image analysis. *Nature methods*, 9(7), 676-682.

- Selever, J., Liu, W., Lu, M. F., Behringer, R. R., & Martin, J. F. (2004). Bmp4 in limb bud mesoderm regulates digit pattern by controlling AER development. *Developmental biology*, 276(2), 268-279.
- Sewertzoff, A. N. (1911). Die Kiemenbogenerven der Fische. *Anat Anz*, 38, 487-495.
- Sewertzoff, A. N. (1928). The head skeleton and muscles of *Acipenser ruthenus*. *Acta Zoologica*, 9(1-2), 193-319.
- Shigetani, Y., Sugahara, F., Kawakami, Y., Murakami, Y., Hirano, S., & Kuratani, S. (2002). Heterotopic shift of epithelial-mesenchymal interactions in vertebrate jaw evolution. *Science*, 296(5571), 1316-1319.
- Shigetani, Y., Sugahara, F., & Kuratani, S. (2005). A new evolutionary scenario for the vertebrate jaw. *BioEssays*, 27(3), 331-338.
- Shih, H. P., Gross, M. K., & Kiousi, C. (2007). Cranial muscle defects of Pitx2 mutants result from specification defects in the first branchial arch. *Proceedings of the National Academy of Sciences*, 104(14), 5907-5912.
- Shimeld, S. M., & Donoghue, P. C. (2012). Evolutionary crossroads in developmental biology: cyclostomes (lamprey and hagfish). *Development*, 139(12), 2091-2099.
- Shu, D. G., Morris, S. C., & Zhang, X. L. (1996). A Pikaia-like chordate from the Lower Cambrian of China. *Nature*, 384(6605), 157-158.
- Shu, D. G., Morris, S. C., Han, J., Zhang, Z. F., Yasui, K., Janvier, P., Chen, L.I.N.G., Zhang, X.L., Liu, J.N., Li, Y.O.N.G & Liu, H. Q. (2003). Head and backbone of the Early Cambrian vertebrate Haikouichthys. *Nature*, 421(6922), 526-529.
- Simakov, O., Kawashima, T., Marlétaz, F., Jenkins, J., Koyanagi, R., Mitros, T., Hisata, K., Bredeson, J., Shoguchi, E., Gyoja, F., Yue, J.X. & Gerhart, J. (2015). Hemichordate genomes and deuterostome origins. *Nature*, 527(7579), 459-465.
- Simonetta, A. M., & Insom, E. (1993). New animals from the Burgess Shale (Middle Cambrian) and their possible significance for the understanding of the Bilateria. *Italian Journal of Zoology*, 60(1), 97-107.
- Siomava, N., Fuentes, J. S., & Diogo, R. (2020). Deconstructing the long-standing a priori assumption that serial homology generally involves ancestral similarity followed by anatomical divergence. *Journal of Morphology*, 281(9), 1110-1132.
- Sleight, V., Gillis, J. A. (2020). Embryonic origin and serial homology of gill arches and paired fins in the skate, *Leucoraja Erinacea*. *Elife* 9: e60635.
- Sommer, R. J. (2008). Homology and the hierarchy of biological systems. *BioEssays*, 30(7), 653-658.
- Song, J. & Boord, R. L. (1993). Motor components of the trigeminal nerve and organization of the mandibular arch muscles in vertebrates: phylogenetically conservative patterns and their ontogenetic basis. *Acta Anatomica* 148, 139–149.
- Sperber, S. M., & Dawid, I. B. (2008). barx1 is necessary for ectomesenchyme proliferation and osteochondroprogenitor condensation in the zebrafish pharyngeal arches. *Developmental biology*, 321(1), 101-110.
- Srivastava, D., Cserjesi, P., & Olson, E. N. (1995). A subclass of bHLH proteins required for cardiac morphogenesis. *Science*, 270(5244).
- Stensiö, E. (1947) The sensory lines and dermal bones of the cheek in fishes and amphibians. *Kongliga Svenska Vetenskaps Akademiens Handlingar*, 24, 1– 195.
- Storm, E. E., & Kingsley, D. M. (1996). Joint patterning defects caused by single and double mutations in members of the bone morphogenetic protein (BMP) family. *Development*, 122(12), 3969-3979.

- Swartz, M. E., Nguyen, V., McCarthy, N. Q., & Eberhart, J. K. (2012). Hh signaling regulates patterning and morphogenesis of the pharyngeal arch-derived skeleton. *Developmental biology*, 369(1), 65-75.
- Talbot, J. C., Johnson, S. L., & Kimmel, C. B. (2010). *hand2* and *Dlx* genes specify dorsal, intermediate and ventral domains within zebrafish pharyngeal arches. *Development*, 137(15), 2507-2517.
- Tanaka, M., Münsterberg, A., Anderson, W. G., Prescott, A. R., Hazon, N., & Tickle, C. (2002). Fin development in a cartilaginous fish and the origin of vertebrate limbs. *Nature*, 416(6880), 527-531.
- Tao W., Lai E. 1992. Telencephalon-restricted expression of BF-1, a new member of the HNF-3/fork head gene family, in the developing rat brain. *Neuron* 8(5): 957-66.
- Tavares, A. L., Garcia, E. L., Kuhn, K., Woods, C. M., Williams, T., & Clouthier, D. E. (2012). Ectodermal-derived Endothelin1 is required for patterning the distal and intermediate domains of the mouse mandibular arch. *Developmental biology*, 371(1), 47-56.
- Tavares, A. L., Cox, T. C., Maxson, R. M., Ford, H. L., & Clouthier, D. E. (2017). Negative regulation of endothelin signaling by SIX1 is required for proper maxillary development. *Development*, 144(11), 2021-2031.
- Tendeng, C., & Houart, C. (2006). Cloning and embryonic expression of five distinct *sfrp* genes in the zebrafish *Danio rerio*. *Gene expression patterns*, 6(8), 761-771.
- Terry, K., Magan, H., Baranski, M., & Burrus, L. W. (2000). *Sfrp-1* and *sfrp-2* are expressed in overlapping and distinct domains during chick development. *Mechanisms of development*, 97(1-2), 177-182.
- Thacher, J. K. (1877.) Median and paired fins, a contribution to the history of vertebrate limbs. *Trans. Connecticut Acad. Sci.* 3: 281-308.
- Theveneau, E., & Mayor, R. (2012). Neural crest delamination and migration: from epithelium-to-mesenchyme transition to collective cell migration. *Developmental biology*, 366(1), 34-54.
- Thomas, T., Kurihara, H., Yamagishi, H., Kurihara, Y., Yazaki, Y., Olson, E. N., & Srivastava, D. (1998). A signaling cascade involving endothelin-1, *dHAND* and *msx1* regulates development of neural-crest-derived branchial arch mesenchyme. *Development*, 125(16), 3005-3014.
- Tissier-Seta, J. P., Mucchielli, M. L., Mark, M., Mattei, M. G., Goridis, C., & Brunet, J. F. (1995). *Barx1*, a new mouse homeodomain transcription factor expressed in cranio-facial ectomesenchyme and the stomach. *Mechanisms of development*, 51(1), 3-15.
- Tomita, T., Toda, M., Miyamoto, K., Ueda, K. and Nakaya, K. (2018). Morphology of a hidden tube: Resin injection and CT scanning reveal the three-dimensional structure of the spiracle in the Japanese Bullhead Shark *Heterodontus japonicus* (*Chondrichthyes*; *Heterodontiformes*; *Heterodontidae*). *The Anatomical Record*, 301, 1336- 1341.
- Tribioli, C., Frasch, M., & Lufkin, T. (1997). *Bapx1*: An evolutionary conserved homologue of the *Drosophila* bagpipe homeobox gene is expressed in splanchnic mesoderm and the embryonic skeleton. *Mechanisms of Development*, 65(1-2), 145-162.
- Trumpf, A., Depew, M. J., Rubenstein, J. L., Bishop, J. M., & Martin, G. R. (1999). Cre-mediated gene inactivation demonstrates that FGF8 is required for cell survival and patterning of the first branchial arch. *Genes & development*, 13(23), 3136-3148.
- Tucker, A. S., Khamis, A. A., & Sharpe, P. T. (1998). Interactions between *Bmp-4* and *Msx-1* act to restrict gene expression to odontogenic mesenchyme. *Developmental dynamics*, 212(4), 533-539.

- Tukel, T., Šošić, D., Al-Gazali, L. I., Erazo, M., Casasnovas, J., Franco, H. L., Richardson, J.A., Olson, E.N., Cadilla, C.L., Desnick, R. J. (2010). Homozygous nonsense mutations in TWIST2 cause Setleis syndrome. *The American Journal of Human Genetics*, 87(2), 289-296.
- Tulenko, F. J., Augustus, G. J., Massey, J. L., Sims, S. E., Mazan, S., & Davis, M. C. (2016). HoxD expression in the fin-fold compartment of basal gnathostomes and implications for paired appendage evolution. *Scientific reports*, 6(1), 1-10.
- Tzahor E., Evans S.M. (2011). Pharyngeal Mesoderm Development during Embryogenesis: Implications for Both Heart and Head Myogenesis. *Cardiovasc. Res.* 91, no. 2: 196–202.
- Van Valen, L. M. (1982). Homology and causes. *Journal of Morphology*, 173(3), 305-312.
- Verreijdt, L., Debiais-Thibaud, M., Borday-Birraux, V., Van der Heyden, C., Sire, J. Y., & Huysseune, A. (2006). Expression of the dlx gene family during formation of the cranial bones in the zebrafish (*Danio rerio*): differential involvement in the visceral skeleton and braincase. *Developmental dynamics*, 235(5), 1371-1389.
- Verzi, M. P., Agarwal, P., Brown, C., McCulley, D. J., Schwarz, J. J., & Black, B. L. (2007). The transcription factor MEF2C is required for craniofacial development. *Developmental cell*, 12(4), 645-652.
- Vieux-Rochas, M., Mantero, S., Heude, E., Barbieri, O., Astigiano, S., Couly, G., Kurihara, H., Levi, G. & Merlo, G. R. (2010). Spatio-temporal dynamics of gene expression of the Edn1-Dlx5/6 pathway during development of the lower jaw. *genesis*, 48(6), 262-373.
- Wada, N., Javidan, Y., Nelson, S., Carney, T. J., Kelsh, R. N., & Schilling, T. F. (2005). Hedgehog signaling is required for cranial neural crest morphogenesis and chondrogenesis at the midline in the zebrafish skull. *Development*, 132(17), 3977-3988.
- Wagner, G.P. (1989). The biological homology concept. *Annu Rev Ecol Evol Syst.* 20(1): 51–69.
- Wagner, G.P. (2007). The developmental genetics of homology. *Nat Rev Genet.* 8(6): 473–79.
- Wagner, G.P. (2014). Homology, genes, and evolutionary innovation. Princeton: Princeton University Press.
- Wagner, G. P. & Hall, B. K. (1994). Homology and the mechanisms of development. Homology: The hierarchical basis of comparative biology, 273-299.
- Walker, M. B., Miller, C. T., Coffin Talbot, J., Stock, D. W. and Kimmel, C. B. (2006). Zebrafish furin mutants reveal intricacies in regulating Endothelin1 signaling in craniofacial patterning. *Dev. Biol.* 295, 194-205.
- Wall, N., Hogan B. (1995). Expression of bone morphogenetic protein-4 (BMP-4), bone morphogenetic protein-7 (BMP-7), fibroblast growth factor-8 (FGF-8) and sonic hedgehog (SHH) during branchial arch development in chick. *Mech Dev* 53:383–392.
- Wang, C. K. L., Omi, M., Ferrari, D., Cheng, H. C., Lizarraga, G., Chin, H. J., ... & Kosher, R. A. (2004). Function of BMPs in the apical ectoderm of the developing mouse limb. *Developmental biology*, 269(1), 109-122.
- Wang, Z., Gerstein, M., & Snyder, M. (2009). RNA-Seq: a revolutionary tool for transcriptomics. *Nature reviews genetics*, 10(1), 57-63.
- Wängsjö, G. (1952). The Downtonian and Devonian vertebrates of Spitsbergen. IX, Morphologic and systematic studies of the Spitsbergen cephalaspids.

- Warga RM, Nüsslein-Volhard C. (1999). Origin and development of the zebrafish endoderm. *Development* 126(4): 827–38.
- Wegner, N. C. (2015). Elasmobranch Gill Structure. *Physiology of Elasmobranch Fishes: Structure and Interaction with Environment*, 101–151.
- Wilson, J., & Tucker, A. S. (2004). Fgf and Bmp signals repress the expression of Bapx1 in the mandibular mesenchyme and control the position of the developing jaw joint. *Developmental biology*, 266(1), 138-150.
- Wotton, K. R., French, K. E., & Shimeld, S. M. (2007). The developmental expression of foxl2 in the dogfish *Scyliorhinus canicula*. *Gene Expression Patterns*, 7(7), 793-797.
- Wyffels, J., King, B. L., Vincent, J., Chen, C., Wu, C. H., & Polson, S. W. (2014). SkateBase, an elasmobranch genome project and collection of molecular resources for chondrichthyan fishes. *F1000Research*, 3.
- Xian-Guang, H., Aldridge, R. J., Siveter, D. J., Siveter, D. J., & Xiang-Hong, F. (2002). New evidence on the anatomy and phylogeny of the earliest vertebrates. *Proceedings of the Royal Society of London. Series B: Biological Sciences*, 269(1503), 1865-1869.
- Xu, D., Emoto, N., Giaid, A., Slaughter, C., Kaw, S., DeWit, D., & Yanagisawa, M. (1994). ECE-1: a membrane-bound metalloprotease that catalyzes the proteolytic activation of big endothelin-1. *Cell*, 78(3), 473-485.
- Xu, P. X., Adams, J., Peters, H., Brown, M. C., Heaney, S., & Maas, R. (1999). Eya1-deficient mice lack ears and kidneys and show abnormal apoptosis of organ primordia. *Nature genetics*, 23(1), 113-117.
- Yamagishi, C., Yamagishi, H., Maeda, J. et al. Sonic Hedgehog Is Essential for First Pharyngeal Arch Development. *Pediatr Res* 59, 349–354 (2006).
- Yanagisawa, H., Yanagisawa, M., Kapur, R. P., Richardson, J. A., Williams, S. C., Clouthier, D. E., de Wit, D., Emoto, N. and Hammer, R. E. (1998). Dual genetic pathways of endothelin-mediated intercellular signaling revealed by targeted disruption of endothelin converting enzyme-1 gene. *Development*, 125(5), 825-836.
- Yao, T., Ohtani, K., Kuratani, S., & Wada, H. (2011). Development of lamprey mucocartilage and its dorsal–ventral patterning by endothelin signaling, with insight into vertebrate jaw evolution. *Journal of Experimental Zoology Part B: Molecular and Developmental Evolution*, 316(5), 339-346.
- Yokoyama, H., Yoshimura, M., Suzuki, D. G., Higashiyama, H., & Wada, H. (2020). Development of the lamprey velum and implications for the evolution of the vertebrate jaw. *Developmental Dynamics*, 250(1), 88-98.
- Young, G.C. and Zhang, G. (1992) Structure and function of the pectoral joint and operculum in antiarchs, Devonian placoderm fishes. *Palaeontology*, 35, 443– 464.
- Yu, J. K., Holland, L. Z., Jamrich, M., Blitz, I. L., & Holland, N. D. (2002). AmphiFoxE4, an amphioxus winged helix/forkhead gene encoding a protein closely related to vertebrate thyroid transcription factor-2: expression during pharyngeal development. *Evolution & development*, 4(1), 9-15.
- Zhang, Y., Parmigiani, G., & Johnson, W. E. (2020). ComBat-Seq: batch effect adjustment for RNA-Seq count data. *NAR genomics and bioinformatics*, 2(3), lqaa078.
- Zhu, M., Yu, X., Ahlberg, P. E., Choo, B., Lu, J., Qiao, T., Qu, Q., Zhao, W., Jia, L., Blom, H. Zhu, Y. (2013). A Silurian placoderm with osteichthyan-like marginal jaw bones. *Nature*, 502(7470), 188–193.

- Ziermann, J. M., Freitas, R., & Diogo, R. (2017). Muscle development in the shark *Scyliorhinus canicula*: implications for the evolution of the gnathostome head and paired appendage musculature. *Frontiers in zoology*, 14(1), 1-17.
- Ziermann, J. M., & Diogo, R. (2018). Development of Head Muscles in Fishes and Notes on Phylogeny-Ontogeny Links. *Evolution and Development of Fishes*, 172.
- Zuniga, E., Rippen, M., Alexander, C., Schilling, T. F., & Crump, J. G. (2011). Gremlin 2 regulates distinct roles of BMP and Endothelin 1 signaling in dorsoventral patterning of the facial skeleton. *Development*, 138(23), 5147-5156